



University  
of Glasgow

McVerry, Ferghal (2014) *Multimodal CT imaging in acute ischemic stroke*. MD thesis.

<http://theses.gla.ac.uk/4868/>

Copyright and moral rights for this thesis are retained by the author

A copy can be downloaded for personal non-commercial research or study, without prior permission or charge

This thesis cannot be reproduced or quoted extensively from without first obtaining permission in writing from the Author

The content must not be changed in any way or sold commercially in any format or medium without the formal permission of the Author

When referring to this work, full bibliographic details including the author, title, awarding institution and date of the thesis must be given

# **Multimodal CT Imaging in Acute Ischemic Stroke**

**Dr Ferghal McVerry**  
**BA, MB, MRCP.**

A thesis which fulfills the requirements of the University of  
Glasgow for the degree of Doctorate of Medicine

Institute of Neuroscience and Psychology  
University of Glasgow  
January 2014

## **Introduction**

Options for imaging in acute stroke are expanding with the potential to select therapy based on imaging targets, as well as providing additional diagnostic and prognostic information. Multimodal CT has been used to image the ischemic penumbra, infarct core, and to detect leptomeningeal collateral flow although the optimum way to image these variables is not clear.

## **Methods**

In addition to a systematic literature review of imaging for leptomeningeal collaterals, Data from observational studies of acute stroke which employed multimodal CT imaging on admission and follow up was used to evaluate feasibility of acute stroke imaging with CT and MRI, Perfusion thresholds for core and ischemic penumbra, methods to quantify leptomeningeal collateral flow and sensitivity of non contrast CT for detecting infarct core pixels.

## **Results**

Advanced imaging in acute stroke and at follow up was more feasible with CT compared to MRI with the possible suggestion that imaging with MRI alone could introduce a bias regarding age and clinical severity for patients entered into clinical studies

Heterogeneity in grading and detecting collateral flow was found in the literature providing an opportunity to devise a novel assessment method.

Well developed collaterals were associated with imaging and clinical markers for good outcome as well as some potential biomarkers including atrial fibrillation and blood fibrinogen level.

Relative cerebral blood flow and delay time were found to be the best predictors on infarct core and ischemic penumbra after derivation of optimum perfusion thresholds and subsequent validation in independent patient groups.

Pixel based comparison of infarct core on CT perfusion and non contrast CT highlighted the lack of sensitivity of CT for detecting infarct core based on Hounsfield unit value alone.

### **Conclusion**

Multimodal CT for acute stroke assessment offers the potential for measuring infarct core, ischemic penumbra and leptomeningeal collateral flow status rapidly according to novel grading scales and thresholds and provides information on tissue viability which cannot be detected on non-contrast CT. Further evaluation on the impact additional imaging should have in clinical practice is needed.

# Table of Contents

Table of Contents .....	4
Publications and Presentations .....	11
Author's declaration.....	13
Chapter 1. Introduction .....	16
1.1 Ischemic Stroke Pathophysiology.....	17
1.1.1 The Ischemic Cascade .....	17
1.1.2 Evidence for Reversible and Permanent Ischemic Damage .....	20
1.1.3 Normal Response to Ischemia .....	21
1.1.4 Identification of Penumbra in Humans with PET .....	22
1.1.5 Factors Affecting the Fate of the Penumbra.....	24
1.2 Treatment Options in Acute Ischemic Stroke.....	27
1.3 CT Imaging for Acute Stroke .....	31
1.3.1 Non Contrast CT .....	31
1.3.2 CT Angiography .....	33
1.3.3 CT Perfusion .....	37
1.4 Magnetic resonance Imaging in Stroke .....	45
1.4.1 DWI .....	45
1.4.2 FLAIR .....	45
1.4.3 Gradient Echo Imaging .....	46
1.4.4 Magnetic Resonance Angiography.....	47
1.4.5 Perfusion Weighted Imaging.....	47
1.5 Conclusion .....	48
Chapter 2. Collateral Circulation .....	49
2.1 Introduction .....	49
2.2 The Cerebral Blood Supply .....	49
2.3 The Circle of Willis .....	52
2.4 Leptomeningeal vessels.....	54
2.4.1 Historical Context .....	54
2.4.2 Collateral Circulation in Animal Models of Stroke.....	55
2.4.3 Collateral Therapeutics in Animal Stroke Models.....	59
2.4.4 Collateral Therapeutics in Human Stroke.....	60
2.5 Systematic Review of Methods for Assessing Leptomeningeal Collateral Flow.....	62
2.5.1 Methods.....	63
2.5.2 Results .....	64
2.5.3 Discussion.....	84
2.5.4 Conclusion.....	90
Chapter 3. Materials and Methods .....	92
3.1 Introduction .....	92
3.2 The Multicentre Acute Stroke Imaging Study (MASIS) .....	92
3.2.1 Data Recording and Transfer .....	98
3.3 POSH- POST Stroke Hyperglycaemia.....	99
3.4 Combined Studies Image Analysis .....	103
3.4.1 Image Transfer, Anonymization and Storage.....	104
3.4.2 Image Analysis .....	104
3.5 Conclusion .....	107
Chapter 4. Feasibility of Imaging Based Study Recruitment .....	109
4.1 Introduction .....	109
4.2 Methods .....	113
4.3 Results.....	114

4.3.1	Acute Imaging.....	118
4.3.2	Subacute Imaging.....	121
4.3.3	Day 30 Imaging.....	121
4.4	Discussion .....	122
4.4.1	Conclusion.....	127
Chapter 5.	Quantifying Collateral Flow Extent in Acute Ischemic Stroke.....	128
5.1	Introduction .....	128
5.2	Quantifying Collateral Flow Using Multimodal CT Imaging. ....	130
5.3	Inclusion Criteria .....	131
5.3.1	Clinical Data .....	132
5.3.2	Image Analysis .....	132
5.3.3	Collateral Flow Grade .....	138
5.3.4	Statistical Analysis .....	142
5.4	Results.....	142
5.4.1	Collateral Flow and Outcome .....	153
5.5	Discussion .....	163
5.6	Conclusion .....	169
Chapter 6.	Derivation and Evaluation of Thresholds for Core and Tissue at Risk of Infarction Using CT Perfusion.....	171
6.1	Introduction .....	171
6.2	Materials and methods.....	172
6.2.1	Patient selection .....	172
6.2.2	Image Acquisition .....	175
6.2.3	Image analysis .....	175
6.2.4	Derivation dataset image analysis .....	177
6.2.5	Validation datasets image analysis .....	181
6.2.6	Statistical analysis .....	182
6.3	Results.....	183
6.4	Discussion .....	193
6.5	Conclusion .....	197
Chapter 7.	Pixel Based Identification of Infarct Core on Non-Contrast CT .....	199
7.1	Introduction .....	199
7.2	Materials and methods.....	200
7.3	Results.....	205
7.4	Discussion .....	211
Chapter 8.	Conclusion .....	215
8.1	Summary .....	215
8.2	Clinical Importance and Future Research Considerations .....	215
8.3	Concluding remarks .....	217
Appendices	.....	218
Gradient Echo	.....	219
DWI	.....	220
Circle of Willis MRA	.....	220
Perfusion.....	.....	221
Post Contrast FLAIR	.....	222
List of References	.....	223

## List of Tables

Table 2-1 Assessment Methods for Measuring Collateral Flow Using Different Modalities .....	65
Table 2-2 Angiographically Defined Collaterals .....	71
Table 2-3CT based Collateral Grading Methods CT based Collateral Grading Methods .....	79
Table 2-4MRI Based Collateral Assessments .....	83
Table 2-5 Original and Modified TIMI and TICl Scales .....	87
Table 3-1 MASIS Study Calendar .....	98
Table 3-2 POSH Study Calendar .....	103
Table 4-1 Recruitment Rates of Trials and Observational Studies of Thrombolysis using CT or MRI .....	111
Table 4-2 Screening Failures for Study Participation in MASIS.....	117
Table 4-3 Comparison of Clinical Characteristics Between Patients Imaged Using CT or MRI on Admission for MASIS .....	120
Table 5-1 Baseline Clinical Characteristics of Subjects with Good and Reduced Collaterals .....	145
Table 5-2 Collateral Status and Associated Imaging Findings on Admission .....	149
Table 5-3 Univariate Logistic Regression Summary.....	153
Table 5-4 Collateral Flow and Clinical Outcome.....	155
Table 5-5 Clinical and Imaging Factors Associated with Clinical Outcome .....	158
Table 5-6 Univariate Logistic Regression Analysis Summaries for Clinical Outcome Prediction (Modified Rankin Scale $\leq 2$ at one month.....	162
Table 6-1 Perfusion Parameter Ranges and Increments Evaluated for Tissue at Risk .....	179
Table 6-2 Perfusion Parameter Range and Increments Evaluated for Core .....	179
Table 6-3 Characteristics of Tissue at Risk Evaluation Group.....	184
Table 6-4 Clinical Characteristics of Infarct Core Groups .....	189
Table 7-1 Sensitivity and Specificity of HU Thresholds for Detecting Infarct Core in Grey Matter .....	210
Table 7-2 Sensitivity and Specificity of HU Thresholds for Detecting Infarct Core in White Matter .....	210

## List of Figures

Figure 1-1 Cascade of Damaging Events in Cerebral Ischemia .....	20
Figure 1-2 Consequences of Reduced Cerebral Perfusion Pressure .....	22
Figure 1-3 Interaction Between CBF Threshold for Infarction and Time .....	25
Figure 1-4 NCCT, CTA MIP and CTA-SI in patient with right MCA occlusion.....	37
Figure 1-5 The Maximal Slopes Method.....	40
Figure 1-6 The Impulse Residue Function .....	41
Figure 2-1 Anatomy of the Middle Cerebral Artery.....	51
Figure 2-2 Illustration of Collateral Scoring Based on Catheter Angiography.....	68
Figure 2-3 Hyperintense Vessels on FLAIR. ....	81
Figure 3-1 MIStar Interface.....	107
Figure 4-1 Flowchart for Recruitment to MASIS Study .....	116
Figure 4-2 Imaging Acquired at Each Study Timepoint.....	122
Figure 5-1 DT Summary Map with ROI Measuring Pixels with DT>2 Seconds .....	134
Figure 5-2 Fusion Tool Before and After Co-registration .....	136
Figure 5-3 Reformatted Structural Image After Co-Registration .....	137
Figure 5-4 4D Angiography Demonstrating Retrograde Collateral Flow .....	139
Figure 5-5 CTA After Application of High-Low HU Threshold .....	141
Figure 5-6 Flowchart for Inclusion in Collateral Flow Evaluation .....	143
Figure 5-7 Collateral Status and NIHSS .....	146
Figure 5-8 Collateral Grade and Fibrinogen Level .....	146
Figure 5-9 Collateral Grade and Atrial Fibrillation .....	147
Figure 5-10 Collateral grade and Volume with DT $\geq$ 2 Seconds .....	150
Figure 5-11 Collateral grade and Volume with DT $\geq$ 4 seconds.....	150
Figure 5-12 Collateral grade and DT $\geq$ 6 seconds.....	151
Figure 5-13 Collateral grade and DT $\geq$ 8 Seconds.....	151
Figure 5-14 Collateral grade and Infarct Core Volume.....	152
Figure 5-15 Collateral Grade and Penumbra Volume.....	152
Figure 5-16 Collateral Grade and Infarct Volume.....	156
Figure 5-17 Collateral Grade and Infarct Growth.....	156
Figure 5-18 Admission NIHSS and Outcome .....	159
Figure 5-19 24hr NIHSS and Outcome.....	159
Figure 5-20 Infarct Volume and Clinical Outcome .....	160
Figure 5-21 Proportion Penumbra Salvage and Clinical Outcome .....	160
Figure 5-22 ASPECTS Score on CBV Maps and Clinical Outcome .....	161
Figure 5-23 ASPECTS Score on NCCT and Clinical Outcome .....	161
Figure 5-24 Collateral Flow and Clinical Outcome .....	162
Figure 6-1 ROI Surrounding Final Infarct Volume .....	177
Figure 6-2 Penumbrogram with Infarct ROI.....	180
Figure 6-3 True & False Positive/Negative Pixels.....	181
Figure 6-4 Effect of Varying Perfusion Threshold on Sensitivity and Specificity	183
Figure 6-5 Youden's Index for Each Perfusion Threshold Evaluated for Tissue at Risk .....	185
Figure 6-6 Frequency Distribution for Optimum DT, Relative MTT and Absolute MTT Thresholds for Tissue at Risk.....	186
Figure 6-7 Bland Altman Plot for DT >2 Seconds, Relative MTT 145 %, Relative MTT 125 % and Absolute MTT 7 Seconds for Detecting Tissue at Risk .....	187
Figure 6-8 Youden's Index for Each Perfusion Threshold Evaluated for Core ...	190
Figure 6-9 Frequency Distribution for Optimum Relative (A) and Absolute (B) MTT Thresholds for Core .....	191
Figure 6-10 Bland Altman Plot for Relative CBF $\leq$ 45%, Absolute CBV 2ml/100g, Absolute MTT > 8 Seconds, and Relative MTT125%, for Detecting Infarct Core..	192
Figure 7-1 Core Grey & White Matter Segmentation .....	202



Figure 7-2 ROC Curve for Presence of Grey Matter Core Pixels on CT.....	206
Figure 7-3 ROC curve for presence of White Matter core pixels on CT.....	207
Figure 7-4 Frequency Distribution for Grey Matter Cut Points .....	208
Figure 7-5 Frequency Distribution for White Matter Cut Points .....	209

## Acknowledgments

This thesis, along with my training in stroke medicine was made possible by the help of my supervisor Professor Keith W. Muir to whom I will be forever grateful. I was given every opportunity during my fellowship to ask questions, explore areas of particular interest and was given lots of encouragement and helpful advice. The skills learnt during this time are invaluable both academically and clinically, and for his role as a supervisor I owe Professor Muir a debt of gratitude.

In addition I acknowledge the support of the other members of the acute stroke team based at the Southern General Hospital; Dr Tracey Baird, Dr Ian Reeves, Dr George Duncan, Dr Phil Birschel, Dr Julie McManus, Dr Fozia Nazir, and Dr Margaret Roberts from whom I learnt a great deal in acute stroke management and who welcomed me into the acute stroke team. The radiography and Nursing staff were excellent in facilitating the research projects. Dr Evelyn Teasdale and Dr Celestine Santosh were sources encouragement and set an example for work ethic and attention to detail in stroke imaging.

My research colleagues Dr Niall MacDougall and Dr Krishna Dani are good friends and provided excellent insights into acute stroke research and imaging, and both made me feel welcome in Glasgow. Christine Aiken, Sandra Greenshields, Angela Welch, Sally Baird and Wilma Smith were always sources of assistance. Dr Mark Parsons was a welcoming host during my visiting fellowship to the John Hunter Hospital, Newcastle Australia and provided excellent training and insight into image analysis in stroke.

I am grateful to both the Translational Medicine Research Collaboration and Chest Heart and Stroke, Scotland for providing funding for my fellowship and conference attendances.

I also wish to express thanks to Professor Jean-Claude Baron and Professor I Mhairi Macrae for taking the time to examine the manuscript and for helpful suggestions on how to improve it following the viva examination.

Finally I must acknowledge my family, my parents who were always at hand to help out especially when travelling over and back from Glasgow, and in

particular my wife Joanne who has dealt with years of disruption and travelling when supporting me in this research project and for whom all of the hard work is dedicated to.

## Publications and Presentations

### Papers

- **Clinical Relevance and Practical Implications of Trials of Perfusion and Angiographic Imaging in Patients with Acute Ischemic Stroke: A Multicentre Cohort Imaging Study.** J.M Wardlaw, K.W. Muir, MJ Macleod, C Weir, F McVerry, T Carpenter, K Shuler, R Thomas, P Acheampong, K Dani, A Murray, JNNP 2013 ( In Press)
- **Systematic Review of Methods for Assessing Leptomeningeal Collateral Flow.** F McVerry, DS Liebeskind, K.W. Muir, AJNR 2012 Mar;33(3):576-82
- **Iodinated Contrast Media and Cerebral Haemorrhage after Intravenous Thrombolysis.**  
N JJ MacDougall, F McVerry, S Baird, E Teasdale, T Baird. K.W. Muir , Stroke 2011 42(8):2170-4

### Abstract Publications

- **Derivation and Evaluation of Thresholds for Tissue at Risk in Stroke Using CT Perfusion**  
F McVerry NJJ MacDougall MJ Macleod J. Wardlaw K.W. Muir JNNP 2012;83:e1  
doi:10.1136/jnnp-2011-301993.48
- **Carotid Stenosis Causes Delay Induced Overestimation of Stroke Lesion Volume on CT Perfusion Imaging.**  
A. Coulter, F.McVerry, K. Muir, International Journal of Stroke Vol 6(s2) December 2011, P65
- **Comparison of CT Perfusion Lesion Volumes from Different Software Processing.**  
F.McVerry, K. Dani, R. Thomas, P. Acheampong, C. Weir, T. Carpenter , P. Rauchaus A. Murray M.J. Macleod J. Wardlaw, K.W. Muir, Cerebrovasc Diseases 2011;31(suppl 2):1–322
- **Short Acquisition Times for Multimodal CT Examination in Acute Stroke.**  
F.McVerry, K. Dani, R. Thomas, P. Acheampong, C. Weir, T. Carpenter , P. Rauchaus A. Murray M.J. Macleod J. Wardlaw, K.W. Muir, Cerebrovasc Diseases 2011;31(suppl 2):1–322
- **Importance of Image Co-registration with Limited Brain Coverage of CT Perfusion.**  
F. McVerry, K. Dani, R. Thomas, P. Acheampong, C. Weir, T. Carpenter , P. Rauchaus A. Murray M.J. Macleod J. Wardlaw, K.W. Muir, Cerebrovasc Diseases 2011;31(suppl 2):1–322
- **Practical Approaches to Improve Feasibility of Patient Recruitment to Hyperacute Stroke trials Using Imaging**  
J.M. Wardlaw, K.M. Muir, M.J. MacLeod, C.J. Weir, T. Carpenter, R.G. Thomas K. Dani, F. McVerry, P. Acheampong, P. Rauchaus, A. Murray, D. Hadley Cerebrovasc Diseases 2011;31(suppl 2):1–322
- **Method For Determining Infarct Growth Significantly Influences the Measurement Obtained**  
F. McVerry, K. Dani, R. Thomas, P. Acheampong, C. Weir, T. Carpenter , P. Rauchaus A. Murray M.J. Macleod J. Wardlaw, K.W. Muir, Cerebrovasc Diseases 2011;31(suppl 2):1–322
- **Patterns of Ischemic Lesion Perfusion in the First Month After Stroke, the “No Reflow” Phenomenon**  
J.M. Wardlaw, K.M. Muir, M.J. MacLeod, C.J. Weir, T. Carpenter, R.G. Thomas K. Dani, F. McVerry, P. Acheampong, P. Rauchaus, A. Murray, D. Hadley Cerebrovasc Diseases 2011;31(suppl 2):1–322
- **CT Assessment of Blood Brain Barrier Permeability and Risk of Haemorrhagic Transformation in Ischaemic Stroke.**

Adam J Couves, Ferghal McVerry, Niall J MacDougall, Krishna A Dani, Keith W Muir.  
Stroke 2011 42;e1111-e35

- **Comparison of Qualitative and Quantitative Mismatch with CT Perfusion.**  
McVerry F, Dani KA, MacDougall NJJ, Wardlaw JM, Macleod MJ, Muir KM, International Journal of Stroke 2010, Volume 5 Issue, Supplement s3 P10
- **Predicting Infarct Core with CT Perfusion, Does Red Mean Dead?**  
F McVerry, MS Ardebelli, JM Wardlaw, MJ Macleod, KW Muir International Journal of Stroke 2010 Vol 5 Issue, Supplement s3, P54
- **Detection of Penumbra and Arterial Occlusions Using Multimodal CT. Where Should Therapy be Targeted?**  
F McVerry, CR Levi, KW Muir, MW Parsons Cerebrovasc Diseases 2010;29(suppl 2):1
- **Access to acute CT and MR imaging techniques in acute stroke research.**  
F. McVerry, JM Wardlaw MJ Macleod, KW Muir. International Journal of Stroke Dec 2009, Vol 4 Issue 0, P1-45
- **Perfusion CT in Acute Ischemic Stroke.**  
F. McVerry K W Muir, International Journal of Stroke Dec 2009, Vol 4 Issue 0, P1-45

#### **Additional Platform Presentations**

- **Role of Advanced Imaging Selection in Acute Ischemic Stroke**  
Invited Speaker. UK Stroke Forum April 2012
- **Derivation and Evaluation of Perfusion Thresholds using CT Perfusion**  
SINAPSE Annual Scientific Meeting 2011

## **Author's declaration**

All analyses presented are the work of the author unless otherwise stated.

Ferghal McVerry BA, MB, MRCP

January 2014

## Definitions

ACA – Anterior cerebral artery  
 ADC - Apparent diffusion coefficient  
 AIF – Arterial input function  
 AUC – Area under the curve  
 ASPECTS - Alberta Stroke Programme Early CT Score  
 CBF – Cerebral blood flow  
 CBV – Cerebral blood volume  
 CI – Confidence interval  
 CMRO<sub>2</sub> – Cerebral metabolic rate for oxygen  
 CPP- Cerebral Perfusion Pressure  
 CSF- Cerebrospinal Fluid  
 CT – Computed tomography  
 CTA – Computed tomography angiography  
 CTP – Computed tomography perfusion  
 CVR- Cerebrovascular resistance  
 DSA – Digital subtraction angiography  
 DT- Delay Time  
 DWI - Diffusion weighted imaging in magnetic resonance imaging  
 FLAIR - Fluid attenuated inversion recovery in magnetic resonance imaging  
 FMISO - <sup>18</sup>F-fluormisonidazole  
 FN- False Negative  
 FP-False Positive  
 FOV - Field of view  
 GE – General Electric  
 GRE – Gradient echo sequences in magnetic resonance imaging  
 Hct - Haematocrit  
 HU – Hounsfield Units  
 ia – Intra-arterial  
 ICA – Internal carotid artery  
 ICC Intraclass Correlation Coefficient  
 ICH – Intra-cerebral haemorrhage  
 IQR – Inter-quartile range  
 iv –Intravenous  
 k=Kappa Statistic  
 LACS- Lacunar Stroke  
 LMF- Leptomeningeal Collateral Flow  
 LMA- Leptomeningeal Arteries  
 MASIS- Multi-centre Acute Stroke Imaging Study  
 MCA – Middle cerebral artery  
 MIP – Maximum intensity projection  
 mm – millimetres  
 MMP – Matrix metalloproteinase  
 MPR- Multiplanar Reformat  
 MRA – Magnetic resonance angiography  
 mRS – modified Rankin Scale  
 MR – Magnetic Resonance  
 MRI – Magnetic Resonance Imaging  
 MREC – Multi-centre Research Ethics Committee  
 MRI – Magnetic Resonance Imaging  
 MRS – Magnetic Resonance Spectroscopy

ms - milliseconds  
MTT – Mean transit time  
NAA – N-acetyl aspartate  
NCCT – Non-contrast computed tomography  
NIHSS –National Institutes of Health Stroke Scale  
OEF – Oxygen extraction fraction  
OR – Odds ratio  
OCSP- Oxfordshire Community Stroke Project  
PACS – Partial anterior circulation Stroke  
PET – positron emission tomography  
POCS- Posterior Circulation Stroke  
POSH- Post Stroke Hyperglycemia  
PS- Surface area product  
PWI - perfusion weighted imaging  
rtPA – recombinant tissue plasminogen activator  
SI-Source Images  
SPECT – single photon emission tomography  
SVD – singular value decomposition  
tPA – tissue plasminogen activator  
TACS- Total Anterior Circulation Stroke  
TCD – transcranial doppler  
TIBI – thrombolysis in brain ischaemia  
TIMI – thrombolysis in myocardial infarction  
TMAX – time to the peak of the deconvolved curve in perfusion analysis  
TN- True Negative  
TOAST- Trial of Org 10172 in acute stroke treatment  
TP – True Positive  
TTP – time to peak  
UK – United Kingdom  
yrs - Years



## Chapter 1. Introduction

Stroke is defined as a rapidly progressive focal or global brain dysfunction of vascular origin lasting more than 24 hours or leading to death within 24 hours(1). As one of the leading contributors to death and disability worldwide, the burden of stroke is felt physically, socially, economically and emotionally on patients, their families and health care services (2). Within stroke, several subtypes exist with ischemic stroke representing the majority, accounting for between 67 and 80 % of stroke cases reported in epidemiological studies (2). Ischemic stroke is more often disabling rather than fatal but remains the most common life threatening neurological disorder(3). 10 % of patients with ischemic stroke will die within 30 days of stroke onset, while half of those who survive have persistent disability 6 months later(4). The remaining 20% of stroke cases are due to intracerebral or subarachnoid haemorrhage which are also potentially devastating conditions with 30 day mortality of primary intracerebral haemorrhage approaching 50%(5-7).

Causes of ischemic stroke are wide(8) .Stroke aetiology may be classified into 5 main groups using the TOAST classification or subsequent variations on TOAST(9-11):

- Large artery atherosclerosis
  
- Cardiac embolus
  
- Small vessel occlusion
  
- Stroke of other determined aetiology
  
- Stroke of undetermined aetiology

## 1.1 Ischemic Stroke Pathophysiology

### 1.1.1 *The Ischemic Cascade*

Transient or permanent occlusion of a cerebral artery by a thrombus or embolus causes a reduction in normal cerebral blood flow in the affected vascular territory. The brain has a high demand for oxygen and glucose delivery for energy production via oxidative phosphorylation which is compromised by the collapse in cerebral blood flow resulting in reduced nutrient delivery to grey and white matter(12). Without the ability to store energy supplies for future use, reduced cerebral blood flow results in the inability to maintain ionic gradients across cell membranes. Persistent or sufficiently severe blood flow reductions result in neuronal death at a rate of approximating 1.9 million neurones per minute(13). Reduced territorial blood flow is not uniform however and interrupted blood flow to the white matter and cortex results in a gradient of hypo perfusion, rather than complete and homogeneous ischaemia of the entire territory(14). The source of persistent blood flow in the setting of complete arterial occlusion is from collateral vessels which may be different depending on the site of occlusion and between different individuals due to other factors(15).

The mechanisms ultimately responsible for cell death in the setting of cerebral ischemia are many and complex, occurring at different times after the onset of ischaemia depending on the pathological process(16).Regions suffering the most severe degrees of hypo perfusion progress most rapidly to necrosis and irreversible cell death, while other regions with more modest blood flow reductions may become infarcted at later time points. This late cell death is mediated via apoptosis at less severe blood flow reductions, and neuronal tissue may be particularly vulnerable in this alternative mode of cell death(17). The potential for tissue infarction late after stroke onset therefore may represent a target for therapeutic intervention.

With loss of energy-dependent cellular processes, ionic potentials across cell membranes are lost and excitatory amino acids are released to the extra cellular space. Glutamate accumulation activates post synaptic NMDA and AMPA receptors leading to  $\text{Ca}^{2+}$  and  $\text{Na}^{+}$  influx, and  $\text{K}^{+}$  efflux, from cells. This results in cell death due to excito-toxicity(12). Anion influx to cells is followed by net

water influx and resultant cellular oedema and ultimately lysis. Loss of normal ionic potentials because of excitotoxicity results in cellular depolarisation which if permanent also results in cellular necrosis. Transient but repeated cellular depolarisation and repolarization can occur in regions with less severe reductions in blood flow which surround the necrotic infarct core in experimental stroke models. Repolarization requires energy and ongoing exposure to glutamate stimulates depolarization again. The likelihood of permanent depolarisation and cell death increases with the number of peri-infarct depolarisations seen in animal models(12). These depolarisations can occur several hours after stroke onset and contribute to the growth of the infarct with time. Glutamate mediated  $\text{Ca}^{2+}$  influx to cells also leads to intracellular production and release of pro-inflammatory cytokines such as TNF and IL-1beta, expression of adhesion molecules on cellular surface and recruitment of neutrophils and macrophages and activation of the complement cascade. The resultant post ischemic inflammatory reaction can further contribute to cell damage by direct toxin production as well as contributing to cell apoptosis. Apoptosis is also linked to activation of intracellular enzymes. Caspase activation after  $\text{Ca}^{2+}$  influx and loss of mitochondrial function results in the generation of reactive oxygen species, intracellular DNA damage, and activation of programmed cell death via apoptosis, potentially occurring with milder levels of blood flow reduction than those responsible for earlier cellular necrosis(18). The time scale for apoptosis induced cell death is over hours to days, while excitotoxicity induced cell necrosis occurs over minutes to hours (Figure 1.1).

Different mechanisms for cell death over time which ultimately contribute to tissue infarction have been the target for neuroprotectant therapies targeting the ischemic cascade. Although the neuroprotectant trials targeting these areas have been negative to date, the cellular processes involved in stroke evolution represent logical targets for therapy. Clinical trials of neuroprotection, for example using therapeutic hypothermia which targets a number of different steps within the ischemic cascade are promising interventions and are currently ongoing(19). Trial design and heterogeneity of subjects recruited to such trials may explain why neuroprotectants targeting cellular processes have failed, and it may be that these treatments could be of benefit in certain stroke subtypes

with specific tissue characteristics. Identifying these subgroups on clinical grounds alone is difficult, highlighting the need to explore additional imaging to identify stroke subtypes(20).

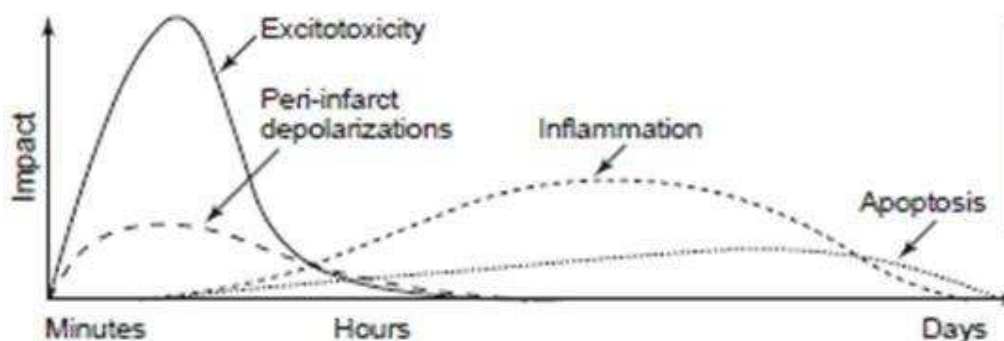


**Figure 1-1 Cascade of Damaging Events in Cerebral Ischemia**

Tissue infarction after cerebral ischemia may be induced by different mechanisms at different time points after stroke. Reproduced from "Dirnagl U, Pathobiology of ischemic stroke: an integrated view" Trends in Neuroscience 1999

### ***1.1.2 Evidence for Reversible and Permanent Ischemic Damage***

Experimental stroke models have shown that impaired brain functional activity and loss of brain structural integrity occur at separate and distinct thresholds of CBF (21). Tissues in receipt of low rates of cerebral blood flow have reduced electrical activity as demonstrated by EEG and cortical evoked potentials (22, 23). Some or all of this electrically silent tissue may have the capacity to recover function however, as the ion concentration changes due to  $K^+$  efflux typically associated with neuronal death may be absent at the level of hypoperfusion required to produce absent EEG activity(24). The concept of tissue states which can be defined according to blood flow thresholds appeared, with two close but distinct thresholds being determined; the threshold for reduced cortical evoked potentials (responsible for the clinical deficit) and the threshold for  $K^+$  efflux and loss of neuronal integrity (responsible for tissue infarction). Tissue between these thresholds, structurally intact but electrically silent, has been defined as the ischemic penumbra, the volume of tissue surrounding the irreversibly damage infarct core resembling the shaded zone surrounding the centre of a complete solar eclipse(14). An important feature was that reversal of the ischemic lesion causing symptoms could actually reverse the clinical deficit, but that interruption to blood flow for long periods ultimately resulted in tissue infarction (25). Hence the presence of penumbra in animals was confirmed and the prompt restoration of flow to penumbral tissue

resulted in recovery of function, supporting the development of strategies to restore flow to ischemic tissue in stroke.

However the original identification and definition of penumbra in animal models, reflecting electrically silent but structurally intact tissue, has limitations when translating the concept of ischemic penumbra to clinical practice as the methods used in the original definition are not practical for examining stroke in humans. The ischemic penumbra has therefore undergone multiple operational definitions since originally proposed, which to varying degrees have defined penumbra according to different imaging modalities and clinical markers. A current definition that embodies many of the concepts of the penumbra is:

“The ischemic penumbra is ischemic tissue which is functionally impaired and is at risk of infarction but has the potential to be salvaged by reperfusion and/or other strategies. If not salvaged this tissue is progressively recruited into the infarct core, which will expand with time into the maximal volume originally at risk”(26).

While this definition describes the key features of the penumbra, incorporating the mechanism(s) of penumbral salvage into the definition is a possible shortcoming, as putative mechanisms of future tissue rescue arguably should not define the actual state of the tissue in question.

### ***1.1.3 Normal Response to Ischemia***

In order to identify core and penumbra using imaging, the normal response to ischemia must be known in order to distinguish tissue which is normal from tissue which is at risk of infarction or irreversibly damaged. CBF is determined by the combination of CPP (cerebral perfusion pressure) and CVR (cerebrovascular resistance). CBF is maintained to a degree despite fluctuations in CPP by autoregulation which protects against hypoxia in the setting of low CPP and against oedema with high CPP (27). In stroke, occlusion of an extra or intracranial artery results in reduced CPP. In an attempt to maintain normal CBF, resistance vessels dilate causing a reduction in CVR and an increase in CBV due to autoregulation. If maximal vasodilation and increases in CBV cannot maintain CBF, tissue hypo perfusion ensues. OEF increases to maintain cerebral

metabolism and function despite the reduction in CBF, and reaches a maximum level in a state of “misery perfusion”(28). If this is insufficient to maintain normal metabolic function, an energy deficit ensues, normal metabolism becomes impaired and  $CMRO_2$  reduces. The response to progressive reduction in CPP is demonstrated visually below, revealing that CBF is maintained by increasing CBV and OEF then increases, but progressive and severe reduction in CBF finally results in a collapse in CBV after loss of autoregulation:

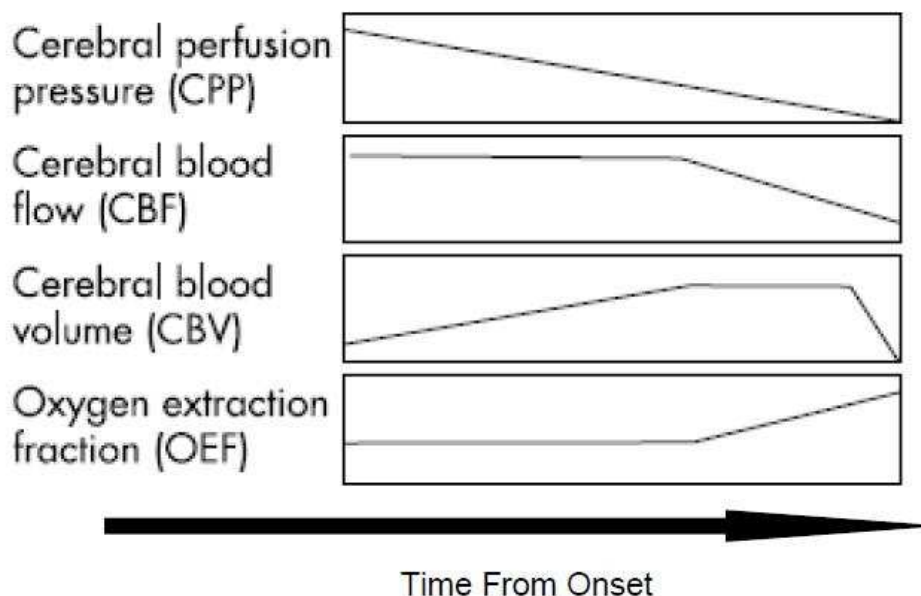


**Figure 1-2 Consequences of Reduced Cerebral Perfusion Pressure**

As CPP falls, CBF is maintained by vasodilation and increasing CBV until compensation is maximal. As CBF falls OEF increases but with ongoing reduction in CPP CBV falls and autoregulation is lost. Adapted from “Markus H. Cerebral perfusion and Stroke. Journal of Neurology Neurosurgery and Psychiatry 2004; 75: 353-361”

Although reductions in CBF are ultimately responsible for tissue to become penumbral or infarcted, indices such as OEF and  $CMRO_2$  clearly can be used to define tissue according to metabolic activity and which ultimately reflect neuronal integrity. These parameters, obtained using PET imaging represent the gold standard methods by which tissue in different states of metabolic and haemodynamic compromise can be determined in humans.

#### **1.1.4 Identification of Penumbra in Humans with PET**

The topography and time course of penumbra in human stroke has been examined using numerous techniques, but the gold standard measurement has been using PET. PET, using oxygen<sup>15</sup> provides quantitative measurement of the

parameters of interest in stroke and penumbra, namely CBF, CMR02 and OEF. Tissue in the state of misery perfusion, with reduced CBF but normal CMR02 is consistent with the concept of penumbral tissue existing between life and death(28). But to meet the above definition of penumbra, the fate of misery perfusion tissue requires examination. To achieve this, Baron and colleagues performed PET imaging in a series of stroke patients between 5-18 hours after onset of stroke symptoms and, in the survivors, obtained final infarct imaging with CT to assess tissue outcome on a voxel by voxel basis(29). In survivors with visualised infarcts, tissue in the misery perfusion state with CBF ranging from 10-22ml/100g/min and OEF above 0.70 was shown to be incorporated into final infarct volume, proving that hypoperfused but metabolically active tissue is truly tissue at risk of infarction and therefore can be defined as penumbra. The viability of tissue suffering from misery perfusion has already been observed in animal stroke models examining the effect of reperfusion at different time points after stroke (25), proving that this tissue state fulfils the ideal definition of penumbra. Importantly, putative penumbral tissue was also seen in non infarcted tissue at follow up. Normal, peri-infarct voxels with penumbral signature on initial PET were found in patients with clinical improvement, the extent of which correlated strongly with the volume of penumbra salvaged suggesting that the penumbra can be salvaged with a corresponding clinical improvement. Irreversibly damaged tissue can also be demonstrated using PET, with a reduction in CBF in tandem with a reduced CMR02 due to loss of normal cerebral metabolism(30).

PET was the first modality to measure penumbra in human stroke. The measurements obtained are quantitative, reflect both blood flow and metabolic activity and remain the accepted gold standard measurement for penumbra. However PET imaging is limited to a small number of sites, is not a routine imaging modality for stroke, is time consuming and requires arterial catheterisation. Therefore, although being the accepted modality for penumbra detection, its use remains as a research tool only. The characteristic PET signatures of penumbra and core have been built upon to achieve penumbra imaging with alternative methods. These include SPECT, CT, MRI, Xenon CT and variations of PET imaging using other tracers such as  $^{11}\text{C}$ -Flumazenil,  $^{18}\text{F}$ -fluoromidazole and  $^{15}\text{O}$ . MRI and CT represent the methods used in clinical



practice with potential to visualise core and penumbra and will be discussed in more detail.

### ***1.1.5 Factors Affecting the Fate of the Penumbra***

The ischemic penumbra exists between life and death with the potential to be rescued, and is therefore subject to influences which determine its ultimate fate. Recovery of penumbra is associated with magnitude of clinical recovery (29) suggesting treatments focussed on maintaining it or rescuing it completely would have a positive impact. The potential influences on penumbral salvage are more than the culprit arterial occlusion however with a number of additional factors implicated;

#### Time

Reperfusion of the penumbra is a target of hyperacute acute stroke treatments which are severely limited by time. Stroke is a dynamic process with neuronal death occurring at times due to different underlying mechanisms. Ultimately however, penumbra becomes recruited to the infarct core with time if not rescued.

After focal ischemia was induced in a group of monkeys, the clinical outcome was dependent on the duration of ischemia with full recovery possible with early reperfusion after stroke onset(25). The interaction between CBF reduction and duration of ischemia is demonstrated in figure 1.3.

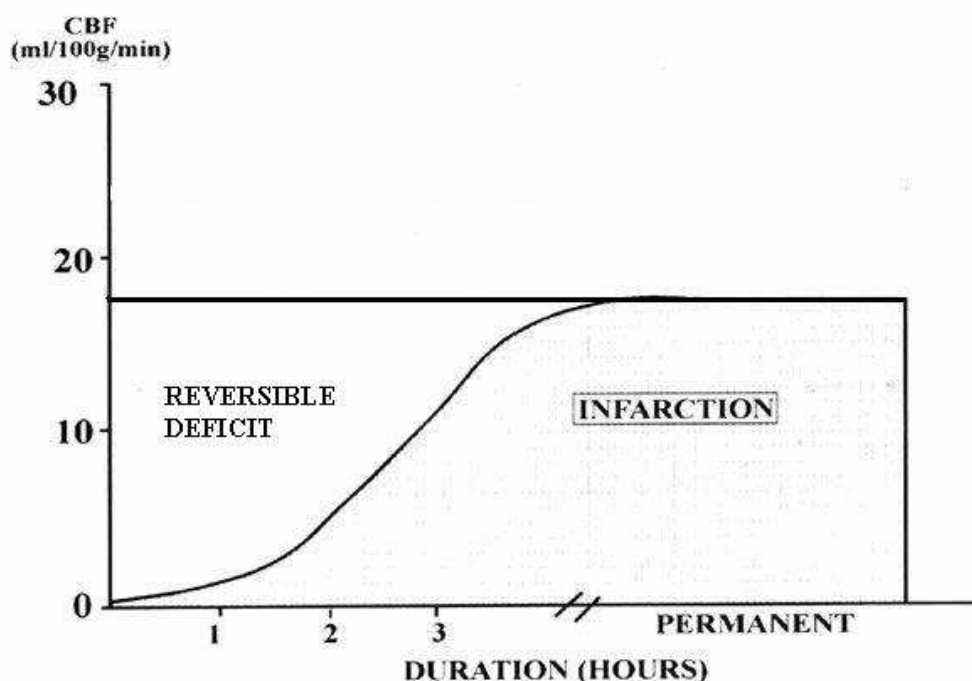


**Figure 1-3 Interaction Between CBF Threshold for Infarction and Time**

The CBF threshold for infarction increases with time from stroke onset. Adapted from “Jones TH, Morawetz RB, Crowell RM et al. Thresholds of focal cerebral ischemia in awake monkeys. *J.Neurosurg.* 1981; 54:773”, courtesy of the American College of Chest Physicians.

Neuronal loss over time has been quantified in a model of supra-tentorial stroke, suggesting that almost 2 million neurons are lost per minute ultimately contributing to the final infarct extent (13). The importance of time is underlined most obviously in the administration of therapies that currently exist to restore perfusion to ischemic tissue, with odds of obtaining good clinical outcome with thrombolytic agents decreasing dramatically with increasing time from symptom onset such that on a population level benefits may not outweigh risks from treatment beyond 4.5 hrs(31). Despite the clear importance of time, it is likely that some patients, such as those with good collateral flow or minimal established ischemic change on imaging, presenting beyond the usual time window would still benefit from treatment if selected appropriately. Although the results of this pooled analysis are not based on documented penumbral salvage, it is likely that infarct extent is greater and penumbral salvage is lesser with increasing time after symptom onset, and the benefit from early reperfusion is due to recovery of penumbral tissue. Stroke is a dynamic process, infarction evolves over time, and for acute stroke, the popular phrase “time is brain” is appropriate.

### Blood Glucose

Persistent hyperglycaemia >7mmol/L is strongly associated with expansion of infarct volume over time while admission hyperglycaemia is associated with increasing lactate production, demise of salvageable tissue and worse clinical outcomes using MRI and MR Spectroscopic imaging(32, 33) . Hyperglycaemia therefore has an independent influence on the fate of tissue likely to be penumbral at the time of imaging. While this offered a potential therapeutic target, trials to date have not shown a therapeutic benefit from using insulin in post-stroke hyperglycemia as lowering blood glucose did not attenuate infarct growth and resulted in episodes of hypoglycaemia (34-36). Hyperglycemia may therefore represent a marker for poor outcomes after stroke, but may not be the direct cause for this effect.

### Age

Increasing age is an independent factor in the risk of penumbra tissue progressing to become infarcted. In an MRI based study using DWI and PWI imaging, Ay et al showed that increasing age was associated with progression of ischemic tissue to become infarcted, with each year of increased age contributing to an additional 0.65% of additional penumbral tissue becoming infarcted(37). Animal studies have revealed that with increasing age, white matter susceptibility to ischemia increases and is mediated predominantly via glutamate release and AMPA and kaianate-type glutamate receptors(38). The impact of age and loss of penumbra interacts with sex, as younger women tended to have 50% less penumbral tissue loss than male counterparts, but older patients had less obvious differences .This interaction of sex and age mirrors cardiovascular risk profiles which are also lower in younger women compared to men, and likely reflects the impact of blood oestrogen levels on cardiovascular risk as well as increased blood flow and decreased vascular tone mediated by increased oestrogen(39).

### Severity of hypo perfusion / Collateral flow

The presence of compensatory collateral circulation in the territory of ischemia may ameliorate the effects of ischemia to a degree(15). Well formed collaterals correlate with less severe hypoperfusion measurements and larger volumes of oligemia. Severity of hypoperfusion does not correlate with the total volume of

ischemic tissue, but does correlate with the volume of irreversibly damaged core within the ischemic zone, suggesting that when development of residual collateral flow is poor, hypoperfused tissue is more likely to become irreversibly damaged (40).

### Haematocrit

Haematocrit contributes to blood viscosity and contributes to poor outcome after ischemic stroke. In a study using serial MRI at intervals up to 90 days after stroke, elevated haematocrit was associated with less reperfusion, more infarct expansion and a trend towards reduced penumbral salvage (41).

## **1.2 Treatment Options in Acute Ischemic Stroke**

The potentially devastating consequences of stroke highlight the need to utilise effective treatments to minimise disability. The spectrum of stroke treatments is wide, involves multiple disciplines and comprises various different interventions depending on the time point and clinical requirement. Given the focus of this thesis will be on acute stroke, treatments given within the first hours after stroke onset will be discussed.

The only licensed treatment of acute ischemic stroke is the administration of rt-PA as a thrombolytic agent in selected individuals (42-45). Trial evidence now supports the administration of rt-PA up to 4.5 hours after symptom onset, although earlier treatment is associated with higher odds for achieving good clinical outcomes (46).

Several randomized controlled clinical trials have been performed using rt-PA in various time windows, with pooled results showing the efficacy and time dependant nature of treatment (31). A total of 6705 patients have been randomised to rt-PA or placebo in several trials with odds ratio of a good clinical outcome after stroke ranging from 2.55(95% CI 1.44-4.52), 1.64 (95% CI 1.12-2.40) and 1.34 (95% CI 1.06-1.61) for 0-90, 91-180 and 181-270 minute time windows respectively, where good clinical outcome was defined as 3 month mRS of 0-1(31). This is despite an increased likelihood of intracerebral haemorrhage

with rt-PA versus placebo (OR 5.37 95% CI 3.22-8.95). These trials confirm the time dependent benefit of thrombolysis for acute stroke.

Other acute stroke therapies exist and are worthy of mention. Alternative thrombolytic agents with theoretical benefits over alteplase include Desmoteplase and Tenecteplase. Desmoteplase in the 3-9 hour window was associated with increased reperfusion rates which corresponded to favourable clinical outcomes in a phase II trial using MRI selection criteria. Extended time window desmoteplase using MRI and CT selection was negative however, possibly relating to less severe clinical severity at entry masking potential clinical benefit of desmoteplase (47, 48) and is the subject of ongoing study.

Tenecteplase is a genetically modified version of TPA with higher fibrin specificity and greater resistance to inhibition in vivo (49) which has been evaluated in dose finding studies and has shown some promise although slow trial recruitment has hampered early studies(50). Low dose tenecteplase (0.1mg/kg) showed better rates of recanalisation and reperfusion than alteplase when selected using multimodal CT imaging, and compared to historical controls (51). In a randomised trial using advanced imaging for patient selection, Parsons et al showed that Tenecteplase had superior recanalisation reperfusion and clinical outcomes in patients with proximal arterial occlusions (52). The results relate to a specific patient cohort with proximal occlusions but suggest that alternative agents could have a superior effect to Alteplase in ischemic stroke but further study is required to identify other subgroups that may benefit.

Recanalisation is strongly associated with good clinical outcome and may be seen as a surrogate marker for clinical outcome(53) . IV rt-PA is not associated with high rates of recanalisation however, with proximal occlusions being the least likely to recanalize (54, 55). The association between recanalisation and outcome, and the low recanalisation rates seen with IV therapy alone has prompted investigation of intra-arterial therapies to improve recanalisation. Intra arterial lysis and mechanical clot retrieval are additional treatment options to achieve recanalisation.

Intra arterial thrombolysis has been evaluated in a number of trials with PROACT II demonstrating efficacy of IA pro-urokinase and heparin against heparin therapy

alone with better clinical outcome at day 90 despite an excess of haemorrhage (56). Only a small proportion of screened patients were eligible for recruitment, but IA lysis resulted in 66% recanalisation and 40% achieved a good clinical outcome (mRS 0-2), both of which were superior to heparin alone. PROACT II also demonstrated that IA therapy may be efficacious up to 6 hours from symptom onset. The MELT trial was terminated early but suggested improved clinical outcome in patients with MCA occlusion treated with IA urokinase compared to control subjects (57). 5 randomised trials of IA fibrinolysis have been undertaken in total with meta-analysis of these suggesting IA fibrinolysis results in improved clinical outcome and higher recanalisation rates compared to controls treated with IV fibrinolysis but also increased rates of both symptomatic and asymptomatic haemorrhage but no difference in mortality (58). Pro-Urokinase, the only agent found to have a positive individual trial result did not get approval for use by the American Food and Drug agency and in the meantime mechanical devices to remove cerebral clots have been developed and have achieved higher recanalisation rates meaning IA Fibrinolytic agents are now seldom used.

Mechanical clot removal or dispersal devices offer some theoretical advantages over chemical fibrinolysis such as improved recanalisation rate and fewer systemic side effects of therapy(59). The MERCI device is a corkscrew shaped device designed to remove blood clot and has been the most widely evaluated device demonstrating up to 69% recanalisation rate in observational non-randomised studies of patients who had failed IV therapy or who were deemed ineligible for IV therapy (60). Intracerebral haemorrhage rate of 9.8 %, good clinical outcome in only 36% and mortality of 34% with the new generation MERCI device are higher than for IV therapy but a direct comparison has not been done in clinical trials. This device has been approved by the FDA for achieving recanalisation but superiority to IV rt-PA has not been demonstrated for clinical outcome. The Penumbra Pivotal Stroke Trial was a single armed study in patients with intracranial occlusion evaluating the penumbra device, a mechanical suction device which can fragment and remove intra-arterial thrombus. Recanalisation rate was 81.6%, although symptomatic intracerebral haemorrhage was seen in 11.2% and only 25% had a good clinical outcome at day 90(61). More recent advances in intra-arterial therapy include the use of stent retriever

devices which combine the features of angioplasty devices and clot retrieval. The SOLITAIRE device has been studied in patients who did not respond to intra-arterial rt-PA or to attempted clot retrieval with the MERCI device and achieved a 90% recanalisation rate along with 10% symptomatic haemorrhage and 20% mortality in a single armed pilot study (62). Further multicentre study of the SOLITAIRE device has demonstrated a similar recanalisation rate of 85% with good clinical outcome in 55% of those treated (63) while a comparison with the MERCI device has shown higher recanalisation rates and better outcomes with the SOLITAIRE device (64). Additional options for stent retrieval such as the TREVO device are being developed which have been shown to have superior recanalisation rates to the MERCI retriever(65) (66).

While the recanalisation rates are higher with IA rt-PA and mechanical devices, their clinical efficacy compared to the standard IV therapy has not yet been demonstrated. The recently published IMS III trial demonstrated that clinical outcomes were unchanged between IA and IV therapies despite superior recanalisation in the IA group (67). In the smaller SYNTHESIS trial, superior recanalisation with IA therapy compared to IV was not associated with improved outcome (68). Reasons for the lack of impact on outcome despite improved recanalisation may be due to multiple factors. Timing of recanalisation is likely to be of critical importance, and delayed transfer to angiography is likely to result in infarct growth, even if subsequent recanalisation occurs. Patients selected for IA therapy have more severe clinical deficits than in trials for IV lysis which also influences outcome. Additional trial design limitations , such as lack of non-invasive angiography in IMS III prior to randomisation would be considered unusual in routine clinical practice and constitute a limitation to the interpretation of the study results, as well as low recruitment rates in centres with experience in delivering IA therapy for stroke, suggesting that those who underwent randomisation may not reflect the bulk of patients treated with IA therapy routinely in those centres(67).Therefore despite the higher recanalisation rates associated with IA stroke treatment, improved clinical outcomes have yet to be demonstrated when compared to IV thrombolytic therapy, meaning further evidence from additional trials is needed to prove the benefit of these promising new treatment options prior to their routine use in stroke (69, 70).

Imaging for all but one of the randomised trials for IV rt-PA was with non contrast CT prior to therapy (31), to exclude stroke mimics and rule out major established ischemic change prior to treatment. Options for imaging prior to therapy have expanded however, and are now being used as part of the selection criteria for some trials in order to reduce heterogeneity of the patient cohort and also to enable outcome measures other than clinical outcome to show proof of efficacy (47, 52). Imaging measures including infarct volume, reperfusion, recanalisation and infarct growth and may be determined using CT or MR imaging and can be used as markers of response to treatment. Additional imaging techniques are likely to be of importance for trial purposes for proof on concept studies and also potentially for enhancing clinical decision making in acute stroke.

## **1.3 CT Imaging for Acute Stroke**

### **1.3.1 Non Contrast CT**

The most widely available and used imaging modality for stroke patients remains non contrast brain CT, used to confirm diagnosis and exclude other mimics such as intracerebral haemorrhage, subdural haematoma and tumour. CT imaging detects different amounts of water content in cerebral tissue measured in HU. Early ischemic changes seen on CT include focal tissue swelling and parenchymal hypoattenuation, grouped together in practice as signs of ischemia, but which may reflect different stages of ischemia and tissue viability (71).

Hypodensity on CT correlates with PET defined infarct core and reduced cerebral blood volume on PWI MRI supporting hypodensity as a marker for irreversibly damaged infarct core (72, 73). Hypodense areas on CT early after symptom onset continue to appear hypodense on follow up CT scanning, emphasising the specificity of hypodensity for infarct core(74). While CT-based hypodensity is highly specific for infarct core, CT has reduced sensitivity for detecting early ischemia. The time taken for hypodensity to appear following symptom onset is longer than for corresponding DWI abnormalities and the degree of hypodensity seen on CT correlates with increasing time from symptom onset (75, 76). Diffusion restriction occurs early after ischemia but does not increase with time beyond 1.5 hours to the same extent as CT hypodensity, which appears later but



continues to evolve with time even after diffusion restriction changes have ceased, which may reflect differences in early cytotoxic oedema, seen with DWI and subsequent vasogenic oedema due to net water uptake demonstrated with CT(75, 77)

Focal swelling (e.g. loss of normal cortical sulcal pattern without hypodensity) is considered to reflect early ischemic changes which are not irreversible and may have increased blood volume suggesting autoregulation consistent with penumbra(71). Detection of focal swelling and hypodensity may not be possible due to limited sensitivity for CT to demonstrate the changes, although hypodensity and focal swelling have high specificity for infarct core and penumbra respectively when seen. Interobserver agreement for presence of ischemic changes can also be low(71).

Extent of ischemic change on CT is associated with increased risk of haemorrhage following thrombolysis and patients with established ischemic change involving more than 1/3 of the MCA territory have been excluded from randomized controlled trials of thrombolysis (44, 78). Detection of ischemic changes varies between readers with improved detection by neuroradiologists compared to non expert raters(74). Systematic evaluation of plain CT in order to improve scan interpretation is possible using scoring methods such as ASPECTS which encompasses both swelling and hypodensity into a composite score for ischemia in the MCA territory examined in ten anatomical regions (79). Interobserver agreement using ASPECTS was shown to be superior to agreement scores on one-third MCA territory ischemia ( $\kappa=0.67-0.82$  and  $0.27-0.76$  respectively). Patients with ASPECTS score  $\leq 7$ , indicative of more severe ischemia were more likely to be functionally dependent at outcome and to suffer symptomatic intracerebral haemorrhage after thrombolysis demonstrating the prognostic significance of ischemic signs on CT in the acute stroke phase (79).

Presence of hyperdense vessels due to clot may help confirm the diagnosis in the absence of hypodensity or swelling, although the sensitivity for this sign is low (30%)(80). Specificity is generally high, although false positive hyperdense vessels can occur. Comparison to the normal hemisphere and measurement of HU intensity can be used to confirm if the vessel is truly hyperdense(81).

Hyperdense vessels have been associated with poor outcomes after stroke, but their presence only suggests an occlusion without independent predictive value as patients with dense vessels had greater clinical stroke severity than control patients at baseline (82, 83). Disappearance of the sign at follow up CT is considered a marker for recanalisation with improved clinical outcome, but the lack of sensitivity of the sign to begin with limits the use of this finding to determine response to therapy (84). Low sensitivity and high specificity for hyperdense vessels is also seen with more distal MCA clot in the Sylvian fissure, known as the Sylvian dot sign, and proximal clot termed the hyperintense carotid artery sign (85, 86). The presence of thrombus on non contrast CT may be visualised more readily using thin slice acquisitions where clot contrasts surrounding structures more clearly due to reduced volume averaging effects than thicker slice CT(87). Thin multi-slice CT may improve sensitivity for thrombus detection and has also shown that in patients with MCA or ICA occlusion, actual clot burden is increased in patients with hyperdense vessels compared to proximal occlusions not associated with a hyperdense vessel(88). Clot burden assessed with thin slice CT may be important in assessing likelihood of response to thrombolysis and could help select patients for intra-arterial therapy(87). In addition to clot burden, clot composition may affect the likelihood of a hyperdense vessel sign being visualised, with low amounts of fibrin content contributing to a reduced clot density appearance(82). High haematocrit which may be associated hyperdense vessels in the absence of thrombus, but the appearances should be bilateral if due to elevated haematocrit alone(89).

CT is the most widely used imaging modality for stroke with high sensitivity for mimics such as intracerebral haemorrhage, high specificity for ischemia when hyperdense vessels or areas of hypoattenuation are seen but low sensitivity for detecting ischemic change is a limiting factor.

### ***1.3.2 CT Angiography***

The limitations of plain CT in terms of sensitivity for detecting ischemia are of obvious importance when assessing acute stroke but improved diagnostic accuracy and information on vascular status is possible with CTA (90). CTA is widely available, non invasive and can be performed without moving the patient

after the initial non contrast CT acquisition making it a feasible adjunct in acute stroke imaging (91). Retrospective analysis of outcomes for patients exposed to IV contrast and those having non-contrast studies alone prior to thrombolysis has demonstrated that contrast administration is not associated with increased risk of haemorrhage following rt-PA administration(92).

CTA is obtained with a volumetric helical acquisition with timed imaging after delivery of a bolus of contrast material, at either a fixed time interval or with scanning triggered automatically by contrast concentration reaching a pre-specified threshold within a ROI placed in the ascending aorta (89). Analysis of CTA may involve interpretation of CTA source images or reconstructions of raw data using multiplanar reformatted images and maximal intensity projections depending on the information required. Coverage by CTA varies between protocols, but may include intracranial imaging alone or an acquisition from the aortic arch superiorly to include neck and intracranial vessels.

Vascular imaging is important in defining stroke subtype and for choosing secondary prevention therapy(9) so the coverage and spatial resolution offered by CTA is of importance. CTA from aortic arch distally permits visualisation of carotid vessels and millimetre exact measurement of carotid artery calibre and stenosis, as well as imaging plaque and vessel wall soft tissues(93). As a carotid imaging modality, it is less widely available than Doppler but the results are reliable, have high specificity and can be crosschecked by different observers in cases of doubt using the same initial acquisition (94). The added benefits of CTA for measuring carotid stenosis is of particular importance in lesser grades of carotid stenosis (50-69%) where it is almost twice as sensitive as Doppler with similar specificity (95). As patients with these degrees of stenosis may still benefit from early carotid endarterectomy this is a potentially important finding when considering options for imaging carotid stenosis on stroke and TIA patients(96). Aortic arch plaques are a risk factor for stroke and for recurrent strokes after initial cryptogenic stroke, which may be visualised with CTA but not with carotid Doppler alone which is restricted in terms of coverage (97). An additional risk factor for stroke which is increasingly recognised is arterial dissection. While some controversy still exists about which imaging modality is best for detecting dissection within carotid or vertebral arteries, CTA may be used to make the diagnosis of dissection, is probably of equal preference to MRA

for detecting carotid dissection and may be superior to MRA for vertebral dissection(98).

CTA findings can also be useful in acute stroke assessment as an adjunct to non-contrast CT. CTA source images (CTA-SI) reveal parenchymal hypoattenuation more readily than CT or even post contrast CT (99). When compared to non-contrast CT, CTA-SI are more sensitive for detection of vascular territory and stroke subtype classification(90). Lesions visible on CTA-SI are strongly correlated with acute DWI and final infarct volume suggesting its use as a marker for infarct core which can produce similar findings to acute DWI (99, 100). The additional predictive value of CTA-SI was confirmed when using the ASPECTS template for image analysis in hyperacute stroke, where patients with normal or near normal ASPECTS on CT were shown to have hypoattenuation on CTA-SI which correlated with the final extent of hypoattenuation on follow-up imaging (101). CTA-SI is also of benefit in posterior circulation stroke where sensitivity of non-contrast CT is a limiting factor. CTA-SI showed increased sensitivity for ischemic change compared to plain CT in patients with acute basilar thrombosis, with lesion extent on CTA-SI correlating with functional outcome at 3 months (102). CTA -SI also correlates more precisely with baseline clinical stroke severity and final neurological outcome than non-contrast CT (54). As CTA-SI lesions correlate with final lesion extent, they are considered a marker for irreversibly damaged tissue, but the extent of agreement with other markers for viability and irreversible damage is debatable. Correlation with DWI and CBV lesions suggest loss of autoregulation and irreversible tissue damage, although this may be related to the timing of contrast administration and scan protocol which may mean that CTA-SI reflect reduced cerebral blood flow rather than reduced cerebral blood volume depending on the acquisition parameters(103). More recent analysis of perfusion measurements for infarct core suggest that reduced CBF may be more accurate than reduced CBV for measuring infarct core(104). Together these findings suggest that hypoattenuation on CTA-SI is likely to represent a marker for irreversibly damaged tissue in ischemic stroke.

As well as demonstrating changes in parenchymal attenuation, CTA may be reconstructed to show vascular anatomy in detail, demonstrating excellent sensitivity and specificity in the assessment of large vessel occlusion and patency (105). When compared to catheter angiography, CTA has a sensitivity and

specificity of 98.4% and 98.1% respectively, with an overall accuracy of 99% (106). Clot location is of prognostic importance and correlates with other clinical markers of stroke severity as proximal occlusions on CTA are associated with higher initial NIHSS scores, while distal/absent occlusions predict early independence after stroke(107). Clot status on CTA can also be used to guide acute treatment decisions beyond usual guidelines for IV thrombolysis. For example, in basilar artery thrombosis both the site of occlusion and the clot burden extent can be assessed using CTA prior to deciding on additional interventions such as mechanical clot retrieval/ IA thrombolysis, although the evidence base for the additional interventions is not yet clear(108, 109). Demonstrating the presence or absence of occluded vessels on reconstructed CTA could be used to select patients more accurately for different reperfusion therapies depending on vascular status (91). The response to therapy in terms of recanalisation is an important marker for clinical outcome, meaning CTA both acutely and sub-acutely has the potential to be used for surrogate measures of outcome in clinical trials(53).

3-D reconstructions of CTA data into MPR and MIPS can demonstrate the site of vascular occlusion and extent of vessel filling via collaterals (110). The impact of collateral flow may be an independent predictor of outcome after stroke although the method which best defines collateral adequacy is not clear(111) (Miteff). Occlusions detected by MIP CTA are highly sensitive and specific, with strong correlation between CTA and DSA (91). A comparison between CT, CTA MIP reconstructions and CTA-SI is shown in figure 1.4

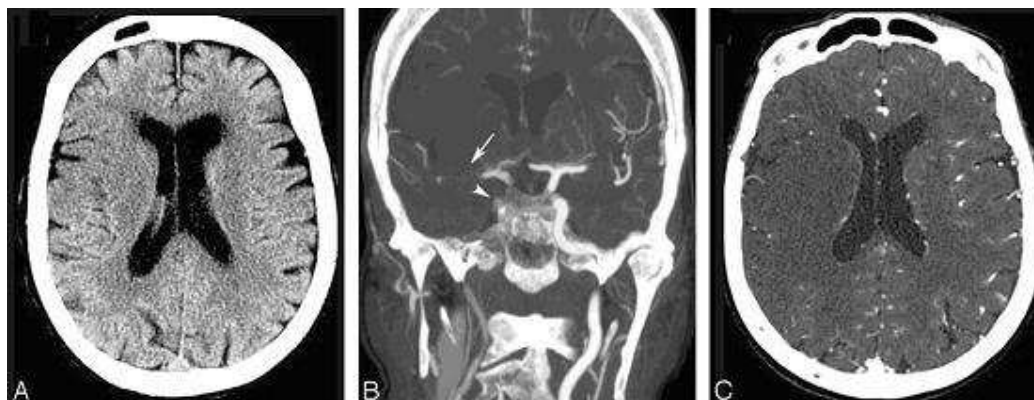


**Figure 1-4 NCCT, CTA MIP and CTA-SI in patient with right MCA occlusion**

Comparison of NCCT (A), 3D CTA reconstruction (B), and CTA-SI (C) in a patient with proximal right MCA occlusion. NCCT shows no obvious ischemic change. There is a filling defect evident in 3D reconstruction (B, arrow shown) while parenchymal hypoattenuation in MCA territory is evident on CTA-SI. This diagram highlights the increased sensitivity of CTA in detecting ischemic lesions, and that 3D or source images from CTA permit visualisation of ischemic change beyond that of NCCT alone. Reproduced from Tan et al "CT angiography clot burden score and collateral score: correlation with clinical and radiologic outcomes in acute middle cerebral artery infarct" AJNR 2009

### **1.3.3 CT Perfusion**

CT Perfusion is a functional imaging technique which derives quantitative brain perfusion parameter measurements by repeated imaging over a portion of the brain during the passage of a bolus of intravenously administered contrast material (112). Multidetector scanners capable of imaging more than one slice of brain per second detect changes in Hounsfield unit values per pixel over time, which are used to derive a number of different perfusion measures including MTT, CBF, CBV and TTP (113). These perfusion measurements provide information on various aspects of tissue integrity and ischemia which may be used to detect features such as infarct core and penumbra. The extent of brain coverage possible with CT perfusion is dependent on the number of detectors and with more modern scanning technology, increasing coverage for perfusion imaging is possible (114). If only limited brain coverage is available, some centres choose to perform 2 CTP scans at different locations to increase brain coverage obtained with CTP, although this is at the expense of increased radiation and contrast exposure meaning the additional imaging should be clinically indicated to be justified (113). The additional radiation exposure for a

multimodal CT examination is approximately 10 mSv, although this is variable as the contribution of CTP may vary between 1.1 and 5 mSv with the total exposure measuring approximately 3 times the annual background rate (115). Vigilance in CTP protocol design is of importance as excessive radiation doses have been administered with potentially serious results(116).

### Perfusion map derivation

Imaging in the Cine-mode over a pre-specified slab of brain tissue is used to quantify perfusion measurements in each pixel. Protocols vary between sites but image acquisition time usually occurs over 45-90 seconds. Post processing of raw CTP data is then undertaken to generate a number of perfusion maps:

1: CBV is defined as the total volume of blood flowing in a given volume of brain, with measurements in ml/100g of tissue

2: CBF is defined as the volume of blood moving through a given volume of brain per unit time and is measured in millilitres of blood per 100 gram of cerebral tissue per minute

3: MTT is defined as the average transit time of blood through a given region of brain, measured in seconds.

4: TTP is defined as the time it takes from the arrival of contrast in a selected arterial pixel to the peak height of the tissue concentration-time curve.

Derivation of each perfusion measure may be according to different mathematical techniques which vary between vendors in how calculations are obtained. The clinical relevance of variations between software packages is unclear, although it appears that some software packages produce maps which overestimate the extent of ischemic tissue due to utilisation of processing packages which are sensitive to the effect of delayed bolus arrival, e.g. in the setting of extracranial stenosis (117).

Different mathematical models to obtain perfusion measurements have been used for CTP.

### Maximal slope model

As contrast material enters the area being imaged, the signal intensity of the time-concentration curve, measured in HU rises linearly( Figure 1.5) (118). The amount of accumulated contrast material  $Q(t)$  is the product of CBF and the difference on arteriovenous concentration:

$$Q(t) = \text{CBF} \cdot \int_0^T [C_{\text{artery}}(t) - C_{\text{vein}}(t)] dt$$

In order to make the CBF calculation less complicated, it is assumed that the output from the capillary bed into the venous system is zero, termed the no venous outflow assumption (119). To satisfy this assumption, injection rates must be very rapid.

Using these assumptions, the equation can be simplified as

$$Q(t) = \text{CBF} \cdot \int_0^T C_{\text{artery}}(t) dt$$

This equation is known as the Mullani- Gould formulation (120).

The rate of contrast accumulation is related to the CBF and the arterial concentration at time (t) and from the Mullani Gould equation the peak rate of contrast accumulation will occur when arterial concentration is maximum:

$$\left[ \frac{dQ(t)}{dt} \right]_{\text{max}} = \text{CBF} \cdot [C_{\text{artery}}(t)]_{\text{max}}$$

The ratio of the maximal slope of  $Q(t)$  to the maximal arterial concentration can therefore be used to measure CBF:



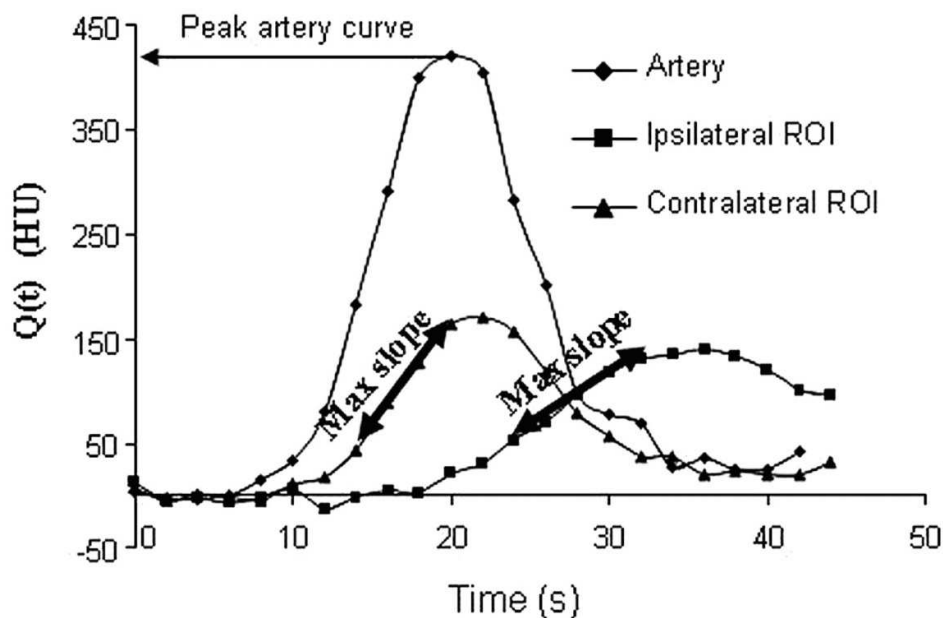


**Figure 1-5 The Maximal Slopes Method**

CBF can be calculated from the ratio of maximal slope of  $Q(t)$  to the maximal arterial concentration. Different maximal slopes in different ROIs reflect different CBF values. Reproduced from "Konstas A.A. et al, Theoretic basis and technical implementations of CT perfusion in acute ischemic stroke, part 2: technical implementations. AJNR 2009. 30; 5: 885-92"

Thus CBF can be determined. However, this equation relies upon assumptions that may influence calculation of CBF. Specifically it is assumed there is no venous flow of contrast flow before the peak arterial enhancement which in turn requires that injection rates of 10-20ml/sec are used to reduce the possibility of venous contamination(119). In clinical practice these rates are not achievable and therefore CBF calculations may be inaccurate(121). As rates of injection for IV contrast material are typically no more than 5ml/sec alternative methods to interpret the time - concentration curves must be considered.

### Deconvolution

Use of deconvolution to derive perfusion measures does not rely on the assumption of no venous outflow, but instead considers outflow in the calculation. The tissue concentration at any time or tissue residue function can be related to CBF ( $F$ ) and contrast media concentration [ $C_a(t)$ ]. If a unit mass of contrast material is deposited into the tissue instantaneously then the tissue residue function becomes the impulse residue function  $R(t)$ . Assuming the contrast remains within the vascular space, the shape of the impulse residue function will be as follows(Figure 1.6)(122):

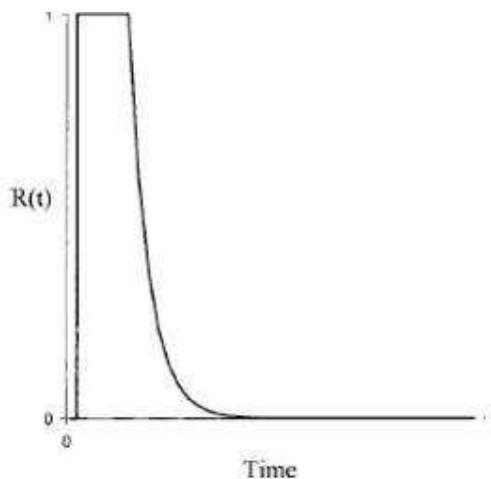


**Figure 1-6 The Impulse Residue Function**

Schematic representing the impulse residue function in a vascular network where the tracer remains intravascular. Reproduced from Eastwood et al "CT perfusion scanning with deconvolution analysis: pilot study in patients with acute middle cerebral artery stroke" Radiology 2002; 222:227-236

The rate of contrast delivery to capillary vessels following IV contrast administration is calculated as:

$$F \cdot C_a(t)$$

Assuming  $F$  is constant and that the mass of contrast in the capillary network is linearly related to the arterial input function (AIF), the following can be calculated:

$$Q(t) = F \cdot C_a(t) * R(t)$$

Where  $*$  is a convolution operator.  $Q(t)$  and  $C_a(t)$  can each be measured and deconvolution produces  $F \cdot R(t)$  which is plotted over time. CBF is obtained from the peak height of the curve, while CBV is the area under the curve. Once CBF and CBV are derived, MTT can be calculated according to the Central Volume Principle (123):

$$CBF = \frac{CBV}{MTT}$$

Thus deconvolution permits calculation of perfusion parameters with lower injection rates but which are in practice easier to achieve.

An additional element in quantifying perfusion measurements with CTP is correction for delayed arrival of contrast bolus. Factors such as extracranial stenosis, congestive cardiac failure or atrial fibrillation may result in delayed bolus arrival, which in turn underestimate values for CBF as deconvolution analysis is sensitive to the effects of delayed transit between the reference AIF and the pixels examined in the tissue concentration-time curves(124). The Anterior cerebral artery is the most widely used AIF for CT perfusion but the assumption that this represents an instantaneous input of contrast material to the brain parenchyma is not met particularly when bolus arrival is truncated (125). Choosing an alternative AIF could theoretically overcome this problem but standardisation of site for AIF placement would be problematic in addition to the likely influence of partial volume effects from selection of AIF from vessels with small calibre. Additional methods to correct for delayed bolus arrival require a delay insensitive deconvolution method such as block circulant Singular Value Decomposition (126). The mathematical modelling behind this is not discussed in this thesis, however the importance is of potential clinical significance as perfusion scans processed without delay correction have been shown to overestimate final infarct volume more frequently and to a greater extent than those with a delay-corrected algorithm (127).

#### CTP Application in clinical practice

The perfusion maps obtained with CTP provide information on various aspects of tissue integrity in stroke patients. Sensitivity for detecting ischemic lesions is generally high for CTP, with TTP maps revealing a sensitivity of 93% for the presence of ischemic stroke, with the “false negative” cases occurring in brainstem and lacunar stroke subtypes rather than territorial hemispheric strokes in patients with acute stroke imaged within 6 hours of symptom onset (128). Patients who have undergone spontaneous recanalisation / reperfusion by the time imaging is acquired may also have “false negative” scans. Perfusion lesion extent has been shown to correlate with baseline clinical stroke severity, while final infarct volume in those who did not recanalize matched baseline lesion extent and was equal or smaller in those who did recanalize, suggesting that CTP can detect the presence of viable tissue but which is at risk of undergoing subsequent infarction (129). When qualitative interpretation of all CTP maps was performed and compared to final infarct volume using the

ASPECTS system, CBV maps were close predictors of outcome lesion extent in patients with major reperfusion by 24 hrs, while MTT and CBF were predictive of infarct extent in those who did not have major reperfusion (130). This finding that different perfusion measures predicted infarct volume depending on the individuals' response to treatment suggests that both infarct core and ischemic penumbra can potentially be detected according to different measurements using CTP. Reduced CBV has therefore been considered a marker for infarct core with prolonged MTT (but with normal CBV) being a marker for ischemic tissue at risk of infarction(113). Attempts to apply thresholds to CTP maps in order to quantify core and penumbra have revealed different results and validated thresholds for each have not yet been defined. When CTP was compared to acute DWI (taken as a measure for infarct core), ROC analysis revealed that absolute  $CBV < 2.0 \text{ ml}/100\text{g}$  was the best measurement of core, while MTT of  $\geq 145\%$  of normal value was the best predictor of infarct volume in those patients with baseline occlusions which did not recanalize on follow up(131). The difference in these two volumes has become a widely used measurement of penumbra in clinical practice being incorporated onto post processing platforms for use in clinical decision making. These volumes for core and penumbra were shown to provide similar results to acute MRI/PWI in terms of mismatch ratio and influence on clinical decision making to the extent that they have been used as part of the imaging criteria for core and penumbra for subsequent clinical trials of novel thrombolytic agents (47, 132). However, threshold derivation from other groups suggested a product of CBV and CBF was the best predictor of core pixels for white matter(133) while ROC analysis using more stringent criteria for defining ischemic tissue which is actually "at risk" has suggested relative CBF rather than absolute CBV provides the closest measurement of infarct core(134). Therefore it remains unclear whether thresholds applied to CTP can be used reliably to measure core and penumbra. Systematic review of the literature surrounding thresholds and the acquisition parameters has highlighted this lack of consensus on agreed definitions(135).

Different post-processing packages for CTP may yield different results on the same raw data which limits the generalisability of suggested core and penumbra thresholds (117). It may be that delayed bolus arrival needs to be corrected for to prevent apparent " Pseudo-reversibility" of some lesions with reduced CBV,

although it has been suggested that there may be important information within the delayed contrast bolus (such as in atrial fibrillation or high grade carotid stenosis), and therefore the need to correct for this could be questioned (136).

Definitions for core and penumbra using CTP require further investigation which will form part of this thesis. Despite some limitations, at present multimodal CT examination for acute stroke patients is the routine in many centres used as part of clinical decision making. It is widely accessible, faster than MRI and has fewer contraindications than MRI, meaning that additional diagnostic and prognostic information can be obtained relatively quickly with CT. Although guidelines require a non contrast CT alone, a multimodal CT examination permits evaluation of the “4 P”s of stroke imaging- parenchyma, pipes, perfusion and penumbra(137) which could ultimately result in tailoring therapy based on the individuals response to ischemia rather than on a rigid and limited time window. Further prognostic information on the risk of developing intracerebral haemorrhage after thrombolysis may be possible using CTP with alternative post-processing to measure blood brain barrier permeability. At present, evidence based decision making prior to thrombolysis is based on a clinical diagnosis of stroke, a known time of onset, and absence of clinical or imaging contraindications to treatment. Extensive ischemic change on CT brain affecting >1/3 of the MCA territory is usually applied as a “rule of thumb” but is imprecise and using imaging to predict haemorrhage more precisely would be attractive(45). In a retrospective review, Aviv and colleagues found that patients who had haemorrhagic transformation following thrombolysis had greater extents of permeability, measured as surface area product (PS) than those who did not have ICH(138) . This finding requires further evaluation but may be limited in practice as the duration of image acquisition to satisfy the theoretical assumptions in measuring permeability is much longer than is obtained in most CTP protocols (139, 140).

The use of CT perfusion in addition to CTA and CT requires prospective evaluation within randomised clinical trials, but further research is needed initially to assess which perfusion thresholds and imaging patterns represent meaningful therapeutic targets.

## **1.4 Magnetic resonance Imaging in Stroke**

A number of MRI sequences are available for stroke imaging for clinical and research purposes. The most widely used methods for determining infarct core, ischemic penumbra and vascular status will be discussed.

### **1.4.1 DWI**

The normal diffusion of molecule or liquid in a gas is random, but diffusion restriction of water molecules is decreased in ischemic brain tissue and these appearances are evident soon after the onset of ischemia representing cytotoxic oedema (141, 142). The presence of DWI lesions has been widely used as a surrogate marker for irreversibly damaged infarct core and subsequently forms part of the perfusion-diffusion mismatch concept for identifying tissue at risk of infarction (143). Although frequently used as a marker for infarct core, the DWI lesion may actually be at least partly reversible(144). PET characteristics for penumbra have been found in DWI “core” lesions supporting the finding that elements of the DWI lesion may be reversible(145). The true extent and significance of DWI reversibility is debated however as the evidence is limited and definitions for reversibility are variable, but a systematic review suggested that approximately 20% of a typical DWI volume may be spontaneously reversible(146). More dedicated image analysis including correction for CSF space and atrophy suggests the reversibility is not clinically meaningful, although this analysis is limited to the 3-6 hr time window alone which may limit the applicability of this finding(147). While some reversibility may occur, DWI remains highly sensitive for detecting ischemic lesions with sensitivities ranging between 83 and 100%, outperforming other MRI sequences and plain CT in the same time window along with high specificity of up to 100% in appropriate clinical context (148-151). Additional prognostic value is obtained from DWI lesion volumes with larger volumes on DWI associated with poor outcome regardless of treatment administered, response to treatment, or extent of mismatch tissue (152, 153).

### **1.4.2 FLAIR**

FLAIR imaging reveals Ischemic lesions as visually hyperintense areas and demonstrates parenchyma well due to heavy T2 weighting and reduction of

signal from CSF. The anatomical detail afforded by FLAIR has resulted in its use as the sequence for measuring final infarct volume in several imaging based stroke trials (153, 154). The timing of FLAIR to optimally measure infarct volume has most often been at day 90 after stroke, although evolution of infarct beyond earlier time points at 30 days or even as soon as 3-7 days after stroke onset may not be significant, supporting the use of an earlier time point to measure infarct volume for trial purposes(155, 156) (157). The time taken for an ischemic lesion to appear on FLAIR is longer than that taken for the same lesion to appear on DWI, but most FLAIR hyperintensities appear within 6 hrs of symptom onset. The use of this “mismatch” between timing FLAIR and DWI lesion appearances has been suggested as a surrogate marker for strokes of recent onset (within 6 hrs) and therefore may be used for trial purposes targeting therapy at patients with wake-up strokes who are usually excluded from thrombolysis(158). In addition to revealing parenchymal change, FLAIR imaging has been used to visualise leptomeningeal collateral flow, with vessel related hyperintensities on FLAIR being associated with smaller DWI volumes and larger mismatch volumes in patients with MCA occlusion suggesting better collateralisation (159). Presence hyperdense vessels on FLAIR are also associated with smaller final infarct volume suggesting preservation of blood flow via collateral routes (160).

### ***1.4.3 Gradient Echo Imaging***

GRE is used in stroke imaging protocols primarily to detect cerebral haemorrhage due to the sensitivity of the sequence to detect the presence of paramagnetic blood substances. GRE has a higher sensitivity for haemorrhage than other MRI sequences. Haem breakdown products including deoxyhemoglobin, methemoglobin and hemosiderin are paramagnetic and detectable on GRE. The sensitivity for detecting haemorrhage with GRE is equal to CT when comparing both modalities on patients with acute ICH within 6 hours of symptom onset (161). Importantly, GRE can also detect small cerebral microbleeds which cannot be detected with CT, and which may confer an increased risk of haemorrhage after ischemic stroke (162). Presence of microbleeds on GRE has not been shown to be associated with haemorrhagic transformation after thrombolysis for ischemic stroke in a large multicentre study, but the number of patients with large numbers of microbleeds were small in this study which limits any conclusions which can be drawn about using GRE to

identify patients who should not receive rt-PA due to risk of haemorrhagic transformation (163).

#### ***1.4.4 Magnetic Resonance Angiography***

MRA can be acquired using time of flight imaging (TOF), Phase contrast or contrast enhanced MRI after the administration of gadolinium. MRA, like CTA can be used for intracranial vascular assessment as well as for extracranial imaging to determine aetiology and subsequent management (e.g. dissection, carotid stenosis)(164). When compared to the gold standard of catheter angiography, TOF-MRA agreed on the presence of a surgical lesion in 80% of cases, although it tended to overestimate the degree of stenosis (165). It is sensitive and specific for detecting intracranial occlusions in acute stroke patients and compares favourably to catheter angiography (84.2% and 84.6% for sensitivity and specificity respectively) although the median time interval between imaging sequences was long(166). Definitions for occlusion on MRA such as the TIMI scale adapted for intracerebral occlusions have been used for trial purposes to classify site and severity of arterial obstruction on admission as well as a marker of response to therapy by recanalisation (154, 167).

#### ***1.4.5 Perfusion Weighted Imaging***

PWI combined with DWI has been the most widely studied method for identifying infarct core or tissue at risk (168). PWI images are obtained by bolus tracking, tracing the passage of a paramagnetic contrast agent through the brain over a period of time (169). An advantage of PWI over CTP is complete brain coverage meaning all potentially ischemic tissue can be assessed by PWI which is not possible for most CTP protocols at present. Lesions on DWI and PWI provide information on likely viability of cerebral tissue and penumbra has been defined operationally as a difference between the extent of abnormalities on each sequence(143). The fate of hypoperfused tissue has been examined using PWI, with DWI lesions expanding into the PWI lesion over time in those patients who had evidence of mismatch on admission, and this expansion can be attenuated with IV fibrinolysis (170). Perfusion maps generated using PWI include CBV, MTT, CBF and Tmax( Time to maximum of the residue function)(171). Thresholds for defining tissue at risk are not yet agreed using PWI/ DWI mismatch.



Multimodal MRI for imaging acute stroke is used routinely in some institutions for obvious reasons such as high sensitivity and specificity for detecting ischemic lesions and prognostic information afforded by measuring lesion volumes. Its use may however be limited by contraindications which prevent some patients undergoing MRI such as implantable defibrillator devices and claustrophobia emphasising the importance to develop alternative imaging methods (172). Multimodal CT may be able to provide similar information to MRI with the advantage of increased availability and fewer contraindications.

## **1.5 Conclusion**

Therapies for acute stroke are evolving and studies evaluating new treatments increasingly use image based markers for outcome. MRI offers excellent sensitivity and diagnostic accuracy, but has restricted availability, some contraindications and takes longer to obtain imaging than CT (20- 30 Mins for MRI compared with 10-15 for CT). CT is widely available and rapidly obtained with few contraindications, but gives less diagnostic accuracy than MRI, involves ionising radiation and at present usually has restricted brain coverage for CT perfusion scanning. While MRI has perhaps been more extensively evaluated, the availability and speed of imaging with CT suggests that additional evaluation of the ability of multimodal CT to enhance understanding of acute ischemic stroke is needed, and this will form the basis of the subsequent work in this thesis.

## Chapter 2. Collateral Circulation

### 2.1 Introduction

Collateral flow in the cerebral circulation refers to the collection of different vascular channels which can contribute to cerebral blood flow when principal pathways of antegrade flow fail(15). Collateral vessels provide an alternative route for cerebral blood flow to compensate for reduced flow via the usual vascular channels when the primary source of blood flow has been diminished.

Different sources and descriptions of collateral flow exist depending on the vessel size and location which provide a route for collateral flow to occur. Primary collateral pathways refer to the different segments of the circle of Willis, namely the anterior and posterior communicating arteries which allow for diversion of flow towards areas with reduced perfusion, occurring from anterior to posterior circulation or vice-versa depending on the site of arterial obstruction. Secondary collateral flow is considered to occur via ophthalmic and leptomenigeal vessels which are probably invoked once primary collateral flow has been exhausted or cannot contribute to supply of ischemic tissue(15). In chronic arterial occlusion proximal to the circle of Willis (e.g. chronic carotid occlusion), primary collateral flow may prevent stroke from occurring when flow to the ischemic territory is derived from the contralateral carotid territory via the anterior communicating artery. Intracranial occlusion distal to the circle of Willis cannot be compensated for by flow in primary collaterals due to anatomical reasons in which cases secondary flow in the leptomenigeal collateral circulation may be invoked to augment cerebral blood flow to that territory.

### 2.2 The Cerebral Blood Supply

The brain requires approximately 20% of the oxygen required by the body and derives this from the internal carotid arteries anteriorly and the vertebral arteries posteriorly.

The internal carotid arteries arise from the common carotid arteries in the neck bilaterally and terminate at the bifurcation to the MCA and ACA. The

extracranial (Cervical) portion of the ICA extends from the carotid bifurcation to the skull base and does not have any branches in the neck (173). The origin of the ICA is a site where atheroma may develop preferentially and from which emboli may originate causing distal occlusions in “large vessel” stroke cases(9). Intracranial segments of the ICA include Petrous, Cavernous and Supraclinoid portions, which may be further sub-divided according to the sites of embryonic precursor vessels(174) . The Petrous ICA portion extends from the skull base to the cavernous sinus giving tympanic branches along its route(175). The cavernous portion travels within the cavernous sinus giving hypophyseal and ophthalmic branches and ends as the artery pierces the dura at the roof of the carotid sinus (173).The supraclinoid portion begins as the artery passes the anterior clinoid process to enter the subarachnoid space and terminates at the carotid T(176).

The Middle cerebral artery arises as the larger of the two terminal branches of the ICA, approximately 75% of the calibre of the ICA. Its trunk is divided into 4 segments: The M1 (Sphenoidal segment) extends laterally within the Sylvian Fissure and gives rise to a series of Lenticulostriate branches along its path which supply deep structures including the Internal Capsule, Globus Pallidus, Putamen and Caudate nuclei. The MCA divides as a bifurcation (78%), trifurcation (12%) or into multiple smaller branches (10%). The M2 (Insular) segment begins at the MCA genu and is the segment where most branching occurs. The M3 (opercular) segments begin at the circular sulcus of the insula and course over the fronto-parietal and temporal opercula. The M4 (cortical) branches begin at the surface of the Sylvian fissure and extend over the cortical surface of the hemisphere(177). The anatomy of the MCA is demonstrated in figure 2.1

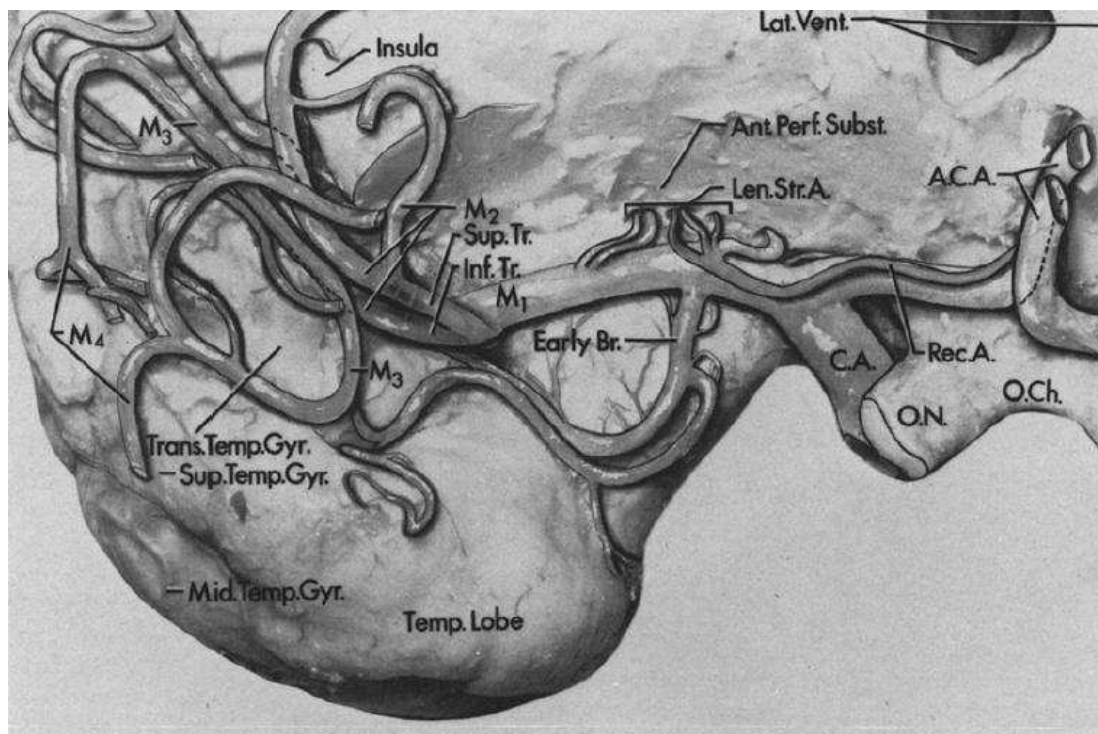


### Figure 2-1 Anatomy of the Middle Cerebral Artery

Anterosuperior view of the right middle cerebral artery and branches with frontal lobe removed showing relationship of the M1, M2, M3 and M4 segments to the temporal lobe (temp lobe). The M1 segment crosses the upper surface of the anterior pole of the temporal lobe and divides into a superior (Sup.Tr.) and inferior (Inf.Tr.) trunk. The M2 Segment lies on the insula, the M3 segment crosses the transverse temporal gyri (Trans.Temp.Gyr.) and the M4 segment passes inferiorly across the superior (Sup.Temp.Gyr.) and middle temporal gyri (Mid.Temp.Gyr.). The anterior cerebral artery (A.C.A.) arises from the carotid artery (C.A.) and passes above the optic nerve (O.N.) and chiasm (O.Ch.) where it gives rise to the recurrent artery (Rec.A.). The Lenticulostriate arteries (Len.Str.A.) enter the anterior perforated substance (Ant.Perf.Subst.). An early branch (Early Br.) to the temporal lobe arises from the M1 segment. The frontal horns of the lateral ventricles (Lat.Vent.) lie above the anterior cerebral arteries. Reproduced from Gibo et al, "Microsurgical anatomy of the Middle Cerebral Artery" *Journal of Neurosurgery*, 1981, 54;2: 151-169.

The ACA originates at the ICA bifurcation and travels antero-medially to cross over the optic nerve and chiasm to communicate with the contralateral ACA via the Anterior Communicating artery. Up until this point the segment is known as the A1 segment which has inferior and superior perforator branches supplying the optic nerve, anterior commissure and hypothalamus. The distal A2 vessel segment extends from the ACOM to the bifurcation and gives rise to the recurrent artery of Heubner, orbito-frontal and frontopolar branches. The distal A3 peri-callosal artery is the terminal segment of the ACA (178).

The right and left vertebral arteries originate from the subclavian arteries bilaterally and travel superiorly in the foramen transversarium to the upper cervical region. The V1 segment extends from the subclavian artery to the C6 transverse process, and is prone to atherosclerotic change at the origin (179). The V2 segment extends until the vertebral artery exits the axis which then continues as the V3 segment until it pierces the dura. The V4 segment is intracranial and extends from the dura until the confluence at the basilar origin (180). The PICA is the most distal branch of the VA 12-13mm proximal to the vertebro-basilar junction supplying the cerebellum and medulla (180). The Basilar artery begins at the junction of the two V4 segments and courses superiorly along the Pons until its bifurcation to the two PCAs. Paramedian and circumferential branches supply the Pons and Cerebellar peduncles. The Anterior inferior Cerebellar artery leaves the basilar at variable points along its course and the superior Cerebellar artery is a distal branch originating close to the PCA origin bilaterally (180).

The bifurcation of the basilar artery gives rise to the PCA bilaterally. The proximal P1 segment is a short segment from the origin to the PCOM and has some small thalamic perforating branches. The P2 segment runs from the PCOM to the midbrain, while P3 and P4 segments are within the quadrigeminal cistern and calcarine fissure respectively (181). A foetal PCOM variant is present when the PCA is supplied from the anterior circulation via a large PCOM with a small or absent P1 ipsilaterally. PCA stroke can have a variety of symptoms depending on the territory affected, including hemianopia, Balint syndrome and reading disorders.

### **2.3 The Circle of Willis**

The anastomotic vascular network at the base of the brain is named after Sir Thomas Willis, (1621-1675) whose studies into human and animal anatomy led him to conclude that “the cerebrum is the primary seat of the rational soul in man, and of the sensitive soul in animals. It is the source of movements and ideas” (182). His post-mortem studies in *Cerebri Anatome* revealed an early but informative description of the anastomotic capacity of the cerebral vessels in vascular disease states: When describing post mortem results on a patient who

died from a mesenteric tumour, he wrote “When his skull was opened we noted amongst the usual intracranial findings, the right carotid artery, in its intracranial part, bony or even hard, its lumen being almost totally occluded; so that the influx of the blood being denied by this route, it seemed remarkable that this person had not died previously of an apoplexy: which indeed he was so far from, that he enjoyed to the last moments of his life, the free exercise of his mental and bodily functions. For indeed, nature had provided a sufficient remedy against the risk of apoplexy in the vertebral artery of the same side in which the carotid was wanting, since the size of this vessel was enlarged, becoming thrice that of the contralateral vessel”(183). Experimental evidence of the connections of the circle of Willis has been shown in his additional description : “ The cephalick arteries, via the carotids and the vertebals do so communicate with another and all of them in several places, are so in grafted one in another mutually that if it happen that many of them should be stopped or pressed together at once, yet the blood being admitted to the head by the passage of one artery only, either the carotid or the vertebral, it would presently pass through all of those parts both exterior and interior; which indeed we have sufficiently proved by an experiment, for that ink being squirted in the trunk of one vessel either carotid or vertebral quickly filled all the sanguiferous passages, and everywhere stained the brain itself” (183, 184).

The circle of Willis functions as an anastomotic network connecting arterial networks from either side as well as anteriorly and posteriorly. Anteriorly, right and left carotid territories are connected by the anterior communicating artery which provides a route for inter-hemispheric blood flow in the setting of unilateral carotid hypo perfusion, and reversed flow in the proximal ACA can be seen in this scenario (15). Cross flow via segments of the circle of Willis can be seen using ultrasound in the setting of proximal vessel stenosis or occlusion(185). Posteriorly, the PCOMs allow for flow from anterior to posterior or vice-versa depending on the direction of flow required. When both posterior communicating arteries are present in addition to an anterior communicating artery, the circle of Willis can be considered to be complete, but this pattern is seen in only the minority of patients examined with angiography(186). Considerable variation in the anatomy of the Circle of Willis exists, with up to 30 % of people having a hypoplastic or absent posterior cerebral artery, absence of

anterior communicating artery in 1% and hypoplasia or absence of the proximal anterior cerebral artery in 10%(187).

Along with the ophthalmic arteries, the segments of the Circle of Willis serve as primary collateral routes(15). In carotid occlusions, the presence of flow via the circle of Willis is associated with low prevalence of watershed infarction(188) and with fewer or less marked symptoms than those without established collateral flow(189). Presence of Willisian collaterals is associated with tolerance of carotid occlusion during angioplasty and stenting (190). Examination with ASL has shown that in independent patients with unilateral ICA occlusions the ipsilateral MCA derives flow from the vertebro-basilar system while the ACA territory is supplied from the contralateral ICA, highlighting the functional capacity of different circle of Willis components in the setting of proximal occlusion (191). Fluctuating demands may reveal the dynamic nature of primary collaterals with hypoplastic segments enlarging according to need(192) which may contribute to the different outcomes seen in carotid occlusion(193).

## **2.4 Leptomeningeal vessels**

While primary Willisian collateral vessels are of obvious importance in the setting of proximal vascular occlusions and stenosis, they are unable to fully compensate for reduced flow in more distal occlusions. Distal intracranial occlusions are anatomically beyond the circle of Willis but may still receive collateral flow from smaller leptomeningeal vessels. Presence of residual flow via collaterals is something that is of increasingly recognised importance, although the contribution made by these secondary collateral routes has not been studied in detail and their capacity for delivering meaningful blood flow via small diameter vessels has been debated for many years(194).

### **2.4.1 Historical Context**

The cortical anastomoses between different arterial territories by leptomeningeal vessels were first studied in detail by Heubner in 1874, who observed that after ligation of a single intracranial artery distal to the circle of Willis, other arteries in both hemispheres were filled through a network of meningeal arteries he termed “Kanalnetzwerk”(Cited by Brozici(194)) . The

importance of LMA in terms of providing a meaningful contribution to cerebral blood flow was contested by other investigators like Duret and Charcot who considered that LMA were of too fine a calibre to provide a meaningful connection between arterial territories, implying that each of the three main arterial territories are in practical terms independent (Cited by Vander Eecken(195)). The anatomy and significance of LMA were examined in a series of 20 adult cadavers by Vander Eecken and Adams in 1953 after injection of a lead based solution into the cerebral arteries(195). They described direct anastomoses between ACA and MCA, MCA and PCA, ACA and PCA, ACA and ACA, and between the Cerebellar arteries. They also asked the question “ Is it possible that the adverse effects of cerebral ischemia following occlusion of a major artery can be ameliorated by collateral blood flow through these pre-existing anastomotic channels?”. In several case examples they demonstrated limited infarction in given arterial distributions despite the presence of proximal occlusions and noted the presence of dilated meningeal vessels reflecting local vascular reaction in the ischemic territory. They concluded that individual variation in the number size and distribution of anastomoses exists, that there is little flow through leptomenigeal vessels under normal conditions, and that they serve a protective function as less extensive infarction is seen if the anastomotic vessels are large and numerous rather than small and poorly developed(195). The ability of neighbouring arterial territories to directly perfuse the MCA territory was demonstrated by de Seze who injected fluid into the ACA and PCA under pressure and demonstrated retrograde flow to the origin of an already occluded MCA, concluding that satisfying irrigation could be obtained without recanalisation of the occluded artery (From Brozici(194) ,article in French).

#### ***2.4.2 Collateral Circulation in Animal Models of Stroke***

Animal studies into collateral anatomy and function have been performed in several species, with most work focussing on rodent stroke and control models. Distal branches of the major intracerebral arteries in the rat form an anastomotic network over the surface of the brain providing a source of flow between neighbouring territories(196).



In rats of different ages, the absolute amount of native anastomoses between the ACA and MCA territories has been shown to be constant with time from birth suggesting that the absolute number of collateral anastomoses remains constant for an individual(196). Inspection of collateral vessels by Coyle at post-mortem in Wistar rats who underwent MCA ligation has revealed that the diameter of anastomotic vessels were significantly larger ipsilateral to the stroke compared with the normal hemisphere and also relative to control specimen rats suggesting that collateral vessel diameter is a variable and can enlarge in response to ischaemia in an neighbouring arterial tree(197). Tortuosity is a measurement for collateral vessel extent being calculated by dividing vessel length by the straight line distance between two vessel ends. Vessel tortuosity has been shown to be increased ipsilateral to an MCA occlusion as a response to focal ischemia. MCA occlusion in the Wistar rat model results in minimal infarction which is considered as evidence of how well-developed leptomenigeal collateral vessels can compensate for occlusions which occur distal to the capacity of primary collaterals(197).

Much additional research into rodent models of stroke has focussed on the spontaneously hypertensive stroke prone rat (SHRSP). In contrast to the Wistar and Sprague Dawley rats, obstruction to the MCA in SHRSP always results in a large infarct within the MCA territory and therefore these rodents have been frequently studied for infarct analysis at post mortem (198). The severity of and propensity to tissue infarction in SHRSP models is not solely related to hypertension however, with additional mechanisms being implicated such as collateralisation. Large infarcts are seen after stroke in young SHRSP before hypertension has even developed highlighting the need to consider additional mechanisms for development of large stroke volumes (199, 200). The importance of factors other than blood pressure is further supported by the finding that non SHRSP rats who had hypertension induced to similar levels as SHRSP prior to MCA occlusion did not suffer large infarcts suggesting other mechanisms were the reason for large infarct volumes (201). Absolute number of anastomoses between arterial territories are the same in both SHRSP and WKY rats at baseline but the internal diameter of anastomotic vessels is smaller in SHRSP and this diameter reduces with increasing age and is not related to hypertension (202). When regional cerebral blood flow was measured and compared between SHRSP and

WKY rats there was no significant difference in blood flow at baseline between strains(203). After MCA occlusion, blood flow was reduced significantly more in SHRSP than WKY, whereas vascular tone was increased in SHRSP compared to WKY(204). Combined, these studies suggest that the number of collaterals does not change in an individual, that size and length of collateral vessels can change in response to ischemia, that the reduction in blood flow following occlusion is augmented to varying extent in different strains due to the ability of collateral vessels to compensate for arterial obstruction. Collateral heterogeneity between strains may point to genetic, anatomical and biochemical differences controlling collateralisation.

### Mechanisms for Collateral Flow Differences

When infarct volumes following MCAO were measured with MRI in WKY , SHRSP and hybrid SHRSP/WKY rats, the propensity to larger infarction in SHRSP was confirmed, as was the finding that the infarct volume was independent of the degree of pre-stroke hypertension (205). The infarct distribution was identical in SHRSP and in the hybrid SHRSP/WKY offspring which suggested a dominant trait for tendency towards large infarct volumes Genetic susceptibility to ischemic damage in SHRSP following MCAO has been co-segregated with a region on the rat's chromosome 5(206). As collateral capacity in response to ischemia is different between rat strains, a genetic component to adequacy of collateral response is a possibility. The genetic influence on collateral flow has been further evaluated in mice. Zhang et al measured collateral length and number of penetrating arterioles following MCAO in 15 different inbred mouse strains and found a wide variation in the extent of native collaterals between strains, that infarct volume correlated inversely with collateral number and density and that change in anastomotic diameter in response to ischemia also displayed wide genetic variation(207). When the two strains with the most difference in cerebral collaterals were compared, variation in native collaterals was evident during the embryonic phase, and the strain with least collaterals displayed slower outgrowth of the cerebral arterial tree which resulted in larger distances between branches of neighbouring arterial territories (208). Levels of VEGF-A, Angiopoietin-2 and PDGF-B expression due to genetic differences were considered as potential mechanisms behind the variation in collaterals between strains(208). Genetic influence on the development of collaterals in skeletal

muscle has also shown the importance of VEGF and Chloride intracellular Channel 4 in determining the number and size of collaterals as well as their effect on tissue perfusion(209, 210).

Reduced functional compliance within collateral vessels in response to ischaemia is considered a potential mechanism for the larger infarction, possibly due to reduced CNS nitric oxide synthetase activity resulting in impaired vasodilation or an excessive inflammatory response(211). The role of NO in stroke has revealed that it may decrease or increase infarct volume, but it may be the source of NO release that is important. NO derived from endothelial cells causes vasodilation and reduces infarct size, while NO derived from, neurones is neuro-toxic and causes an increase in infarct volume. (212, 213)NO release and infarct volumes were measured by Kidd et al to evaluate the effect of NO on collateral flow. (198)NO release measured by a porphyrinic microsensor was significantly reduced in SHRSP compared to control Sprague Dawley rats, which inversely correlated with infarct volume. When control rats had NO release inhibited by a NO synthetase blocker ( $N^G$ -nitro-L- Arginine [L-NNA]), NO measurements were reduced which correlated with an increase in infarct volume as well as increased wall thickness. The authors concluded that reduced endothelial NO release may be a contributory cause of reduced collateral flow(198). The importance of endothelial NO release has also been confirmed in mice models of stroke where endothelial NO synthetase (eNOS) knockout mice were shown to have larger infarct than wild-type mice as well as reduced CBF confirming that endothelial NO exerts a protective role by inducing vasodilation of the collateral circulation and thereby increasing flow capacity in collateral vessels(212, 214).

Presence of leptomenigeal collateral flow has been considered a marker of severe cerebral hypo perfusion induced after the circle of Willis has failed, but it is the actual reduction in cerebral perfusion which is an important factor for inducing flow via leptomenigeal pathways (215). Adult mice after common carotid artery occlusion showed increased ipsilateral leptomenigeal vessel diameter compared to sham operated mice and this change to collateral architecture was dependant on time(216). Cortical perfusion measured by laser-doppler flowmetry was more severely reduced in the MCA rather than ACA territory following CCA occlusion, demonstrating a pressure gradient between the neighbouring arterial territories and that this pressure gradient is

responsible for collateral vessel growth (216). Possible mechanisms include increased fluid shear stress in collateral vessels or increased activity of monocytes/macrophages.

The impact of hyperglycaemia on collateral flow has also been evaluated in animal models. After MCA occlusion followed by reperfusion in Diabetic (Goto-Kakizaki [GK]) and control (Wistar) rats, expression of VEGF reduced significantly in GK rats, while angiostatin, an anti-angiogenic factor, was increased compared to controls. These correlated with reduced capillary density in GK rats, suggesting impaired collateral ability in diabetic rats which may be due to impaired collateral growth/ enlargement (217). Comparing the effect of hyperglycaemia in different rat strains to evaluate the effect on collaterals is limited however by the fact that any perceived effects could be related to genetic factors rather than solely due to hyperglycaemia(218) When coronary collaterals in diabetic dogs were evaluated, impaired collateral development was seen in chronic hyperglycaemia in association with increases in angiostatin and MMP-9(219).

Hypoxia has an additional influence on angiogenesis and collateral flow, and adaptation to hypoxia is regulated by hypoxia inducible factors (HIF) which regulate the expression of genes involved in metabolism, vascular remodelling and collateral development(220). When HIF- containing plasmids were placed on the cortex of male Wistar rats prior to MCAO, the length of collateral vessels was significantly increased compared to control rats that also underwent MCAO(220). As a target gene of HIF is that of erythropoietin (EPO) which has been associated with tolerance to stroke in mouse models, response to hypoxia mediated by EPO has been considered as a means of inducing collateral flow. EPO levels have also been associated with better degrees of collateral flow in the coronary circulation in human patients with stable angina(221).

### ***2.4.3 Collateral Therapeutics in Animal Stroke Models***

The genetic link to ischemia following MCAo in SHRSP has been linked to chromosome 5(206). This region is where genes responsible for 20-hydroxyeicosatetraenoic acid (20-HETE) are located. 20-HETE, is derived from arachadonic acid(AA) by cytochrome P-450 and acts as a potent vasoconstrictor

which controls vascular tone and autoregulation(222, 223). Levels of 20-HETE are significantly increased in SHRSP compared to WKY rats, and this increase is specific to the cerebral circulation.(224) This increase appears to be independent of blood pressure, as levels of 20 HETE were not significantly different between WKY controls and WKY rats treated to induce hypertension, implying that elevated levels, although associated with hypertension in SHRSP are not markers of hypertension, but rather of another characteristic of the SHRSP's susceptibility to stroke. When synthesis of 20 HETE was blocked by a selective inhibitor, HET0016, infarct volume was significantly reduced as was the amount of reactive oxygen species generated (224). When 20 HETE was selectively inhibited by TS-011 in different rat strains, reduction in 20-HETE levels, infarct volume and neurological deficits were seen (225-227). As 20 HETE causes vasoconstriction, and reduced collateral diameter is associated with larger infarct in SHRSP, the beneficial effects of blocking 20 HETE may be due to improved collateral flow following MCAO, but this has not been confirmed.

As stated previously, the action of macrophages has been linked to leptomeningeal collateral growth following CCA occlusion in mice (216). Granulocyte-macrophage colony stimulating factor (GM-CSF) is produced by macrophages/ monocytes, and has receptors on endothelial cell surfaces(228). GM-CSF injection following CCA occlusion but prior to a subsequent permanent MCA occlusion was associated with significantly increased vessel diameters, while GM-CSF treatment did not alter vessel diameters in sham operated mice. GM-CSF treatment also significantly reduced infarct volume following MCA occlusion (216). This model suggests that hypo perfusion is essential for the diameter of leptomeningeal collaterals to be altered and also that growth factors could be associated with increased collateral dimensions and a subsequent reduction in infarct volume.

#### ***2.4.4 Collateral Therapeutics in Human Stroke***

The potential role of endothelial NO in determining blood flow and infarct volume has been discussed in animal models. Statins lower cholesterol by inhibition of HMG-CoA reductase, but they also exert other effects including improved endothelial function and increased NO bioavailability(229). Statins reduce risk of recurrent stroke and TIA(230) but the effect may be independent

of cholesterol level, as other cholesterol lowering mechanisms do not have the same effect(231, 232). In addition to reducing stroke risk, statins may improve outcomes after ischemic stroke. In a follow up of the SPARCL study, there was a trend towards less severe strokes in those patients randomized to receive Atorvastatin compared to placebo (233). The potential mechanisms for this effect are many, including neuro-protection against glutamate effects, reduced superoxide production, reduced cytokine gene expression, and up-regulation of NO-synthetase. Statin therapy prior to stroke has been associated with better degrees of collateral flow on angiography, with no difference in clinical stroke severity at baseline (234). These findings suggest that statins may improve microcirculatory capacity increasing collateral flow in stroke patients which may be a contributory factor to the suggestion of better outcomes following statin therapy, although the association between statins and collaterals requires confirmation.

Transdermal Nitrates may lower BP and maintain cerebral blood flow in recent stroke via enhancing flow in leptomenigeal collaterals (235). The effect of nitrates on stroke outcome is the subject of ongoing investigation, although evaluation of collaterals is not part of the study(236). Additional methods for augmenting blood pressure for clinical effect in stroke may mediate effects via collaterals but collaterals have not been specifically measured in these studies (237).

Sphenopalatine ganglion stimulation may increase ipsilateral cerebral blood flow via parasympathetic nerve stimulation(238). The safety and efficacy of sphenopalatine ganglion stimulation to enhance collateral flow in stroke is the subject of current investigation (239). Flow diversion by redirecting flow to the brain by performing partial aortic occlusion after stroke has also been attempted. Aortic balloon pump occlusion is a safe and potentially efficacious means of providing additional blood flow in stroke but requires further evaluation (240, 241). other methods of achieving flow diversion includes application of external compression devices to enhance venous pressure in the setting of carotid occlusion, but this has been evaluated in case reports only(242).

In summary, several attempts to improve outcome after stroke by enhancing collateral flow have been attempted and form part of an expanding therapeutic field. However the effects of any of these methods on direct measures of collateral flow have yet to be assessed which may be partly due to the lack of an agreed method to measure and grade collateral flow extent. In order to target collaterals, a reliable means of grading collaterals using imaging may be required in order to prove that different interventions mediate an effect via collateralisation.

## **2.5 Systematic Review of Methods for Assessing Leptomeningeal Collateral Flow.**

Studies of leptomeningeal collateral flow in animals have suggested that the adequacy of flow via anastomoses could be important in affecting infarct volume and outcome after stroke but most of these studies have measured collaterals at post mortem, permitting quantitative measurements of vessel diameter or qualitative measurements of vessel tortuosity. Early works on collaterals in human stroke have also been at post-mortem, but imaging at stroke onset may be used to measure collateral flow adequacy for stroke patients in real time. Different imaging modalities can be used to evaluate the cerebral circulation and collateral flow, including catheter angiography, CT and MR angiography and Trans-cranial Doppler, but the modality and grading assessment method which can best evaluate the presence and adequacy of collaterals is not clear. Numerous studies have evaluated collaterals in acute settings using different modalities and grading scales. Poor collaterals when assessed using catheter angiography have been associated with haemorrhage after intra-arterial thrombolysis (243). Better grades of collateral flow measured with angiography and CTA have been associated with lesser amounts of infarct growth and better clinical outcomes after stroke (111, 244). These studies, while demonstrating the importance of collateral flow adequacy in stroke, have each used different scales with which to grade collaterals and there is no consensus on how collateral flow should be graded, which limits any potential future research into clinical, genetic or blood biomarkers of collaterals flow.

Part of the purpose in writing this thesis was to evaluate the impact of collateral flow on clinical and imaging outcomes after stroke as well as to investigate the

presence of biomarkers for adequacy of collateral flow status. In order to measure collateral flow adequacy in my dataset later in this thesis, a grading scale which could be used to grade collaterals was required. As consensus on grading collaterals was lacking from initial review of the literature, a systematic literature review was therefore undertaken in order to consider all of the currently available methods with which to grade collateral flow, as well as to confirm the importance of collateral flow on outcomes in stroke and to determine how collaterals could be best classified in order to permit further study of collateral flow in this and other future work.

### **2.5.1 Methods**

#### Search Strategy

The Ovid on-line Portal was used to search Medline and Embase from inception to week 32, 2009 for methods to describe leptomeningeal collateral assessments. The search strategy is attached in Appendix 1. In addition the search was supplemented by review of electronic tables of contents in neurological journals and by hand-searching the references and citations of all relevant articles identified by the initial literature search. Where full text was unavailable (e.g. Conference poster presentations published in abstract form only) the relevant authors were contacted directly to obtain copies of the grading scale used to grade collateral flow.

#### Inclusion criteria

All publications which were written in English and performed on humans in whom collateral flow of any kind was described were initially selected for review. Publications which only evaluated primary collateral flow (i.e. through the segments of the circle of Willis or via the ophthalmic artery) were subsequently excluded from analysis. Terms which were considered to reflect leptomeningeal collaterals according to different nomenclature included pial collaterals and cortical anastomoses. Studies of collateral flow described using these terms were included in the final group of selected publications. A specific disease state not included was Moyamoya, as the collateralisation seen in this condition, although occurring in the leptomeningeal vessels, was not considered



to be reflective of the flow dynamics seen in stroke patients due to presumed different pathophysiology of collateral development and recruitment.

Imaging modalities for inclusion were those that may be employed in acute stroke consideration were not pre-specified at the time of literature search, but in practice the inference of collateral flow using PET or SPECT in different publications did not specifically evaluate collateral flow. Instead PET and SPECT measured the responsiveness/capacity of collaterals or inferred the presence of collaterals according to flow or metabolic indices and were not ultimately included in the final analysis.

### Data extraction

Information recorded from each relevant publication included imaging modality, description of collateral flow grade, number of subjects evaluated, clinical setting (i.e. acute stroke, less than 24hrs from symptom onset, or chronic cerebrovascular disease states with imaging performed more than 24 hrs after initial symptom onset). Inter and intra observer agreement was recorded if it was analysed in any publication as was the impact (positive, negative or neutral) collateral flow adequacy had on imaging and clinical outcomes. If more than one modality or grading scale was evaluated, correlations between methods for measuring collateral flow were recorded. Included publication dates ranged from January 1965 to October 2010.

### **2.5.2 Results**

Medline and Embase searches yielded 9456 and 6847 publications respectively, 195 of which were screened as being potentially relevant and had full texts reviewed. After screening, 39 articles were included. A further 42 articles were obtained by hand searching bibliographies and review of electronic tables of contents from different journals providing a total of 81 different publications for inclusion (n=4686 patients, Table 2.1).

Modality	Different assessment methods	Number of Publications	Methods with inter/intra observer agreement assessed
Angiography	41	58	2 <sup>(243, 245, 246)</sup>
CT	7	12	5 <sup>(110, 111, 247-249)</sup>
MRI	9	13	0
TCD	6	7	0

**Table 2-1 Assessment Methods for Measuring Collateral Flow Using Different Modalities**

Two grading scales had reliability assessed for angiography, but three publications are referenced as one had reliability assessed in a second publication by the same author. Five different methods using CT tested reliability.

## Catheter Angiography for Collateral Flow Assessment

The majority of leptomeningeal flow assessments were performed using catheter angiography. A total of 3467 patients in 58 publications had leptomeningeal flow assessed by a total of 41 different criteria. 36 publications investigated collateral flow in acute stroke/TIA, and 18 assessed collaterals in non acute patients (191, 250-268). Time from symptomatic event was unclear in 5(160, 267-270) and a combination of acute and non acute patients was reported once (271). Two publications reviewed collateral flow in the posterior circulation alone (267, 272) with the remaining relating to either anterior circulation alone or a combination of anterior and posterior circulation (Table 2.2).

Reliability assessments were available for two of these methods, demonstrating good and very good inter/intra observer agreement (n=172) (243, 245, 246). Arterial injection sites, when described, included unilateral carotid/MCA (n=3)(273-275), bilateral carotid (n=3)(253, 276, 277), minimum of ipsilateral carotid and vertebral (n=10)(250, 251, 261, 262, 269, 271, 278-281), and other combinations (n=5)(257, 265, 266, 282, 283).

A simple inspection of the angiogram appearance without use of specifically defined grading system (i.e. leptomeningeal collaterals termed as being present or not) was identified in 25 publications (160, 191, 251, 253-266, 268-270, 277, 278, 282-284) . Each of these used a different subjective interpretation of the angiographic appearances to assess for leptomeningeal collateral flow presence. Inter/intra-observer reliability was not assessed for any of these assessment methods.

One grading method used in three different publications from a single group was based on a scale that took into account both the actual site of the arterial occlusion as well as the degree of collateral flow around it as determined by the adequacy of vessel filling. This method is known as the Qureshi grading scale and showed good inter-observer reliability ( $\kappa=0.73$ ) for grading among three different readers on a sample of 15 patients when it was first used (246). When this method was used again, reliability in terms of observer agreement was not re-assessed (285, 286). This method had a total of 8 different grades which

varied according to the initial occlusion site as well as the collateral flow state, and therefore does not solely describe collaterals.

The absolute number of individual leptomeningeal vessels visualised at angiography was used in 7 publications to grade collateral flow adequacy (271, 274-276, 280, 281, 287). Other grading scales which were broadly considered to be based upon interpretation of the rapidity of vessel filling or anatomic extent of leptomeningeal flow were used in 22 publications (40, 234, 243-245, 250, 252, 267, 271, 272, 275, 276, 279-281, 287-293). A combination of absolute collateral vessel number along with speed and extent of collateral flow was used in 6 publications (271, 275, 276, 280, 281, 287). An illustration of one of the grading methods using catheter angiography is shown in figure 2.2.

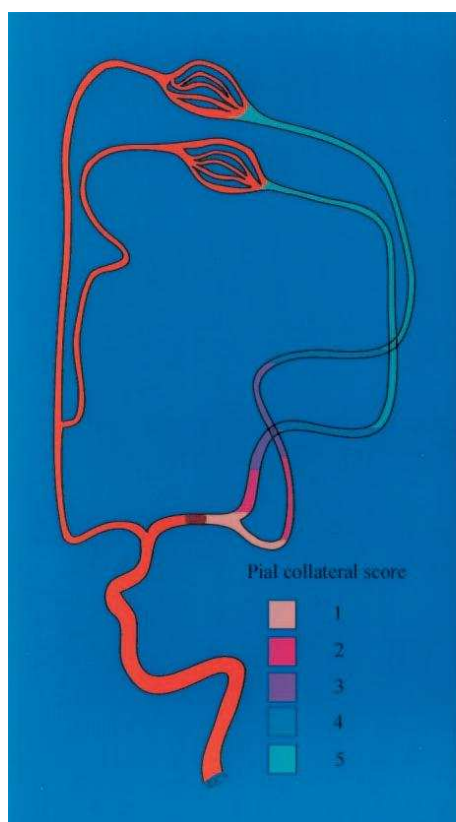


**Figure 2-2 Illustration of Collateral Scoring Based on Catheter Angiography**

Illustration showing collateral scoring based on extent of retrograde flow from the anterior cerebral artery towards a proximal occlusion in the middle cerebral artery scoring corresponds to the angiographically visible retrograde reconstitution of the middle cerebral artery segments on the delayed venous phase. Each colour depicts the furthest extent of retrograde opacification depicted on the anteroposterior cerebral angiograms for each leptomeningeal collateral score. Reproduced from Christoforidis et al "Angiographic assessment of pial collaterals as a prognostic indicator following intra-arterial thrombolysis for acute ischemic stroke" *AJNR Am J Neuroradiol.* 2005 26(7):1789-97

### Impact of Angiographically Defined Collaterals

Not all publications described the impact or importance of flow in collateral vessels as the purpose of the literature review was primarily to obtain information on how collateral flow can be graded. When stated however, the presence of adequately developed collaterals appeared to be associated with markers for better outcomes when assessed using catheter angiography. Christoforidis et al revealed that in addition to known predictors of haemorrhagic transformation after intra arterial thrombolysis (Time to treatment, diabetes, low platelet count); poorly developed collaterals were associated with haemorrhagic transformation as well as larger size of haemorrhage following IA thrombolysis (243). In addition collateral flow grade was shown to predict infarct volume and clinical outcome, and may be associated with better response to thrombolysis (245). In acute stroke patients undergoing angiography <5 hrs from symptom onset, Toni et al found that collateral flow was a predictor of early clinical improvement along with arterial patency(277). Von Kummer stated that reperfusion and collateral flow were two important factors associated with small infarct volume and better clinical outcome in patients with MCA/ICA occlusion receiving IV rt-PA(280). Infarct volume, clinical outcome, clinical presentation and evolution of ischemic CT changes were correlated with collateral status in patients with MCA occlusion in the PROACT II trial (273, 279). When compared with other indices using Multimodal MRI in acute stroke patients, collateral flow was associated with larger volumes of benign oligemia, less infarct growth even without recanalisation and was associated with a trend (although not statistically significant) towards better grades of recanalisation(244). In the setting of basilar occlusions, Arnold et al found that better residual collateral flow was more likely to be seen in patients who had good clinical outcomes after therapy(294) while Cross et al found that patients with collateral filling of the basilar artery tolerated longer symptom duration after basilar artery stroke, although the collateral source may have included both primary and secondary flow collateral routes(272). Good collateral flow grade was a significant univariate predictor and the only multivariate predictor of favourable clinical outcome in a group of patients treated with Intra-arterial or intravenous thrombolysis when inspected by Kucinski et al (287). No publication assessing collaterals demonstrated a negative association between well developed collaterals and clinical or radiological outcome, although the effect was neutral or not mentioned in

several publications (160, 234, 268, 270, 283). The published articles describing collateral flow defined using catheter angiography are summarised in Table 2.2. The number of different methods and grading scales published highlights heterogeneity in how collateral flow has been quantified. Where numerical scales were used, lower numbers reflected poorly developed collaterals while higher numbers signified better collateral flow, although these varied between publications.

Description	Grading	Author(n)	Acute(<24hr from symptom onset)/Non acute	Reliability assessed?	Prognostic Significance (NS= Not Stated)
Extent of antero/ retrograde vessel filling	0-3	Brandt <sup>(267)</sup> (20) Arnold <sup>(294)</sup> (40)	Acute	No	Beneficial <sup>(267, 294)</sup>
Number and rapidity of collateral vessel filling	0-2	Von Kummer <sup>(281)</sup> (53)	Acute	No	Beneficial
Number and rapidity of collateral vessel filling	n/a	Bozzao <sup>(283)</sup> (36) Bozzao <sup>(282)</sup> (36) Toni <sup>(277)</sup> (80)	Acute	No	NS <sup>(283)</sup> NS <sup>(282)</sup> Beneficial <sup>(277)</sup>
Filling extent of main and distal vessels via collaterals	0-3	Wu <sup>(252)</sup> (51)	Non acute	No	n/a
Vessel filling relative to occlusion	1-5	Christoforidis <sup>(243)</sup> (104) Christoforidis <sup>(245)</sup> (53)	Acute	Yes	Beneficial <sup>(243)</sup> (245)

**Table 2-2 Angiographically Defined Collaterals**



Description	Grading	Author(n)	Acute(<24hr from symptom onset)/Non acute	Reliability assessed?	Prognostic Significance (NS= Not Stated)
Retrograde MCA flow to insula	Present, absent, indeterminate	Derdeyn <sup>(254)</sup> (117)	Non acute	No	n/a
Rapidity and extent of retrograde collateral flow	0- 4	Bang <sup>(244)</sup> (44) Higashida <sup>(289)</sup> (0)* Bang <sup>(40)</sup> (119) Ovbiagele <sup>(234)</sup> (95) Sanossian <sup>(288)</sup> (74) Liebeskind <sup>(293)</sup> (120) Liebeskind <sup>(292)</sup> (120) Liebeskind <sup>(290)</sup> (50) Liebeskind <sup>(291)</sup> (66)	Acute	No	Beneficial <sup>(40, 244, 293)</sup> n/a <sup>(289)</sup> No effect <sup>(234)</sup> NS <sup>(288, 290-292)</sup>
Flow extent across cortical surface	n/a	Powers <sup>(253)</sup> (19)	Non acute	No	n/a
Visual inspection	n/a	Klijn <sup>(255)</sup> (76)	Non acute	No	n/a
Delayed contrast washout	n/a	Essig <sup>(256)</sup> (30)	Non acute	No	n/a
Visualisation of slow flow	n/a	Kamran <sup>(160)</sup> (8)	Acute	No	NS
Visualising flow pattern	Grade 4= LMF	Ozgur <sup>(257)</sup> (27)	Non acute	No	n/a
Cortical branches from contralateral ACA/PCA	n/a	Rutgers <sup>(258)</sup> (112)	Non acute	No	n/a

**Table 2-2 Angiographically Defined Collaterals (continued)**

Description	Grading	Author(n)	Acute(<24hr from symptom onset)/Non acute	Reliability assessed?	Prognostic Significance (NS= Not Stated)
Visualisation of Pial vessels	n/a	Zappe <sup>(270)</sup> (86)	Unclear	No	NS
Visualising flow from adjacent vascular territories	n/a	Noguchi <sup>(278)</sup> (5)	Acute	No	NS
Visualising arteriogram	n/a	Grubb <sup>(259)</sup> (81)	Non acute	No	n/a
Cortical arteries from PCA	n/a	Fukuyama <sup>(260)</sup> (3)	Non acute	No	n/a
Number and rapidity of vessel filling	0-2	Lee <sup>(275)</sup> (8)	Acute	No	NS
Distal MCA branches filling through ACA or PCA	n/a	Kim <sup>(284)</sup> (51)	Acute	No	NS
Retrograde vessel filling	n/a	Kinoshita <sup>(269)</sup> (10)	Unclear	No	NS
Cortical branches from PCA to MCA	n/a	Van Laar <sup>(191)</sup> (23)	Non acute	No	n/a
Retrograde filling of MCA branches	n/a	Yamauchi <sup>(261)</sup> (42)	Non acute	No	n/a

**Table 2-2 Angiographically Defined Collaterals (continued)**

Description	Grading	Author(n)	Acute(<24hr from symptom onset)/Non acute	Reliability assessed?	Prognostic Significance (NS= Not Stated)
Extent and number of vessels filling via collateral flow	Absent, mild, or prominent	Uemura <sup>(271)</sup> (25)	Combination	No	NS
Occlusion site and extent of collateral flow combined	0-5	Qureshi <sup>(246)</sup> (15) Mohammad <sup>(286)</sup> (57) Mohammad <sup>(285)</sup> (55)	Acute	Yes k=0.73 <sup>(246)</sup>	Beneficial <sup>(246, 285, 286)</sup>
Extent of retrograde flow in MCA	Good, poor	Kucinski <sup>(287)</sup> (111) Gasparotti <sup>(295)</sup> (27)	Acute	No	Beneficial
Capillary blush in MCA territory	Grade 4= leptomeningeal flow	Russell <sup>(262)</sup> (14)	Non acute	No	n/a
MCA/PCA filling from posterior circulation	n/a	Bischopps <sup>(263)</sup> (68)	Non acute	No	n/a
Basilar artery opacified by collaterals	Distal vs. distal & proximal	Cross <sup>(272)</sup> (24)	Acute	No	Beneficial
Cortical branches filling MCA/ACA from PCA	n/a	Bokkers <sup>(264)</sup> (17)	Non acute	No	n/a
Pial collateral flow from ACA and PCA	n/a	Derdeyn <sup>(265)</sup> (10)	Non acute	No	n/a

**Table 2-2 Angiographically Defined Collaterals (Continued)**

Description	Grading	Author(n)	Acute(<24hr from symptom onset)/Non acute	Reliability assessed?	Prognostic Significance (NS= Not Stated)
Flow via channels on brain surface	n/a	Smith <sup>(266)</sup> (18)	Non acute	No	n/a
Collateral flow assessment based on ASPECTS (13 areas)	0-3	Chng <sup>(250)</sup> (18)	Non acute	No	n/a
Number and rapidity of vessel filling from ACA	Good or scarce	Von Kummer <sup>(276)</sup> (77)	Acute	No	No effect
Number and rapidity of vessel filling from ACA and PCA	0-2	Von Kummer <sup>(280)</sup> (32)	Acute	No	Beneficial
Filling extent of at risk territory	1-3	Roberts <sup>(273)</sup> (180)	Acute	No	Beneficial
Collateral flow assessment based on ASPECTS(15 areas)	0-3	Kim <sup>(279)</sup> (44)	Acute	No	Beneficial
MCA branch filling in early venous phase	Good, moderate, poor	Ringelstein <sup>(274)</sup> (34)	Acute	No	Beneficial

**Table 2-2 Angiographically Defined Collaterals (Continued)**

Description	Grading	Author(n)	Acute(<24hr from symptom onset)/Non acute	Reliability assessed?	Prognostic Significance (NS= Not Stated)
Retrograde arterioles visualised in capillary phase	n/a	Weidner <sup>(268)</sup> (4)	Unclear	No	NS <sup>(268)</sup>
Presence of superficial PCA/ACA cortical branches	n/a	Hoffmeijer <sup>(251)</sup> (70)	Non acute	No	n/a
Extent of LMF in occluded territory	Poor, Good	Arnold <sup>(296)</sup> (98) Meier <sup>(297)</sup> (311)	Acute	No	No effect <sup>(296)</sup> Beneficial <sup>(297)</sup>
Presence of collaterals in affected territory	None/ minimal/ Moderate/ maximal	Gonner <sup>(298)</sup> (43) Brekenfeld <sup>(299)</sup> (294)	Acute	No	No effect <sup>(298)</sup> Beneficial <sup>(299)</sup>

**Table 2-2 Angiographically Defined Collaterals (Continued)**

List of publications using catheter angiography to define collateral flow extent are summarised. The wide variation in methods and scales limits full explanation in a single table, so a brief summary of each is included.

## Computed Tomography for Collateral Flow Assessment

Studies using CT imaging to investigate collateral flow focussed on qualitative interpretation of CTA appearances, either CTA-SI or CTA reconstructions. A total of seven grading scales using CTA were identified from nine publications with assessments performed on a total of 593 patients suspected of having acute ischemic stroke (91, 99, 110, 111, 247-249, 275, 300-303) (Table 2.3).

Interobserver agreement was assessed for 5/7 CTA methods, ranging from moderate to excellent (total patients assessed for reliability of method n=247).

One grading scale used a combination of CTP and CTA to grade collaterals by confirming that collateral flow was truly retrograde using 4-D angiographic images obtained from raw CTP data (111).

Collaterals were scored exclusively in cases of MCA stroke in 3 publications (111, 300, 301) . Whole anterior circulation strokes were assessed for collaterals in 4 (91, 99, 247, 248) while a combination of anterior and posterior circulation strokes were included in 1 publication (110). The different processing steps for interpretation of CTA included MIP images (301) CTA source images(99, 247, 300) and a combination of source images and 3D reconstructions (91, 110, 248, 249).

Grading scales for collaterals were based upon the extent of peri-lesional vessel filling on CTA source images(247), comparison of ipsilateral and contralateral filling in the Sylvian fissure(91, 110, 300-302), peri-lesional enhancement on source images and reconstructions(99, 303), lesion extent on tri-phasic perfusion CT(275) and extent of retrograde flow towards a proximal MCA occlusion(111)

### Impact of CT defined collaterals.

Extent of collateralisation was shown to correlate with clinical outcome after thrombolysis when examined by Wildermuth et al, suggesting that those with poor collaterals, alongside subjects with ICA occlusion or with thrombi which had auto-lysed may have little benefit when receiving IV thrombolysis (91). When source images and MIP reconstructions were blindly compared in the same patient group, Tan et al found that CTA source images for collateral assessment did not predict infarct volume, but that 3D reconstructions were predictive of final infarct volume(249). Maas et al found that neurological deterioration

(defined by any subsequent increase in NIHSS after admission measurement) was four times more likely in the group with diminished collaterals(301). Rosenthal et al compared the predictors of clinical outcome between those patients who did and did not show recanalisation of a symptomatic arterial occlusion and found that leptomeningeal collaterals only had a positive influence on outcome in patients who did not recanalize, and that this impact was proportionally less than that of baseline lesion volume and admission NIHSS(300). Schramm et al showed that clinical outcomes were significantly better in patients with good collateral status and that patients at risk of infarct growth could be identified on the basis of poor collateralisation, although baseline lesion volume (defined on DWI/ CTA source image) and therapy with IV rt-PA were not corrected for in the analysis (99). The independent predictive value of collaterals on clinical outcome after stroke in proximal occlusions was confirmed in relatively large patient samples by Tan et al and Miteff et al(111, 248) (n=85 and 92 respectively ) in addition to the association of good collaterals with smaller baseline perfusion defects and smaller final infarct volumes. No clear clinical or blood biomarkers for collateral flow were found from these studies, although patients imaged more than one hour from symptom onset were more likely to have good collateral flow than those imaged earlier which suggests that collateral flow might improve with time(301). However, serial imaging in individuals to determine whether or not collateral flow improved over time was not performed meaning an association between collateral flow and time from stroke onset remains speculative.

Modality	Method	Grading	Author (n)	Acute (<24hr from symptom onset)/ non acute	Reliability assessed?	Prognosis (NS= not stated)
Axial CTA-SI	Extent of peri-lesional vessel filling	None, moderate, good, excellent	Liebeskind <sup>(247)</sup> (36)	Acute	Yes ICC=0.81	NS
CTA-SI	Sylvian LMF compared with contralateral side	Absent, less, equal to, greater than contralateral side	Rosenthal <sup>(300)</sup> (44) Maas <sup>(301)</sup> (135) Lima <sup>(302)</sup> (196)	Acute	No	Beneficial <sup>(100, 300-302)</sup>
CTA-SI and MPR	Extent of peri-lesional filling	Good, poor	Schramm <sup>(99)</sup> (20) Tan <sup>(249)</sup> (113)	Acute	Yes k=0.494	Beneficial <sup>(99, 249)</sup>

**Table 2-3CT based Collateral Grading Methods**



Modality	Description	Grading	Author (n)	Acute (<24hr from symptom onset)/ non acute	Reliability assessed?	Prognosis (NS= not stated)
CTA SI and MPR	MCA filling in Sylvian fissure	Good, moderate, absent	Wildermuth <sup>(91)</sup> (40) Knauth <sup>(110)</sup> (21)	Acute	Yes 88% agreement between raters (110)	Beneficial <sup>(9)</sup> 1, 110)
CTA MIPS	Extent of filling in territory of occluded vessel	0-3	Tan <sup>(249)</sup> (113) Tan <sup>(248)</sup> (85) Soares <sup>(303)</sup> (22)	Acute	Yes k= 0.669 <sup>(249)</sup> ICC 0.87	Beneficial <sup>(2)</sup> 48, 249, 303)
CTA MIP & CTP	Retrograde filling of MCA	Good, moderate, poor	Miteff <sup>(111)</sup> (92)	Acute	Yes k=0.93	Beneficial
Tri-phasic CTP (TPCT)	Extent of perfusion deficit on TPCT	Severe, moderate	Lee <sup>(275)</sup> (8)	Acute	No	NS

**Table 2-3 CT based Collateral Grading Methods (Continued)**

A summary of each method for grading collateral flow with CT is included as full methods could not be incorporated to a single table. k=Kappa statistic. ICC= Intraclass Correlation Coefficient

## MRI based Collateral Assessments

A total of 9 different assessment methods determined or inferred the presence of leptomeningeal collateral flow using MRI in 13 publications (n=358, 244 acute stroke patients, 114 non-acute).

Detection of vascular hyperintensities on FLAIR imaging was used as a marker of delayed arterial transit within leptomeningeal vessels in 5 publications (159, 160, 278, 288, 304), 4 of which compared findings on FLAIR with an additional “gold standard” measurement of collaterals using with catheter angiography (160, 278, 288, 304). An example of FLAIR hyperintense vessels is shown in figure 2.3

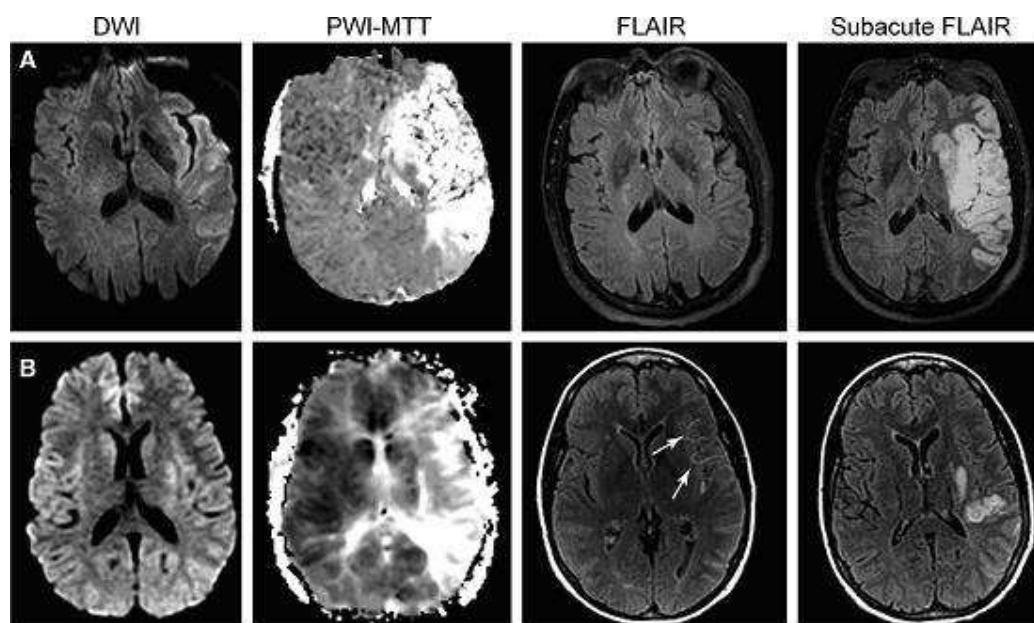


**Figure 2-3 Hyperintense Vessels on FLAIR.**

Two patients are shown with right MCA occlusion and similar perfusion deficits (PWI-MTT) at baseline. The patient with hyperintense vessels on FLAIR (panel B, Arrows) had a smaller subacute infarct volume than the patient without (Panel A) demonstrating the effect of good collaterals. Reproduced from Lee et al “Distal hyperintense vessels on FLAIR: an MRI marker for collateral circulation in acute stroke?” *Neurology* 2009; 72(13) 1134-9

Delayed contrast arrival using Perfusion weighted imaging (PWI)(305) Factor analysis of Dynamic Studies (FADS)(306), Quantitative MRA (QMRA)(307), Phase contrast MRA(308) and arterial spin labelling (ASL) (250, 252, 309) have been inferred as markers of leptomeningeal collateral flow markers in a total of 7 publications.

Abnormal visualisation of leptomeningeal vessels (AVLV) on T2\* weighted MRI was used in one series as a representation of leptomeningeal collateral supply(310)

Although multiple different methods and imaging sequences have inferred the presence and adequacy of collateral flow, none of these reported measurements compared the presence of collaterals with clinical or radiological outcomes after stroke. In addition, no agreement or observer error rates using MRI to grade collaterals were performed in any of the included assessment scales. The different publications using MRI to define collateral flow extent are summarised in Table 2.4.

Modality	Description	Author (n)	Acute(<24hr from symptom onset) /non acute	Reliability assessed?	Prognostic significance of good collateral flow grade in acute stroke (NS= not stated)
FADS	Late FADS implies collateral flow	Martel <sup>(306)</sup> (22)	Acute	No	NS
QMRA	Increased flow ipsilateral to steno-occlusive disease	Ruland <sup>(307)</sup> (16)	Non Acute	No	n/a
Phase contrast MRA	Flow from posterior to anterior circulation	Schomer <sup>(308)</sup> (29)	Non acute	No	n/a
FLAIR	FLAIR hyperintensities as a marker of collateral flow	Liebeskind <sup>(304)</sup> (91) Kamran <sup>(160)</sup> (8) Noguchi <sup>(278)</sup> (5) Sanossian <sup>(288)</sup> (74) Lee <sup>(159)</sup> (52)	Acute	No	NS <sup>(304)</sup> (159, 160, 278, 288)
T2* weighted MRI	Abnormal visualisation of leptomeningeal vessels	Hermier <sup>(310)</sup> (48)	Acute	No	NS
PWI	Delayed perfusion sign visualised on PWI	Hermier <sup>(305)</sup> (29)	Acute	No	NS
ASL	Quantitative distal collateral flow measurement	Wu <sup>(252)</sup> (51)	Non acute	No	n/a
TASL	Collateral flow assessment based on ASPECTS	Chng <sup>(250)</sup> (18)	Non acute	No	n/a
CASL	Collateral flow inferred from delayed arterial flow	Chalela <sup>(309)</sup> (15)	Acute	No	NS

**Table 2-4MRI Based Collateral Assessments**

TASL= Territorial Arterial Spin Labelling, CASL= Continuous Arterial Spin Labelling, FADS= Factor Analysis of Dynamic Studies, QMRA= Quantitative Magnetic Resonance Angiography,

### Transcranial Doppler Measurements of Collateral Flow

A total of 6 different assessment tools from 7 publications measured leptomeningeal collateral flow using transcranial Doppler measurements. At least 268 patients were assessed using TCD, although the number examined in one publication was unclear(311) . Asymmetry of blood flow measured in different arterial segments was used in most TCD based collateral methods, either in isolation(215, 312) or in combination with reduced pulsatility of the vessel under investigation(284, 313, 314). The degree of asymmetry required to define flow via leptomeningeal vessels varied between different publications. Additional definitions of collateral flow on TCD included accelerated flow in the A1 segment of the ACA feeding flow in the smaller leptomeningeal vessels(315) and retrograde flow relative to the TCD probe(311). None of the TCD based collateral assessments had measurements of observer agreement/reliability assessed, and none of them compared the grade or presence of collaterals with any outcome measurement.

### Comparisons between Modalities

A total of 8 publications compared non-invasive LMF assessments with MRI (n=5) CT (n=2) or TCD (n=1) to a reference “gold standard” using catheter angiography. Each time a comparison was made however, a different grading scale or definition for measuring collaterals using the gold standard imaging modality was performed limiting the potential to compare assessment methods between different modalities (160, 250, 252, 269, 275, 278, 284, 288).

### **2.5.3 Discussion**

The quality of leptomeningeal collateral flow is reported in several of the reviewed publications to be an independent predictor of outcome after acute ischemic stroke even after adjustment for other known prognostic factors such as age, clinical stroke severity, baseline imaging characteristics, occlusion site, treatment and recanalisation/reperfusion, (111, 244, 248, 249, 277, 287, 300) which suggests that as a minimum there is a need to account for its influence on outcomes after stroke particularly when imaging modalities used at baseline assessment in therapeutic trials in stroke have the potential to detect and grade

collateral flow . Good collateral flow is assumed to be associated with favourable outcome as a consequence of maintaining the ischemic penumbra for longer until reperfusion occurs. However the effect of collaterals appears to be independent of conventional indices of penumbra such as arterial recanalisation or reperfusion as even after correcting for these outcome predictors, collateral flow extent has an additional impact on clinical outcome after proximal arterial occlusion (111, 300).

It is unclear whether collateral grade represents an inherent characteristic of individual subjects or a potential therapeutic target .Collateral flow grades on CTA are reportedly better in patients who undergo imaging later after symptom onset, while better collateral flow grades on catheter angiography have been reported in patients treated with statins prior to stroke (234), suggesting collateral flow is dynamic, develops over time and could potentially be modified by medications or other interventions such as partial occlusion of the abdominal aorta which increases blood flow proximal to the aortic occlusion, including cerebral blood flow, and is used to improve cardiac perfusion following myocardial infarction(241). In order to target collaterals in terms of therapy, agreement on how collaterals are graded is likely to be needed in order to measure response to interventions. At present there is no consensus on collateral grading within and between different imaging modalities.

Collateral flow is not accounted for in most occlusion classification systems which may be important in defining arterial occlusion severity at entry to clinical trials and adoption of scoring systems from coronary artery disease, notably the TIMI(167) system, or minor modification of such systems (e.g. TICl) ignores fundamental differences in the acquisition of images and the anatomy of the different vascular beds. The original TIMI scale defines the extent of both recanalization and reperfusion based on interpretation of *dynamic* angiography appearances, but translation of this scale to a non-dynamic imaging modality such as CTA or MRA has some limitations. Patients with complete occlusions but good distal collateral flow could be wrongly classified as having a high TIMI score, because without dynamic information it is impossible to say whether or not the flow into an ischemic territory is anterograde or retrograde in origin. Guidelines have been developed for agreed reporting methods in determining recanalization/ reperfusion, but have focussed on angiography and have

acknowledged that individual CTA/ MRA scales have not been developed, requiring adaptation from TIMI/TICI or others. However these have been variably applied and therefore have been acknowledged as a possible source of confusion (316). The presence of collaterals as a contribution to the imaging appearances seen is seldom considered when defining occlusions at baseline (47). The original TIMI and TICI scales are illustrated in Table 2.5 along with subsequent adaptations of each(51, 316).The Modified TICI (mTICI) score has recently been shown to be a better outcome predictor than TIMI(317). None of these scales incorporate collateral flow adequacy which may not be so important when using dynamic imaging such as catheter angiography, but this could be seen as a limitation when the same scales are applied to non-dynamic imaging methods such as CTA or MRA as the source of flow distal to the occlusion (i.e. antegrade versus retrograde) is not defined using these imaging methods alone.

Scale + Grade	Description
TIMI 0	No recanalization/ reperfusion
TIMI 1	Minimal recanalization/ reperfusion
TIMI 2	Partial recanalization/ reperfusion
TIMI 3	Complete recanalization/ reperfusion.
TIMI 0*	Complete occlusion
TIMI 1*	Minimal flow
TIMI 2*	Partial flow
TIMI 3*	Normal flow
TICI 0	No Perfusion.
TICI 1	Penetration With Minimal Perfusion
TICI 2	Partial Perfusion
TICI 2a	Only partial filling (2/3) of the entire vascular territory is visualized
TICI 2b	Complete filling of all of the expected vascular territory is visualized, but the filling is slower than normal
TICI 3	Complete Perfusion
mTICI0	No reperfusion
mTICI1	Flow beyond occlusion without distal branch reperfusion
mTICI2a	Reperfusion of less than half in the downstream target arterial territory
mTICI2b	Reperfusion of more than half , yet incomplete, in the downstream target arterial territory
mTICI3	Complete reperfusion of the downstream target arterial territory, including distal branches with slow flow

**Table 2-5 Original and Modified TIMI and TICI Scales**

\* Adapted TIMI scale describing the occlusive lesion using CTA (reference 51). The original TIMI scale was used in coronary angiography. Even with revisions of the scales, they remain somewhat subjective particularly in defining the extent of filling in distal territories.

In order to investigate collaterals in acute stroke, a consistent method for assessment and grading is required. This literature review revealed wide variation in methods for grading LMF, few of which are supported even by measurement of observer agreement.

Catheter angiography, considered the gold standard for assessing cerebrovascular anatomy can reveal retrograde collateral perfusion in a dynamic fashion and has been used for LMF assessments in the largest number of patients. The most frequently employed scale was proposed by the American Society of Interventional and Therapeutic Neuroradiology in an effort to homogenise grading with angiography (289) , but an assessment of inter-observer



agreement has not yet been reported which may be a limitation. Good intraobserver agreement has been demonstrated with angiography when LMF was graded according to the anatomical extent of retrograde flow ( $\kappa= 0.81$ ) (243, 245). The Qureshi scale also demonstrates good interobserver agreement, but does not focus on LMF independently as each grade is dependent on the index arterial occlusion as well as the collateral flow, which could be a limitation when trying to address the impact of collaterals alone. One additional grading scale anecdotally used in clinical practice quantifies collateral flow according to time taken for contrast to travel from ICA to the M2 segment of the MCA via collaterals but this method describes flow through primary collaterals of the circle of Willis rather than specifically through cortical anastomoses(318). As there may be specific influences on collateral development (including genetic factors as suggested from experimental models) it is important to find a method of measuring flow in leptomeningeal vessels alone in order to further understand their properties. As LMF is derived from neighbouring arterial territories, its quality may only be fully evaluated when the contribution of all potential inflow sources is assessed. Descriptions of arterial injection sites are infrequently provided for catheter angiography and even when available, the contribution of the whole cerebral circulation is seldom evaluated. Catheter angiography is invasive and is usually performed when a patient is being considered for IA therapy which in general, is reserved for those patients with contraindications to IV treatment (e.g. presentation beyond 4.5 hours with favourable appearances on CT) meaning that angiographic assessments for collaterals will be predominantly restricted to this relatively small patient group. As multimodal CT and MRI are increasingly used in clinical practice and prior to entry to clinical trials, they offer a larger potential population in which LMF can be assessed non-invasively.

Although lacking dynamic information, CTA alone permits visualisation of the anatomical extent of collateral flow. The independent predictive value of collaterals has been confirmed with different CTA based collateral grading methods and interobserver agreement within different grading scales has been assessed with good to excellent measures of agreement (110, 247-249). Retrograde flow relative to a proximal arterial occlusion provides a measurement of LMF adequacy, but grading LMF this way for more distal

occlusions may be more difficult due to the specific anatomical landmarks used. A collateral scoring system based upon contrast enhancement in defined regions of interest provides a scale not dependent on a specific occlusion which could potentially be applied in a larger patient population(247). The addition of CT perfusion to CTA adds potentially important dynamic information to confirm that collateral flow is truly retrograde, and has been shown to have excellent inter-observer agreement (111). This additional dynamic information obtained with CTP requires further imaging, contrast administration and radiation exposure at present, although the development of new multidetector scanners which enable simultaneous acquisition of both CTA and CTP now allows dynamic collateral flow assessment from a single combined CTA/CTP acquisition without the current requirement for additional scanning(114).

LMF assessments with MRI use various imaging characteristics to infer the presence of collateral flow. FLAIR Vascular hyperintensities (FVH) due to retrograde flow in leptomenigeal vessels have been associated with larger mismatch volumes, and smaller subacute infarct volumes, while abnormal vessels on T2\* imaging may be due to de-oxygenated blood in collaterals and are associated with smaller infarct volumes (159, 310). ASL using different criteria has also been used to grade collateral flow with MRI (250, 252, 309). These and other LMF assessments with MRI have not been replicated nor had interobserver reliability graded and it remains to be seen if they represent robust means of assessing collateral flow.

Relative blood flow velocity and vessel pulsatility have been used as surrogate markers for leptomenigeal collateral flow using TCD in a small number of studies but the criteria for defining LMF varied among publications . The lack of an agreed definition for LMF on TCD, absence of direct collateral visualisation and difficulty in finding acoustic windows are limitations for TCD, although these are offset by the lack of radiation and contrast requirements.(319). Flow diversion on TCD, defined as increased flow velocity in ipsilateral ACA/PCA did correlate with angiographic collateral grade when methods were compared, suggesting a possible role for TCD to measure LMF (284).

Where collaterals were measured using digital subtraction angiography, CTA and MRI, CTA compared favourably, but the methods used for grading LMF on CTA were not clearly stated so this finding must be interpreted with caution(269).

### **2.5.4 Conclusion**

This review of the imaging modalities which can evaluate collateral flow as well as the literature regarding historical considerations of collaterals and investigations into collateral flow using experimental models of stroke has revealed some important findings:

- 1: There is little consistency in how flow via leptomeningeal collaterals are graded within and between various imaging modalities,
- 2: Despite this inconsistency, the positive impact collateral flow can have on various markers in stroke seems secure with independent predictive value being demonstrated in some studies,
- 3: Terms describing severity of arterial occlusions such as TIMI or TICI may inadvertently incorporate good and reduced collaterals into different occlusion descriptions, but the fact that these scales do not actually describe collateral flow which may be a limitation of their use given that collaterals may influence outcome,
- 4: Experimental and post-mortem studies of collaterals have proven that leptomeningeal vessels have many anastomotic connections, with various influences on their development, and that anastomotic development are associated with markers for improved outcome,
- 5: A small number of studies have suggested that collateral flow may be influenced by ischemia (increasing in capacity with increasing time from ictus) and medications, offering the potential of a new therapeutic target for stroke.

The influence of well developed collaterals is likely to be positive, in addition to other known prognostic indicators but the reasons behind collateral development in humans are not understood. No blood or clinical biomarker for collaterals has been described: if found, such a biomarker may offer insights into the factors

which control the development of collateral circulation. Further confirmation of the benefit of collaterals, consensus on grading, and study into biomarkers for collateral flow will hopefully improve understanding of the mechanisms behind collateral formation and adequacy, and could potentially represent novel targets for therapy in stroke.

## **Chapter 3. Materials and Methods**

### **3.1 Introduction**

The material presented in the different chapters presented in this thesis is focussed on multimodal CT imaging in acute stroke, exploration of some of the additional information this provides, how thresholds are generated for defining core and penumbra with CT perfusion, Collateral flow, and how these tissue compartments relate back to standard imaging in acute stroke with non contrast CT. Imaging and clinical data presented here were obtained during a research fellowship based at the Institute of Neurological Sciences, Southern General Hospital, Glasgow and the University of Glasgow from February 2009 to August 2011. Image analysis for different chapters varied with the specific analysis required and will be discussed in the relevant individual chapters but the entire cohort of patients and data available will be discussed initially. Recruitment to two observational studies into acute stroke took place during the fellowship period and elements of each were combined for several of the analyses undertaken. Both studies focussed on obtaining imaging data on patients soon after stroke onset, and imaging at later time points to use as potential surrogate markers for measuring outcome. Several overlapping features of the two studies meant that imaging and clinical data from each could be combined for some of the analyses within this thesis. The study protocols, procedure and timelines are discussed below.

### **3.2 The Multicentre Acute Stroke Imaging Study (MASIS)**

MASIS was a study performed at three acute stroke centres in Scotland between August 2008 and March 2010. The study was designed to investigate different imaging modalities, blood biomarkers and clinical aspects of acute ischemic stroke. Funding was provided by the Translational Medicine Research collaboration (TMRC), Dundee. The recruitment sites were Aberdeen Royal Infirmary, Western General Hospital, Edinburgh and Institute of Neurological Sciences, Southern General Hospital, Glasgow.

#### Study Objectives

- 1: To define parameter thresholds for tissue damage at presentation with MR diffusion/perfusion imaging and CT/CTP imaging
- 2: To refine imaging biomarkers for salvageable brain tissue
- 3: To define what proportion of patients can be scanned using advanced CT and MRI
- 4: To define what proportion of acute stroke patients have evidence of salvageable tissue at the time of presentation to hospital
- 5: To compare the practicality of CT and MRI based imaging techniques
- 6: To explore the relationship between imaging findings and blood biomarkers for haemostasis and inflammation
- 7: To explore the relationship between specific imaging findings and clinical progress and blood biomarkers
- 8: To use the acquired data to determine the practicality of using additional imaging methods in a clinical trial

As this was a multicentre collaborative study, only some of the overall objectives were carried out by me. These included the feasibility of performing advanced imaging with CT or MRI, and refining the thresholds for salvageable tissue and irreversibly damaged tissue in stroke and will be presented in later chapters.

### Study Design

MASIS was a prospective, observational study of the natural history of acute ischemic stroke conducted at three sites specifically relating CT and MRI methods, blood biomarkers and follow up imaging with clinical change. No therapeutic interventions specific to the study were involved. The aim was for equal recruitment with CT and MRI at baseline, and with follow up imaging at 72 hrs and 30 days with MRI (or CT if MRI contraindicated)

### Patient Selection-MASIS

The target for recruitment was 80 acute stroke patients, with baseline imaging performed within six hours of symptom onset; 40 patients with admission MRI and follow up MRI, 40 patients with admission CT and follow up MRI. No study specific procedures could be performed until consent was provided by the patients or assent was provided by the next of kin. Screening logs were kept at each site to help determine the barriers to patient recruitment.

If patients were eligible for thrombolysis, as the local imaging practice was to obtain CT prior to thrombolysis, all potential thrombolysis patients would have CT regardless of subsequent study specific imaging. Eligibility for receiving thrombolysis did not influence eligibility for study inclusion.

#### Inclusion Criteria:

- 1: Clinical Diagnosis of acute ischemic stroke
- 2: <6 hours after symptom onset

#### Exclusion Criteria:

- 1: Known non stroke diagnosis (e.g. Primary intracerebral haemorrhage, tumour, subarachnoid haemorrhage, epilepsy)
- 2: Inability to lie in a recumbent position for the duration of additional imaging (e.g. severe cardiac failure, desaturation on lying flat, high risk of aspiration)
- 3: Intercurrent illness likely to limit survival to less than 30 days
- 4: Coma
- 5: Chronic or acute renal failure
- 6: Known sensitivity to iodinated contrast media (including previous contrast reactions or severe asthma) for CT based imaging studies

7: Known sensitivity to gadolinium contrast, recently implanted ferromagnetic foreign bodies, intracranial aneurysm clip, or dependence on a cardiac pacemaker or implantable defibrillator for MRI studies.

Men and woman from all ethnic groups were considered eligible for the study. Children less than 18 years of age were excluded on the grounds that stroke in childhood is rare and is likely to have causes that differ significantly from that in older populations. All patients with suspected acute ischemic stroke meeting the inclusion criteria could therefore be considered for inclusion.

Patients admitted to the stroke unit of each hospital who were seen by a member of the research team at each site could be screened for inclusion. There was no specific restriction in terms of time of day or day of week when patients could be approached, but in practice the recruitment took place during the normal working week when members of the research time were available which usually corresponded to the times when MRI scanning was potentially available.

Patients were able to withdraw from the study at any time for any reason. An option to continue with clinical follow up was offered to subjects unwilling to undergo further imaging studies. All data collected prior to withdrawal were retained. Patient registration was managed at each site independently, and each patient was assigned a study number in the form X-XX with the first digit representing the site and the second representing the unique patient identifier at that site.

Study protocol and consent forms were reviewed by the Multicentre Research Ethics Committee for Scotland and ethical approval for the study was granted in October 2007 (reference 07/MRE00/96). Patient and relative information sheets along with accompanying consent and assent forms are attached in the appendix.

#### Baseline imaging

Imaging on admission was with either CT or with MR (aim was for 50:50 recruitment with each) with exclusion criteria for each modality considered and



documented as appropriate. If both imaging modalities were equally available MRI was the preferred option.

CT imaging at baseline included whole brain non contrast CT, CT perfusion and CT angiography from aortic arch to vertex. Multimodal CT examination was obtained using a Multidetector Scanner (Philips Brilliance 64 Slice). Whole brain NCCT was acquired first (5 mm slice thickness FOV 218 x 218 mm, 120kV, 171 mA or 0.9 mm slice thickness, FOV 250x250mm, 120 kV, 404 mA) followed by CTP with 40mm slab coverage (8x5mm slices, FOV 25cm, 80kVp, 476 mAs, 2 second cycle time, 30 cycles) using a 50 ml contrast bolus administered at 5mls/second (350 Xenetix) via a large-gauge venous cannula, usually placed in the antecubital fossa. CTP was followed by CTA from aortic arch to the top of the lateral ventricles (0.67 mm slice thickness, 120 kV, 475 mA) using bolus tracking to enable correct timing of image acquisition.

MRI on admission included DWI, PWI, T2, FLAIR post contrast, gradient echo, Circle of Willis Time-Of-Flight MR angiography. MRI acquisition parameters are included in Appendix 2.

### Clinical Assessment

All patients had full clinical assessment on admission to hospital using validated scales including NIHSS and OCSP classification. Additional clinical information included blood pressure, capillary blood glucose, body temperature, concomitant medications, ECG, social history (e.g. smoking) and family history. NIHSS was repeated at 24hr, 72hr, day 7 and day 30, Blood pressure and glucose were recorded at 4 hourly intervals for the first 48 hours, and thereafter at the same intervals as NIHSS. Pre-morbid modified Rankin scale was recorded at baseline and was repeated using structured questionnaire at day 30 and 90 after stroke onset. Blood samples for biomarkers were taken at baseline, 2hrs post lysis administration (only if given lysis), 24, 48,72hrs, 7 days and 30 days post stroke. Other bloods taken as part of routine clinical care included baseline full blood count, urea and electrolytes, and coagulation profile, the results of which were recorded .

### Follow up imaging

All MRI compatible patients were scheduled to have followed up MRI at 72hrs and day 30 irrespective of the choice of baseline imaging modality. For those patients who were unable to undergo follow up MRI at 72hrs, non-contrast CT and CT angiography were performed instead. Day 30 imaging was not performed using CT.

72 hr MRI included DWI, PWI, T2, FLAIR post contrast, gradient echo and Circle of Willis MRA. Day 30 MRI included DWI, PWI, T2, FLAIR post contrast and Gradient Echo.

Follow up CT imaging if MRI was unavailable or contraindicated was with whole brain NCCT followed by intracranial CTA from base of skull to the top of the lateral ventricles. If the initial occlusion was extracranial, the subacute CTA was extended using the same protocol as the admission CTA. The MASIS study calendar is shown in table 3.1

Procedure	Baseline	24h	48h	72h	Day7	Day30	Day90
Informed consent/Assent	✓						
Non contrast CT brain	†	*					
CT Perfusion	*						
CT Angiography	*	✓					
MRI brain	*			✓		✓	
NIHSS	†	✓	*	✓	✓	✓	
Blood Samples	✓	✓	✓	✓	✓	✓	
Modified Rankin Scale	✓					✓	✓

**Table 3-1 MASIS Study Calendar**

MASIS study calendar with procedures at different time points. ✓ denotes study-specific procedure † denotes clinically routine procedure, data captured for study, \* denotes procedure clinically routine in some patients

### **3.2.1 Data Recording and Transfer**

All study specific data were recorded on a paper case record form for each patient kept at the site of recruitment. The data were subsequently transferred to a web based electronic database (<http://tmrc-openclinica.lifesci.dundee.ac.uk>) for centralised data checks and statistical analysis by research fellows at each site. Image analysis for all patients was recorded on pre-specified data collection sheets and transferred centrally. The image analysis undertaken for the overall study is not covered in this thesis, although specific subgroup analysis will be included in due course.

Raw imaging data were transferred between the recruiting centres via the national Picture Archiving and Communication System for Scotland. Scans were downloaded from there onto radiology workstations locally for anonymization of data prior to study specific image analysis. Anonymization of imaging data from each study will be discussed later in this chapter.

Although all image data were collected, the only data that will be discussed within this thesis relate to those patients imaged with multimodal CT on admission as these patients could be combined with patients from an additional study using multimodal CT on admission.

### **3.3 POSH- P<sub>O</sub>st Stroke Hyperglycaemia**

The second observational study into acute stroke which took place during my research fellowship was the POSH study (Pathophysiology of acute post-stroke hyperglycaemia in relation to brain perfusion and arterial patency). The purpose of POSH was to define the interaction of early and delayed hyperglycaemia with arterial patency and brain perfusion in acute stroke patients, which was a single centre, prospective, observational study in with an aim to recruit approximately 100 acute stroke patients. Much of the imaging and clinical data for the POSH study overlapped with the MASIS study allowing elements of each to be combined for the work presented.

Funding for the POSH study was from an award from the Stroke Association (awarded July 2006)

#### Study Objectives-POSH

The primary research question was whether there is a difference in the growth of irreversibly damaged tissue after stroke between patients in whom blood glucose remains normal throughout, in whom blood glucose is increased early (within 6 hours of onset), and in whom blood glucose is initially normal but increases later (>6 hours after onset). Additional secondary outcomes included:

- 1: Interaction between blood glucose and recanalisation
- 2: Interaction between recanalisation and infarct growth
- 3: Penumbra salvage according to recanalisation and glucose status
- 4: Clinical progression and glucose status
- 5: Influence of glucose on death and dependency at day 30 after stroke

## Patient Selection-POSH

Acute Stroke patients presenting to the Institute of Neurological Sciences, Southern General Hospital, Glasgow within 6 hrs of symptom onset were considered for study entry. No study specific procedures were performed without written consent was obtained from the patient (or assent from a relative if appropriate). All imaging protocols for the POSH study used CT, both at baseline and at follow up. If CT CTP and CTA were obtained for clinical reasons (meaning at the discretion of the stroke physician dealing with the patient on admission), patients were offered participation in the study in retrospect as the other information obtained during the first 24hrs of study participation was the same as that obtained during routine care for acute stroke and would not have altered the information obtained for study purposes.

### Inclusion Criteria:

- 1: Clinical diagnosis of acute ischemic stroke
- 2: <6 hours after symptom onset

### Exclusion Criteria:

1. Known non-ischemic stroke diagnosis prior to consent )(e.g. primary intracerebral haemorrhage, tumour, subarachnoid haemorrhage, epilepsy)
2. Known sensitivity to iodinated contrast media (including previous contrast reactions or severe asthma)
3. Inability to lie in a recumbent position for the duration of additional imaging (e.g. severe cardiac failure, desaturation on lying flat, high risk of aspiration)
4. Intercurrent illness likely to limit survival to less than 30 days

Again only patients seen by a member of the research team on admission (or soon after if additional imaging was performed for clinical reasons) were able to be entered into the study. Informed written consent was obtained from the patient where possible, while assent from the next of kin was obtained if the

patient was unable to provide consent (e.g. aphasia). Patients could withdraw from the study at any time for any reason and all data collected prior to withdrawal was retained.

Ethical approval for the study was granted by the Scotland A research ethics committee on 22<sup>nd</sup> Feb 2007. Patient and relative information sheets and consent/assent forms are attached in the appendix.

### Imaging

Initial imaging for POSH comprised whole brain non-contrast CT, CT perfusion, and CT angiography from the aortic arch to the vertex. Parameters for CT were identical to those for MASIS. Follow up imaging was scheduled for 24-48 hrs and comprised whole brain non-contrast CT and CT angiography of the intracranial vessels only. If no occlusion was seen on the admission CTA and there was no clinical suspicion of a new/repeat occlusion, CTA was not performed at 24-48 hrs. Where the treating clinician requested MRI for follow up imaging for clinical reasons (typically performed if minor clinical deficit and normal admission imaging), CT/CTA was not routinely requested for study purposes as it was considered that MRI would be more likely to reveal the final infarct extent and that additional CT imaging in this setting would not necessarily be required.

### Clinical assessment

Clinical assessment at baseline included NIHSS, OCSP classification and pre-morbid Modified Rankin Scale. NIHSS was repeated at 24hrs, 72hrs and day 7 after stroke onset. Clinical outcome following stroke was assessed at day 30 using the Modified Rankin scale according to a structured questionnaire, along with Barthel Index. Clinical measurements of blood pressure, capillary blood glucose and temperature were assessed at 4 hourly intervals for 48 hours and thereafter at 72hrs and 7 days.

Concomitant medications including thrombolysis were recorded, but no study specific therapeutic interventions were performed for the study. Blood samples specific to the study included HbA1C and a single serum sample frozen and stored for future analysis, although other blood samples were taken on most

patients as part of routine clinical practice such as blood count, urea and electrolyte profile and coagulation profile.

Data were recorded on a paper case record for each patient which was stored locally. Once completed, data from the paper CRFs were transferred to a master database in SPSS format locally for analysis. Study procedures are summarised in table 3.2

Procedure	Baseline (<6h)	6-24h	24-48h	72h	Day 7	Day 30
Informed consent or assent from next of kin	✓					
Non-contrast CT brain	×		*			
CT Perfusion	×					
CT Angiography	×		✓			
NIHSS	×		*	✓	✓	
Blood Sample - biomarkers	✓					
Blood sample – HbA1c, glucose	×					
Blood sample – U&Es	×		*			
Capillary Blood Glucose	×	×	×			
TCD	*	✓	✓			
Modified Rankin Scale						✓

**Table 3-2 POSH Study Calendar**

✓ Denotes study-specific procedure

×

\* denotes procedure clinically routine in some patients

### 3.4 Combined Studies Image Analysis

Imaging data from each study were used for this thesis as the inclusion criteria, baseline CT imaging protocol and clinical follow up showed overlap and therefore permitted amalgamation of both datasets relatively easily. Follow-up imaging from each study was similar in terms of assessing infarct volume and recanalisation at subacute time points (24-72hrs) and as a proportion from MASIS had contraindications to MRI, the same imaging modality at follow up was used for many patients was used (non-contrast CT and CTA). All image analysis on the combined datasets was performed blinded to clinical information, and therefore required anonymization of imaging data prior to analysis.



As the focus of the thesis is on CT based imaging in acute stroke, a combined database from both studies with CT imaging on admission was compiled, forming the bulk of the data presented.

### **3.4.1 Image Transfer, Anonymization and Storage**

After imaging data were acquired locally, the raw images in DICOM format were transferred to a workstation where interpretation of images was undertaken for clinical purposes. A copy of the raw image data were made on the same workstation for study purposes, which included a DICOM header specific to that patient and imaging time-point so that the images could be identified for future use. Patient identifiers from the initial raw data were removed (including name, age, date of birth, physician) and were replaced with study specific DICOM headers. The programme used for this purpose was Philips Brilliance Workstation package. The same procedure was followed for both CT and MRI data after initial transfer to the workstation. Imaging data from remote sites for the MASIS study was anonymized using the same technique after the raw data were downloaded to the workstation from the National radiology archive for Scotland.

After initial anonymization, a CD copy of each study scan was made which were subsequently archived on an external hard drive for storage. The hard drive was password protected for security purposes. In addition, all other remaining DICOM headers were removed using an additional anonymization tool (Neologica Dicom Anonymizer Pro version 1.1.19, [www.neologica.it](http://www.neologica.it)) ensuring that all imaging data stored externally had no DICOM headers which could be used to identify the patient apart from a study specific DICOM header and date of acquisition.

### **3.4.2 Image Analysis**

Different methods used for image analysis will require detailed descriptions specific to the relevant chapters, but all scans were processed and interpreted by me according to the same method initially in order to classify study recruits into different groups according to different characteristics (e.g. perfusion deficit, occlusion status, recanalisation, intracerebral haemorrhage). This interpretation was performed blinded to treatment and clinical outcome.

Admission imaging

Initial imaging was evaluated beginning with Non contrast CT for the hemisphere affected (if any), presence/absence of a hyper-intense vessel sign indicating arterial occlusion and for ASPECTS(320).

CTP was processed next on the proprietary software present in the Philips Brilliance brain perfusion module obtained for clinical use in the Neuroradiology department of the Institute of Neurological Sciences, Glasgow. Raw data were loaded and underwent an automated motion correction. The arterial input function was selected manually by placing a region of interest within the anterior cerebral artery contralateral to the ischemic lesion, and the venous output function was selected after placing a region of interest in the superior sagittal sinus. Perfusion maps including CBF, CBV, MTT and TTP were automatically generated and were interpreted for presence/ absence of ischemic lesion on each of the ASPECTS regions (79). After initial qualitative analysis of the CTP, thresholds for core and penumbra were applied and displayed in a final summary map “penumbragram”. Penumbra pixels were defined by those pixels ipsilateral to the stroke lesion with prolonged MTT  $\geq$  145% of the normal contralateral hemisphere with normal cerebral blood volume. Core pixels were defined as those with prolonged MTT ( $\geq$ 145% of normal) but with reduced cerebral blood volume below 2.0ml/100g (131)). As core and penumbra were presented visually on each perfusion scan slice, an overall qualitative measurement of mismatch was taken (mismatch defined as perfusion lesion >20% larger than the core lesion). Volume of core and penumbra were also calculated using the total area of core and penumbra according to the thresholds mentioned (area measured in mm<sup>2</sup>) multiplied by the slice thickness (5mm). If the processed CTP parameter maps had no obvious perfusion deficit present visually (e.g. lacunar stroke, brainstem stroke missed by perfusion slab) thresholds were not applied for core and penumbra as this was likely to have resulted in false positive volumes for each.

CT angiography for each patient was evaluated for presence / absence of arterial occlusion and if occlusion was present, the arterial segment occluded was recorded. CTA source images were reviewed initially from the aortic arch to the vertex and each arterial segment was followed proximally to elucidate any segments which did not fill with contrast. 3D MIP reformats in sagittal, coronal and axial planes were reviewed for occlusion site and collateral status. An

occlusion was defined as absence of contrast in a vessel which separated the proximal portion of the vessel from the distal portion(111), and occlusions were classified as extracranial ICA, intracranial ICA, M1 segment MCA, M2 segment, M3, ACA and PCA. Circle of Willis anatomy was also recorded.

### Follow-up Imaging

Presence or absence of a visualised infarct was recorded after assessment of the non contrast CT or MRI FLAIR sequence of the subacute imaging scans (usually obtained at 24-72hrs). Final infarct ASPECTS was recorded using the same method as for the admission scan ASPECTS grading, while presence or absence of haemorrhage was recorded , and classified as HI1 (Small patchier along margins of infarct) ,HI2 (more confluent patchier within the infarcted area), PH1( blood clot not exceeding 30 percent of the infarcted area with some mild space occupying effect) and PH2(dense blood clot/clots exceeding 30 percent of the infarcted area with significant space occupying effect)(44).

Follow up CTA or MRA were evaluated for change in the appearance of the baseline occlusive lesion. Again, source angiographic data were viewed initially followed by MIP images in 3 planes as before. Recanalisation was determined by comparing the initial and follow up angiographic appearances which were measured using an adaptation of the TIMI score; TIMI 1=no recanalisation, 2= minimal recanalisation, 3=partial recanalisation, 4=complete recanalisation.

### Additional Imaging Platform: MIStar

In addition to the baseline characterisation of each patient described above, further imaging analyses were undertaken which required an alternative imaging platform which permitted image co-registration, evaluation of a variety of different perfusion thresholds, volumetric measurement of infarct volumes, and dynamic interpretation of raw CTP data to confirm the direction of collateral blood flow distal to arterial occlusions. A licence for the imaging platform was obtained in April 2010, after I received initial training in its use during a 6 week visiting fellowship to the John Hunter Hospital, Newcastle, New South Wales Australia under the Supervision of Dr Mark Parsons in November/December 2009. MIStar is a software package that provides manipulation, visualization and

processing of medical images in a diagnostic imaging setting, and was used for the majority of image analysis covered in this thesis. A number of different modules were available for use including a stroke module designed for CTP processing using a fully deconvolved methodology and a fusion tool permitting accurate co-registration of subacute imaging with CT/MRI to CTP raw data and interpolating the follow up images to match the orientation of the CTP scan. An ROI tool was also available which permitted manual drawing or semi-automated generation of ROIs to map out areas of interest such as infarct extent with an automated calculation of lesion volume as needed. These ROIs could be copied, saved for future use, and transposed to images different to those on which they were originally obtained. Exact descriptions are provided in later chapters. The MIStar interface screen is shown for descriptive purposes in figure 3.1

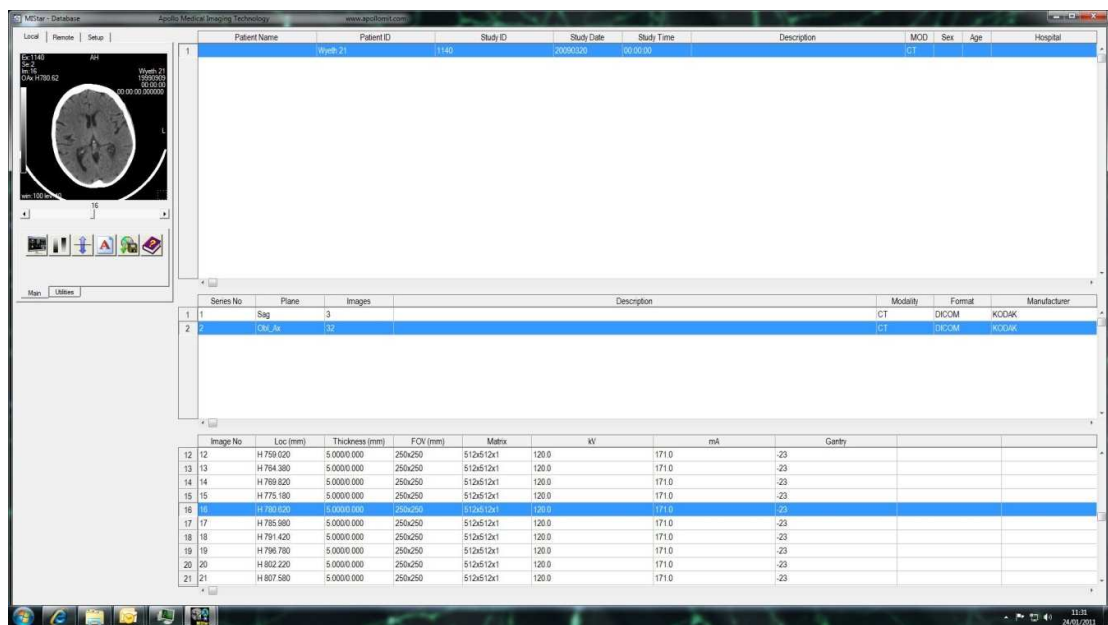


**Figure 3-1 MIStar Interface**

MIStar stored imaging files for analysis in the format shown above. Anonymized scans could be highlighted and examined in a variety of image processing modules accessed from the icons on the top right of the screen. Data characteristics from each slice are shown in the bottom third of the screen

### 3.5 Conclusion

Data included in this work were obtained from two observational studies into acute stroke which were undertaken at the Institute of Neurological Sciences during my research fellowship based there and at the University of Glasgow from February 2009 to August 2011. As a member of the stroke research team, I was

involved in many different aspects of each study, including patient screening, obtaining informed consent/assent, performing clinical assessments, requesting imaging procedures, maintenance of paper and electronic case record forms and imaging data transfer, anonymization and storage prior to analysis. All image analysis was performed by me after appropriate training both locally and abroad. Other members of the research team locally and in other centres made major contributions to each study, the end result of which resulted in a relatively large population of acute stroke patients with imaging data available for examination in the upcoming chapters of this thesis. The two studies used had several similar characteristics such as inclusion and exclusion criteria, baseline imaging protocols for multimodal CT, clinical information and follow up permitting the amalgamation of much of the data from the two studies for analysis.

## Chapter 4. Feasibility of Imaging Based Study Recruitment

### 4.1 Introduction

Advanced brain imaging with either MRI or multimodal computed tomography CT offers the potential to select specific treatment strategies for individual patients based on the volumes of irreversibly damaged core tissue and tissue with characteristics of the ischemic penumbra (131, 143). Although further validation of the imaging based targets for therapy is required, a number of stroke trials and open label studies have used advanced imaging techniques, predominantly using MRI in order to identify patients with specific imaging patterns prior to therapy or to measure imaging findings such as reperfusion, recanalisation or infarct growth as potential surrogate markers for outcome(47, 48, 51, 154). Most of these studies have focussed on acquiring, but not necessarily interpreting MR imaging prior to trial entry and have shown several findings supportive of the use of additional imaging for trials in acute stroke. The DEFUSE Study showed that early reperfusion was associated with clinical benefit in those with perfusion/diffusion mismatch, but that reperfusion was not beneficial in those without mismatch (153). The DIAS I trial showed that dose dependant reperfusion after desmoteplase was correlated with clinical outcome in patients selected on the basis of pre-defined perfusion/diffusion mismatch while the DEDAS trial suggested efficacy of Desmoteplase at a dose of 125micrograms/litre in stroke patients with perfusion and diffusion mismatch(48, 321). EPITHET suggested that alteplase was associated increased reperfusion in patients with PWI/DWI mismatch between 3 and 6 hrs after stroke onset compared with placebo and that reperfusion was correlated with improved clinical outcome, although no clear effect on infarct growth was seen (154).

These studies confirm that MRI measures such as mismatch between infarct core and potentially salvageable penumbral tissue are attractive (if not yet uniformly defined) therapeutic targets which can be visualised using MRI, and that imaging findings before and after therapy may correlate with response to therapy. However some limitations of these studies should be considered; MRI was not reviewed prior to entry to the EPITHET study partly due to slow post processing

which would have caused unacceptable delays in treatment even after the additional imaging was performed. Recruitment to most MRI based trials in acute stroke has been restricted to a relatively small number of expert centres with sufficient resources to perform such studies. Despite adequate resources in terms of imaging availability and staff, rates of patient recruitment to these trials have been slow in comparison to earlier trials of rt-PA which required only non contrast brain CT at entry, although time window and entry criteria varied between different trials and observational studies which could also influence recruitment rate. A recent study using multimodal CT based selection criteria prior to randomisation to IV tenecteplase or alteplase has demonstrated the excellent potential for CT based trial recruitment with high recruitment rates even with a very specific imaging target(52) .Importantly, this study required interpretation of imaging prior to randomization and mean time from symptom onset to treatment administration was rapid, demonstrating that time taken for multimodal CT acquisition and interpretation is not a barrier to rapid treatment or to trial participation. However the centres recruiting to this study were large centres with extensive experience in use of multimodal CT, and still the proportion of patients recruited was just 3% of those screened, reflecting inherent barriers to recruitment including the pre-specified imaging criteria. This finding highlights the importance of centres with high volumes of stroke admissions as well as experience in advanced imaging interpretation when designing such trials. Recruitment rates for trials and observational studies of IV thrombolysis and their different imaging requirements are shown in figure 4.1

Study	Modality	Time Window (h)	Duration (years)	Participating Centres	Number recruited	Crude Rate per centre per year	Mean Age	Median NIHSS
EPITHET	MRI	3-6	7	15	101	1.0	71.6	13
DEFUSE	MRI	3-6	4	7	74	2.6	70.9	11.5
DEDAS	MRI	3-9	2.6	25	37	0.6	73*	11
DIAS	MRI	3-9	2.7	44	104	0.9	68*	12
DIAS II	CT/MRI	3-9	1.7	52	186	2.1	71	9
NINDS	CT	0-3	3.7	43	624	3.9	67-69 <sup>†</sup>	14-15 <sup>†</sup>
ECASS	CT	0-6	1.5	75	620	5.5	65-66 <sup>†</sup>	12-11 <sup>†</sup>
ECASS II	CT	0-6	1.3	108	800	3.2	68 <sup>†</sup>	11 <sup>†</sup>
ECASS III	CT	3-4.5	4.3	130	821	1.5	65-66 <sup>†</sup>	9-10 <sup>†</sup>
TNK-NEJM	CT/CTP/CTA	0-6	3	3	75	8.3	68-72	14.4 $\Omega$

**Table 4-1 Recruitment Rates of Trials and Observational Studies of Thrombolysis using CT or MRI**

Key characteristics of randomised trials and observational studies of IV thrombolysis and imaging modality are demonstrated, including crude recruitment rates. Trials using imaging selection for Intra-arterial therapy are not included as additional factors such as restricted access to IA therapy are additional barriers to recruitment to these studies.\* Median age, † Placebo and treatment groups,  $\Omega$  Mean NIHSS,



Designing clinical trials which select patients with specific occlusion subtypes or perfusion patterns are likely to result in a more homogenous study population which will have the advantage of reduced sample size requirements in order to prove a beneficial effect of the agent being investigated(20). This benefit could be offset by higher numbers of screening failures due to more stringent inclusion or exclusion criteria, while the practical difficulties of obtaining and processing additional imaging before deciding on eligibility represents another potential recruitment barrier. An additional consideration for trial design is that the choice of imaging modality may also affect the ability to recruit patients. This may be the case as those with contraindications to undergo MRI may differ from those without, while the centres recruiting may also be different depending on the availability of different imaging modalities.

Multimodal CT is generally more widely accessible than MRI, is better tolerated with shorter acquisition times, and has fewer contraindications although renal impairment and hypersensitivity to contrast material may preclude additional imaging with CT and excessive radiation dose is a concern(116). The limited brain coverage offered by most CTP protocols is also a limitation compared to MRI, although whole brain coverage may eventually become available (114). While multimodal CT imaging may provide information similar to that obtained with MRI in acute stroke, it has been less frequently studied as an entry selection criterion (47).

Better understanding of the impact of imaging biomarker selection on key factors such as recruitment rates and study population characteristics is needed to aid the design of future therapeutic trials. These issues were therefore investigated prospectively as part of the MASIS study comparing acute CT and MRI as initial imaging modalities in acute stroke.

Some of the content of later chapters will be focussed on the validation of CT thresholds for core and penumbra which would be important for trial selection criteria. Initially however the question of whether there is a need for multimodal CT imaging for trial purposes was examined using data from the

MASIS study, which was designed in part to compare advanced MR and CT-based techniques for imaging in acute stroke. This chapter will examine the feasibility of performing each modality in the acute time window after stroke, as well as the difficulties encountered in obtaining imaging based outcomes at different time points after stroke and will argue that imaging with multimodal CT could be used to expand the number of patients potentially entered into imaging based stroke trials.

## 4.2 Methods

Feasibility of imaging with CT and MRI at different time-points was examined as part of the MASIS study. Recruitment, study protocol, ethical approval and data collection was described in chapter 3. In summary, acute stroke patients admitted to the three participating stroke centres between August 2008 and March 2010 were prospectively screened for recruitment to MASIS, an observational study examining clinical, imaging and blood biomarkers of salvageable tissue and outcome after ischemic stroke. Each site had access to MRI scanners with the ability to perform stroke imaging including DWI, PWI, FLAIR, GRE and MRA, and multimodal CT including non contrast brain CT, CT CTA and CTP (CTP/CTA was unavailable in Aberdeen for the first 18 months of the study meaning MRI was the exclusive imaging modality at this site for the majority of the recruitment period). Acute imaging was performed within 6 hours of symptom onset, and thereafter was scheduled for 72 hrs and 30 days. Acute imaging could be with either CT or MRI, whichever was available, while follow-up imaging was with MRI unless there were contraindications or MRI was not available.

Screening logs were maintained at each study centre in order to document reasons for inclusion or exclusion of patients from study participation after initial screening. As the aim was to recruit equally with CT and MRI after admission, the reasons for choosing one modality over the other were recorded prospectively. If both CT and MRI were equally available, MRI was the default imaging choice. As scans were obtained for research purposes, they were not routinely evaluated to aid decision making on acute management including thrombolysis unless specifically requested by the treating physician

All clinical and imaging data from the three sites were examined together after the last patient follow up was completed and data were entered into the online database. Imaging modality used per time point (CT or MRI) and the reasons for each were documented. Clinical characteristics examined included age, sex, smoking status, alcohol intake, stroke risk factors, pre-morbid modified Rankin scale, medication history, NIHSS, OCSP, blood pressure, body temperature and hemisphere affected. Clinical characteristics of those imaged using CT or MRI on admission were compared using the t-test and Mann-Whitney test for normally and non-normally distributed variables respectively. Associations between categorical variables were assessed using the chi-squared test.

### **4.3 Results**

Patient screening commenced on 21/04/2008 and completed on 31/03/2010, with the last patient follow-up performed in June 2010. 360 patients were screened as potential study recruits within the time period, and informed written consent or assent for study participation was obtained from 93. Reasons for non study participation were:

- 1: Refusal of consent (n=17)
- 2: Recruitment to other study (n=52)
- 3: Unknown (n=5)
- 4: Non ischemic stroke diagnosis (n=69)
- 5: >6hrs from symptom onset (n=36)
- 6: Renal failure (n=7)
- 7: Medical co-morbidities (n=3)
- 8: MRI incompatible (n=16)
- 9: MRI unavailable (n=9)

10: Research staff unavailable (n=50)

11: Comatose (n=4)

12: Onset time unclear (n=8)

13: Incorrect diagnosis on admission (n=1)

Study recruitment is summarised in Figure 4.1, with screening log data from each site summarised in table 4.2.

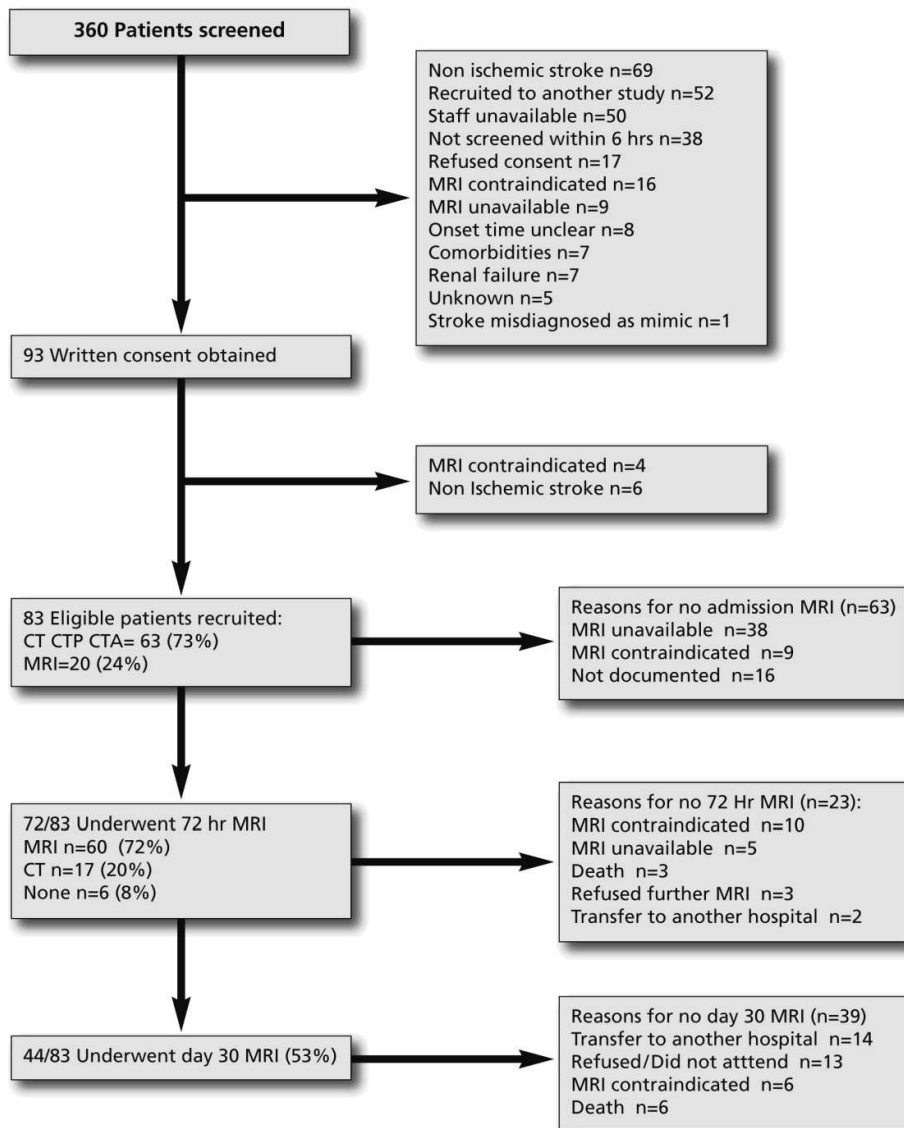


Figure 4-1 Flowchart for Recruitment to MASIS Study

	Aberdeen	Edinburgh	Glasgow	All
Screened	45	185	130	360
Consented to study	12	42	39	93
Completed Study	8	37	38	83
Refused consent	3	3	11	17
Other Study	0	5	47	52
Unknown	1	3	1	5
Non ischemic stroke	4	37	28	69
>6hrs	0	34	2	36
Renal Failure	0	6	1	7
Co morbidities	0	2	1	3
MRI incompatible	9	6	1	16
MRI unavailable	9	0	0	9
Staff not available	10	40	0	50
Coma	0	4	0	4
Onset time unclear	0	8	0	8
Incorrect non-stroke diagnosis on admission	0	1	0	1

**Table 4-2 Screening Failures for Study Participation in MASIS**

Reasons for failure to recruit after screening in each site are shown. The reasons varied considerably between sites which likely reflects differences in imaging availability at each site, but also different practices for screening and recruiting patients which limits what conclusions can be drawn from the study on feasibility of imaging based study recruitment

As consent was obtained prior to performing study-specific imaging, some patients who had provided written consent in fact had a non-ischemic stroke diagnosis. These included:

1: Primary intra-cerebral haemorrhage (n=4)

2: Migraine with focal neurological deficit (n=2)

These 6 patients were recruited but withdrawn from study participation thereafter when the correct clinical diagnosis was confirmed. One patient recruited locally in Glasgow became claustrophobic prior to acquisition of study imaging with MRI acutely and chose to withdraw from study participation immediately. 3 patients consented to the study in Aberdeen but could not tolerate MR imaging due to:

1: Claustrophobia (n=1)

2: Body habitus (n=1)

3: Inability to tolerate MRI scanner noise (n=1)

After removal of these 10 patients unable to participate despite providing written consent, a total of 83 eligible patients remained in the study for the final analysis.

There were 50 males and 33 females recruited to the study, with a mean age of 70 years (SD 14). 18 (22%) had a previous diagnosis of stroke, 54 (65%) had hypertension, 23 (28%) had atrial fibrillation and 28 (33%) had previous ischemic heart disease. Median NIHSS on admission was 7 (Range 1-30) with a mean NIHSS of 9.8 (SD 7.52). In terms of OCSF classification, 20 (24%) had TACS, 42(51%) were PACS, 6(7%) were POCS and 15 (18%) were LACS. 31 (41%) received IV rt-PA with a further 2 randomized to the control arm of the IST3 study(322).

#### **4.3.1 Acute Imaging**

Baseline imaging was with CT for 63 (76%) and with MRI for 20 (24%) patients, rather than the target of equal distribution between both modalities. For those

imaged using CT at baseline, MRI was unavailable (38, 60.3%) was contraindicated (9, 14.3%) or an exact reason was not documented (16, 25.4%). Patients imaged with CT or MRI on admission did not differ in most baseline characteristics including stroke risk factors, medications, and blood pressure. However, those who were imaged acutely with MRI differed from those imaged with CT in respect of some characteristics:

1: Younger age. Mean age for MRI group = 65 years (SD 15) Mean age for CT group =72 years (SD 11),  $p=0.024$

2: Pre-morbid disability. Pre-morbid mRS was 0 for 19/20(95%) of MRI group and 35/63 (56%) of CT group,  $p=0.0013$ )

3: Non dominant hemisphere stroke location. Right hemisphere strokes accounted for 13 (72%) of the MRI group and 15 (33%) of the CT group,  $p=0.0041$ )

Differences in groups depending on admission imaging modality are summarised in table 4.3.



Parameter	Baseline MRI	Baseline CT	P
Age, years, mean (SD)	64.7 (14.9)	71.9 (11.4)	0.024
Male Sex	14 (70.0%)	36 (57.1%)	0.31
Smoking Status			
Never	8 (40.0%)	24 (38.1%)	0.57
Ex-smoker	5 (25.0%)	23 (36.5%)	
Current	7 (35.0%)	16 (25.4%)	
History of Previous Stroke	5 (25.0%)	13 (20.6%)	0.58
Hypertension	13 (65.0%)	41 (65.1%)	0.99
Diabetes	1 (5.0%)	8 (12.7%)	0.52
Atrial Fibrillation	4 (20.0%)	19 (30.2%)	0.38
Ischemic Heart Disease	5 (25.0%)	23 (36.5%)	0.48
Pre-morbid Modified Rankin Scale			
0	19 (95.0%)	35 (55.6%)	0.0013
1	1 (5.0%)	10 (15.9%)	
2	0 (0%)	11 (17.5%)	
3	0 (0%)	6 (9.5%)	
4	0 (0%)	1 (1.6%)	
NIHSS on admission, mean (SD)	8.0 (6.0)	10.3 (7.9)	0.22
Right Hemisphere Affected	13 (72.2%)	15 (32.6%)	0.0041

**Table 4-3 Comparison of Clinical Characteristics Between Patients Imaged Using CT or MRI on Admission for MASIS**

MASIS patients imaged at baseline with MRI were more likely to have non dominant strokes, had lower pre-morbid Rankin scales and were younger than those imaged with CT. The Students t test and Mann Whitney U test were used for testing differences between continuous and categorical variables, respectively.

### **4.3.2 Subacute Imaging**

At 72hrs most patients (n=60, 72.3%) were able to undergo imaging with MRI as planned in the study protocol. A subset of patients (n=16, 19.3%) had imaging with CT rather than MRI and 7 patients (8.4%) had no imaging performed at this time-point. Reasons for MRI not being performed at 72hrs included:

- 1: MRI contraindicated n=10 (12%)
- 2: MRI scan unavailable n=5 (6.3%) (e.g. due to administrative reasons or scanner malfunction)
- 3: Death n=3 (3.6%)
- 4: Transfer to another hospital for rehabilitation n=2 (2.4%)
- 5: Patient refusal of MRI scanning n=3 (3.6%)

### **4.3.3 Day 30 Imaging**

Day 30 imaging with MRI was performed in just over half of the eligible patients recruited to the study (n=44, 53%). Reasons for study imaging not being performed included:

- 1: Patient refusal of further imaging n=10 (12%)
- 2: Transfer to another hospital for rehabilitation n=11 (13.4%),
- 3: Death n=8 (9.6%)
- 4: MRI incompatibility /contraindications n=10 (12%)

Study imaging at each time point is summarised in Figure 4.2

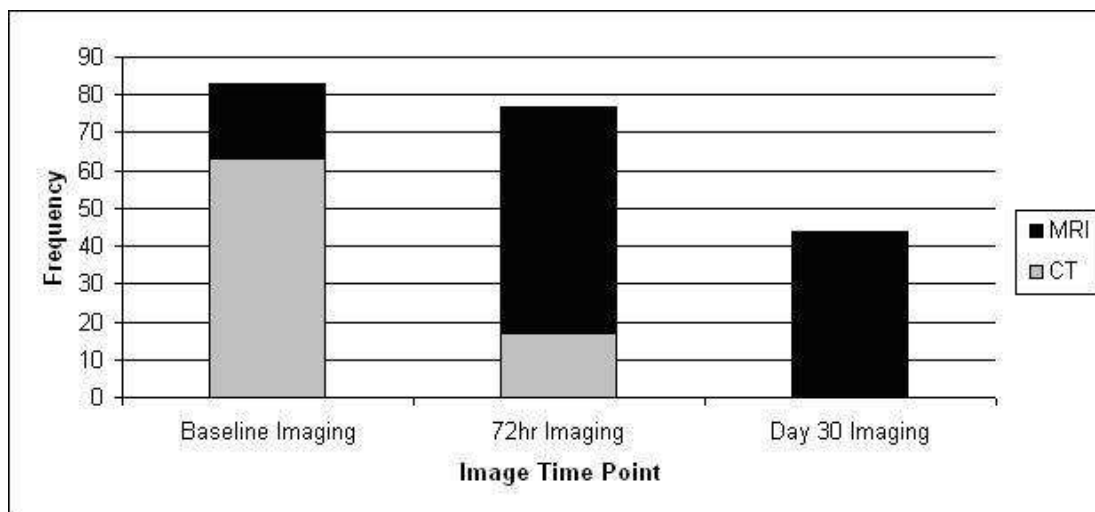


**Figure 4-2 Imaging Acquired at Each Study Time point**

Most patients at study entry had CT based imaging, with the majority being imaged with MRI at 72 hours. A high proportion did not have day 30 imaging.

## 4.4 Discussion

This analysis highlights some important issues regarding the practicality and feasibility of performing multimodal imaging with CT and MRI for research or trial purposes. Trials or open label studies of thrombolysis in the later time window after stroke which predominantly used MRI for case selection at baseline have had low overall recruitment rates from a smaller number of centres when compared to trials that used only non-contrast CT. This suggests that choice of imaging modality and acquisition of additional information beyond what is obtained with plain CT alone may be at the expense of the ease with which trials in acute stroke can be conducted. While other factors such as service changes over time and differing inclusion and exclusion criteria will also affect study recruitment, complexity of image acquisition can have a major influence on recruitment rate as evident in the recruitment rates of EPITHET and ECASS III which both studied alteplase in the extended time window but with different imaging protocols. Acute stroke trials and studies inevitably involve patients who are potentially clinically unstable and therefore additional imaging must be both safe and acceptable for the patients involved.

The present results confirm that limited access to MRI may be a major barrier to stroke trial recruitment. This is despite specific research funding and research

dedicated MRI scan time at each of the participating sites. Limited MRI access may be seen solely as an administrative barrier which reflects local circumstances and resources, but the limited number of sites capable of recruiting to other trials that select on the basis of complex imaging suggests that this is actually a widespread issue for acute stroke trials employing MRI as the imaging method of choice. Many patients remain unable to undergo MRI scanning due to relatively common contraindications such as metallic heart valves, pacemakers and claustrophobia. Even if MRI access was equal to that of CT, clinical instability and presence of hypoxia in acute stroke patients represent additional limiting factors for MRI given the longer time required for image acquisition(172). The MASIS study confirms that contraindications to MRI alone prevent imaging in a proportion of patients, similar to that reported previously (14%)(323). This finding has implications for trial design as a sizeable portion of otherwise eligible patients would be excluded from trials selecting on the basis of MRI findings alone(323). By comparing patients recruited with CT and MRI, this study has shown that the imaging modality chosen to select patients for research studies may directly influence the population recruited, with those imaged with MRI on admission being younger, more likely to have a non-dominant hemisphere stroke, and having less pre-morbid disability than those able to undergo multimodal CT examination using the same inclusion /exclusion criteria and time window. Although these results could just reflect investigator bias in selection of imaging modality, it is also consistent with reduced tolerability of longer examination times for MRI by older and more disabled patients, and, if representative of wider clinical practice, would restrict the generalisability of the results of randomised trials of treatments based on MR selection criteria to a younger and less disabled population than what would be representative of most stroke patients. No previous clinical study has compared imaging modality in a randomised manner and most insisted on either CT or MR but did not allow both freely. Indirect comparisons of trial reports do not identify any consistent difference in age or clinical stroke severity where MRI rather than CT selection has been used (Table 4.1). However DIAS II, the only trial that allowed recruitment based on either multimodal CT or multimodal MRI found significantly greater stroke severity in terms of NIHSS among CT-selected patients compared to MRI-selected patients, among other differences such as mismatch volume (47). Patients recruited to DIAS II with MRI

also had a trend towards younger age also but no statistically significant difference was detected. It is therefore possible that, in addition to restricting generalisability of overall trial results, imaging modality for patient selection will in itself systematically influence trial population characteristics and in turn potentially impact upon key parameters such as rates of favourable clinical outcome. These outcome measures are used to prove therapeutic effect and are determinants of sample size calculations. These results suggest that a greater proportion of patients, with a wider range of stroke severities and greater pre-morbid disabilities, more reflective of the complete range of patients that experience a stroke, are able to undergo multimodal CT compared to MRI within 6 hours of symptom onset. Based on these results, the recruitment rate for a trial with multimodal CT selection might be as high as 3-fold greater than for one based on MRI alone.

However, while minimising barriers to trial participation is important in order to maximise study participation, recruitment rates are not the only parameters of relevance in trial design and other important issues require discussion when considering multimodal CT as part of research and clinical imaging protocols. Limited brain coverage by the majority of CTP scans relative to that covered by MRI means that the volume of tissue covered per scan must be chosen manually at the time of scanning and even if the perfusion scan is appropriately located, volumes of core and penumbra or mismatch tissue which are present outside the reaches of the perfusion slab will inevitably be missed with a possible influence on penumbra volume or mismatch ratio for that patient. The definitions for core and penumbra on CT as well as the acquisition parameters used to obtain and process CTP scan are not yet agreed and there has been heterogeneous image acquisition in many CTP studies (168). Imaging with CTP and CTA requires exposure to ionizing radiation when screening patients for a trial based on utilising multimodal CT, requiring consent / assent for this exposure prior to scanning. Reports of excessive radiation dose with CTP with disfiguring consequences could conceivably influence patient choice, emphasising the need to standardise how scans are obtained (324). The requirement for administration of iodinated contrast materials restricted in patients with renal impairment, known contrast hypersensitivity, or diabetes are other important considerations (325).

These findings are consistent with previously published results where the use of late imaging time-points for determining infarct volume was associated with patient drop-out (157). The reasons for patient drop-out were diverse and some (death, transfer to remote rehabilitation facilities) will affect trials regardless of imaging modality used. Patient refusal however, accounted for a high proportion of the numbers lost to follow-up in the MASIS study, and it appears that this is more commonly a problem with MRI for reasons such as claustrophobia and scanner noise. The high proportion able to be imaged at 72h supports the benefit for trials of using a subacute time-point for determining imaging outcome biomarkers since delaying until day 30 (or later) would require larger sample sizes to compensate for losses to follow-up which may in turn bias results as larger infarcts may be more likely to result in death prior to imaging at late time points. Using subacute imaging as an imaging outcome has some limitations; for example lesion swelling may result in overestimation of infarct volume in the first week in some patients(326), and some trials have used even later imaging time points to measure infarct volume(154). Use of an earlier imaging outcome this is likely to represent a reasonable compromise between accuracy of infarct volume measurement and ability to obtain useful study imaging because of patient drop out. This approach is supported by recent research suggesting that earlier time points for measuring infarct volume correlate well with later time points and therefore could represent an appropriate end point for trials measuring infarct volume. Therefore subacute imaging (i.e. 3-6 days) post stroke appears to be a time point which could be used for measuring infarct volume after stroke (156). Even earlier endpoints could potentially be used, as acute and subacute DWI lesions have been shown to be similar in patients with major reperfusion, but comparison of these to an accepted gold standard has yet to be performed (134).

Where imaging selection or analyses have been used in acute stroke studies, a single imaging modality has generally been used both on admission and at follow up. The data presented indicate that a flexible approach using acute CT on admission with follow up MRI is perhaps the most feasible approach. A combination of acute CT and follow-up MRI for study design could permit penumbral imaging rapidly and safely, but also allow infarct volumes to be measured accurately on FLAIR (156). When Multimodal CT was used to select

patients for trial entry for patients recruited to DIAS II, CT was also used for day 30 imaging outcome on this patient group (47). CT can be used to measure infarct volumes (327), although MRI if available has some advantages over CT including infarct delineation (328).

Using the same image modality throughout has advantages for image analysis in terms of calculating changes in lesion extent over time. Measurement of infarct growth from baseline to the final outcome measurement can be determined by a simple calculation of the difference between two volumes at different time points (e.g. final infarct volume on FLAIR - acute DWI volume = infarct growth (154)). As CTP has only limited brain coverage, simple measurements of the differences in CTP defined core and final infarct volume may reflect changes in brain coverage between scans rather than true evolution of infarct volume, meaning such simple calculations could be misleading. CT and MRI can however be combined in a relatively straightforward fashion by co-registration, placing acute and follow up imaging pixels into the same anatomical space for accurate measurement of outcome in tissue covered by the CTP slab. With imaging software this step can be performed easily permitting the combining of different modalities for trial purposes. Image co-registration may be required even when using MRI alone at each time point as has been highlighted in a reanalysis of the EPITHET trial results suggesting this image processing step is likely to be required regardless of image modality chosen at baseline and follow up (329). This fact implies that additional image post-processing is needed in determining tissue outcome and therefore combining imaging modalities is not necessarily a barrier to using a combination of image modalities. Other studies have demonstrated that Acute CT and follow up MRI can be relatively easily combined for these purposes (51).

Some limitations of this study do however limit the conclusions which can be drawn. Lack of success in recruiting using MRI acutely is likely to have been affected by treatments received by the patients acutely. Institutional protocols at each site required CT prior to thrombolysis, meaning any potential study recruit would have had CT rather than MRI acutely. This suggests that each site could have a bias towards obtaining CT initially despite each site having dedicated research slots and staff for MRI. Furthermore, the number of patients screened per site, as well as the different recruitment patterns suggests that

study recruits were not identified in the same way at each site. This also limits conclusions based on the overall cohort. In particular the clinical differences observed between MRI and CT based study recruits may reflect this bias, although the fact that the findings replicate previous work make it worthy of ongoing evaluation. Accessing MRI was more problematic for later time points with a high degree of drop out for late imaging, suggesting MRI at late time points as a measure of radiological outcome has clear limitations.

#### **4.4.1 Conclusion**

One of the purposes of the MASIS study was to explore the feasibility of obtaining advanced imaging for research purposes by adopting a flexible approach to image acquisition on admission and at follow up. The results suggest that acute stroke imaging with perfusion and angiography is generally more feasible using CT rather than MRI, but that follow up MRI can generally be obtained, particularly in the subacute time window after stroke. MRI was contraindicated in a proportion but limited availability was also an important factor which has implications when planning imaging based trials .

These results, along with DIAS II (47) which used both CT and MRI suggest that patients recruited on the basis of MRI alone may not be reflective of the wider stroke populations and this could limit the applicability of results from these studies on wider clinical practice. A number of patients were unable to have MRI follow-up at later time points which included a proportion of patients who refused MRI because of tolerability issues, although some loss to follow up would have occurred regardless of imaging modality. Subacute MRI, which was more feasible than day 30 imaging, may therefore have important advantages for trials that employ an imaging outcome marker.

As acute multimodal CT imaging is likely to be more feasible than MRI for acute stroke trials, further study of CT CTP and CTA will help validate its use for trials and for clinical practice.



## Chapter 5. Quantifying Collateral Flow Extent in Acute Ischemic Stroke

### 5.1 Introduction

Chapter one reviewed the evidence for therapeutic interventions in acute ischemic stroke which, considering the burden of disease and research activity remain relatively limited, focussing on techniques to recanalize occluded vessels with intravenous or intra-arterial rt-PA, or with mechanical clot removal.

Additional therapeutic options focussing on neuroprotection have not shown benefit in clinical trials despite promising experimental data (20). The reasons proposed for the failure of neuroprotective agents are numerous, with trial design being a consistent reported explanation, as the heterogeneity of patients recruited in trials may mask a subgroup(s) who may have benefited.

Identification of these specific patient subgroups with the use of additional imaging may be one way to improve trial design. Poor collateral blood flow has been suggested as an additional explanation for failure of neuroprotectants due to limited delivery to the site of action. While this is likely to be an overly simplistic view due to the fact that neuroprotectants should eventually reach a site of action if any residual flow is present, it has been one of the reasons suggested for considering collateral flow adequacy in trial design. In addition, collateral flow to the area served by an occluded vessel via a developed collateral circulation may also be associated with reduced severity of ischemia in that area. Residual perfusion distal to an occluded vessel varies between stroke patients, which may explain to a degree why successful recanalisation does not result in the same outcomes despite being treated in a similar time window(330).Recanalisation may be futile if parenchymal tissue distal to an occlusion has insufficient flow to prevent tissue infarction, therefore strategies which could augment collateral flow are of potential clinical relevance..

Improved understanding of the factors which determine collateral flow adequacy is likely to be needed in order to use collaterals as a therapeutic target. The importance of collateral flow is shown by the fact that despite a variety of imaging modalities and techniques used to grade collaterals, the presence of good collateral flow corresponds to direct or indirect markers of good outcome as discussed in Chapter 2. Most of these methods have been qualitative

assessments of collateral flow extent in the ischemic territory or hemisphere, only some of which had inter-observer agreement documented. In addition the factors which govern collateral flow recruitment have been less well evaluated.

Efforts to augment collateral flow are already the focus of clinical trials focussing on partial occlusion of the abdominal aorta in an effort to enhance cerebral blood flow although a benefit has yet to be clearly demonstrated(240, 331). Additional potential interventions to augment collaterals include vasodilation and induced hypertension although the evidence that these interventions have a meaningful impact on collaterals or clinical outcome is limited (332, 333). Factors which could negatively affect collateral flow extent have been suggested such as congenital anatomy variation, dehydration, hyperthermia, hyperglycemia, increased blood viscosity, systemic infections, pulmonary compromise, cardiac failure, renal dysfunction, antihypertensive agents , and widespread intracranial atherosclerosis, but there is no direct evidence thus far to support the interaction between these and collateral adequacy and they remain therefore speculative associations (237).

Before collateral flow can be targeted for therapeutic effect in stroke, improved understanding of the mechanisms which govern collateral recruitment is needed. Research up to this point has sought to evaluate the impact of collateral flow using multiple different imaging modalities and suggests collateral flow confers a benefit although uncertainties remain regarding the methods for grading collaterals and their absolute impact. Markers for collaterals have not been previously studied in detail. Some factors have been associated with collateral flow extent, including pre-morbid medication with statins (234) and with time taken from symptom onset(301). These potential influences have not previously been evaluated for impact on collateral flow in independent populations which may limit the emphasis that can be placed up on them at present. Further understanding of the potential influences on collateral flow and agreement on how it should be measured are likely to be needed to further any therapy aimed at improving collateralisation, or even to incorporate collateral adequacy into decision making processes such as therapy in the extended time window. The aims of this chapter therefore are as follows:

- 1: To derive a novel grading scale for measuring collateral flow extent in acute hemispheric stroke.
- 2: To demonstrate intra-observer reliability of the grading scale.
- 3: To use the grading scale to demonstrate the impact of collateral flow on clinical and imaging markers of outcome after stroke
- 4: To examine baseline clinical characteristics and blood biomarkers of patients with good and reduced collateral flow to evaluate which, if any, are associated with collateral flow extent.

Blood biomarkers for collateral flow have yet to be identified. Although serum, plasma and DNA were obtained from recruits to MASIS, only serum was obtained and stored for patients recruited to POSH, therefore a specific blood biomarker applicable to the combined study recruit cohort was not analysed for association with collateral flow. All patients did however have blood testing for clinical purposes on admission to hospital which included fibrinogen as part of a coagulation blood assay. Blood fibrinogen has been suggested as a potential marker for collateral flow in a single publication by Lee et al where lower fibrinogen measurements were associated with presence of a dominant posterior cerebral artery ipsilateral to an occluded middle cerebral artery (334). This sign has been suggested by the authors as a marker of flow from posterior to anterior circulation via leptomeningeal collaterals. Blood fibrinogen levels have also been associated with poorer outcomes following stroke and methods to reduce fibrinogen have been studied in a number of randomized clinical trials, although these have not examined collateral flow specifically (335, 336). In the absence of other candidate biomarkers and with the suggestion of an association between fibrinogen and collaterals, blood fibrinogen was examined for any association with collateral flow extent.

## **5.2 Quantifying Collateral Flow Using Multimodal CT Imaging.**

Although catheter angiography is often considered the gold standard for assessing vascular anatomy and therefore collateral flow extent (40), its use is

generally restricted to a smaller number of adequately resourced institutions while the patients undergoing angiography may have contraindications to IV rt-PA, meaning collaterals measured by angiography may not be generalisable to other patient populations. CT is more widely available and non-invasive and although lack of dynamic information with CTA is a potential limitation(113), the use of raw CTP data to confirm the retrograde direction of collateral flow is complementary to the anatomical detail of CTA(111). Not all patients who have previously had collaterals graded using CTA had a documented arterial occlusion meaning that the extent to which flow in ischemic territory was truly collateral or not is debatable. Using anatomical grading scales of collaterals in the setting of lacunar stroke for example may be misleading and conclusions derived from collateral measurements without visualised occlusions need to be viewed with caution. All previous methods using CTA graded collateral flow extent qualitatively.

Given the lack of consensus regarding collateral flow grading, the opportunity to explore a novel method for collateral measurement was taken.

### **5.3 Inclusion Criteria**

The combined databases from MASIS and POSH studies comprising patients who underwent multimodal CT imaging on admission to hospital were used to evaluate collateral flow. For consistency in methodology, only those patients imaged with CT at study entry to MASIS were considered for inclusion. Overall study inclusion criteria, recruitment, consent, imaging protocols, anonymization and clinical assessments for POSH and MASIS are described in Chapter 3.

Patients selected for collateral flow evaluation met the following conditions:

- 1: Diagnosis of acute ischemic stroke.
- 2: Written consent and imaging obtained as part of participation in either POSH or MASIS studies.
- 3: Baseline CTA confirmed an acute symptomatic arterial occlusion in ICA or proximal MCA vessels.

4: Retrograde direction of collateral flow demonstrated using 4-D Angiogram from baseline CTP raw data.

### **5.3.1 Clinical Data**

The clinical evaluations performed were discussed in detail previously. In brief, baseline and follow-up clinical assessments included NIHSS(337), mRS(338), OSCP classification (339), routine physiological monitoring including blood pressure and blood glucose, age, sex, time of symptom onset and therapy given. Risk factors for stroke and medication history were recorded. Good clinical outcome was defined as mRS  $\leq 2$  at 1 month following stroke. Presence and degree of carotid stenosis was determined on admission CTA. Degree of stenosis was graded for clinical purposes by consultant radiologists who were not involved in subsequent research-specific analyses. Presence of Atrial fibrillation was determined from ECG on admission to hospital or if paroxysmal, from previous medical notes. Blood fibrinogen measurement was determined from coagulation samples obtained on admission to hospital as part of routine clinical practice.

### **5.3.2 Image Analysis**

CT imaging on admission, comprising CT, CTP and CTA, was analysed after DICOM anonymization. Evaluation was performed blind to treatment received and clinical outcome. A single reader performed all analyses (FMV).

Baseline non-contrast CT was evaluated qualitatively for ASPECTS (79).

Presence and location of arterial occlusions were determined from CTA. An occlusion visualised using CTA source images and 3-D MIP reconstructions was defined as the absence of contrast filling in a vessel which separated the proximal and distal portions of the vessel(111).

After post-processing, CTP scans were examined qualitatively for ASPECTS on MTT, CBF and CBV summary maps. Core volume, penumbra volume and total perfusion lesion volume were recorded. Core volume was defined as tissue with reduced CBV (Absolute CBV $\leq 2.0$ ml/100g). Penumbra was defined as tissue with prolonged MTT (Relative MTT  $\geq 145\%$  that of contralateral hemisphere) but with

normal CBV (131). Total perfusion lesion volume was calculated as the volume of core and penumbra combined.

Severity of hypoperfusion in the affected ischemic territory was measured using a newer perfusion measure, Delay time (DT), (340) according to four thresholds of hypo perfusion severity;  $DT \geq 2$  seconds,  $DT \geq 4$  seconds,  $DT \geq 6$  seconds and  $DT \geq 8$  seconds. To calculate DT as part of the deconvolution algorithm, a series of delay time values,  $DT_i$  ranging from 0 to  $T_{max}$  were applied and for each delay time value a modelled arterial transport function was convolved with the measured global AIF to produce  $AIF_i$  which is used for SVD deconvolution of the tissue curve to produce an impulse residue function  $IRF_i$  with its maximum appearing at  $T_{max}(i)$ . Delay time (DT) was determined as the minimal  $DT_i$  value which produces  $T_{max}(i) = 0$  (341).

DT value in any given pixel is a measurement of hypo perfusion severity. A series of thresholds was applied to the DT perfusion maps according to the principle used by Bang et al to grade severity of hypo perfusion according to time taken for contrast arrival (40). A masking ROI was manually drawn over the affected hemisphere. Non parenchymal pixels were excluded. A further ROI seed was placed in the hemispheric ROI which was then grown according to a series of pre-specified thresholds:  $DT \geq 2$  seconds,  $DT \geq 4$  seconds,  $DT \geq 6$  seconds and  $DT \geq 8$  seconds. Volume of hypoperfused tissue within each threshold group was automatically calculated. The process was repeated for each perfusion scan slice and added together to provide a volume of tissue within the different DT thresholds for each patient evaluated (Figure 5.1)

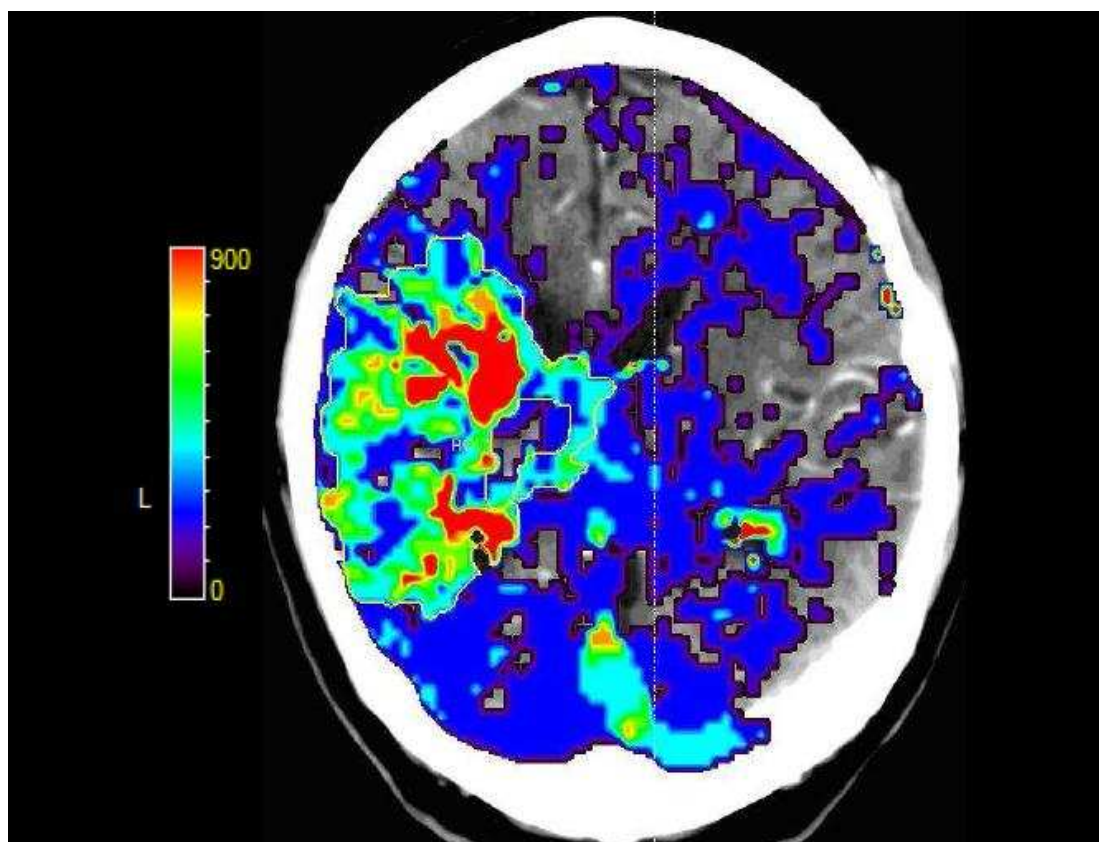


**Figure 5-1 DT Summary Map with ROI Measuring Pixels with DT>2 Seconds (Units = seconds x 100)**

Colour coded map displaying region of interest over pixels with DT>2 seconds. Key on left shows perfusion deficit severity depending on colour. Most severe perfusion deficit shown in red (>9 seconds)

Recanalisation was determined on subacute imaging using an adapted Thrombolysis in Myocardial infarction (TIMI) scale where recanalisation was defined as none (TIMI 0), minimal recanalisation/ persistent severe stenosis (TIMI 1) partial (TIMI 2) and complete (TIMI 3)(167). Recanalisation was further dichotomised; TIMI 0-1 was considered non-recanalisation, TIMI 2-3 represented recanalisation.

Subacute structural imaging with CT or FLAIR was evaluated for presence / absence of intracerebral haemorrhage. Infarct Volume was determined from follow up structural imaging after co-registration with the baseline perfusion

scan. Follow up CT or FLAIR was loaded along with CTP into a fusion tool function using MIStar. A rigid body 3-D transformation was used to register the follow up structural imaging to the perfusion scan. Structural CT/ MRI-FLAIR sequences were subjected to a series reformatting procedures in the axial, sagittal, coronal and oblique planes to obtain an orientation which matched that of the original CTP scan. The co registration process is shown in figure 5.2.



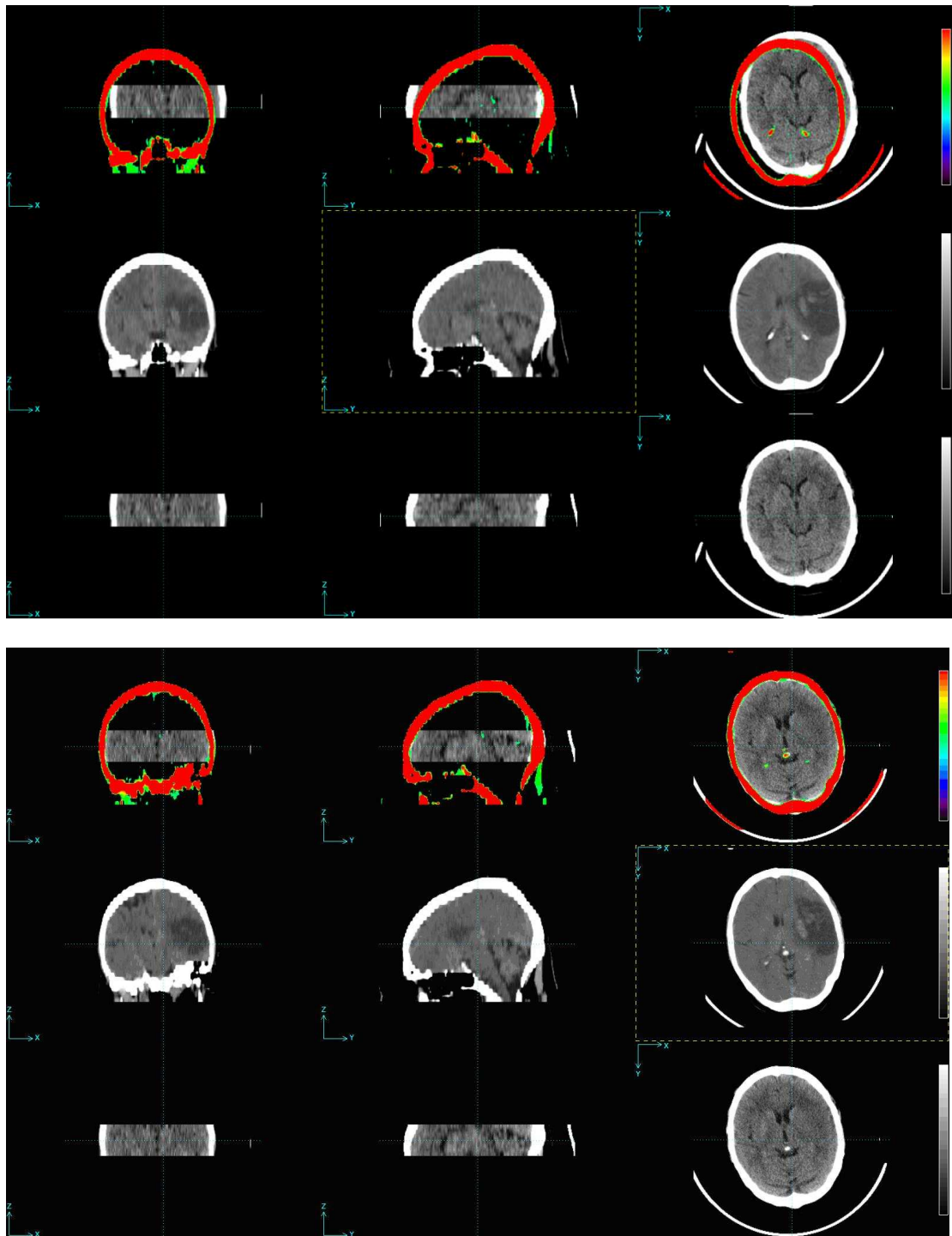


**Figure 5-2 Fusion Tool Before and After Co-registration**

Baseline CTP and follow up CT from one patient are shown before (top panel) and after ( lower panel) coregistration. In each panel, the follow-up CT is shown in the middle row, CTP is shown in the lower row, and the fusion overlay of each is shown in the top row. After co registration, the fusion overlay images show a close fit (top row from lower image screen save)

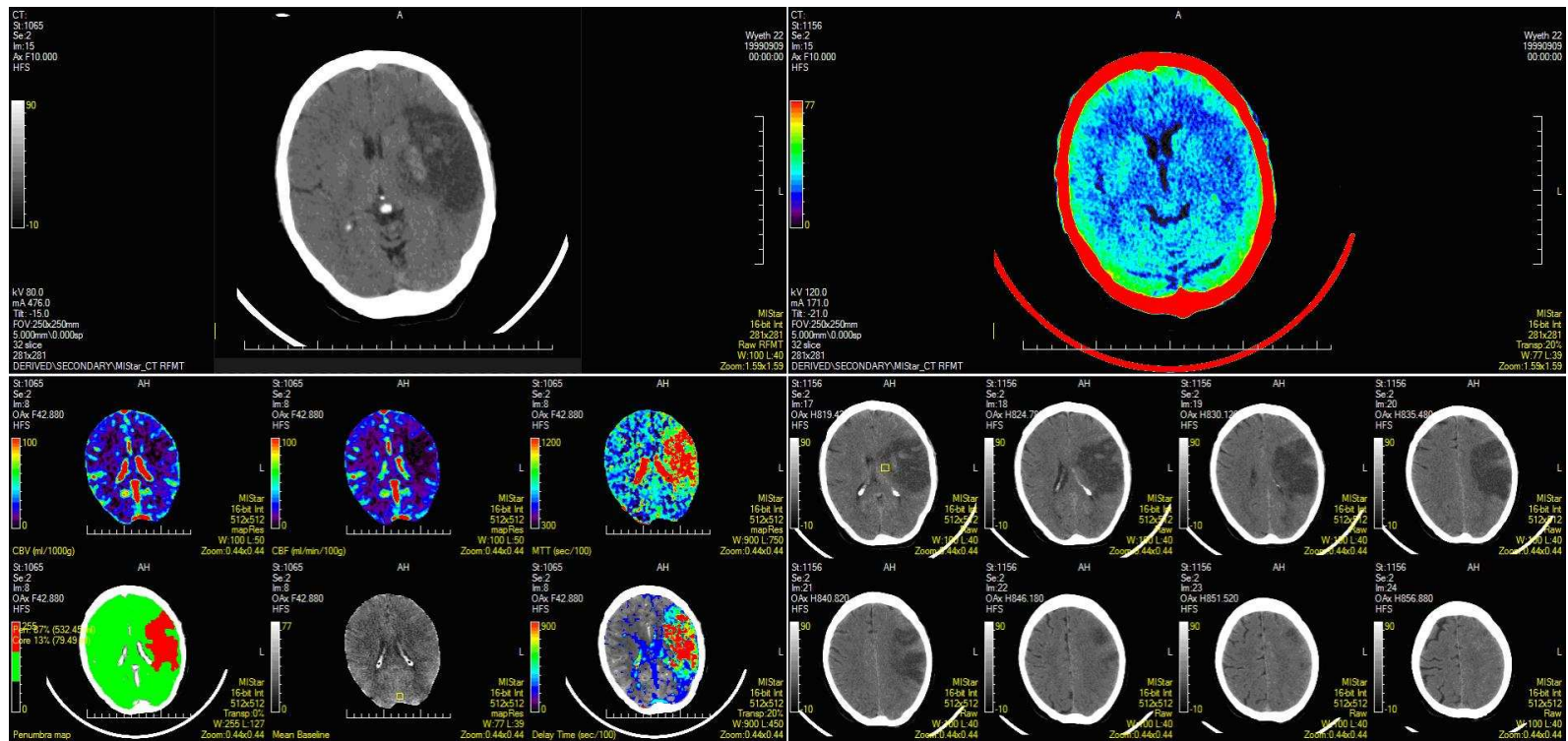


**Figure 5-3 Reformatted Structural Image After Co-Registration**

Screen save showing imaging output after using the MIStar co registration tool. Processed CTP scan (Bottom left panel) and follow up structural CT (bottom right panel) have been co registered as shown in figure 5.2. The fusion overlay is shown on the top right panel, and the reformatted structural CT, which now matches the 3D orientation of the original CTP scan, is shown on the top left. This reformatted CT scan is used to measure infarct volume in the same pixels covered by the original CTP acquisition,

After co-registration, the reformatted follow-up images were used to measure final infarct volume. A ROI seed was placed within the visualised area of final infarction. This ROI was subsequently adjusted by HU threshold semi-automatically to match the extent of visualised infarct. Manual correction was used if needed to map the infarct extent precisely. ROI seed placement and growth/adjustment was repeated for each scan slice and combined to obtain a total infarct volume for each patient.

As the CTP scan did not provide complete brain coverage, infarct volume was measured separately for those pixels which were covered by the perfusion scan and additionally for all parenchymal pixels which went on to become infarcted but which were not necessarily covered by the perfusion scan at baseline. Two separate measurements for infarct volume were therefore obtained; a total final infarct volume and a co-registered infarct volume which was used to determine the fate of tissue pixels covered by the perfusion scan.

Measurements for core and penumbra volumes on CTP and co-registered infarct volume were used to determine tissue outcome according to a number of calculations;

- Infarct Growth=Co-registered infarct volume-Core volume
- Penumbra salvage= Penumbra Volume - Penumbra volume which infarcted
- Proportion Penumbra Salvage= (Penumbra salvage/Penumbra Volume) x100
- Relative Growth= Co-registered infarct Volume/ Core Volume

### **5.3.3 Collateral Flow Grade**

A novel, semi-quantitative method based on CTA and CTP for measuring collateral flow extent was devised. Patients with arterial occlusion in the ICA or proximal MCA vessels had perfusion scans evaluated to determine the direction of blood flow distal to the vessel occlusion. 4-D angiographic appearances of the 4 cm perfusion slab were displayed as a MIP image and evaluated in cine mode.

The 4D angiographic appearances permitted visualisation of arterial filling in normal and ischemic tissue beds in real time or at faster rates if needed, adjusted by the operator. This effect permitted the presence of contrast enhancement in distal portions of an arterial distribution to be seen prior to filling of the proximal portions and thereby confirming that flow in the relevant territory is truly collateral in nature. Without being able to confirm the retrograde direction of flow it would be impossible to say if CTA appearances were due to collateral filling and not simply due to delayed antegrade flow due to an incomplete arterial occlusion/ stenosis. The use of perfusion data to confirm flow direction has been previously demonstrated using the same software package(111). The effect is best appreciated when viewed in the cine mode, but can be appreciated using a series of screen shots taken at 2 second intervals as seen in figure 5.4

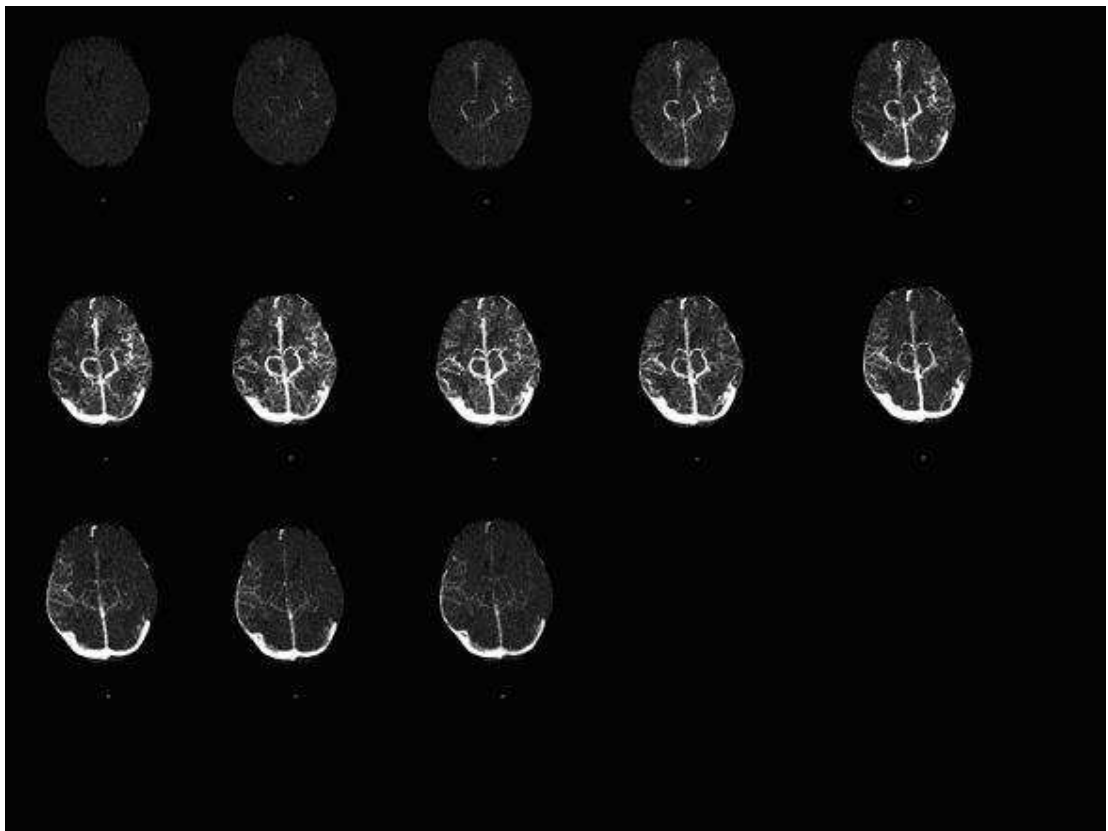


**Figure 5-4 4D Angiography Demonstrating Retrograde Collateral Flow**

Right MCA occlusion with perfusion scan MIP shown at 2 second intervals. The right MCA demonstrates delayed contrast filling, but the distal portion fills prior to proximal portion confirming that flow in ischemic area is retrograde and collateral in origin.

CTA was evaluated for collateral flow in those with retrograde flow on CTP. The intracranial CTA portion was viewed and if necessary underwent a 3-D Multiplanar reconstruction to ensure the orientation for each hemisphere was symmetrical when viewed in the axial plane when centred over the level of the basal ganglia (lower ASPECTS level)(79). Images were then converted to maximal intensity projections with a slice thickness of 40mm in order to include most of the MCA territory in a single image.

A ROI was drawn over the vessel portions in the unaffected MCA territory. The MCA origin was defined as the confluence of ICA MCA and ACA vessels. The most distal portion covered by the ROI was the most distal portion of the vessel seen which had continuity with the proximal MCA portion. Use of the unaffected hemisphere with full contrast enhancement was in order to remove any bias when drawing ROIs according to the visualised extent of collateral vessel filling. A mirror ROI was then generated in symptomatic hemisphere, each ROI containing the same absolute number of pixels. A high-low HU threshold was applied to the ROIs to permit inclusion of pixels measuring between 90 and 350 HU. This threshold range included pixels which contained contrast within vessels and excluded pixels representing brain parenchyma, ventricles and bone. The range chosen is also the HU threshold range for vascular pixels used on CTA post-processing packages used in clinical practice (e.g. Philips Brilliance) and therefore was considered to represent a reasonable attempt at visualising vascular pixels alone. ROI appearances after applying the HU thresholds is shown in figure 5.5.



**Figure 5-5 CTA After Application of High-Low HU Threshold**

An ROI was generated over the right MCA territory (blue) and mirrored to the symptomatic left MCA territory (yellow). Applying the high-low HU threshold permitted calculation of the absolute number of vascular pixels within each ROI.

The importance of quantifying vascular filling in both hemispheres was due to the fact that CTA acquisition and appearances vary between individuals. Differences such as timing of image acquisition after contrast bolus injection, cardiac output, atrial fibrillation and blood pressure variability result in large variation in the absolute number of vascular pixels measured within a vascular territory between different individuals. This inter-patient variability was seen during the present analysis with large differences in the absolute number of vascular pixels measured in vascular territories which appeared similar on inspection, thus preventing the use of absolute numbers of vascular pixels as a measure of collateralisation. These factors are constant however for a given individual meaning that contrast enhancement in each hemisphere should be symmetrical in the absence of an occlusive lesion. This principle was employed to compare affected and unaffected hemispheres for vascular filling and a ratio was determined as;

$$\text{Collateral ratio (\%)} = (\text{Ipsilateral pixels} / \text{Contralateral pixels}) \times 100$$

using only the number of vascular pixels measured within the ROIs over the affected and unaffected hemispheres.

Collateral ratio was generated as a continuous variable and then dichotomised into two groups, good (collateral ratio  $\geq 75\%$ ) and reduced collaterals (collateral ratio  $< 75\%$ ) for analysis. This cut point was chosen based on interpretation of the best available qualitative scales.

To determine agreement for collateral grading, all anonymized CTA scans were re-evaluated for collateral flow grade one month after initial assessments were made.

### **5.3.4 Statistical Analysis**

Statistical analysis was performed using PASW statistics 18 ([www.SPSS.com](http://www.SPSS.com)). Analysis was performed for collateral flow grade as the outcome measure in order to investigate factors which may impact collateral flow, as well as clinical outcome to assess the contribution of different factors including collateralisation to final clinical outcome after stroke. Group comparisons were performed using the student's T test and Mann-Whitney test for continuous and ordinal data, or the Pearson Chi Squared test for categorical data. Binary logistic regression was performed for predictors of collateral grade and clinical outcome using univariate analysis. Those univariate predictors with p values  $< 0.1$  were included in multivariate analysis. Intra-observer agreement for collateral grade was assessed using an un-weighted kappa score

## **5.4 Results**

From the combined MASIS and POSH databases, 151 subjects were available for analysis. Of those, 62 had no visual occlusion on CTA and a further 11 had arterial occlusions in the posterior circulation. Of the 78 patients with CTA-defined anterior circulation occlusion, 45 patients had evidence of retrograde flow on CTP while 33 patients did not, 3 of whom had chronic extracranial ICA occlusions which were not responsible for the individuals' presentation. The remaining 42 subjects had ICA /proximal MCA occlusions with retrograde flow on CTP demonstrated and were included in the final analysis (Figure 5.6).

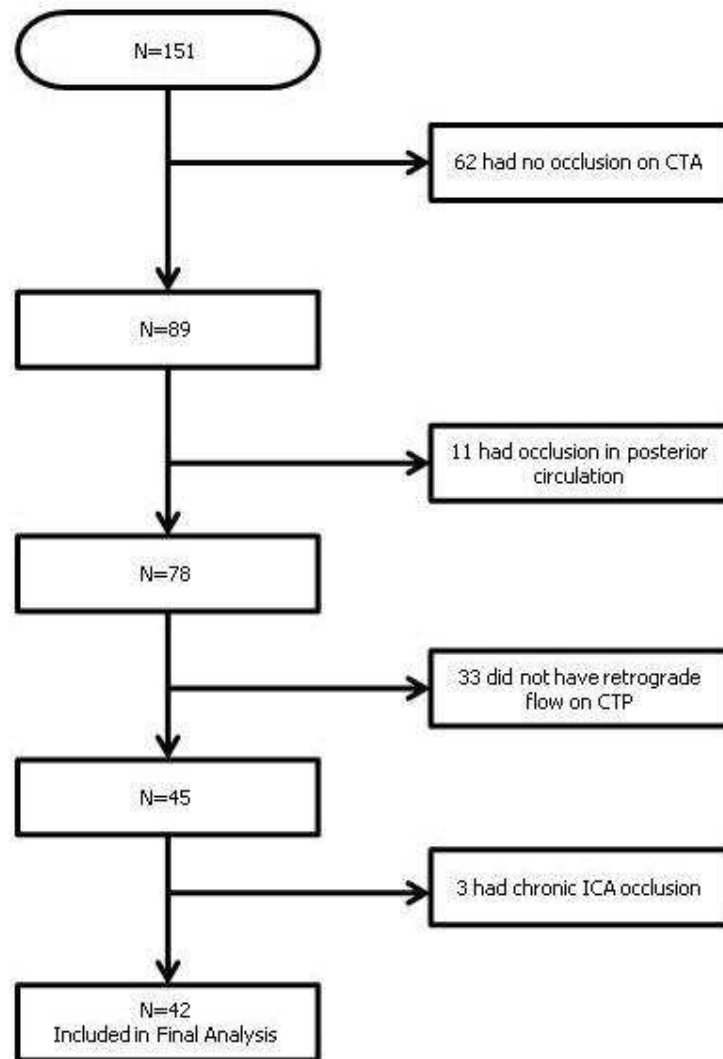


**Figure 5-6 Flowchart for Inclusion in Collateral Flow Evaluation**

Collateral flow was reduced in 29 (69%) and good in 13 (31%) subjects. Both groups were well matched in terms of age, sex, blood pressure and blood glucose. There were no significant differences in frequency of occlusion subtypes between collateral subgroups but those with good collateral flow had lower NIHSS measurements on admission. Stroke risk factors and previous medical conditions were generally similar between groups but atrial fibrillation was detected significantly more frequently in those with reduced collateral flow ( $n=15$  vs.  $n=2$ ,  $p=0.013$ ). Pre-morbid medications including statins were not



significantly different. Time taken from symptom onset to image acquisition was similar in both groups. Plasma fibrinogen level was lower in those patients with good collateral flow ( $p=0.012$ ). Carotid stenosis was not more frequently seen with good collateral flow. Baseline clinical characteristics of both groups are summarised in table 5.1 and figures 5.7 to 5.9. Intra-observer agreement for collateral flow grade was excellent ( $k=0.86$ ).

Variable	All (n=42)	Good Collaterals (n=13)	Reduced Collaterals (n=29)	p
Age(SD)	73.1(11.8)	69.1(11.3)	74.9(11.7)	0.138
Male sex (% of group)	16(38%)	9(21.4%)	7(16.7%)	0.159
NIHSS (Range)	18 (6-33)	13(6-21)	19(9-33)	<0.001
Systolic BP (SD) (mmHg)	146.7(21.2)	139.2(13.5)	150.5(23.4)	0.119
Diastolic BP (SD) (mmHg)	75.4(20.5)	68.8(17.6)	78.8(21.4)	0.154
Blood Glucose (Range (mmol/L))	6.7(3.8-9.0)	6.4(3.8-9.0)	7.0(5.0-9.0)	0.157
ICA occlusion (% of group)	13(31%)	2(4.8)	11(26.2)	0.144
MCA occlusion (% of group)	29(69%)	11(26.2)	18(42.9)	0.144
Pre-morbid Statin use (% of group)	22(52.4%)	7(16.7%)	15(35.7%)	0.899
Carotid stenosis >70% (% of group)	5(11.9%)	2(4.8%)	3(7.1%)	0.641
Atrial Fibrillation *(% of group)	17(40.5%)	2(4.8%)	15(35.7%)	0.013
Hypertension (% of group)	26(61.9%)	7(16.7%)	19(45.2%)	0.471
Diabetes (% of group)	7(16.7%)	2(4.8%)	5(12.0%)	0.941
Never smoked (% of group)	14(33%)	4(9.5%)	10(23.8%)	0.807
Previous stroke (%of group)	7(16.7%)	1(2.4%)	6(14.3%)	0.296
Fibrinogen (SD) (g/L)	3.6(0.8)	3.0(0.8)	3.8(0.8)	0.012
Onset to Imaging Obtained (Mins) (Range)	147.5(57-355)	126(57-220)	154(82-355)	0.105

**Table 5-1 Baseline Clinical Characteristics of Subjects with Good and Reduced Collaterals**  
T test and Mann-Whitney test used for normal and non-normal continuous variables. Chi Square test used for categorical variables. \* No data on atrial fibrillation for 3 subjects

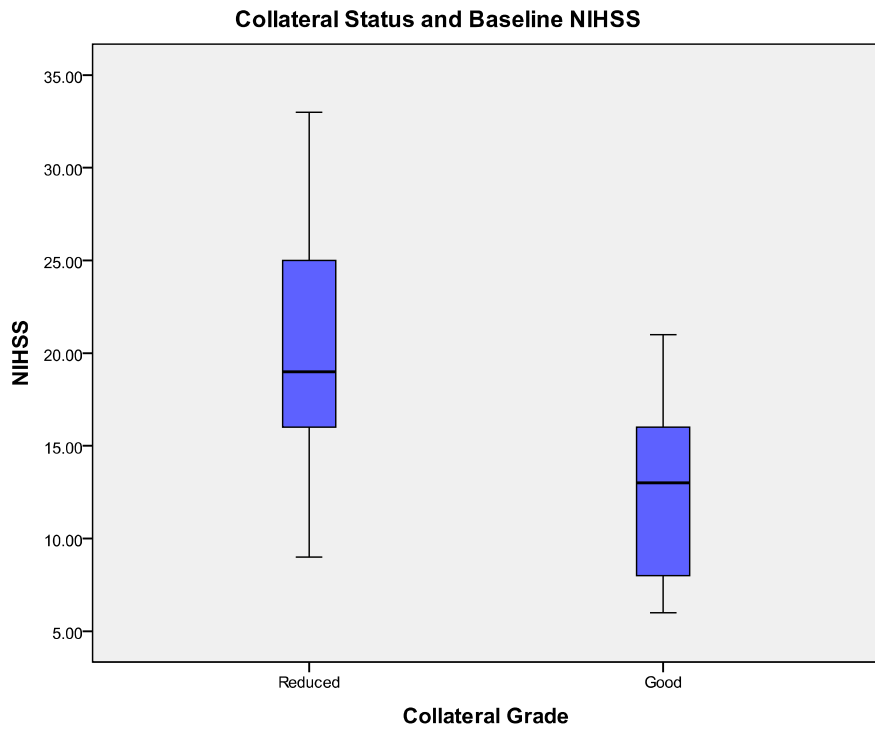


**Figure 5-7 Collateral Status and NIHSS (Median +IQR +Range)**  
Mann Whitney U test  $p < 0.001$

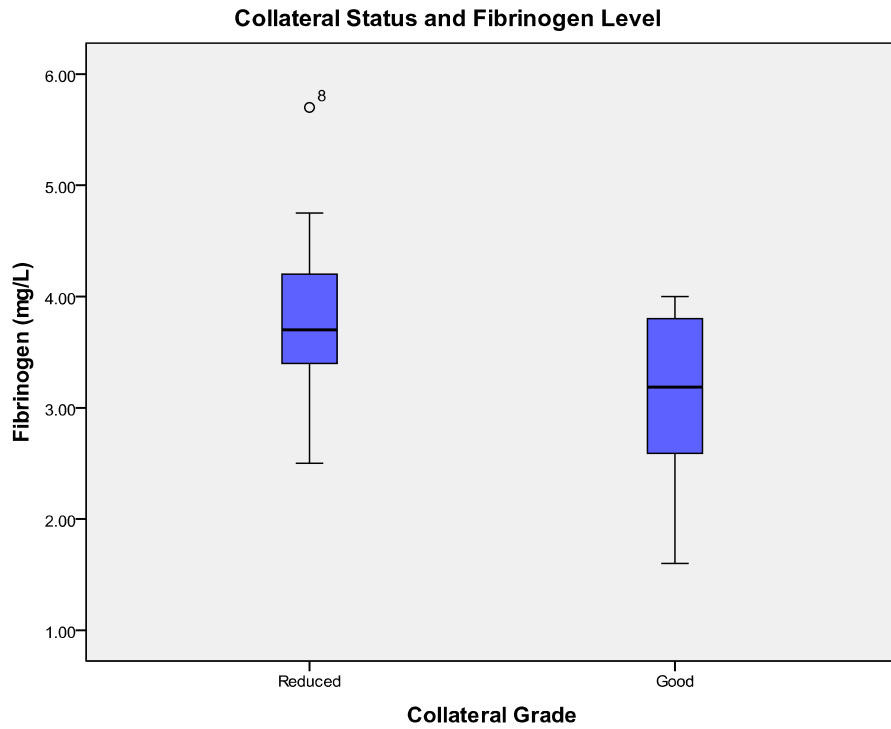


**Figure 5-8 Collateral Grade and Fibrinogen Level (Mean +SD + Range +Outlier)**  
T test  $p = 0.012$

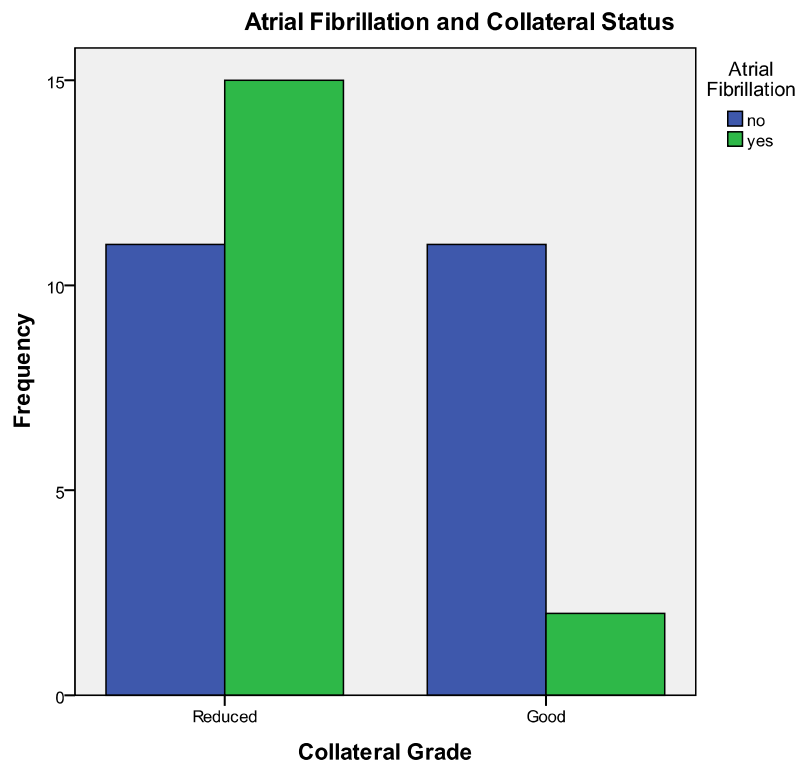


**Figure 5-9 Collateral Grade and Atrial Fibrillation**

Good collateral flow was less frequently seen in patients with atrial fibrillation. Data on atrial fibrillation status on 3 subjects are missing. Chi-Squared Test  $p=0.012$

Collateral flow extent was studied for association with other baseline imaging characteristics. Qualitative assessment of NCCT and processed CTP maps were similar in both groups apart from CBV-ASPECTS score which was significantly lower in the group with reduced collaterals (Median scores 8.0 and 6.5  $p=0.006$ ). Core volume, penumbra volume and thresholded perfusion lesion volume were similar in each group. The volume of hypoperfused tissue on  $DT \geq 2$  second maps was significantly greater in those with reduced collateral flow compared to good collateral flow ( $p=0.031$ ). Volumes were also significantly larger for  $DT \geq 6$  and  $DT \geq 8$  second thresholds in the reduced collateral groups suggesting larger volumes of severely hypoperfused tissue in association with reduced collateral flow, although proportion of tissue with severe hypo perfusion ( $DT \geq 8 / DT / 2 \geq$ ) was not significantly different between groups. Imaging features and collateral status are summarised in Table 5.2 and figures 5.10 to 5.15

Measurement	All (n=42)	Good Collaterals (n=13)	Reduced Collaterals (n=29)	p
NCCT ASPECTS (Range)	6.0 (1-10)	7.0 (2-10)	5.5 (0-10)	0.336
CBV ASPECTS (Range)	8.0 (1-10)	8.0 (5-10)	6.5 (1-10)	0.006
CBF ASPECTS (Range)	4.0 (0-10)	5.0 (1-9)	4.0 (0-10)	0.295
MTT ASPECTS (Range)	3.0 (0-9)	3.0 (1-9)	3.0 (0-9)	0.585
Core Volume (ml) (Range)	25.6 (4.8-131.0)	20.5 (4.8-92.9)	30.0 (6.4-131.0)	0.117
Penumbra Volume (ml)(Range)	31.7 (5.1-76.9)	22.7 (5.1-69.6)	33.5 (12.1-76.9)	0.256
Perfusion lesion volume (ml) (Range)	68.8 (19.5-194.7)	45.2 (19.5-148.4)	82.1 (27.8-194.7)	0.053
DT $\geq$ 2 Seconds Volume (ml)(Range)	77.3 (13.0-185.0)	43.6 (17.5-139.0)	94.5 (13.0-185.0)	0.031
DT $\geq$ 4 Seconds Volume (ml) (Range)	39.4 (3.5-161.0)	23.2(3.5-100.2)	44.7 (5.9-161.0)	0.056
DT $\geq$ 6 Seconds Volume (ml)(Range)	22.5 (0.0-121.0)	10.0 (0.0-66.3)	27.5 (0.7-121.0)	0.037
DT $\geq$ 8 Seconds Volume (ml) (Range)	11.1 (0.0-96.0)	5.3 (0.0-25.5)	15.2 (0.0-96.0)	0.05
DT $\geq$ 8/DT $\geq$ 2 ratio (Range)	0.19 (0.0-0.52)	0.14 (0.0-0.25)	0.23 (0.0-0.52.)	0.116

**Table 5-2 Collateral Status and Associated Imaging Findings on Admission**  
Groups were compared using the Mann Whitney U test

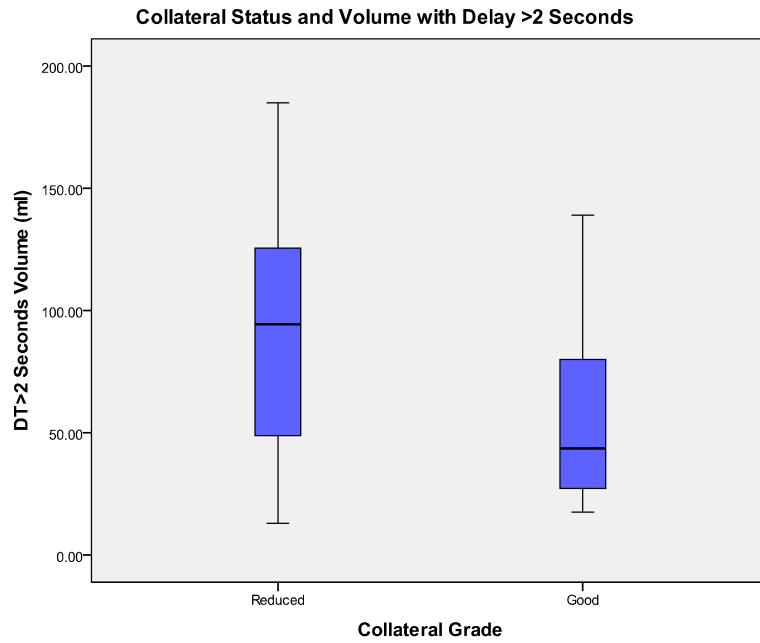


**Figure 5-10 Collateral grade and Volume with DT  $\geq$  2 Seconds (Median +IQR, +Range)**  
 Mann Whitney U test p=0.031

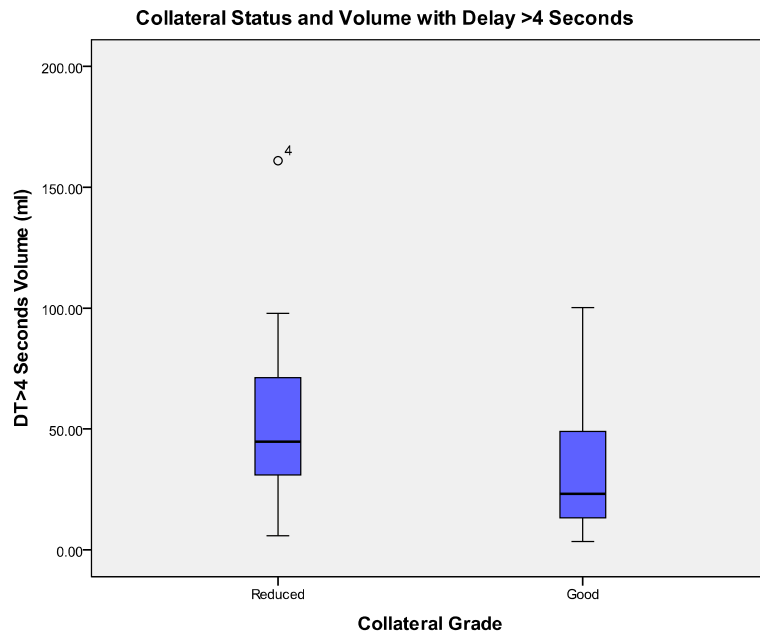


**Figure 5-11 Collateral grade and Volume with DT  $\geq$  4 seconds (Median +IQR, +Range+ Outlier)**  
 Mann Whitney U test p=0.056

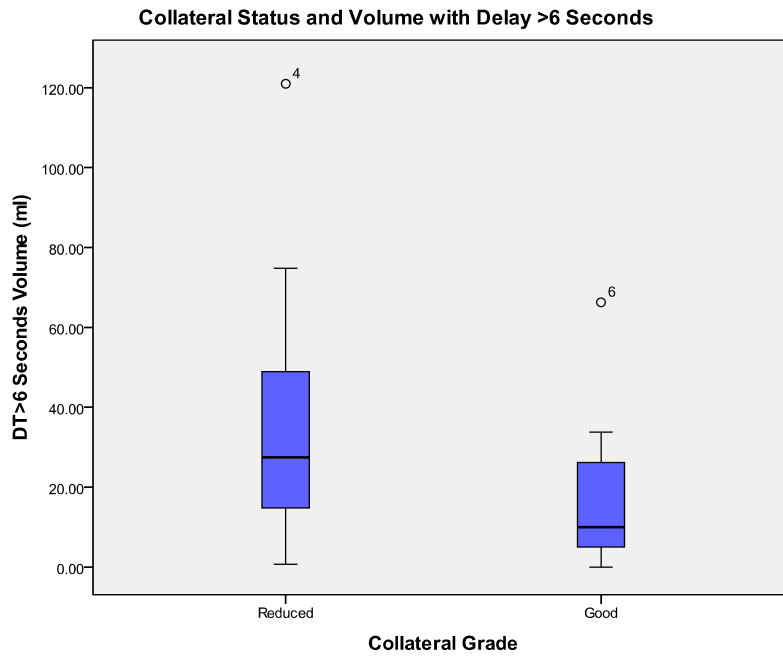


**Figure 5-12 Collateral grade and DT ≥ 6 seconds** (Median +IQR +Range +Outliers)  
Mann Whitney U test p=0.037

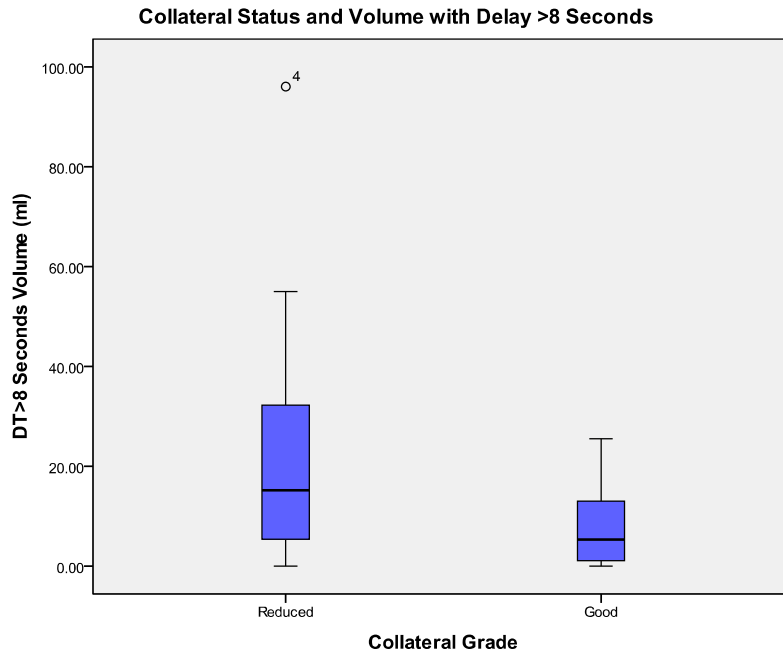


**Figure 5-13 Collateral grade and DT ≥ 8 Seconds** (Median +IQR+ Range + Outlier)  
Mann Whitney U test p=0.05



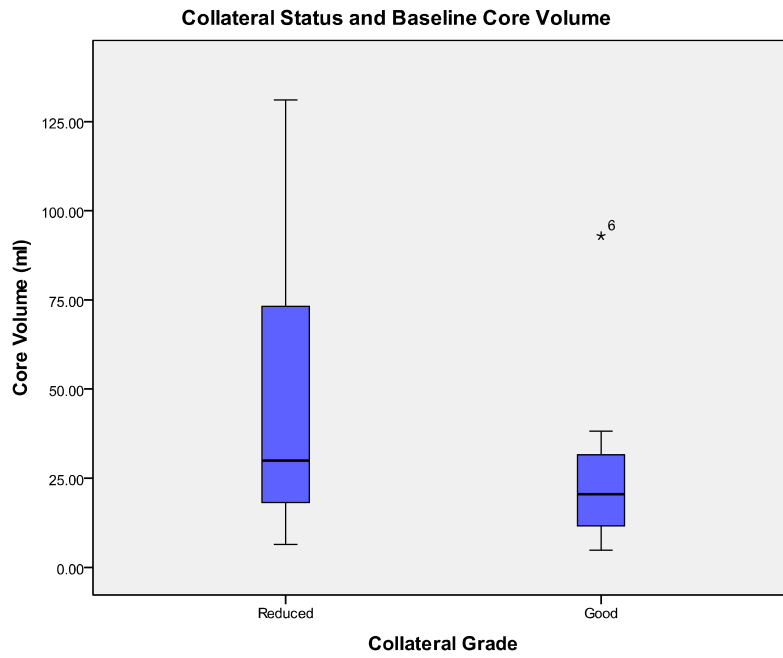


**Figure 5-14 Collateral grade and Infarct Core Volume (Median +IQR +Range + Outlier)**  
Mann Whitney U test  $p=0.117$

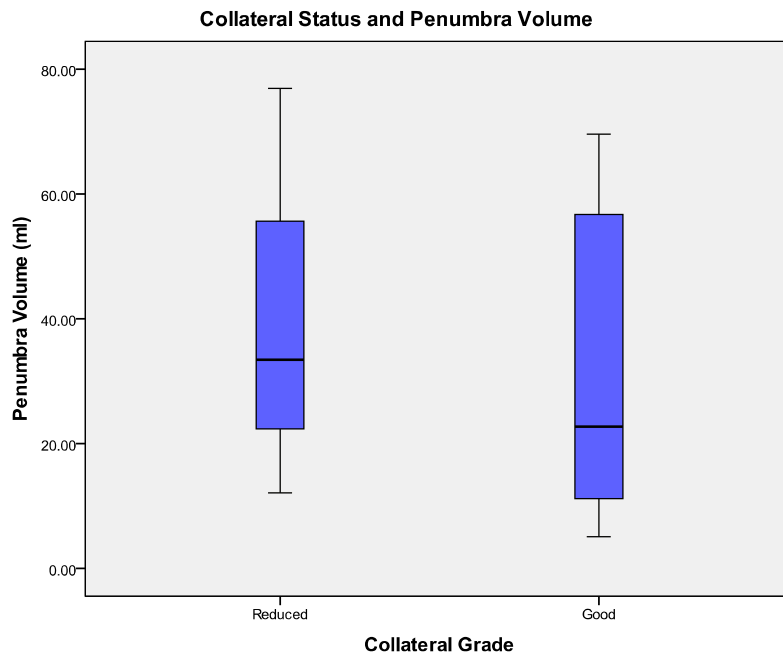


**Figure 5-15 Collateral Grade and Penumbra Volume (Median +IQR +Range)**  
Mann Whitney U test  $p=0.256$

Variables with significant association with good collateral grade from a univariate logistic regression analysis included NIHSS, CBV ASPECTS, atrial Fibrillation, plasma fibrinogen and DT $\geq$  2 seconds volume.

Predictor	OR (CI)	p
NIHSS	0.763 (0.637-0.914)	0.03
CBV ASPECTS	1.762 (1.116-2.781)	0.02
Atrial Fibrillation	0.133 (0.024-0.727)	0.02
Fibrinogen	0.227 (0.062-0.833)	0.03
DT >2 seconds	0.980 (0.960-0.999)	0.04

**Table 5-3 Univariate Logistic Regression Summary**

These elements were entered to a multiple logistic regression model but none achieved statistical significance.

#### **5.4.1 Collateral Flow and Outcome**

Recanalisation on subacute angiography appeared to occur more often in those with poor collaterals although the result was not statistically significant for both groups with no statistical difference seen. Intracerebral haemorrhage was present for 7 subjects all of whom had reduced collaterals. No ICH was detected in the good collateral flow group. Of the 7 with ICH at follow up, recanalisation was assessed in 5. 4/5(80%) had evidence of recanalisation on follow up, although the result was not statistically significant (Chi Square p=0.523). Collateral flow was associated with smaller infarct volume, less absolute and relative infarct growth from baseline and larger proportions of penumbra salvage.

Good clinical outcomes were more likely in the good collateral flow group who also had significantly lower NIHSS measurements at 24 hrs. Absolute NIHSS reduction from admission to 24 hrs was not statistically different between groups. Proportional NIHSS reduction at 24hrs appeared higher in those with good collaterals, although statistical significance was not seen. Two subjects were lost to clinical follow up meaning final outcome measurement was

available for 40 of 42 subjects. Results are summarised in table 5.4 and figures 5.16 and 5.17.

<b>Outcome</b>	<b>All (n=42)</b>	<b>Good Collaterals (n=13)</b>	<b>Poor Collaterals (n=29)</b>	<b>p</b>
ICH (% of total)	7 (16.7%)	0 (0)	7 (16.7 %)	0.039
Recanalisation (% of total)	23 (54.7%)	7 (16.7%)	16 (38.1%)	0.73
Infarct Volume (ml) (Range)	39.3 (0.0-364.8)	21.6 (0.0-151.0)	60.9 (1.1-364.8)	0.006
Infarct Growth (ml) (Range)	13.9 (0-79.5)	10.2 (0-43.4)	22.7 (0-79.5)	0.017
Penumbra Salvage (ml)(Range)	14.9 (3.1-76.8)	17.2 (3.1-68.1)	14.7 (4.9-76.8)	0.861
Proportion Penumbra salvaged (%) (Range)	74.0(16.0-100.0)	89.0(50.0-100.0)	71.5 (16.0-100.0)	0.034
Relative Growth (Range)	1.4(0.0-8.5)	0.9(0.0-1.9)	1.6(0.1-8.5)	0.005
NIHSS 24hrs (Range)	14 (0-30)	6 (0-20)	15 (1-30)	0.013
24hr NIHSS reduction (Range)	4(-11.0-32.0)	6(-9.0-16.0)	3 (-11.0-32.0)	0.643
Proportional NIHSS reduction 24hrs (%) (Range)	12.9 (-88.9-100.0)	38.9 (-81.8-100.0)	10.5 (-88.9-97.0)	0.110
Good Clinical Outcome(% of total)	8(19.0%)	3 (7.1%)	5(11.9%)	0.043

**Table 5-4 Collateral Flow and Clinical Outcome**

Categorical variables compared using the Chi-Squared test. Continuous variables compared using the Mann Whitney U test.

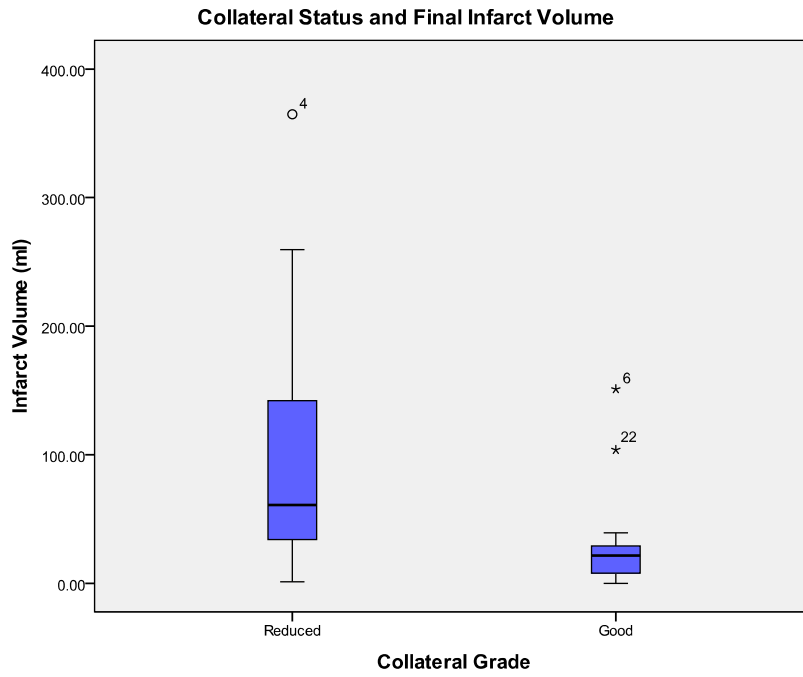


**Figure 5-16 Collateral Grade and Infarct Volume** (Median +IQR +Range +Outliers)  
Mann Whitney U test p=0.006

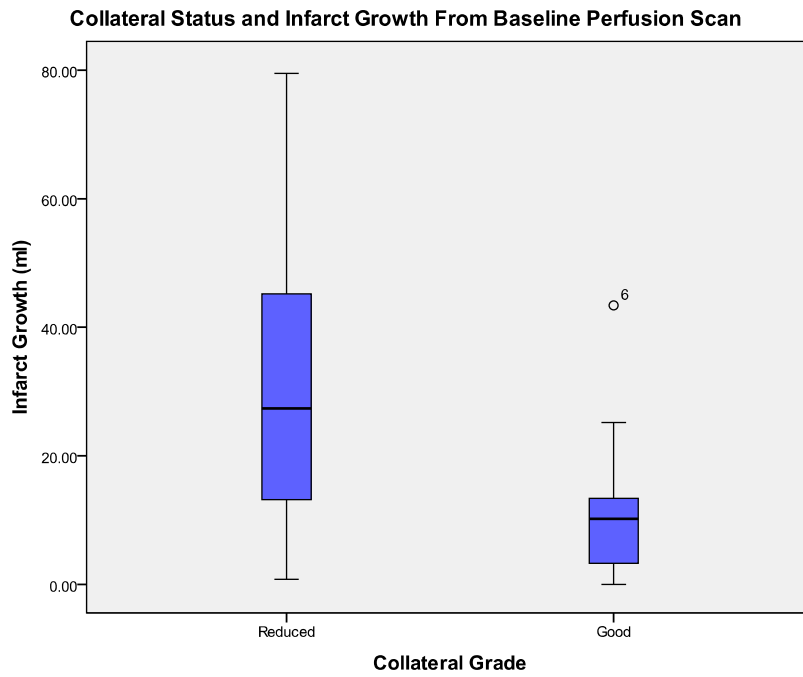


**Figure 5-17 Collateral Grade and Infarct Growth** (Median +IQR +Range +Outlier)  
Mann Whitney U test p=0.017

Additional measurements significantly associated with clinical outcomes included baseline NIHSS measurement, NCCT-ASPECTS and CBV-ASPECTS on admission, infarct volume, and proportion of penumbra salvaged. Collateral grade expressed as a continuous measurement was significantly greater in those who achieved good outcomes. Lower NIHSS measurements at 24 hrs were seen in those with good outcome. Recanalisation, administration of alteplase, occlusion site, atrial fibrillation, blood fibrinogen and volumetric measurements of core and penumbra were not associated with clinical outcome. Results are summarised in table 5.5 and figures 5.18 to 5.24.

NIHSS, ASPECTS on CBV and NCCT, Collateral flow grade and infarct volume were significant univariate predictors of good outcome after logistic regression analysis (Table 5.6). Statistical significance for each was lost after entry to a multivariate logistic regression analysis.

Variable	Good Clinical Outcome? (mRS ≤2)		P
	No (n=32)	Yes (n=8)	
Age (SD)	73.8 (11.5)	68.6 (13.7)	0.276
Admission NIHSS (Median)(Range)	18.0 (6.0-30.0)	15.5(8.0-19.0)	0.050
Blood Glucose mmol/l (SD)	8.9 (5.5)	6.7 (1.2)	0.403
Carotid occlusion	10 (25%)	2 (5%)	0.730
M1 Occlusion	17 (42.5%)	5 (12.5%)	0.634
M2 Occlusion	7 (17.5%)	3 (7.5%)	0.361
Good Collaterals?	8 (20%)	5 (12.5%)	0.043
Alteplase	22 (55%)	6 (15%)	0.768
Recanalisation?(n=32)	15 (46.8%)	6 (18.8%)	0.519
Atrial Fibrillation?	15 (46.8%)	1 (2.5)	0.086
ASPECTS NCCT (Range)	5 (0-10)	8 (5-10)	0.042
ASPECTS CBV (Range)	7 (1-10)	9 (7-10)	0.017
ASPECTS CBF (Range)	4 (0-9)	4 (1-10)	0.860
ASPECTS MTT (Range)	4 (0-9)	3 (1-6)	0.433
Core Volume (ml) (Range)	34.6 (4.8-121.2)	25.5 (10.8-37.0)	0.279
Penumbra Volume (ml) (Range)	24.1 (5.1-68.7)	35.2 (15.2-19.6)	0.772
Hypoperfused Volume (ml) (Range)	72.0(19.5-148.4)	61.0 (35.1-106.6)	0.382
Proportion Core (%) (Range)	57.6(18.5-58.2)	34.7(18.5-58.2)	0.196
Infarct Volume (ml) (Range)	70.2(0-264.8)	29.0(9.7064.4)	0.034
Absolute Infarct Growth (ml) (Range)	23.2 (0.0-79.5)	10.2 (7.5-37.9)	0.128
Relative Infarct Growth (Range)	1.5(0.0-8.6)	0.9 (0.2-2.0)	0.122
Volume Penumbra Salvaged (ml) (Range)	12.7 (3.1-62.5)	32.3 (11.5-68.1)	0.166
Proportion penumbra salvaged (%) (Range)	65.0(16.0-100.0)	91.0(42.0-98.0)	0.041
24 hr NIHSS	15.5 (0.0-30.0)	7.0(5.0-15.0)	0.016
24hr NIHSS reduction	3.0(-11.0-16.0)	7.0(2.0-10.0)	0.295
Fibrinogen (mg/L) (SD)	3.7(3.3-4.3)	3.2(2.7-3.5)	0.167

**Table 5-5 Clinical and Imaging Factors Associated with Clinical Outcome**

Admission /24hr NIHSS, ASPECTS on NCCT and CBV, proportion of penumbra salvaged and final infarct volume were all associated with clinical outcome status. Categorical variables compared using the Chi Squared test. Normal and non-normal continuous variables compared using the t test and Mann Whitney U test, respectively.

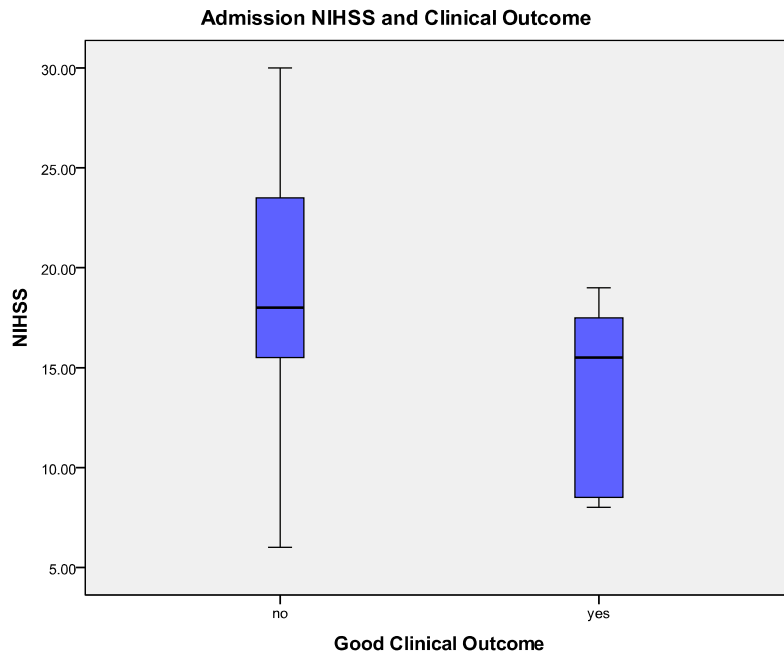


**Figure 5-18 Admission NIHSS and Outcome (Median +IQR +Range)**  
Mann Whitney U test p=0.05

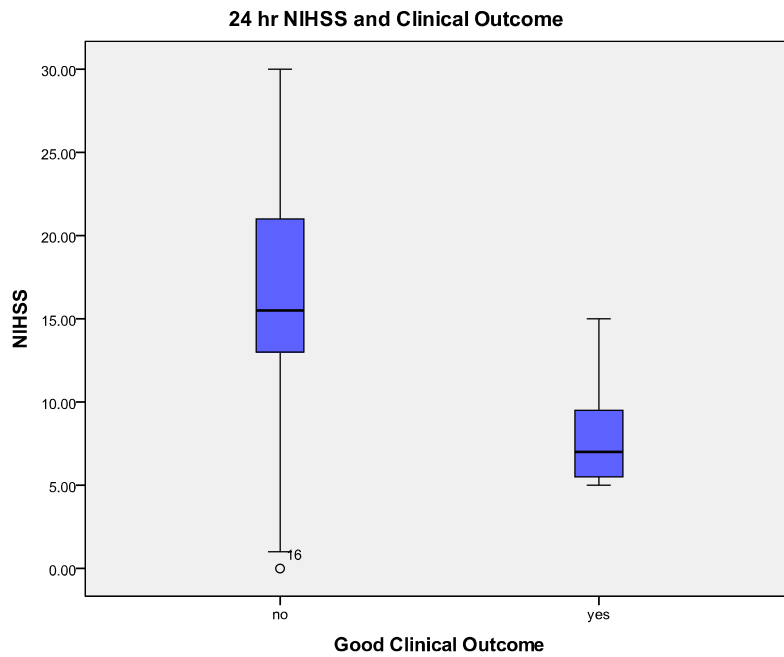


**Figure 5-19 24hr NIHSS and Outcome (Median +IQR +Range)**  
Mann Whitney U test p=0.016



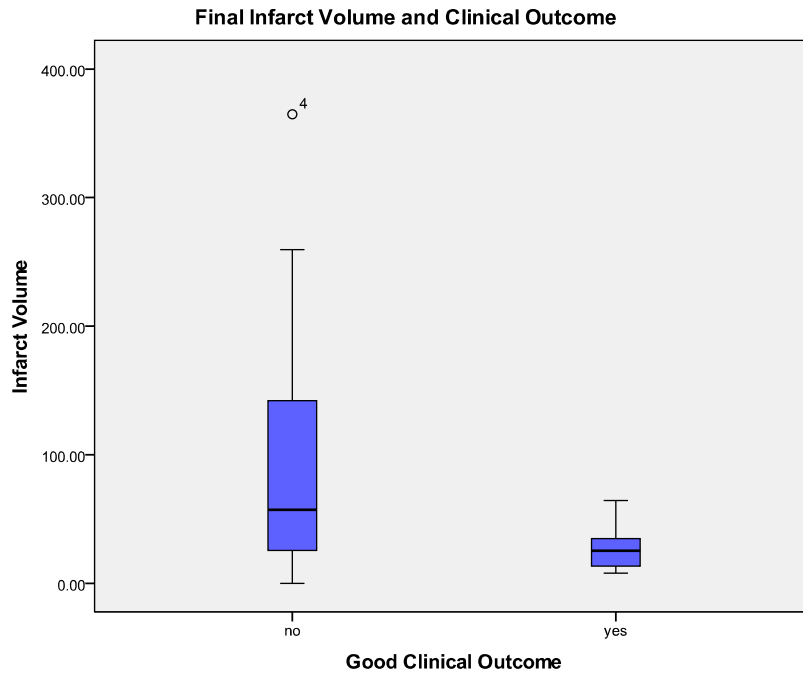


**Figure 5-20 Infarct Volume and Clinical Outcome** (Median +IQR +Range +Outlier)  
Mann Whitney U test p=0.034

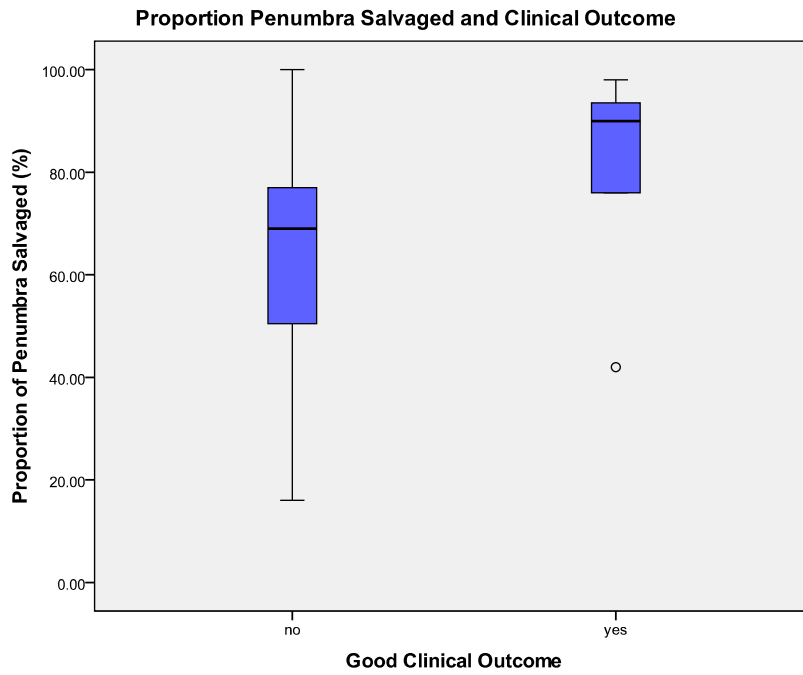


**Figure 5-21 Proportion Penumbra Salvage and Clinical Outcome** (Median +IQR +Range +Outlier)  
Mann Whitney U test p=0.041

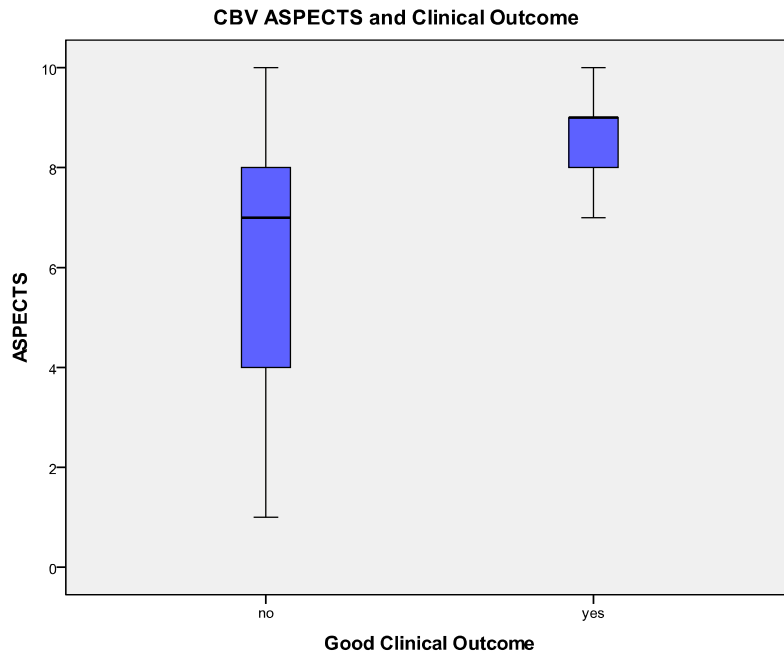


**Figure 5-22 ASPECTS Score on CBV Maps and Clinical Outcome (Median +IQR +Range)**  
 Mann Whitney U test p=0.017

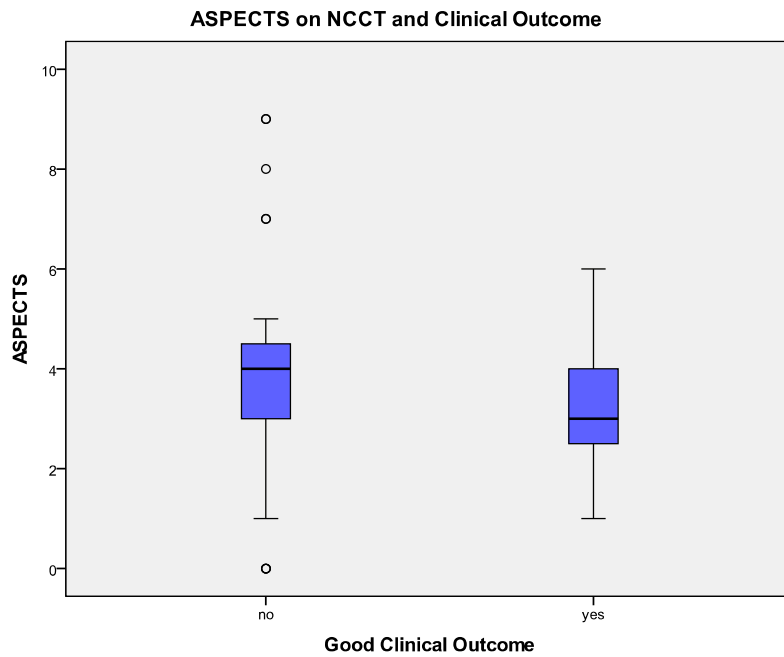


**Figure 5-23 ASPECTS Score on NCCT and Clinical Outcome (Median +IQR +Range+ Outliers)**  
 Mann Whitney U test p=0.042

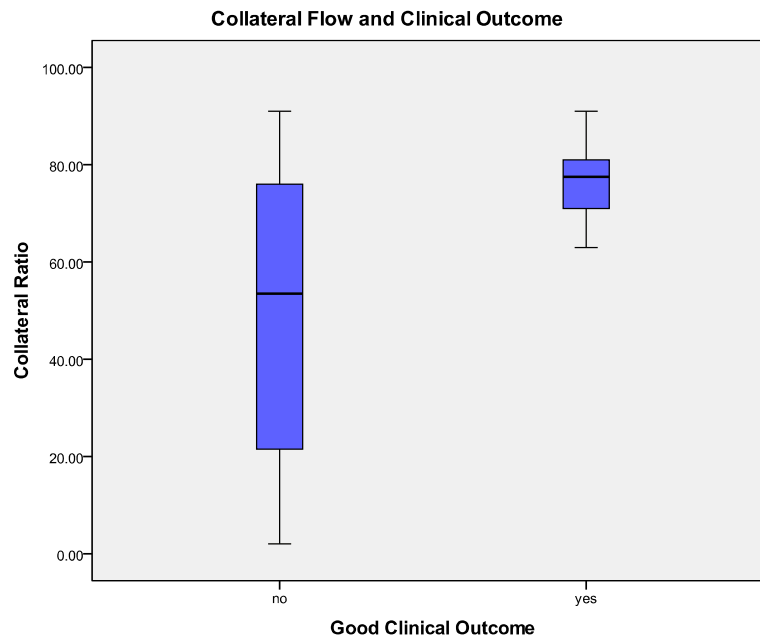


**Figure 5-24 Collateral Flow and Clinical Outcome (Median +IQR +Range)**  
 Collateral ratio, when measured as a continuous variable was associated with better clinical outcomes. Median 77.5 % ( Range 63-91%) and 53.5 % ( range 2-91%) for good and poor clinical outcome groups, respectively .Mann Whitney U test p=0.017

<b>Predictor</b>	<b>OR (CI)</b>	<b>P</b>
ASPECTS NCCT	1.426(0.990-2.055)	0.057
ASPECTS CBV	1.856 (1.023-3.366)	0.042
Infarct Volume	0.974 (0.946-1.003)	0.080
Collateral flow	1.006 (1.004-1.119)	0.037
NIHSS	0.852 (0.727-0.998)	0.047
24hr NIHSS	0.850 (0.733-0.987)	0.033

**Table 5-6 Univariate Logistic Regression Analysis Summaries for Clinical Outcome Prediction (Modified Rankin Scale  $\leq 2$  at one month)**

## 5.5 Discussion

This study evaluated collateral flow extent using a novel semi-quantitative measurement based on quantifying the extent of vessel filling in a region affected by stroke relative to the normal contralateral region. The method was devised after considering the merits of other available grading scales summarised in chapter 2. All previous methods using CTA to measure collaterals were based on qualitative interpretation of images with only some studies reporting inter/intra observer agreement. This method design attempted to avoid subjective interpretations of what may appear as good or poor vessel filling and risk of bias by drawing a ROI over the normal hemisphere and quantifying the number of vascular pixels in the mirror region. This assumes that vascular territories are relatively symmetrical which in practice they usually are, although this may not be true for all subjects (e.g. previous stroke with established infarction, previous intracranial steno-occlusive disease, presence of arteriovenous malformation). Similar to previous studies, only proximal anterior circulation strokes were evaluated. The use of CTP to determine the direction of flow was considered an important additional feature in order to evaluate features associated with different collateral flow and has been used in a previous study(111). This may have resulted in a smaller final patient cohort but is likely to have made the population more homogenous. If subjects with residual antegrade (e.g. high grade stenosis/incomplete occlusion) rather than retrograde flow were included, patient characteristics specifically relating to collateralisation may not have been evident. Intra-observer agreement was excellent although inter-observer reliability was not assessed. Measuring collaterals in a quantitative fashion is not something likely to be possible in clinical practice but as a way of studying collateral flow influences and minimising subjective interpretation, a quantitative assessment appears useful and promising for further work.

Patients with well developed collateral flow had some differences from those with poor collateral flow although the two groups were generally well matched at baseline. Collateral flow extent was not associated with increased time between symptom onset and scan acquisition as had been previously suggested, and pre-morbid statin therapy did not appear to affect collateral flow grade in this population (234, 301). Although the occlusion subtypes, core, penumbra and

perfusion lesion volumes were not significantly different in this cohort those with good collateral flow had significantly lower admission NIHSS values. Right and left hemisphere strokes may be represented differently by the NIHSS but this is not likely to account for this difference alone. The volumes of hypoperfused tissue on DT maps at 2, 6 and 8 second thresholds were significantly larger in those with poor collateral flow, although the ratio of severe to mild levels of hypo perfusion was not significantly different. The difference in absolute DT volumes appears at odds with the core and penumbra measurements, but these are based on perfusion thresholds which are not yet validated and therefore using combined core/penumbra volume as the only measure of hypoperfused tissue on CTP should be interpreted with some caution. Although use of DT thresholds also has limited validation the observed trend could suggest that collateral flow may result in smaller volumes of severely hypoperfused tissue. A reduction in volume of severely hypo perfused tissue could potentially result in less tissue being at risk of infarction, and as ischemic penumbra is by definition associated with a clinical deficit, a reduced penumbra volume could result in less clinically severe strokes measured using the NIHSS. However, although groups were not significantly different at baseline, the higher proportion of proximal occlusions ( particularly ICA occlusions ) seen with reduced collaterals means an effect from occlusion site as a confounder cannot be excluded.

The similarity in the qualitative measurements of hypoperfusion (ASPECTS on MTT or TTP) between patient groups suggests that the overall volume of tissue which is experiencing any hypoperfusion is not significantly different between groups with good and reduced collaterals. This visualised area of perfusion disturbance on ASPECTS does not measure the severity of hypoperfusion, but just its overall extent and therefore could include mildly hypoperfused tissue or “benign oligemia” which is not at risk of infarction and unlikely to contribute to the clinical deficit(342). The reduced collateral group did however have significantly lower ASPECTS scores measured on CBV, an indicator of tissue which is likely to be irreversibly damaged(130) . Viewed in combination these findings suggest that volumes of hypoperfusion are broadly similar in those with good and reduced collaterals, but those with good collateral flow have smaller volumes of core. If this is a true effect it is suggestive of a beneficial effect of well developed collateral flow, resulting in larger volumes of ischemic tissue being in

a potentially viable state compared to those with reduced collaterals. However as previously stated, the potential for differences based on baseline occlusion to be a confounding variable needs to be considered.

Collateral flow grade was associated with beneficial outcome on imaging markers. No patient with good collaterals underwent haemorrhagic transformation post thrombolysis. Recanalization after IV thrombolysis was not influenced by collateral flow extent in this study as had been previously suggested due to enhanced drug delivery to the site of action(343) but final infarct volume and volume of infarct growth from baseline core measurement were significantly less in the group with good collaterals. Proportional penumbra volume salvaged and relative lesion growth from baseline were significantly different between groups with good and reduced collaterals. These findings are supportive evidence of the beneficial effect of collaterals by maintaining residual flow to the ischemic zone despite the presence of a proximal occlusion. Recanalisation is an important predictor of outcome and is used as a surrogate marker for outcome, but collateral flow has also been shown to impact imaging and clinical outcomes (53, 111, 244). Prompt recanalisation even with poor collaterals can have good outcomes, while collateral status is also predictive of outcome, suggesting that good collaterals and recanalisation are likely to result in the best outcomes(245).The effect on imaging outcomes measured support the protective effect of collateral flow in reducing severity of hypo perfusion, limiting the progression of ischemic tissue to infarction before and after the time of initial image acquisition and importantly the overall infarct volume, a surrogate marker for clinical outcome (47, 321).

Baseline characteristics associated with collateral flow included NIHSS, atrial fibrillation and blood fibrinogen. The association with less clinical severity may reflect milder strokes and consequently a confounding measurement when determining predictors of outcome. The similar volumes of hypoperfused tissue measured could point towards collaterals maintaining tissue in a state of benign oligemia and therefore less symptomatic penumbra/ core tissue for the reasons outlined above, as truly penumbral tissue should be associated with a clinical deficit(26).

Patients with good collateral flow were less likely to have a history of atrial fibrillation. This has not been previously reported. Cardio-embolic stroke may be associated with a different response to ischemia than large artery atherothrombotic stroke as animal models have suggested that previous reduction in blood flow may serve a protective role by pre-conditioning the cerebrum to the effects of ischemia(344). Mechanisms for induction of ischemic tolerance are unclear with neuronal gene expression and protein synthesis being suggested as potential methods (344, 345). Reduction in cerebral perfusion pressure prior to a stroke has been shown to be associated with preserved cerebral blood flow mediated via leptomeningeal collaterals in rat models suggesting ischemic preconditioning may be mediated via an enhanced collateral flow network(346). Sudden onset of brain ischemia without previous warning, such as in cardio-embolic stroke could possibly be associated with reduced ability to compensate compared to those with extracranial / intracranial atherosclerotic disease but the association is unclear. This study did not find a relationship with the presence or degree of carotid stenosis and collateral flow, although large artery /non cardio-embolic related strokes are not necessarily associated with carotid stenosis. As this association has not been previously reported it should be viewed with caution but given the proposed mechanism of collateral development by previous transient ischemia in animal models, additional studies to investigate whether the response to stroke mediated via collaterals may be influenced by stroke mechanism should be considered.

Baseline fibrinogen level was significantly lower in patients with good collateral flow which is intriguing given the association of fibrinogen with stroke risk but also stroke outcome. The fibrinogen studies collaboration have shown in a meta-analysis of 31 studies that higher fibrinogen levels influences risk of stroke, cardiovascular death and all vascular mortality implicating fibrinogen as a marker for cardiovascular risk(347). In addition, fibrinogen has been identified as a marker for outcome after stroke by Tanne et al who found higher baseline fibrinogen levels in those with a poor clinical outcome in subjects recruited to the original NINDS study (348). Reducing fibrinogen in a rodent stroke model by plasma exchange has been shown to reduce blood viscosity , improve CBF and reduce ischemic injury potentially via enhanced collateralisation(349). Fibrinogen reduction has therefore been studied in a number of randomised

clinical trials for a potential treatment effect, although the results are conflicting. Ancrod is a purified extract from Malayan Pit Viper *Agkistro donrhodostoma* which rapidly induces defibrinogenation in humans (350). The STAT study suggested that using Ancrod to reduce fibrinogen within 3 hrs of stroke onset was associated with better clinical outcomes (351). The European ESTAT study did not show any beneficial effect when Ancrod was administered in subjects recruited within 6 hours of symptom onset(335). A recently updated Cochrane review of defibrinogenation for ischemic stroke did not support the routine use of fibrinogen-lowering agents but suggested some patients could possibly benefit and further study was required in order to identify subgroups appropriately(352). Those trials included in the Cochrane review did not report use of additional imaging which may have provided insights into subgroups that may have benefited from lowering fibrinogen levels. As fibrinogen is a marker for blood viscosity and micro vascular occlusion, the association with collateral flow grade demonstrates a potential mechanism for the possible benefit seen with lower fibrinogen level(349). There is a single previous study which investigated fibrinogen and collateral flow, although only an indirect imaging marker for collaterals was used. Lee et al found an association between low fibrinogen and the presence of a dominant posterior cerebral artery ipsilateral to an occluded Middle cerebral artery. The enlarged posterior cerebral artery in this study was considered a sign of collateral recruitment to the ischemic site from the adjacent arterial network and flow was suggested to be enhanced in those with lower fibrinogen levels(334). Imaging characteristics of those with elevated and reduced fibrinogen have not otherwise been reported previously. Fibrinogen level may have a number of effects, but if collateral flow is influenced by fibrinogen, it may be that some patient subgroups would have little to benefit from lowering fibrinogen acutely. Lenticulostriate arteries which are affected in lacunar stroke are anatomically end arteries which do not benefit from collateral supply, while patients with very distal occlusions may not benefit from reduced viscosity/ improved collaterals compared to more proximal occlusions with larger volumes at risk but also more potential for collateral flow derivation. These mechanisms remain speculative but point towards heterogeneous stroke subtypes in whom increasing collateral flow (and lowering fibrinogen) could potentially have a meaningful effect depending on the site of arterial occlusion. This study cannot prove a direct relationship between



collaterals and fibrinogen, but if this relationship was evident it could mean that some subgroups have potential benefit by reducing fibrinogen level acutely such as those with vessel occlusion and poor collaterals, while others would have little to benefit from enhanced collaterals, such as lacunar strokes. Improved characterisation of subgroups using imaging will be needed to see if fibrinogen depletion can be of benefit in some groups, but this study suggests that collateral flow and fibrinogen may have a relationship which could potentially be targeted for effect.

Good clinical outcome was seen significantly more often in those with good collaterals, although overall numbers with good clinical outcome were low overall. Other univariate predictors of good outcome were also associated with collateral flow grade when good and reduced groups were compared. None had a significant impact on outcome in a multivariate analysis, and therefore an independent effect for any of the variables, including collateral grade, on outcome was not demonstrated. Although the effect of collaterals may be confounded by other variables, in particular admission NIHSS, the results suggest that collateral flow extent is variable among patients with similar baseline occlusions, that hypoperfused volume is similar overall but less severe in those with good collaterals, that core and infarct volume are smaller when collaterals are developed, and that both fibrinogen and stroke mechanism could influence the degree of collateral recruitment.

Strengths of this study include the precise identification of collateral flow using both CTA and CTP, the objective semi-quantitative measurement used and the excellent intra-observer reliability. Limitations include that the population is highly selected and therefore the results may not apply to other stroke subtypes, although even after selection based on occlusion and flow direction on CTP, the different occlusion subtypes could be seen as a limitation as more proximal occlusions are associated with markers for poor clinical outcome. The study population was small, which limits the ability to draw firm conclusions on the reported findings associated with good and reduced collateral flow which have not been previously reported. These findings should therefore be evaluated in larger independent populations. Outcome imaging was early which may result in overestimation of lesion volume due to swelling in the first days after stroke. Given the extent of image post processing involved, the method is not one which

can be used in “real time” limiting use in clinical practice, but it is important to study collateral flow characteristics first as the degree to which collateral development could /should influence clinical decision making remains unclear. CTA appearances can however be rapidly evaluated meaning that other qualitative scales could potentially be used in acute stroke decision making without major delays in treatment. Should the case for considering collaterals in treatment decisions be proven, a more pragmatic scoring system would need to be employed. In the meantime, this novel grading scale has shown the beneficial effects of collateral flow on imaging and clinical measurements of outcome after ischemic stroke and has suggested additional areas for research. In particular the possibility of fibrinogen being a blood biomarker for collaterals is of potential significance with the possibility of exploring collateral therapeutics with agents to reduce fibrinogen such as Ancrod in selected populations. As collaterals seem to be associated with less severe blood flow reduction and smaller infarct volumes, methods to enhance collateral flow could be of real clinical importance to acute stroke patients.

## **5.6 Conclusion**

The application of a novel and semi quantitative method for grading collaterals in proximal arterial occlusions has demonstrated good intra-observer reliability and could represent a robust method in which to study characteristics of collaterals. No previous study has evaluated collaterals with blood biomarkers, and although the results require confirmation, the possibility of fibrinogen being associated with collateral adequacy is supported by other studies which suggested collaterals and fibrinogen may be interrelated and is an interesting finding worthy of further study, particularly as fibrinogen lowering has been linked with positive effects in stroke. Good and poor collaterals were associated with similar volumes of perfusion disturbance, but better collaterals seemed to have less severe degrees of hypo perfusion suggesting a beneficial effect in real time. Smaller infarct volumes also support the concept of collaterals being beneficial for stroke outcome. Small numbers are a limitation and this study did not show that collaterals were independently predictive of outcome but overall the results are strongly supportive of the positive impact of collaterals and suggest further evaluation of clinical and blood biomarkers should be undertaken to understand collaterals as a potential future therapeutic target.



## Chapter 6. Derivation and Evaluation of Thresholds for Core and Tissue at Risk of Infarction Using CT Perfusion

### 6.1 Introduction

The limited overall sensitivity for NCCT to detect acute ischaemia in the first hours after stroke onset has led to the use of alternative or complementary imaging modalities to provide additional information in acute stroke assessment (74, 151). Physiological imaging identifies distinct groups of patients that are clinically indistinguishable but have different brain imaging profiles with respect to blood flow and metabolic activity, and potentially divergent outcomes based on the presence or absence of viable tissue(29). Brain perfusion imaging with CT or MRI offers a practical means of identifying brain tissue viability in individual patients, with the potential to improve patient selection for reperfusion therapies such as IV thrombolysis. While MRI based perfusion imaging has been extensively used to operationally define core and penumbra, and to demonstrate the impact of thrombolysis on stroke lesion evolution (143, 170), multiple other factors impact on the feasibility of performing MRI based penumbra and core imaging highlighted previously. Multislice CT scanners are widely available resulting in the potential for acquiring CTP in addition to CT and CTA in hyperacute stroke with only a few additional minutes required to complete imaging(353). CTP offers potentially quantifiable assessment of perfusion parameters that can be acquired rapidly and predict volumes of potentially salvageable tissue(113)

Thresholds to define irreversibly damaged core and tissue at risk of infarction/ penumbra have been proposed for CTP, equivalent to the MRI diffusion-perfusion mismatch concept (131). These proposed thresholds have been used as selection criteria for entry to clinical trials of novel thrombolytic agents and appear in post-processing packages on CT workstations for use in clinical practice (47, 52). However, CTP thresholds for core and penumbra have been derived from only a limited number of subjects and scanners, and no study has validated the proposed thresholds in an independent dataset to assess the accuracy of each threshold in practice. Moreover, different studies have reached differing conclusions regarding optimal indices and thresholds for core or penumbra based

on CTP suggesting that further validation of thresholds is needed before their routine application in clinical practice (104, 131, 133, 134, 354, 355).

Methods for core measurement have used concurrently acquired DWI volume as a gold standard measurement of infarct core against which to test CTP parameters (131). Comparison between acute and 24 hr DWI volumes in patients who showed major reperfusion demonstrated similar results however, suggesting lesion evolution after initial image acquisition may be negligible if early reperfusion occurs (134).

Tissue at risk of infarction on CTP has been measured using final infarct volume as the gold standard reference in patients who did not show recanalisation of a baseline arterial occlusion. The differences between the thresholds for core and tissue at risk have been used as a measurement of penumbra (131).

Post-processing algorithms vary among different manufacturers with the result that generated perfusion maps can be different despite use of the same raw imaging data (117). An important feature of post-processing packages highlighted more recently is the algorithmic correction for tracer bolus delay in order to avoid pseudo-reversibility of some perfusion lesions (127). Delay correction may not have been performed for all previous CTP threshold derivations which could produce unreliable results if applied on a scan processed using a delay corrected algorithm.

Given the uncertainty over which thresholds best represent core and penumbra, possible unreliable map generation without correction for tracer delay, and lack of validation in independent cohorts, I sought to derive the perfusion thresholds which best represent core and penumbra on CTP and evaluate the accuracy of the derived thresholds along with those from the literature to determine which thresholds perform best in independent validation.

## **6.2 Materials and methods**

### ***6.2.1 Patient selection***

Patients included in the present analysis were selected from those recruited to the POSH or MASIS studies between August 2008 and September 2010 at the

Institute of Neurological Sciences, Southern General Hospital, Glasgow. Entry criteria to the studies, imaging protocols, and clinical assessments are described in more detail in Chapter 3. For the present analysis patients were selected from the combined dataset based on specific imaging characteristics. As stated in chapter 3, some patients recruited to MASIS underwent MRI imaging at baseline instead of CT, but only those imaged with CT were considered for this analysis as MRI perfusion thresholds would require separate evaluation which is beyond the scope of this work. After recruitment to each study imaging characteristics including occlusion status, recanalisation status clinical severity at baseline and 24 hrs were recorded. From the combined dataset, 2 sets of selection criteria were used to identify patient and imaging data on which threshold analysis could be performed.

Tissue at risk was evaluated in patients with the following imaging characteristics:

- 1) Arterial occlusion on admission CTA
- 2) Non recanalization of baseline occlusion at subacute CTA/ MRA at 24-72 hrs (TIMI 0)
- 3) Follow-up structural brain imaging at 24-72 hrs obtained to enable quantification of final infarct volume

These inclusion criteria are similar to those used in previous threshold derivation work (131). The presence of an arterial occlusion which does not recanalize on follow up scanning permits the assumption that all hypoperfused tissue which was at risk of infarction at baseline will have infarcted at follow up. In this assumption even small degrees of recanalisation could potentially result in reperfusion to some of the ischemic zone and subsequently influence the derived threshold. For this reason only those with no recanalisation of any degree were selected for inclusion. Hypoperfused tissue which does not infarct despite the lack of recanalization or reperfusion may be considered to be benign oligemia, hypoperfused but not actually at risk of infarction (356).

Patient data were selected for inclusion in the core threshold dataset based on the following characteristics:

- 1) Arterial occlusion on admission CTA
- 2) Evidence of recanalisation on subacute CTA/MRA at 24-72 hrs
- 3) Clinical evidence suggestive of major reperfusion - Improvement in NIHSS by  $\geq 4$  points at 24 hrs
- 4) Follow-up structural brain imaging at 24-72 hrs obtained to enable quantification of final infarct volume

A concurrently acquired DWI was not available as a measure of infarct core but as infarct volume at 24 hrs in patients who undergo major reperfusion have been shown to be similar to baseline DWI volume subacute imaging characteristics can serve as a reference for core lesion volume in selected patients(134). Imaging evidence of reperfusion was not available for all patients due to the imaging protocols within the POSH study so patients with recanalisation combined with major early clinical improvement were chosen as this is likely to represent a group with salvaged penumbra and minimal infarct growth between baseline and subacute imaging time-points. Final lesion volume in this cohort was used as the reference for measuring infarct core extent.

Patients who met entry criteria for core or tissue at risk analysis were then further divided into subgroups. Within the tissue at risk group, patients were divided randomly into a threshold derivation group used to test a large range of absolute and relative thresholds and a validation group in which to test the best performing thresholds from the derivation dataset and a selection of those from the literature. The same sub-group division was performed for those meeting core group entry criteria, where patients were randomly divided to derivation and validation cohorts in which to derive and then test the best performing thresholds along with a selection from the literature. Cases were listed within the core and tissue at risk groups in Microsoft excel and a randomisation formula was used to select patients for inclusion in either threshold derivation or threshold validation subgroups separately for core and tissue at risk.

## **6.2.2 Image Acquisition**

Multimodal CT examination was obtained using a Multidetector Scanner (Philips Brilliance 64 Slice) comprising non contrast CT, CT perfusion and CTA from aortic arch to the Circle of Willis. Imaging parameters are describe in detail in chapter 3.

Follow up CT imaging for was with whole brain NCCT followed by intracranial CTA from base of skull to the top of the lateral ventricles as described in chapter 3.

Follow up MRI, where applicable was performed on a 3T MRI using post -contrast FLAIR to demarcate the final infarct volume (GE, 3.0T Signa Excite, TR 10000 ms, TE 144.4 ms, slice thickness 5mm matrix 284x286).

## **6.2.3 Image analysis**

### CTA interpretation

Initial image analysis is described in chapter 3. In summary, patent identifiers were removed and each scan was given a unique study Identification header. Presence of arterial occlusion was determined from the acute CTA processed on a Philips Brilliance workstation (Advanced Vessel Analysis tool) using source images and MIP reconstructions in axial, coronal and saggital planes. An occlusion was defined as an absence of contrast material in the vessel which completely separated the proximal portion of the vessel from the distal portion(111). Recanalisation was determined using an adapted Thrombolysis in Myocardial infarction (TIMI) scale where recanalisation was defined as none (TIMI 0), minimal (TIMI 1) partial (TIMI 2) and complete (TIMI 3)(167)

### CTP processing

CTP post-processing was performed using MISTar. This provided 4 perfusion parameters for analysis, CBF, CBV, MTT and DT. Motion correction was automatically applied by the programme after loading the raw CTP dataset. AIF and VOF were selected semi-automatically after placing a ROI in the anterior cerebral artery and superior saggital sinus respectively.



Deconvolution of the tissue enhancement curve and the AIF was performed using a modified singular value decomposition (SVD) method. A tissue impulse residue function (IRF) was derived, where the maximum of the IRF appears at certain time point known as  $T_{max}$ . Usually where  $T_{max}=0$  this reflects normal blood supply in normal tissue without delay. In contrast,  $T_{max}>0$  is considered to be associated with arterial delay and dispersion effect due to the presence of an ischemic lesion. While the physiological meaning of  $T_{max}$  is unclear, its value could be dependent on various factors including arterial delay and dispersion, tissue transit time and dispersion, as well as the cut-off threshold for the SVD deconvolution algorithm. In order to properly compensate for the effect of arterial delay and dispersion, a vascular transport model involving an arterial transport function with a delay time and a relative dispersion was used(341). The effect of the arterial transport function is to shift and broaden the AIF profile, more reflective of true physiology in acute stroke. A delay-corrected SVD deconvolution approach applied a series of delay time values,  $DT_i$ , ranging from 0 to  $T_{max}$ . For each delay time, a modelled arterial transport function was convolved with the measured global AIF to produce an AIF (i), which is used for SVD deconvolution of the tissue curve to generate an IRF (i) with its maximum appearing at  $T_{max}$  (i). The actual delay time,  $DT$ , was determined as the minimum  $DT_i$  value which produces  $T_{max}$  (i) =0.

Subsequently, CBF and CBV were determined from the deconvolved tissue concentration-time curve. CBV was measured as the area under the deconvolved curve while CBF was measured as the peak height of the deconvolved curve. Knowledge of these values for each pixel measured in turn permitted the calculation of MTT according to the following:

$$MTT=CBV/CBF$$

A constant relative dispersion value of 0.35 was used in this study, automatically incorporated by the processing software. This figure is based upon the best fit from internal validation of the MISTar software performed by the software designers. While this figure has been used in CTP validation in other cohorts, the accuracy of the dispersion correction alone has not been subject to external validation (134, 340, 341, 357).

Follow up imaging was co-registered to the baseline CTP frames as previously described.

#### **6.2.4 Derivation dataset image analysis**

Final infarct ROIs were delineated semi-automatically from co-registered images by growth of a ROI seed placed within the infarct according to threshold with subsequent manual correction as required for each slice to ensure the ROI matched the visualised region of infarction (Figure 6.1)

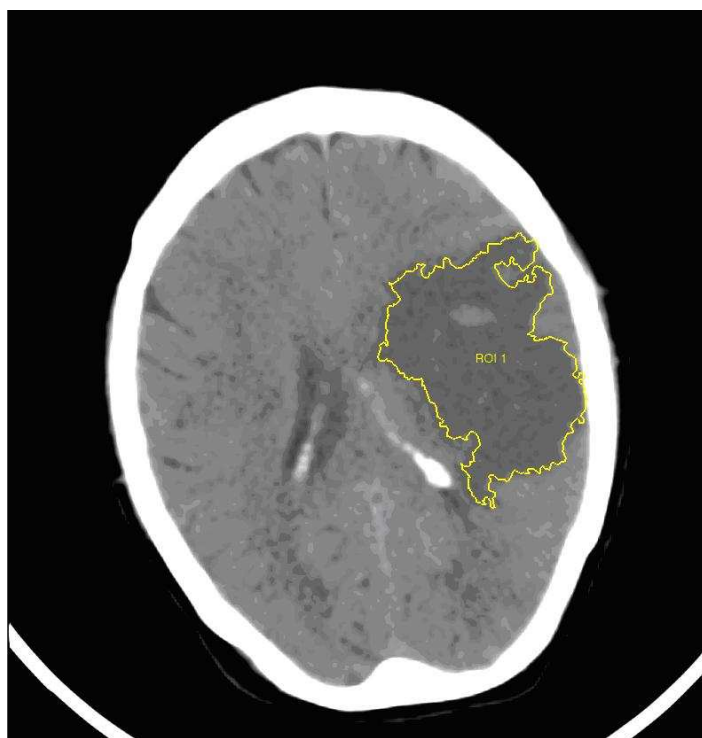


**Figure 6-1 ROI Surrounding Final Infarct Volume**

Subacute NCCT showing left MCA territory infarction with ROI superimposed on the visualised area of hypodensity.

ROIs were transposed onto the corresponding perfusion map slices which could be altered according to perfusion threshold so as to test the predictive value of several different perfusion parameters and thresholds. Seven different perfusion parameters were tested: Absolute CBV, Relative CBV, Absolute CBF, Relative CBF, Absolute MTT, Relative MTT and DT in core and penumbra groups, with 66 and 65 different thresholds assessed for core and penumbra in total respectively. The thresholds tested were chosen to reflect the range of those previously

tested in the literature. The range of thresholds evaluated are shown in Tables 6.1 and 6.2

Perfusion Parameter	Threshold Range	Increment
Relative MTT	100-250%	25%
Absolute MTT	4-14 seconds	1 second
Relative CBF	40-90%	5%
Absolute CBF	5-45ml/100g/min	4ml/100g/min
Relative CBV	40-90%	5%
Absolute CBV	0.5-3.5ml/100g	0.3ml/100g
Delay(DT)	0-10 seconds+ baseline	2 seconds

**Table 6-1 Perfusion Parameter Ranges and Increments Evaluated for Tissue at Risk**  
Relative measures are percentages relative to the mean value in the contralateral hemisphere

Perfusion Parameter	Threshold Range	Increment
Relative MTT	125-300%	25%
Absolute MTT	4-14 seconds	1second
Relative CBF	10-60%	5%
Absolute CBF	3-17 ml/100g/min	2ml/100g/min
Relative CBV	10-70%	5%
Absolute CBV	1-2.5ml/100g	0.25 ml/100g
Delay (DT)	0-10seconds + baseline	2seconds

**Table 6-2 Perfusion Parameter Range and Increments Evaluated for Core**

The ranges of thresholds were evaluated for each slice after placing the infarct ROI onto the Penumbrogram which could be manipulated according to a chosen perfusion threshold. All pixels within the Penumbrogram could be dichotomised as either within or out-with a certain pre specified threshold. In order to test a single threshold at a time, all pixels within the threshold were defined as core within the programme and all others defined as penumbra. This meant that the absolute number of pixels within and out-with a certain threshold could be quantified based on the pixel being represented by one of two possible colours.

“Positive” pixels which were within a given threshold appeared as red and those outside that threshold appeared as green “negative” pixels (Figure 6.2).

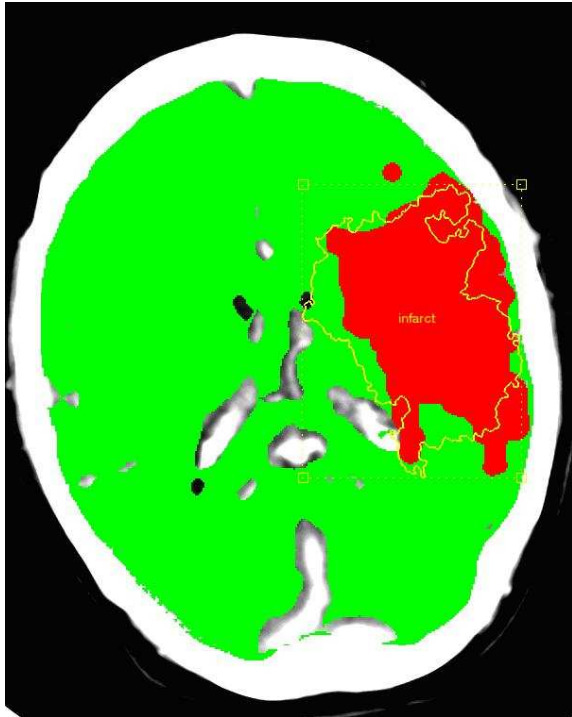


**Figure 6-2 Penumbrogram with Infarct ROI**

Red pixels represent pixels within a given threshold; green pixels represent all other parenchymal pixels. Final Infarct ROI is superimposed in yellow.

Pixels within a chosen CTP threshold which appeared within the final infarct volume were defined as “true positives” (TP), while pixels which were within the chosen threshold but were not within in the final infarct volume were classified as “false positives” (FP). Pixels which were within the final infarct but were not predicted by the chosen threshold were “false negatives” (FN) and non-infarcted pixels not within the thresholded perfusion lesion were “true negatives” (TN) (Figure 6.3). Only pixels in the affected cerebral hemisphere were considered for this analysis as inclusion of whole brain pixels would result in an over-representation of “true negative” pixels which correctly predict that pixels in the hemisphere contralateral to the ischemic lesion would not undergo infarction and result in an overestimation of the true specificity of the threshold tested(134)

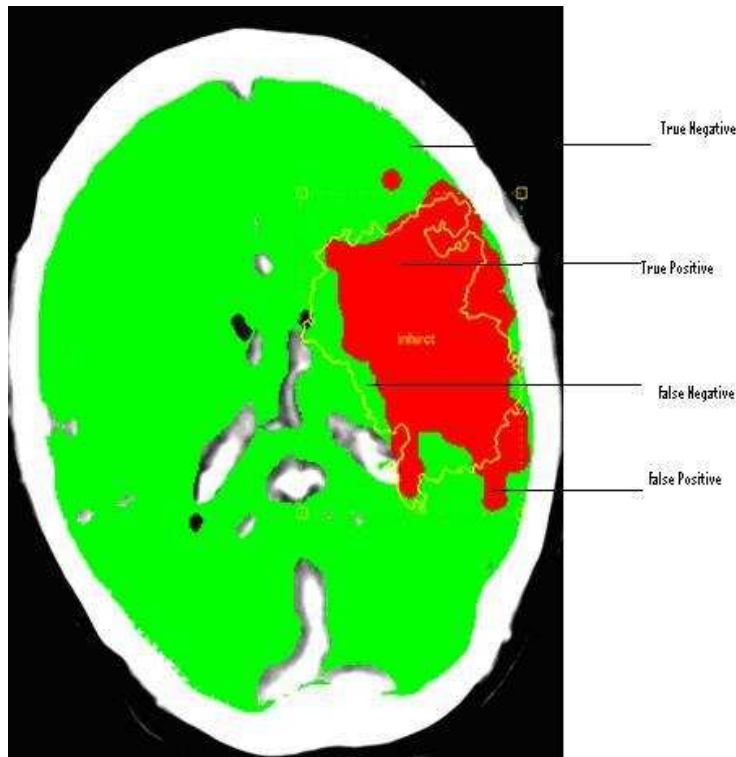


**Figure 6-3 True & False Positive/Negative Pixels**

Positive pixels appear red, negative pixels appear in green. Their relation to the final infarct ROI defines whether or not each is a true or false positive/ negative.

### **6.2.5 Validation datasets image analysis**

A total of 4 perfusion parameter thresholds were evaluated in the independent validation datasets for both core and penumbra. After the optimum parameter thresholds were derived from each the derivation datasets, the best performing thresholds from the ROC curve analysis were tested along with selected thresholds from the literature for accuracy in predicting core and tissue at risk volume. For core analysis, absolute CBV  $\leq 2.0$ ml/100g and relative CBF  $\leq 45\%$  of normal were evaluated with the best derived thresholds, while for penumbra relative MTT  $\geq 145\%$  of normal was evaluated in addition to the best thresholds from derivation dataset. AIF and VOF selection and co-registration were performed as previously described for the derivation group image analysis. Volume of tissue defined according to each chosen parameter threshold was measured. Final infarct volume in the corresponding slices on follow up imaging was determined from ROI analyses using semi-automated ROI growth with subsequent manual correction in the same way as previously described.

Infarct volume for the validation datasets were evaluated on two occasions separated by approximately 2 months blind to the results of the first reading in order to determine intra-observer agreement for infarct volume determination.

### **6.2.6 Statistical analysis**

#### Derivation Datasets

Sensitivity for each threshold was calculated as  $TP / (TP+FN)$ , while specificity was defined as  $TN / (TN+FP)$ . The combination of sensitivity and specificity were plotted for each threshold on a ROC curve of sensitivity (Y-Axis) against 1-specificity (X-axis) for all pixels evaluated. AUC for each perfusion parameter and Youden's index for each threshold tested were derived from the ROC curve for each perfusion parameter [Youden's index  $Y = (\text{sensitivity} + \text{specificity}) - 1$ ](358). The parameters with highest Youden's index values, reflecting the best overall combination of sensitivity and specificity, were examined in more detail to determine the optimum threshold within the perfusion parameter tested for each patient within the derivation datasets. The thresholds which corresponded to the best sensitivity and specificity combination per perfusion parameter per patient were plotted using a histogram, with the most frequently occurring threshold(s) chosen for testing in the validation datasets. The comparison of thresholds with different sensitivity and specificity illustrated in figure 6.4

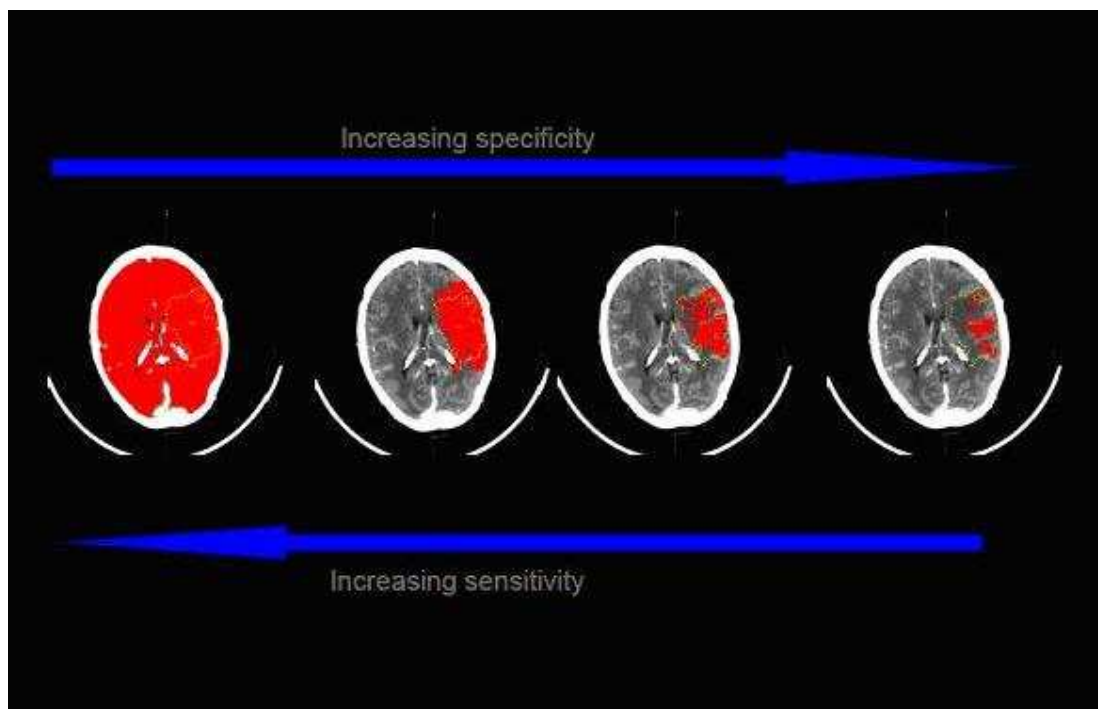


**Figure 6-4 Effect of Varying Perfusion Threshold on Sensitivity and Specificity**

The effect of varying the perfusion threshold on the number of true and false positive pixels measured. Relative MTT of 100%, 150% 200% and 250% of normal are shown. Large numbers of false positive pixels reflect sensitivity but poor specificity of the MTT threshold 100 % (on left). The converse is seen with a higher threshold of 250%, with fewer false positives but also fewer true positives – seen on right.

### Validation Datasets

Volume of predicted infarct volume from CTP according to the selected thresholds were compared to the actual final infarct volume using a Bland Altman plot comparing means and differences in predicted and actual infarct volume for core and penumbra groups .

Baseline clinical characteristics of each group were compared using the Mann-Whitney test. Statistical analysis was performed using Graphpad Prism ([www.graphpad.com](http://www.graphpad.com))

## 6.3 Results

### Tissue at Risk Group

Of 118 patients recruited to the combined studies for the present analysis, 44 had no visualised occlusion, 6 did not have recanalisation assessed, 42 had



evidence of some recanalisation on subacute CTA/MRA, 4 had chronic ICA occlusions which were not responsible for the acute presentation, 1 CTP was acquired with jog mode, 1 stroke lesion was outside the CTP coverage (Superior Cerebellar Artery occlusion) leaving 20 patients with persistent symptomatic arterial occlusions for analysis. One was later excluded from analysis because of massive and ultimately fatal space occupying oedema on follow up imaging as the range of perfusion thresholds tested would inevitably underestimate the apparent infarct volume in this setting.

Of those included, eleven were male and 8 were female. Median age was 72 years (IQR 63-81) and median NIHSS on admission was 18 (IQR 11-19). Occluded vessels included internal carotid artery (ICA) (n=6), M1 segment Middle Cerebral Artery (MCA) (n=6), M2 segment (n=5), M3 segment (n= 1) and Posterior Cerebral Artery (PCA) (n=2). Median time from symptom onset to imaging with CTP was 164 minutes (IQR 136-196) and hemisphere affected was the left side in 13/19 cases. 17/19 had follow up brain imaging with CT with a median time from onset to follow up scan of 26 hours (IQR 24-31). There were no significant differences in age, NIHSS or imaging times between validation and derivation datasets (Table 6.3).

	<b>All (n=19)</b>	<b>Derivation Dataset (n=12)</b>	<b>Validation Dataset (n=7)</b>	<b>P</b>
Age (Mean +SD)	71(11)	69 (11)	74(11)	0.35
NIHSS (IQR)	18(11-19)	17(11-19.8)	19(8-19)	0.93
Onset to CTP (Mins)(IQR)	164 (136-196)	156 (138-196)	169(130-247)	0.47
Time to follow up imaging (Hours)(IQR)	26(24-31)	27(24-30)	25(24-48)	0.77

**Table 6-3 Characteristics of Tissue at Risk Evaluation Group**

Groups were compared using the t test or the Mann Whitney U test for normal and non-normally distributed data, respectively.

Over 3.8 million pixels were analysed in total. ROC curves and Youden's index for each perfusion parameter showed that the best overall predictors for tissue at risk were relative MTT, absolute MTT and delay time. (Figure 6.5)

The best combination of sensitivity and specificity for these perfusion parameters were determined for each patient showed clustering around  $DT \geq 2$  seconds, absolute MTT  $\geq 7$  seconds and relative MTT of 125% for the three parameters evaluated suggesting that these thresholds had the best predictive value of infarct volume in this setting (Figure 6.6).

In the validation dataset, Bland-Altman plots to assess the accuracy of each chosen threshold (Relative MTT  $\geq 125\%$ , Absolute MTT  $\geq 7$  seconds,  $DT \geq 2$  seconds) and one from the literature (relative MTT  $\geq 145\%$ ) revealed that the cut point with most accuracy in predicting final infarct volume was  $DT \geq 2$  seconds (95% limits of agreement -44 to +30, Bias -6.89) followed by relative MTT  $\geq 145\%$  (95% limits of agreement -75.1 to +96.8 Bias +10.8), relative MTT  $\geq 125\%$  (95% limits of agreement -70.1 to +108.5 Bias 19.2) and Absolute MTT  $7 \geq$  seconds (95% limits of agreement -65.7 to +112.2 Bias 23.3)(Figure6.7).

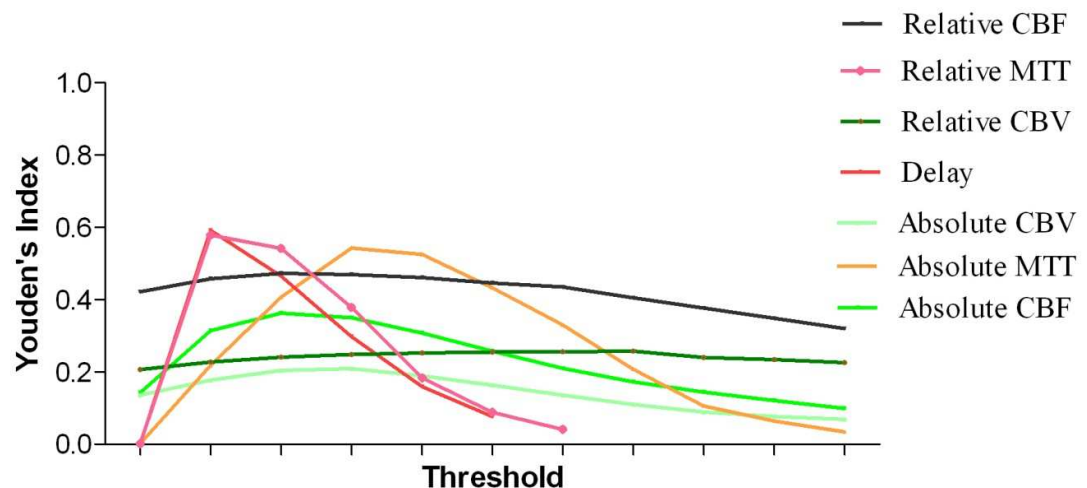
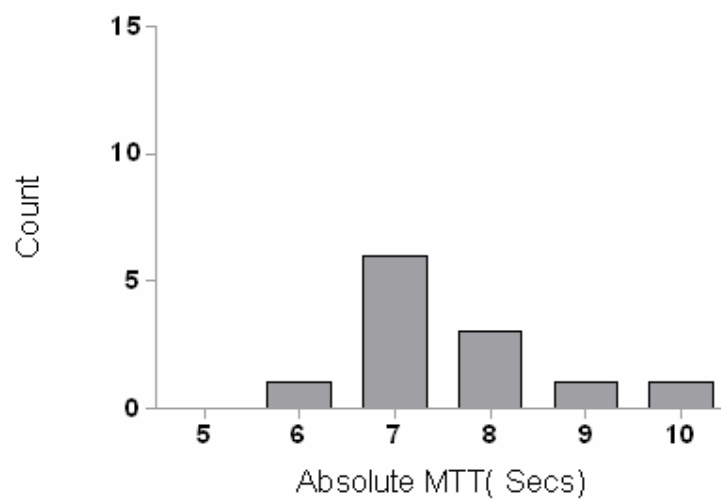
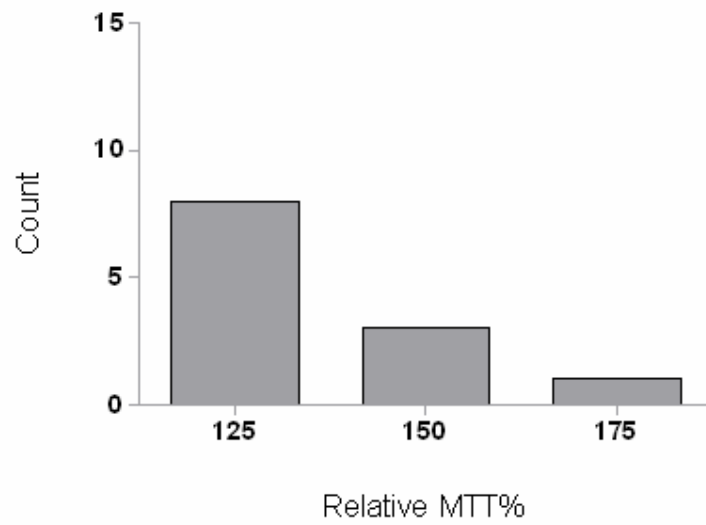
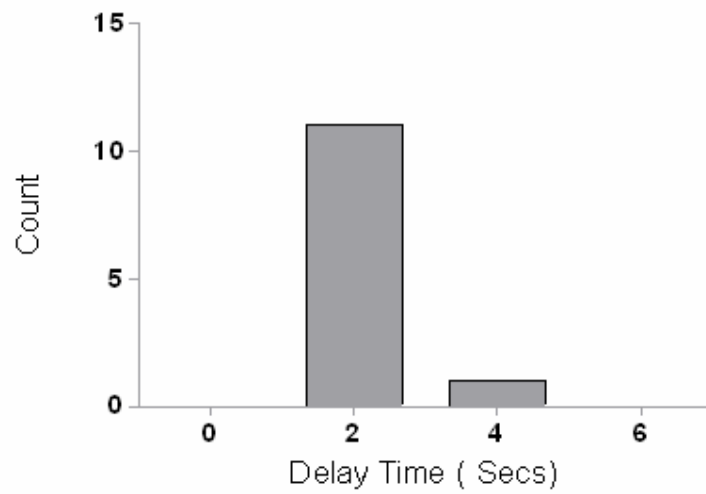
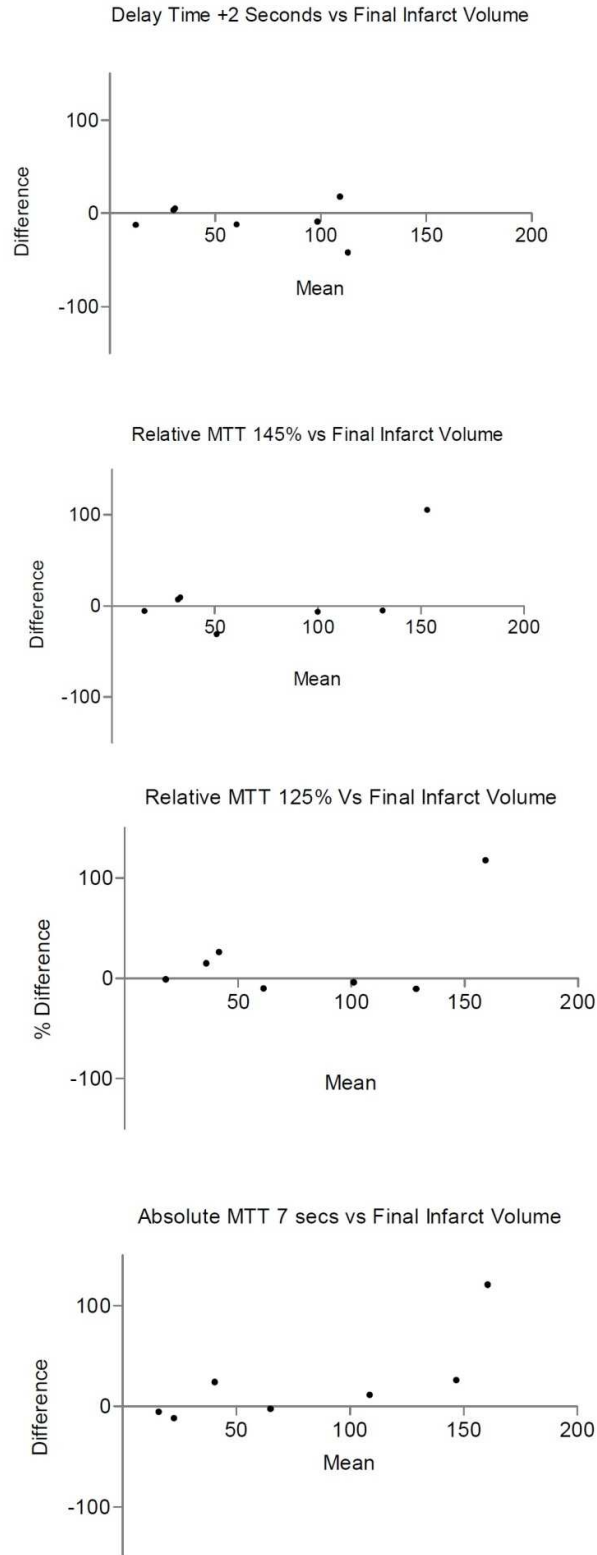


Figure 6-5 Youden's Index for Each Perfusion Threshold Evaluated for Tissue at Risk



**Figure 6-6 Frequency Distribution for Optimum DT, Relative MTT and Absolute MTT Thresholds for Tissue at Risk**



**Figure 6-7 Bland Altman Plot for DT >2 Seconds, Relative MTT 145 %, Relative MTT 125 % and Absolute MTT 7 Seconds for Detecting Tissue at Risk**

### Core Group

16 patients were included in the core threshold analysis, 7 were male and 9 were female. Median age was 75 (IQR 65-83), Median NIHSS on admission was 15 (IQR 7-15) and median time to subacute imaging with CT/MRI was 29 hrs (IQR 27-63), with subacute CT being performed for 15/17 cases. Left hemisphere was affected in 6/17 occasions. Vessel occlusions at baseline included M1 MCA (8) M2 (5) PCA (2) and ACA (1).

There were no significant differences in clinical characteristics at baseline between derivation and validation groups (Table 6.4). Over 2.9 million pixels were analysed.

	All	Derivation Dataset	Validation Dataset	p
Age (Mean + SD)	72(14)	73(13)	70(15)	0.62
NIHSS (Median + IQR)	15(7-18)	8(7-16)	18(12-22)	0.08
Onset to CTP (Mins) (Median + IQR)	196 (149-233)	219 (154-284)	188(143-227)	0.35
Time to follow up imaging (Hours) (Median +IQR)	29(27-63)	28(25-52)	30(27-123)	0.63

**Table 6-4 Clinical Characteristics of Infarct Core Groups**

Groups were compared using the t test or the Mann Whitney U test for normal and non-normally distributed data respectively.

Cut points derived from the ROC curves for each perfusion measurement showed that absolute and relative MTT were the best predictors of final infarct volume in the trial dataset (Figure 6.8) and histograms of the most frequently occurring thresholds for each parameter demonstrated clustering at absolute MTT of 8 seconds and relative MTT of 125% of normal (Figure 6.9)

Bland-Altman plots for these two derived thresholds and two from the literature (Absolute CBV  $\leq$  2.0 ml/100g and relative CBF  $\leq$  45%) revealed that the best performing threshold was relative CBF  $\leq$  45% (bias -3.9ml, 95% limits of agreement -51.6 to +43.6) followed by absolute CBV  $\leq$  2.0 ml/100g (bias 6.4ml 95% limits of agreement -49.3 to +62.3), absolute MTT of 8 seconds (bias 24.4ml, 95% limits of agreement -38.8 to + 87.6) and relative MTT of 125% (bias 39.2ml 95% limits of agreement -47.4 to +127.8 ) (Figure 6.10).

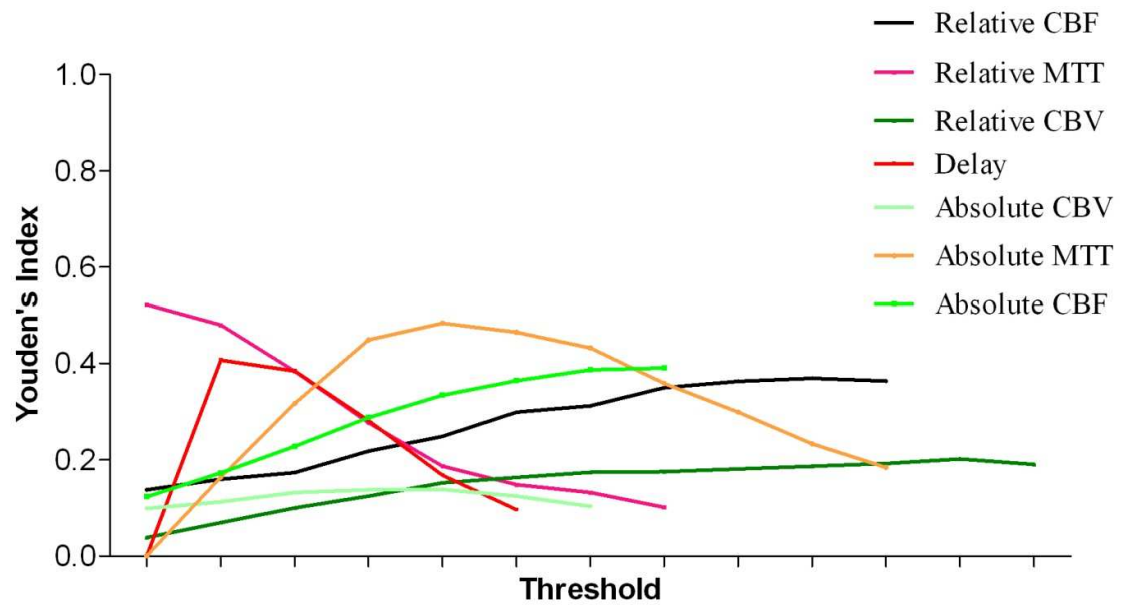
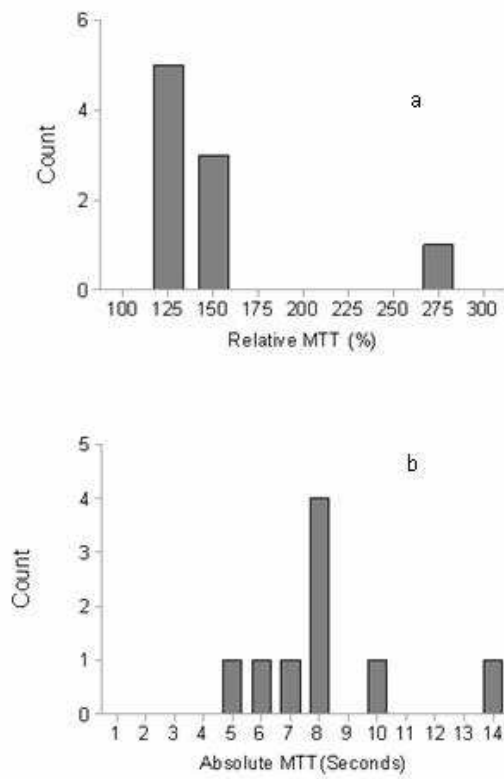
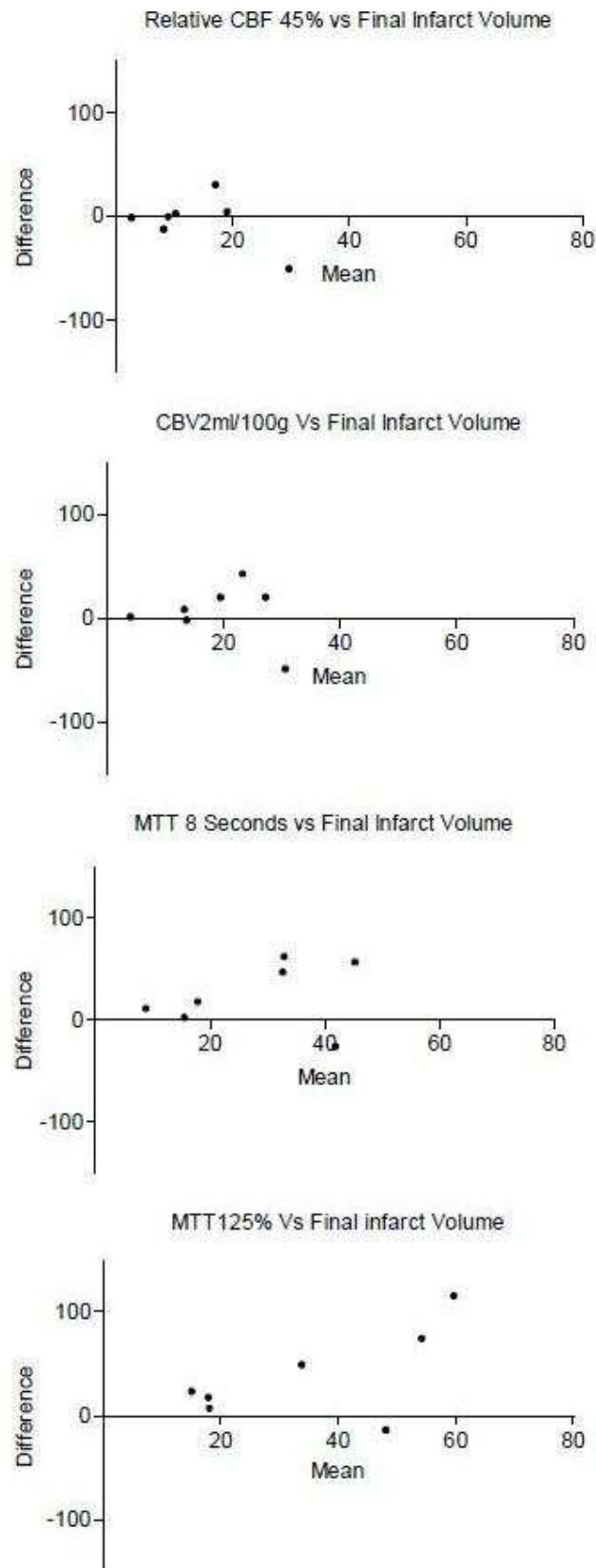


Figure 6-8 Youden's Index for Each Perfusion Threshold Evaluated for Core



**Figure 6-9 Frequency Distribution for Optimum Relative (A) and Absolute (B) MTT Thresholds for Core**





**Figure 6-10 Bland Altman Plot for Relative CBF  $\leq$ 45%, Absolute CBV 2ml/100g, Absolute MTT > 8 Seconds, and Relative MTT125%, for Detecting Infarct Core**

## 6.4 Discussion

The previous studies that sought to establish thresholds for core and penumbra with CTP have proposed different perfusion parameters and values for viability thresholds. The differing results highlight the need to find agreement on which perfusion measures are best for measuring core and tissue at risk using CTP. Validation of any derived thresholds in an independent dataset has not been previously performed but some of the proposed thresholds have been used in selection criteria for clinical trials (47). The importance of validation is highlighted in the variation in performance of some thresholds within the validation studies.

The results show that time based perfusion measures are best for defining hypoperfused tissue which is at risk of infarction in the setting of persistent arterial occlusion. Relative MTT, Absolute MTT and DT all performed similarly in the derivation group as shown in figure 6.5 implying the best available combinations of sensitivity and specificity for detecting tissue at risk. MTT has been used as a marker for tissue at risk with CTP previously, and both relative and absolute measurements had similar values for AUC in ROC curve analysis. DT is a more recently used measurement for hypo perfusion and has been recently reported as a marker for tissue at risk in another study (357). Although these perfusion indices performed similarly in the derivation group, the performance in the validation group showed variation in predictive value of each, with the best measurement being  $DT \geq 2$  seconds which performed best in the Bland Altman plot comparison between predicted and final infarct volumes (figure 6.7). This measurement was close to final infarct volume in the validation dataset over a range of infarct volumes, but had a tendency to underestimate the final infarct volume. The MTT measurements tended to overestimate the infarct volume, but relative measurements performed better than absolute measurements of MTT in keeping with previous work on threshold derivation for tissue at risk (131). MTT of 145% performed best of the three MTT measures tested in the validation dataset, but was not predicted by the derivation dataset. This shows that relative MTT is a good measurement of tissue at risk but emphasises the importance of validating the performance of any proposed threshold as ROC curve derivation alone does not give a measure of how closely a chosen threshold will perform in practice. MTT of 145% was tested because it

is widely used in practice and a comparison with the best derived thresholds could help compare accuracy in practice. As DT provided closer measurements of infarct volume it appears to be a superior predictor of infarct volume to relative MTT which has been reported elsewhere(134).

The predictive value of the perfusion measures tested in the derivation dataset seems less in comparison to previous studies(131). Important methodological differences may account for the apparent difference. When determining threshold sensitivity and specificity using a ROC curve Wintermark et al included pixels in the contralateral hemisphere as true negatives, meaning a chosen threshold under evaluation correctly did not predict infarction in those pixels which were contralateral to the stroke lesion(131). This would inevitably result in a much larger number of true negative pixels being measured for each scan evaluated relative to the number of false positive pixels. As specificity is determined as  $TN/(TN + FP)$ , the inclusion of contralateral negative pixels would result in larger values for specificity at all points increasing the AUC for the ROC curve. By including only pixels ipsilateral to the stroke lesion, this study included fewer true negative pixels for each scan slice resulting in lower apparent specificity but a result which is likely to be more reflective of the true measurement. Not all pixels ipsilateral to the stroke lesion will be at risk of infarction such as distal MCA occlusions. Even in this setting specificity may be overestimated by including all hemispheric pixels but for consistency in methodology this was performed as the territory of any given arterial occlusion could not be accurately demarcated. The variability in what pixels may be considered as potentially at risk and counted for in ROC curves underscore the importance of performing a subsequent validation of chosen thresholds.

The perfusion threshold which most accurately measured core in the validation dataset was relative CBF of  $\leq 45\%$ , which was the closest measurement of infarct core when compared using Bland Altman plots (figure 6.10). This tended to underestimate the core lesion volume but all other thresholds tested in the validation group overestimated lesion volume. As two thresholds from the literature were available for testing, I chose only the best 2 from the validation datasets for comparison. Again the importance of threshold validation was underscored as the best threshold from the validation dataset was not actually predicted by the derivation dataset. MTT measures had the best Youden's index

values from the derivation dataset. As stated, this is usually considered a marker for tissue at risk but not for core, although recent work has demonstrated that MTT can have a predictive value in defining core within the DWI lesion on MRI suggesting it may be helpful in detecting core(359). As core tissue is usually located within a volume of hypoperfused tissue and MTT can be used to measure hypoperfusion it is not surprising that MTT is sensitive for infarct core and therefore can have relatively high AUC and Youden's index values for core detection. Its specificity is not likely to be as good because MTT would be expected to include penumbra as well as core. In the model used for this study, the measurement of core was performed on subacute images in a selected patient group with clinical evidence suggestive of major reperfusion. Infarct growth even to a small degree after the timing of initial scanning could result in infarct core expansion into the space occupied by penumbra which may account for the apparent predictive value of MTT in this setting. The large overestimation of infarct volume by MTT measures in the validation dataset suggest that the choice of recanalisation and clinical improvement is likely to represent a model of minimal infarct growth overall. The overestimation of infarct volume by absolute CBV in the validation dataset is of importance given its widespread use as a marker for core on CTP post-processing packages in practice. CBV may not be accurately determined in situations of severe hypoperfusion, and this may explain differing values proposed in the literature to define core tissue (including  $\leq 2.0\text{ml}/100\text{g}$  and  $< 2.3\text{ml}/100\text{g}$ (131) and CBV/CBF interaction (133). The results suggest absolute CBV may not be a reliable marker for infarct core as it still overestimates lesion volume in a model where some lesion growth cannot be excluded. Relative measurements of CBF have been suggested as superior markers for infarct core in a number of studies and the present results support this finding(104, 355, 357). Stroke severity, although not statistically different between groups, did appear to be greater in the validation dataset. As this stroke severity is likely to increase with increasing lesion volumes, a confounding effect on threshold accuracy cannot be excluded.

The CTP processing algorithm is different to previous studies examining thresholds for determining tissue at risk. Delay insensitive deconvolution has been shown to be important when examining reversibility of perfusion lesions after recanalisation(127). Delay insensitive algorithms produce perfusion maps

that are less sensitive to tracer delay, a problem that may result in an overestimation of the volume of tissue at risk particularly in cases of extracranial stenosis. The post processing package in this study used a delay-insensitive deconvolution algorithm which also took into account the effect of bolus dispersion.

This study has some strengths and also limitations. The small sample size in each group places a limit on the generalisability of the results to all patients, and differences in stroke severity seen between groups could have a confounding effect, despite the lack of statistically significant differences, due to the small sample size. A large number of pixels were included for analysis despite the sample size. Inclusion of patients with different arterial occlusions at baseline reflects clinical practice, although different thresholds may exist for different arterial territories. Although a minimal sample size calculation has not been done, larger cohorts could have produced different results. The results are consistent with other work on threshold derivation suggesting that future studies could focus on validation of existing perfusion thresholds. The choice of imaging modality at follow up is a potential limitation. Other studies have used MRI at 24- 120 hours for final infarct volume determination while the majority in this analysis had volumes measured on CT which may be more difficult (131, 134). The clinical severity and proximal occlusions included however were typically associated with large infarct volumes which were readily demonstrated on CT. Early swelling may mask the true final infarct volume. Although the timing for a “gold standard” infarct volume has been suggested as 90 days, changes after the subacute period may be negligible (156). Furthermore as illustrated in chapter 4, imaging at later time points is less feasible than early time points. A pragmatic approach to study design for POSH and MASIS, along with the amalgamation of the datasets to identify suitable recruits necessitated the use of early imaging outcomes. All data were acquired from a single institution with the same scanner specifications and imaging protocols. Therefore the results may not necessarily be applicable to other centres with different image acquisition protocols. The need to harmonise CTP acquisition protocols has been emphasised elsewhere and threshold validation on different scanner types is needed (168). Image analysis was performed by a single reader with the potential for error. Differences in lesion volume measurements were small when intra observer

agreement was assessed but co-registration errors, if present may also have had an influence on the outcome.

The fully deconvolved processing algorithm with correction for bolus delay/dispersion is strength of the study as delay correction is being increasingly recognised as an important feature of CTP post processing (127). The large perfusion slab permitted coverage of a large portion of the ischemic area, although some hypoperfused tissue may have been beyond the CTP coverage. A large range of perfusion parameters and thresholds were tested comprising absolute and relative measures. Dividing groups into derivation and validation datasets had not previously been done which is a strength of the study because no assessment of how precisely perfusion thresholds predicted core or tissue at risk was previously available. Previous publications derived thresholds for tissue at risk in 46 patients and core in 25, 57 and 48 patients but did not evaluate the performance of chosen thresholds in independent datasets (134, 355). Different perfusion parameters and thresholds may underestimate or overestimate core and tissue at risk, but the closest matches are likely to indicate reasonable markers for each tissue compartment. There was little difference in measured volumes at different time points highlighting consistency in ROI analysis performed for determining infarct volume.

## 6.5 Conclusion

This study demonstrated that the ability to predict tissue at risk of infarction with CTP is best using  $DT \geq 2$  seconds which is a superior measure to the previously used relative MTT of 145% of the contralateral normal hemisphere. Irreversibly damaged core tissue is best predicted using relative CBF of 45%. As optimum thresholds may depend on processing software and scanner type, evaluation of these thresholds in different populations and scanner types is required.

In order to realise the promise of CTP for patient treatment selection in clinical trials or routine management, standard definitions of core and penumbra thresholds are required. Clinical, imaging and scanner specific differences exist between different studies which have evaluated perfusion based definitions for core and penumbra which may limit their use as in acute stroke assessment and

as outcome markers in trials. These results should be tested in a wider setting using different scanner protocols and manufacturers. Prospective evaluation of these and other thresholds in independent cohorts is needed to examine how they perform in wider clinical practice.

## Chapter 7. Pixel Based Identification of Infarct Core on Non-Contrast CT

### 7.1 Introduction

Early ischemic changes including hypodensity and brain swelling may be visualised in most MCA territory strokes within 3 hours of symptom onset when viewed by expert readers although hypoattenuation and brain swelling are likely to represent distinct stages of the ischemic cascade (71, 360-362). Water uptake into cells results in visualised hypoattenuation(78). Hypo attenuated regions on CT correspond to regions of DWI abnormality(320). Reduced CBV and CBF are seen in regions with hypoattenuation while focal swelling is associated with increased CBV(363). Areas of hypoattenuation within 6 hours of stroke onset almost always progress to infarction on follow up MRI whether reperfusion occurs or not, and larger volumes of hypoattenuation are associated with larger infarct volumes and less favourable outcomes(74, 363). The presence of hypoattenuation on CT indicates core with high specificity, but sensitivity for detection is low and interobserver agreement can be low even using methodical grading tools such as ASPECTS (71, 79). It has been suggested that a normal CT may not imply solely a lack of sensitivity, but instead represents a favourable situation where ischemic oedema has not yet developed (99). However the presence of infarct core markers on CTP acquired concurrently to CT suggests that sensitivity is a genuine limitation of CT and core may be present at a cellular level but not necessarily visible on CT(130). CTP acquired after CT can measure core according to thresholds with CBF being suggested as the most appropriate marker for core from earlier chapters and other work (104, 134, 355). Given that interobserver agreement for detecting hypodensity can be poor while expert readers may report better sensitivity when interpreting CT scans, a less subjective interpretation of CT for the presence of infarct core could be of interest in demonstrating the sensitivity of CT alone or in outlining the importance of additional imaging for measuring infarct core(74). For example, if absolute values for HU attenuation could be shown to be sensitive and specific for core, an analysis of CT based on absolute HU thresholds could potentially add helpful information beyond what is obtained by a standard visual interpretation of a CT scan. Grey and white matter have different attenuation on CT, with loss of distinction between compartments a sign of early ischemic change(364). The



definition of hypodensity for each may be different given the variation in baseline appearances so accounting for differences in HU attenuation in grey and white matter separately would be important. I sought to measure the absolute HU values of pixels on CT which were considered infarct core on CTP in order to determine the sensitivity and specificity for infarct core detection on non-contrast CT for both grey and white matter.

## **7.2 Materials and methods**

### Patient selection

Consecutive patients who participated in the POSH study between January 2009 and January 2011 were considered for inclusion. From this dataset, scans were selected for analysis according to the following criteria:

- 1: Confirmed diagnosis of ischemic stroke
- 2: Baseline occlusion visualised in ICA or MCA territory
- 3: Core lesion volume >5ml on baseline CTP scan

Clinical characteristics and measurements are described in the materials and methods chapter.

### Image analysis

Anonymized scans were processed using the MIStar image processing platform as previously described. Admission CT scans were first co-registered to the baseline frames of the CTP using a rigid body 3-D transformation as previously described. Slices reformatted to match the CTP orientation were used for core quantification. Two 5 mm slices corresponding to the lower and upper ASPECTS reading areas were chosen to give a representative sample of both grey and white matter for each patient included.

Grey and white matter segmentation was performed using the time-averaged mean arterial phase sequences at each ASPECTS level which produced maximal contrast between grey and white matter in normal tissue(355). Normal grey and

white matter were segmented according to HU threshold in the hemisphere contralateral to the stroke region by placing ROI seeds within each on the time averaged maps and adjusted according to threshold with manual correction if necessary. Normal grey and white matter ROIs were then transposed onto the reformatted CT scan and then mirrored to the contralateral (symptomatic) hemisphere in order to give a map of the territories comprising grey and white matter. The unaffected hemisphere was used to delineate normal grey and white matter as the presence of a stroke lesion would be likely to obscure the normal boundaries between each.

CTP data were then processed as previously described according to a delay corrected deconvolution algorithm with AIF and VOF selected from the Anterior Cerebral Artery and Superior Saggital Sinus respectively. Given the results of the thresholds derivation and evaluation chapter, along with developments in the literature suggesting CBF is the optimum marker for core rather than CBV core pixels were defined by relative cerebral blood flow of  $\leq 45\%$  of normal(104, 134).

ROIs were drawn semi-automatically around areas of core tissue on the final “Penumbrogram” map on the upper and lower ASPECTS slices and saved. These ROIS were transposed to the appropriate slices on the reformatted CT along with the grey and white matter ROIs (Figure 7.1).

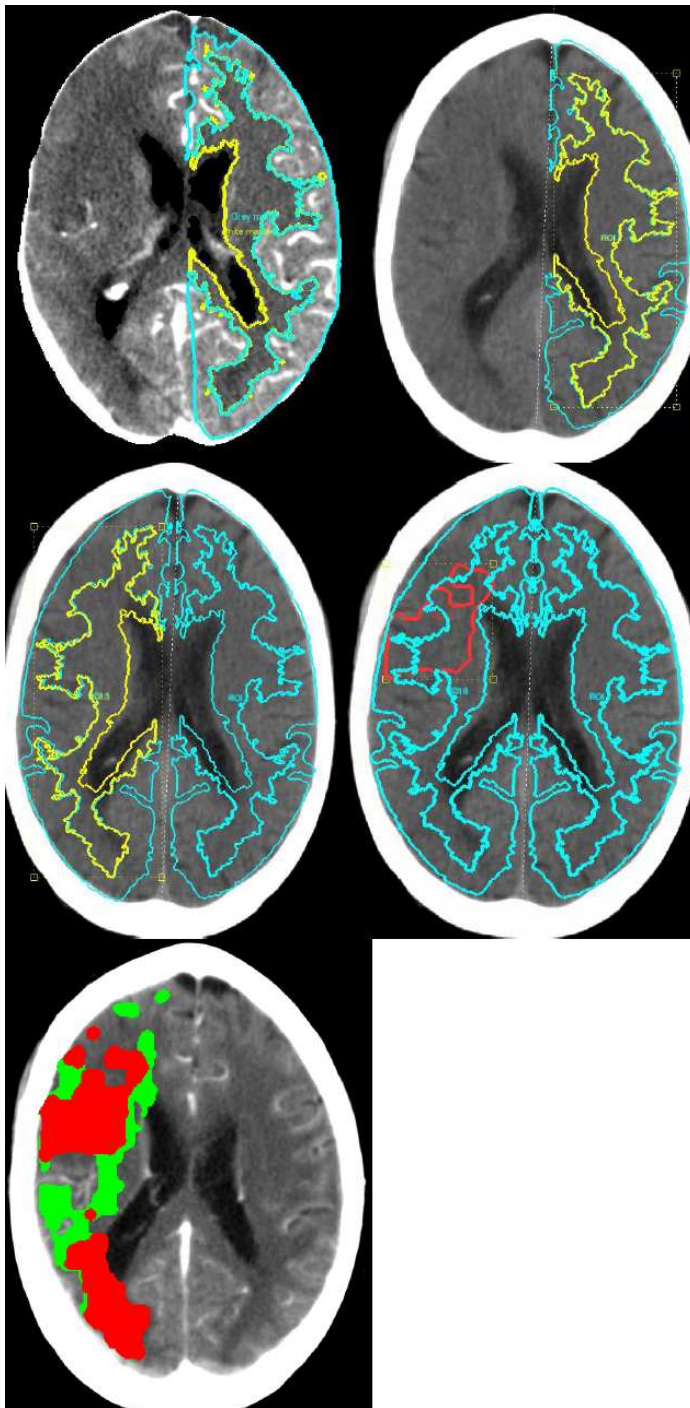


**Figure 7-1 Core Grey & White Matter Segmentation**

Grey and white matter are segmented in the right hemisphere on time averaged CTP, transposed to CT and mirrored to the affected hemisphere. ROI for core pixels are also transposed (only 1 core ROI shown). Penumbrogram revealing extent of core and penumbra is shown at bottom for reference. Core pixels shown in red, penumbral pixels shown in green.

Pixels within each ROI in the stroke hemisphere had a Hounsfield unit value and a spatial location given by an x and y coordinate which were combined for each patient and saved as a text file. The HU values for Grey, white matter and overlapping core were therefore recorded. The saved ROI data comprising

spatial and HU value information for each pixel in text format was exported to Microsoft Excel and manipulated in a series of steps that permitted separation of normal and core tissue for both grey and white matter:

- 1) The core ROI and Grey matter ROI data were combined in an excel file with separate columns for pixel number, x coordinate, Y coordinate and HU value. Duplicate rows in this composite of 2 saved ROIS reflected pixels identical spatial positions. These were selected from the overall list using an excel formula and saved. The saved pixels corresponded to those grey matter pixels which were defined as core on the CTP (Termed A).
- 2) The remaining “non duplicate” pixels were a combination of both normal grey matter and core pixels which were spatially within the white matter. This composite was also selected and saved(Termed B)
- 3) White matter ROI pixels were combined with the same core ROI pixels in Excel as above (see step 1) and duplicate pixels were again highlighted and saved. Duplicate pixels corresponded to white matter pixels that were defined as core on CTP (Termed C)
- 4) The remaining pixels after removing the duplicates were a combination of normal white matter pixels and core pixels which occupied white matter space (Termed D)
- 5) D and A were combined in single document and duplicate pixels were selected and deleted. This removed any grey matter core pixels from the combined list (D and A). The remainder represented all normal white matter pixels for that scan slice (Termed E)
- 6) C and B were combined in a single document and duplicate pixels were selected and deleted in order to remove any white matter core pixels from the combined list (C and B). The remaining list represented all normal grey matter pixels for that scan slice (Termed F).

In summary:

A= Grey Matter core

B= Normal Grey matter along with some White Matter core pixels

C= White Matter core

D= Normal White Matter along with some Grey Matter core pixels

E= (A+D) minus any duplicates = normal White Matter pixels

F= (C+B) minus any duplicates= normal Grey Matter

By subjecting the raw numerical data to the series of steps described, the HU values for normal and infarcted grey and white matter were listed for each slice examined and combined for individual patients. Core pixels were assigned a value of 1 and normal parenchyma was assigned a value of 0 for subsequent statistical analysis.

#### Statistical analysis

SPSS version 18 was used for all statistical analysis undertaken. For each patient sensitivity and specificity for quantifying core pixels was assessed using ROC curve generation, with the area under the curve indicating the overall diagnostic performance of CT compared to the chosen gold standard. Optimum cut-points per patient were derived from the ROC curve to determine the HU threshold with best sensitivity/specificity combination for detecting core pixels. Youden's index was used to quantify the combination of sensitivity & specificity for each threshold tested. Histograms were generated to identify which HU cut-points with highest Youden's Index value occurred most frequently. HU values of pixels for all patients were additionally combined to produce a ROC curve for overall performance of CT in detecting CBF defined core. Sensitivity and specificity measurements for each threshold were interpolated from the ROC curve and overall sensitivity and specificity for the most frequently occurring HU cut-point for grey and white matter was calculated from the ROC curve.

### 7.3 Results

89 subjects were considered for inclusion. 32 had no occlusion on CTA, 2 had problems with AIF selection due to movement rendering perfusion maps unusable, 2 had Anterior Cerebral Artery occlusions, 7 had posterior circulation occlusions, 12 had no core on CTP despite having an arterial occlusion, and 1 patient's admission CT scan was not available leaving 33 in the final analysis cohort. Clinical and imaging characteristics are shown in table 7.1

<b>Variable</b>	<b>Result</b>
Age (Mean +SD)	72 (12)
NIHSS( Median +IQR)	16 (11-20)
Carotid occlusion (n)	9
M1 occlusion (n)	11
M2 occlusion (n)	13
ASPECTS- NCCT (Median +IQR)	6.0 (4.5-9.0)
ASPECTS- CBV (Median +IQR)	8.0 (6.0-9.0)
ASPECTS CBF (Median +IQR)	4.0 (1.0-7.0)
ASPECTS MTT (Median +IQR)	4.0 (3.0-6.0)
ASPECTS TTP (Median +IQR)	4.0 (3.0-6.0)
24 hr NCCT ASPECTS (Median +IQR)	6.0(3.0-6.0)

**Table 7.1 Clinical Characteristics of patients included in analysis of core pixels on NCCT**

A total of 320845 pixels were included in the analysis, comprising 180960 grey matter and 139885 white matter pixels. AUCs for CT based quantification of infarct core were 0.641 and 0.601 for grey and white matter respectively (Figure 7.2 and 7.3)

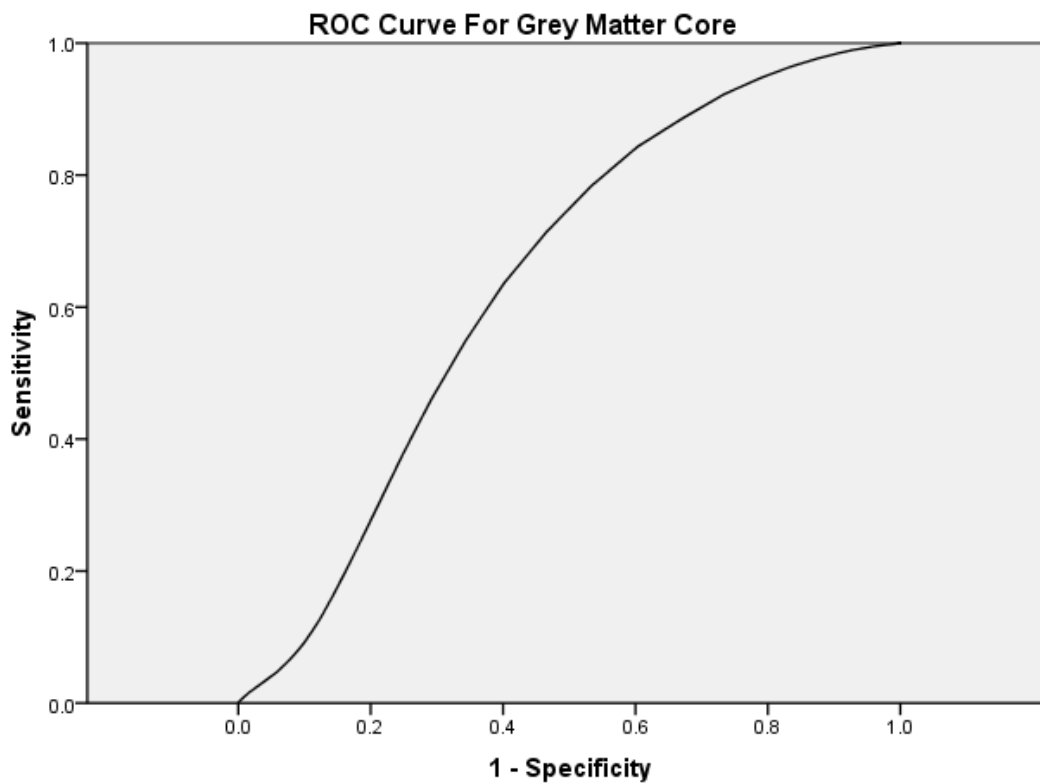


**Figure 7-2 ROC Curve for Presence of Grey Matter Core Pixels on CT**  
AUC for detecting core in grey matter based on HU value alone=0.641

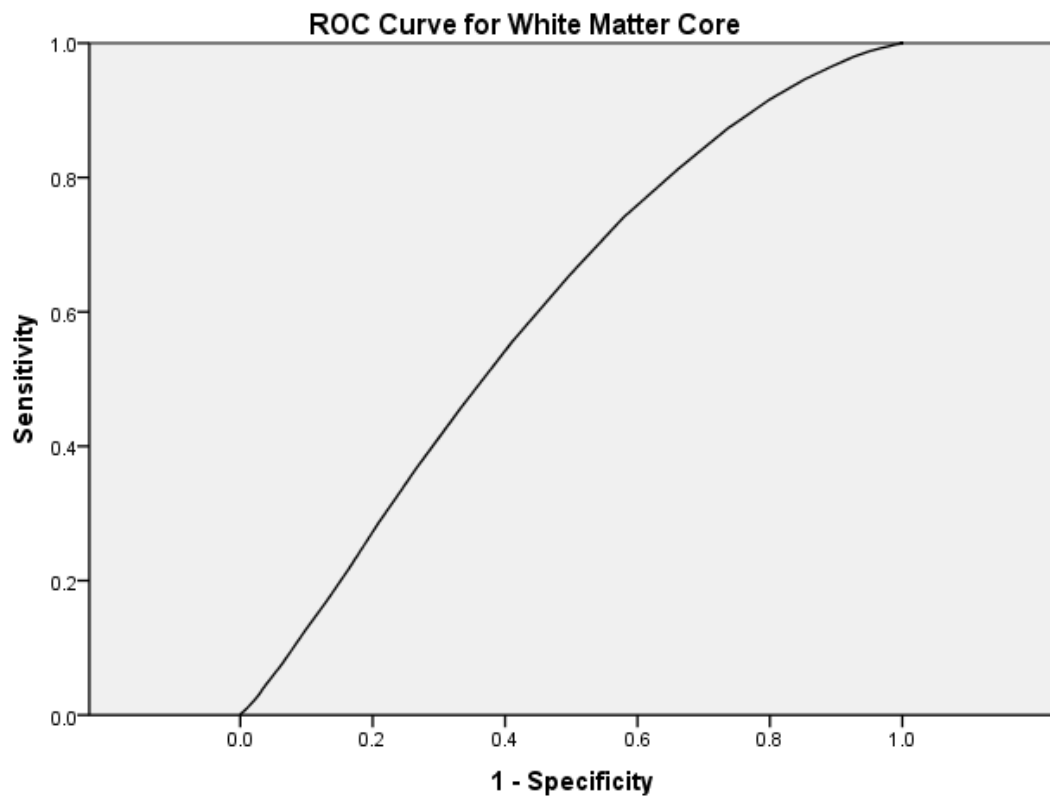


**Figure 7-3 ROC curve for presence of White Matter core pixels on CT**  
AUC for detecting core in white matter based on HU value alone=0.601



Frequency distribution for the best performing grey matter thresholds showed 29 HU to be the most frequent threshold (Figure 7.4). The most frequently occurring threshold for white matter core was 28 HU (Figure 7.5)

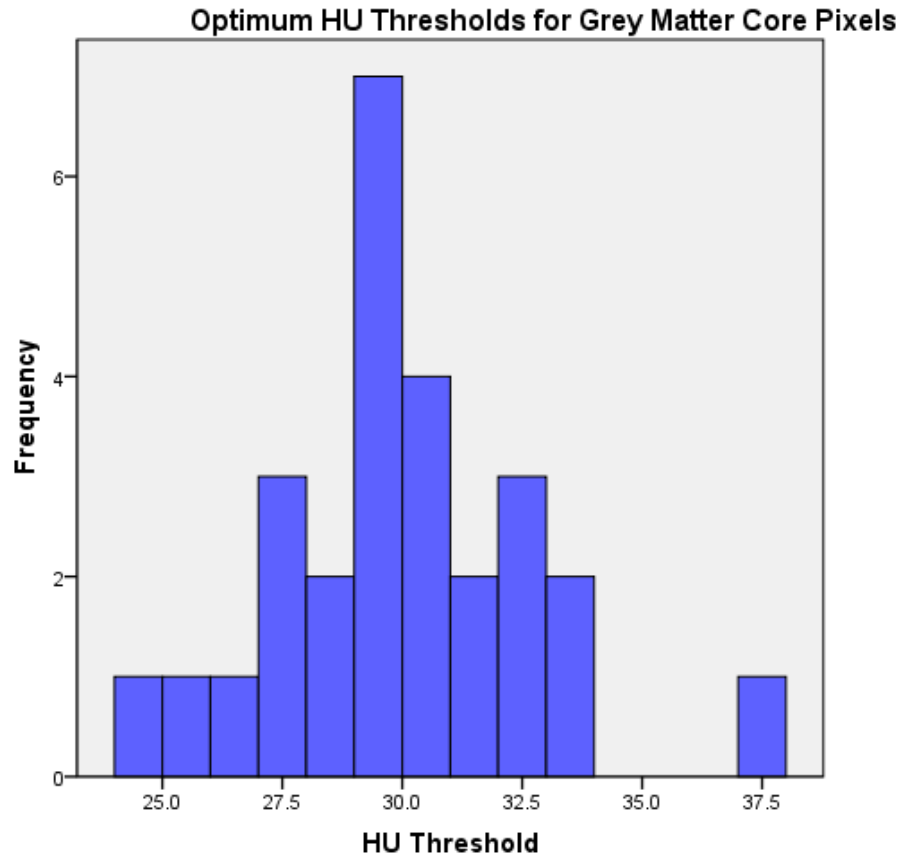


**Figure 7-4 Frequency Distribution for Grey Matter Cut Points**

Optimum cut points for each patient varied with 29 HU being the most frequently recorded threshold.

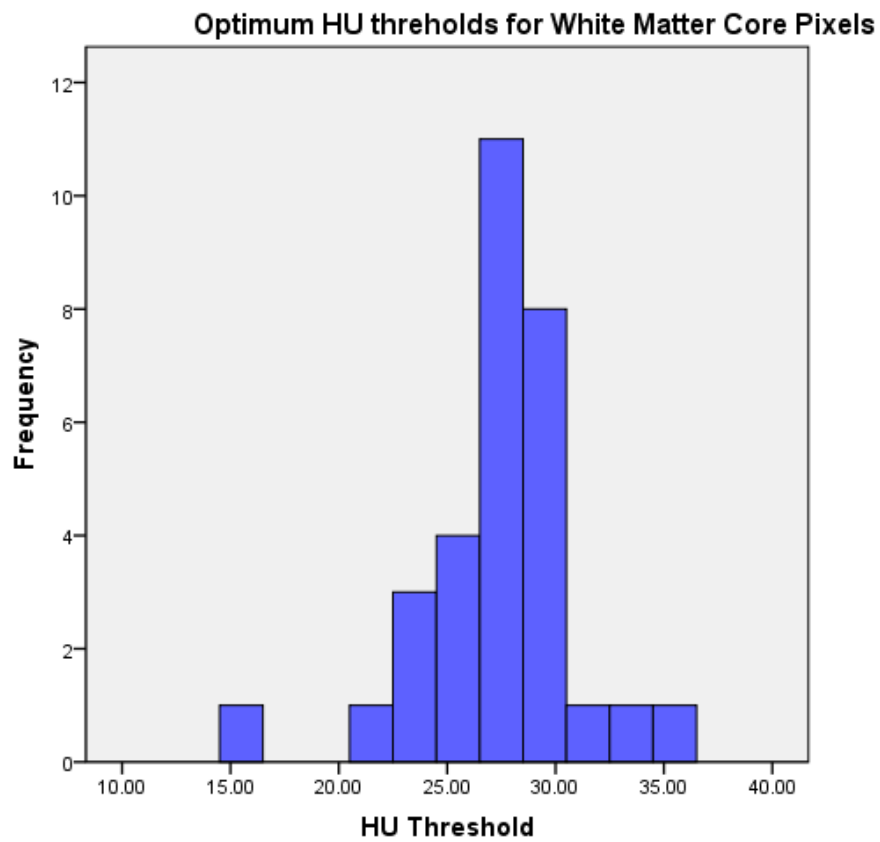


**Figure 7-5 Frequency Distribution for White Matter Cut Points**

Optimum cut points for each patient varied with 28 HU being the most frequently recorded threshold.

29 HU had a median sensitivity of 0.79 and specificity of 0.48 for detecting infarct core in grey matter. Lower HU thresholds had increased specificity but reduced sensitivity. Examples are shown in Table 7.1

<b>HU</b>	<b>Sensitivity (Median %+IQR)</b>	<b>Specificity (Median %+IQR)</b>
29	79 (62-87)	48 (32-59)
20	15 (9-23)	86 (80-91)
25	44 (28-57)	70 (62-79)
30	81 (72-90)	47 (25-52)

**Table 7-1 Sensitivity and Specificity of HU Thresholds for Detecting Infarct Core in Grey Matter**

Lower HU values demonstrate higher specificity for infarct core but at the expense of sensitivity

28 HU had a median sensitivity of 0.83 and specificity of 0.36 for detecting infarct core in white matter. Again, lower HU thresholds demonstrated increased specificity with reducing sensitivity. Examples are shown in Table 7.2

<b>HU</b>	<b>Sensitivity (Median % +IQR)</b>	<b>Specificity (Median % +IQR)</b>
28	83 (74-89)	36 (26-43)
20	17 (8-23)	88 (82-94)
25	57 (43-69)	60 (50-70)
30	92 (86-96)	19 (12-25)

**Table 7-2 Sensitivity and Specificity of HU Thresholds for Detecting Infarct Core in White Matter**

Areas with lowest HU values were most specific for detecting infarct core, but these were relatively insensitive

## 7.4 Discussion

This study has evaluated the predictive value of CT for detecting CBF defined infarct core based on absolute HU values for grey and white matter. Even with expert review of images, CT scans for ECASS II and NINDS were reported as normal in approximately 1/3 cases which were found to have infarction on follow up imaging, reflecting a limited sensitivity for detecting ischemic changes (74, 365). Hypoattenuation on CT is caused by net increase of water in cells experiencing reduced cerebral blood flow (78). Animal studies have suggested a 1% increase in brain water results in a reduction of 2-3 HU on CT(366). The detection of hypoattenuation in practice may be difficult with CT as large water shifts are needed for the human eye to detect hypoattenuation(367). As large shifts are needed before hypoattenuation can be visually appreciated, this study was performed to evaluate whether or not attenuation changes may be present on CT if not necessarily visible to the human eye. By performing a pixel based quantification of the attenuation values of infarct core on CT this study has revealed that pixels which are likely to represent infarct core on CTP are not reliably detected on CT based on an absolute HU value. The AUC for grey and white matter of 0.641 and 0.601 demonstrate only a modest ability for core to be quantified on CT based on HU value alone. Irreversibly damaged tissue which can be seen on CTP is therefore not necessarily detectable on a concurrently acquired non-contrast CT. As subjective interpretation of CT was not undertaken, the present findings suggest that CT has limited ability to identify core tissue in hyperacute stroke regardless of the interpreter's experience. A "normal" CT scan, therefore, which may represent a good imaging target, does not exclude the presence of irreversibly damaged brain tissue.

The HU values of 29 and 28 for grey and white matter were associated with modest sensitivity and low specificity. This initially appears at odds with the generally accepted view that hypodensity is specific if not sensitive for infarct core(74, 363) but how hypodense any given HU value appears to a reader was not evaluated in the study and the trend for increasing specificity with lower attenuation values (Table 7.1 and 7.2) confirm that increasingly hypodense parenchymal pixels are highly specific for infarct core. While low HU value pixels in this study confirm a high probability of tissue infarction, the overall performance of CT is limited by the compensatory reduction in sensitivity as

indicated by the overall ROC curve values. The two chosen cut-points are close to each other in terms of absolute attenuation values and this difference is unlikely to be appreciated clinically (367). The AUC for grey matter was higher than that of white matter for detection of infarct core. As grey matter attenuation is higher at baseline than the adjacent white matter(368), a relative reduction from baseline may be more easily detected. However the values for both reflect a limited capacity for CT to reveal all core pixels in this time window after stroke onset.

The definition for core on CTP used was reflective of progress in the literature and previous results within the thesis, but independent validation of relative CBF of 45% as the best measure of core has not been performed which limits the interpretation of the results. Not all core pixels measured by CTP may have been truly core, while others may have been considered penumbral or even normal on CTP. Therefore the choice of a “gold standard” reference for this work is potentially questionable. However relative CBF is increasingly recognised as a marker for core and has the advantage of being acquired at virtually the same time as the CT which limits any natural progression of the stroke lesion being responsible for the differences between modalities(104, 134, 355). An additional measure could have been to use follow up imaging to confirm that those pixels defined as core on CTP were infarcted on follow up but the likely evolution of the infarct over time would have limited this as a “gold standard” comparison. Only two scan slices were examined per patient but other studies based on pixel based comparisons have shown large numbers of pixels can be studied when performing a single scan slice comparison and in this study the same scan slices based on anatomical landmarks were used for each patient(355). Only pixels ipsilateral to the stroke lesion were quantified as the measurement for “normal” grey and white matter pixels. Incorporating those in the contralateral hemisphere as well would result in a disproportionately large number of negative (non -core) pixels and potentially influence the AUC values derived from the ROC curves.

Strengths of this study include the pixel based analysis of CT which provided a novel quantitative approach to assessing stroke on non contrast CT, the large number of pixels examined for the ROC curve generation, and the separation of grey and white matter into compartments for individual analysis. Limitations of

this study include the lack of a validated definition for infarct core as a gold standard reference using CTP. In addition , using ROIs from a processed CTP scan to measure core and penumbra is potentially an over-simplistic method, as within a given ROI, there are likely to be pixels with various different perfusion values which may have different predictive value to detect core. The use of an ROI based on the “penumbragram” output from CTP ignores the individual perfusion characteristics of single pixels. In addition only a limited number of slices were examined per patient which may limit any conclusions, although the absolute number of pixels examined overall was large. An additional step which could have made the work stronger would have been to prospectively evaluate the accuracy of absolute HU values in a validation cohort rather than relying on the low AUC values alone from the dataset alone to infer the limited ability for plain CT to define core based on HU value.

The results of this study are of importance when interpreting imaging in acute stroke for clinical decision making. The presence of a normal or nearly normal scan in clinical practice is seen as a good prognostic sign while extensive changes on CT are excluded from treatment as little benefit is likely to be achieved (45). Scans in practice may be reported as having “no established change” if obvious hypodensity is not seen. This pixel based quantification of core tissue suggests that a scan with little or no hypodensity could in fact have irreversibly damaged tissue which is not salvageable with treatment but that this tissue cannot be detected with certainty on CT. Absence of hypodensity on CT therefore may not imply absence of core tissue. The impact this may have in practice is unclear however as selection criteria for thrombolysis based on additional imaging with CTP are not available. Large core volumes on DWI have a crucial influence on outcome (152) but it is unclear who should / should not be treated with reperfusion strategies based on additional imaging criteria with CTP. Core on CTP still requires validation and thereafter evaluation in clinical trials to assess if additional imaging should be used to select patients for therapy, while treatment with IV thrombolysis based on a non contrast CT and clinical examination is supported by a strong evidence base (369). Imaging based methods to improve patient selection for acute stroke treatments have been suggested previously(130, 363). This study illustrates the inherent limitations of

CT compared to other imaging modalities, but the impact this may have on patients receiving treatment should be the subject of further study.

## **Chapter 8. Conclusion**

### **8.1 Summary**

The work presented within this thesis has evaluated a number of areas of importance with regard to acute stroke imaging for both clinical and research purposes. There is certainly a need for additional imaging beyond a non-contrast CT which was used in most trials of IV alteplase for stroke, as trials evaluating novel treatment options have already begun to use imaging markers as surrogates for clinical outcome(52, 154). The rationale for using imaging markers in trials is clear, but what has been incompletely evaluated previously is the range of possible means of which could be employed and how reliable they may be in practice. Recanalisation offers an insight into possible effect of lytic agents, but reperfusion or infarct growth may provide additional information about the usefulness of any vessel recanalisation in terms of tissue salvage. Reperfusion and infarct growth are measurements which are feasible to determine using multimodal CT but are not the only predictors of outcome.

### **8.2 Clinical Importance and Future Research Considerations**

The contents of the preceding chapters are of relevance for clinical practice in acute stroke and highlight areas of uncertainty which should be addressed in future research projects.

Choice of imaging modality in acute stroke assessment has been debated, with MRI and CT each having pros and cons. In the MASIS study, centres recruited more frequently using CT rather than MRI even though both modalities were available at each site. Those who underwent MRI on admission had milder degrees of stroke severity at baseline, while MRI was contraindicated or not tolerated in some patients suggesting that ongoing focus using CT is important for patients with acute stroke. This work cannot answer the question over which modality should be used in practice or for trials, but suggests that flexibility with use of imaging modality may result in a wider /more clinically relevant



population being recruited to studies if CT is used. Given contraindications, additional patient factors and access issues, the need for ongoing access to and used of CT for acute stroke evaluation remains essential for clinical practice.

Multimodal CT is being used in many centres as part of routine clinical imaging, but the results of the threshold derivation chapter show that further evaluation of the accuracy of perfusion thresholds is needed in the first instance prior to their use in clinical practice. Anecdotally, CTP appearances have been used to justify treatment in late time windows and in wake-up strokes, as well as withholding treatment in the current 4.5hr window ( e.g. large volumes of core, little or no penumbra) based on the attractive prospect of tailoring treatment towards an imaging target, but the results show that the proposed thresholds must be validated first as relying on previously derived thresholds could result in less accurate measures of core and penumbra. Finding what the range of perfusion-imaging targets for acute stroke therapy exist (if any) is likely to form part of future stroke research trials. In order to treat based on imaging targets however, they must be reliable measures of different tissue states before a trial of treating based on mismatch or other marker can be considered. Use of perfusion imaging as a surrogate marker for outcome in other trials is also limited until thorough validation of thresholds is completed. Which CTP based measures most accurately represent core and penumbra? This difficult question has yet to be fully answered but the current work suggests relative CBF is the best marker for core , while DT may be the best marker for penumbra, which are supported by other studies which evaluated perfusion thresholds (355, 357).

As absolute HU values do not appear to identify core tissue on a pixel by pixel basis, it suggests that treating based on NCCT alone could mean administering thrombolysis to patients with established core which could not be detected on CT. The reassurance of a “normal” CT scan may be limited therefore due to impaired sensitivity for detecting core as core volumes at baseline may identify patients who have no benefit from rt-PA(152). This analysis is preliminary and did not take lesion volume and time from symptom onset into account, both of which could affect the predictive value of a given HU to measure core and these could be assessed in future.

The question of whether or not collateral flow augmentation can impact on outcome is being evaluated in stroke trials which are ongoing at present. The impact of collaterals on outcomes seems to be secure despite the current lack of consensus on how to best grade collateral flow. This work has presented a novel method to quantify collateral vessel filling and should be evaluated by additional raters and in additional populations to assess its suitability as a collateral measurement. This simple system could potentially then be used to measure an effect from the proposed measures of collateral flow enhancement such as volume expansion, induced hypertension and partial aortic occlusion (237, 241). The mechanisms which control collateral flow adequacy remain unclear however and may require much more study before treatments based on collateral flow enhancement can be found. Future questions which should be addressed include whether or not stroke mechanism influences collateral flow, whether blood biomarkers( such as fibrinogen) can be confirmed to have a relationship with collateral flow adequacy, and whether the grading scale employed can be used in additional populations in order to study the factors which govern collateral flow.

### **8.3 Concluding remarks**

The work presented advances what was previously known about each component of a multimodal CT examination in hyperacute stroke; the limited sensitivity of CT based on absolute HU values, the potential of CTA to quantify leptomeningeal collateral flow, the accuracy of both previously accepted and novel measures of infarct core and ischemic penumbra, as well as the individual advantages of CT for obtaining imaging in a way that is rapid, feasible and acceptable for patients compared to MRI in acute stroke. Each component is worthy of further study in an effort to improve selection for current treatments, and hopefully as part of the process in demonstrating the benefit of new treatments for acute stroke, all of which is of the utmost importance for stroke patients in the future.

## Appendices

### Appendix 1: Search Strategy for Literature review( Chapter 2)

#### Search Strategy:

- 
- 1 stroke.mp. or \*Stroke/ (116364)
  - 2 acute stroke.mp. or \*Stroke/ (26935)
  - 3 \*Adult/ or \*Aged/ or \*Ischemic Attack, Transient/ or \*Cerebrovascular Circulation/ or \*Cerebrovascular Disorders/ or \*Brain/ or \*Middle Aged/ or \*Brain Ischemia/ or ischemic stroke.mp. or \*Cerebral Infarction/ (292864)
  - 4 cerebral infarction.mp. or \*Cerebral Infarction/ (20246)
  - 5 occlusion.mp. (104641)
  - 6 stenosis.mp. or Constriction, Pathologic/ (124777)
  - 7 carotid stenosis.mp. or \*Carotid Stenosis/ (9718)
  - 8 \*Cerebral Arteries/ or \*Cerebrovascular Disorders/ or \*Aged/ or \*Carotid Artery Diseases/ or \*Ischemic Attack, Transient/ or \*Cerebral Infarction/ or \*Arterial Occlusive Diseases/ or intracranial occlusion.mp. or \*Stroke/ (121544)
  - 9 middle cerebral artery occlusion.mp. or \*Infarction, Middle Cerebral Artery/ (4891)
  - 10 \*Thrombosis/ or \*Intracranial Thrombosis/ or \*Carotid Artery Thrombosis/ or \*Intracranial Embolism and Thrombosis"/ or thrombosis.mp. (113612)
  - 11 clinical outcome.mp. (28006)
  - 12 contrast media.mp. or \*Contrast Media/ (50776)
  - 13 tomography, x-ray computed.mp. or \*Tomography, X-Ray Computed/ (211017)
  - 14 \*Angiography, Digital Subtraction/ or \*Angiography/ or Angiography.mp. or \*Cerebral Angiography/ or \*Magnetic Resonance Angiography/ (169715)
  - 15 ct angiography.mp. (2950)
  - 16 CT angiogram.mp. (129)
  - 17 CT angiography source images.mp. (8)
  - 18 \*Brain Ischemia/ or \*Brain/ or \*Diffusion Magnetic Resonance Imaging/ or \*Magnetic Resonance Imaging/ or Magnetic resonance, diffusion weighted.mp. (278212)
  - 19 Magnetic resonance angiography.mp. or \*Magnetic Resonance Angiography/ (12426)
  - 20 digital subtraction angiography.mp. or \*Angiography, Digital Subtraction/ (5088)
  - 21 angiogram.mp. (6160)
  - 22 \*Ultrasonography, Doppler, Transcranial/ or transcranial.mp. (13511)
  - 23 \*Cerebrovascular Circulation/ or \*Collateral Circulation/ or pial collaterals.mp. or \*Cerebral Arteries/ (32495)
  - 24 leptomeningeal collaterals.mp. (31)
  - 25 collateral circulation.mp. or \*Collateral Circulation/ (11376)
  - 26 collateral vessels.mp. (1561)
  - 27 collateral flow.mp. (1430)
  - 28 collateral blood supply.mp. (246)
  - 29 CT perfusion.mp. (278)
  - 30 recanalization.mp. (4939)
  - 31 \*Thrombolytic Therapy/ or thrombolysis.mp. or \*Stroke/ (40155)
  - 32 angiogram.m\_titl. (580)

- 33 angiography.m\_titl. (22374)  
 34 collateral.m\_titl. (5252)  
 35 33 or 32 or 21 or 17 or 12 or 20 or 15 or 14 or 22 or 34 or 30 or 13 or 16 or 19 (414417)  
 36 6 or 11 or 3 or 7 or 9 or 2 or 8 or 1 or 4 or 30 or 10 or 5 (714893)  
 37 27 or 25 or 28 or 30 or 24 or 26 or 23 (46110)  
 38 35 or 29 (414446)  
 39 38 and 36 and 37 (14037)  
 40 limit 39 to humans (12346)  
 41 limit 40 to English language (9487)  
 42 from 41 keep 7-8,12,29,41,52-53,58,70,72,78,102,113,116,141-142,168,174,198,202,211,218,225-226,230,232,243,248,259-260,283,301-302,307,309,313,326,342,348,357-358,360,370-372,391,397,416-417,438,447,457,486,505-507,512,528-529,538,585,636,674,688,725,733,735,744,758,778,780,797,805,811,813,825,832-833,849,856,885,910,916,930,958 (85)

## Appendix 2: MRI acquisition parameters for MASIS study

### General

	Edinburgh	Aberdeen	Glasgow (1.5T)	Glasgow (3T)
<b>B<sub>0</sub></b>	1.5T	3.0T	1.5T	3T
<b>Manufacturer</b>	GE	Philips	GE	GE
<b>System</b>	HDx Excite	Achieva	Signa Excite	Signa Excite
<b>Software</b>	14.04	R2.5	11.0_0403a	12.0_0606.b
<b>Gradients</b>	Echospeed+	Quasar Dual	Twin	Twin
<b>Head coil</b>	Quadrature	SENSE NV-16	8 channel	8 channel

### Gradient Echo

	Edinburgh	Aberdeen	Glasgow (1.5T)	Glasgow (3T)
<b>Sequence</b>	Axial T2 GRE	T2W-FFE	Ax T2* GRE	Ax T2* GRE
<b>TR</b>	660ms	780ms	500	670
<b>TE</b>	15ms	16.11	20	22
<b>Flip angle</b>	20°	18°	20°	10°
<b>NEX</b>	1	1	1	1
<b># slices</b>	28	24	24	24
<b>Slice thickness</b>	5	5	5	5
<b>Slice gap</b>	0	0	<b>0</b>	<b>0</b>
<b>Matrix</b>	256*192	286x170	256x224	256x256
<b>Φ FOV</b>	0.75	0.8	0.75	0.75

<b>FOV</b>	24 x 24	240x240	24	24
<b>Slice orient</b>	Straight axial	Straight axial	AC-PC	AC-PC
<b>Tscan</b>	1:42	2:14	2:56	2:11

## DWI

	<b>Recommended</b>	<b>Edinburgh</b>	<b>Aberdeen</b>	<b>Glasgow (1.5T)</b>	<b>Glasgow (3T)</b>
<b>Sequence</b>	Single-shot DW EPI	Single-shot DW EPI	Single-shot DW EPI	Ax DWI	DWI ASSET
<b>TR</b>	>4000ms	10000	7600	8000	9000
<b>TE</b>	min	Min (87.3)	Min (68)	Min	65.7
<b>B (s/mm<sup>2</sup>)</b>	0 and 1000	0 and 1000	0 and 1000	0 and 1000	0 and 1000
<b># directions</b>	>3	3	3	3	3
<b>Flip angle</b>	90°	90°	90	90	90
<b># slices</b>	>12 (whole brain)	28	24	28	24
<b>Slice thickness</b>	5mm	5	5	5	5
<b>Slice gap</b>	0-1mm	0	0	1.5	0
<b>Matrix</b>	128 x 128	128 x 128	256x256	128x128	256x256
<b>Φ encoding dir<sup>n</sup></b>	AP	R/L		AP	AP
<b>FOV</b>	24 cm	24 x 24 cm	256x256	26	24
<b>Slice orient</b>	// to hard palate	Straight axial	Straight axial	AC-PC	AC-PC
<b>T<sub>scan</sub></b>	90-120secs	0:40	1:39	2:08	3:36 (plus 12secs for calibration)

## Circle of Willis MRA

	<b>Edinburgh</b>	<b>Aberdeen</b>	<b>Glasgow (1.5T)</b>	<b>Glasgow (3T)</b>
<b>Sequence</b>	3D TOF 2 slab HR			3D TOF
<b>TR (ms)</b>	23			21ms
<b>TE (1) (ms)</b>	2.7			3ms
<b>TE (1) (ms)</b>	20 / 2000			
<b>Flip angle</b>	20°			15
<b>Locs / slab</b>	32			50
<b>Slice thickness</b>	1.6			1.2
<b>Slice gap</b>	0			0

<b>Matrix</b>	320 x 224			512 x 320
<b>Φ FOV</b>	1			1
<b>FOV</b>	16			22
<b>Slice orient</b>	Straight axial			Oblique
<b>Tscan</b>	5:46			2:52

## Perfusion

	<b>Recommended</b>	<b>Edinburgh</b>	<b>Aberdeen</b>	<b>Glasgow (1.5T)</b>	<b>Glasgow (3T)</b>
<b>Sequence</b>	Single-shot EPI	Single-shot EPI	Single-shot EPI	GRE-EPI	SS-EPI
<b>TR</b>	1500±250ms	1600	1600	<b>2000</b>	<b>1500</b>
<b>TE</b>	35-45ms@1.5T 25-30ms@3T	30	30	60	22.1
<b>Flip angle</b>	90°@1.5T 60°@3T	90	<b>90</b>	90	60
<b>Tscan</b>	90-120seconds	2:08	2:06	1:05	2:00
<b>T before contrast</b>	10secs (10-12 baseline images)	16	16 sec (10 baseline scans)	<b>6-8 sec</b>	<b>15s</b>
<b># slices</b>	>12 (whole brain)	22	30	18	Whole brain
<b>Slice thickness</b>	5mm	5	5	5	5
<b>Slice gap</b>	0-1mm	0	0	<b>1</b>	<b>0</b>
<b>Matrix</b>	128x128	96 x 96*	96x96*	128x64	128x128
<b>Φ encoding dir<sup>n</sup></b>	AP	AP	AP	AP	AP
<b>FOV</b>	24 cm	24 x 24	240x240	26	24
<b>Slice orientation</b>	// to hard palate	Straight axial	Straight axial	<b>AC-PC</b>	AC-PC
<b>Contrast</b>	Gad-based	Gad-based	Gad-based	Gad-based	Gad-based
<b>Contrast flow rate</b>	4-6ml/sec	5ml/sec	5ml/sec	5	5
<b>Contrast vol</b>	~20ml for 100kl person	20ml	20ml	20	Per Patient
<b>Saline flow rate</b>		5ml/sec	5ml/sec	5	5
<b>Saline volume</b>	20-40ml	20ml	20ml	20	20
<b># phases</b>		80	75	32 per location	40 per location

### Post Contrast FLAIR

	<b>Edinburgh</b>	<b>Aberdeen</b>	<b>Glasgow (1.5T)</b>	<b>Glasgow (3T)</b>
<b>Sequence</b>	Ax FLAIR	IR-TSE	Ax T2 FLAIR	Ax T2 FLAIR
<b>TR (ms)</b>	9000	11000	8000	10000
<b>TE (ms)</b>	140	125	120	144.4
<b>TI (ms)</b>	2200	2800	2000	2250
<b># slices</b>	28	24	24	24
<b>Slice thickness</b>	5	5	5	5
<b>Slice gap</b>	0	0	1.5	0
<b>Matrix</b>	256*224	368x216	256x224	384x256
<b>Φ FOV</b>	1	0.8	0.7-1	0.7-1
<b>FOV</b>	24 x 24	240x190	24	24
<b>Slice orient</b>	Straight axial	Straight axial	AC-PC	AC-PC
<b>Tscan</b>	4:12	6:36	3:44	3:20

## List of References

1. Hatano S. Variability of the diagnosis of stroke by clinical judgement and by a scoring method. *Bull World Health Organ*1976;54(5):533-40.
2. Feigin VL, Lawes CM, Bennett DA, Barker-Collo SL, Parag V. Worldwide stroke incidence and early case fatality reported in 56 population-based studies: a systematic review. *Lancet Neurol*2009 Apr;8(4):355-69.
3. Biller J, Ferro J. Evidence-Based Management of Stroke 2011.
4. Warlow C, Dennis M, Van Gijn J, Hankey GJ, Sandercock PA, Bamford J, et al. *Stroke A practical guide to management*1996.
5. Broderick J, Connolly S, Feldmann E, Hanley D, Kase C, Krieger D, et al. Guidelines for the management of spontaneous intracerebral hemorrhage in adults: 2007 update: a guideline from the American Heart Association/American Stroke Association Stroke Council, High Blood Pressure Research Council, and the Quality of Care and Outcomes in Research Interdisciplinary Working Group. *Stroke*2007 Jun;38(6):2001-23.
6. Bederson JB, Connolly ES, Jr., Batjer HH, Dacey RG, Dion JE, Diringer MN, et al. Guidelines for the management of aneurysmal subarachnoid hemorrhage: a statement for healthcare professionals from a special writing group of the Stroke Council, American Heart Association. *Stroke*2009 Mar;40(3):994-1025.
7. Fogelholm R, Murros K, Rissanen A, Avikainen S. Long term survival after primary intracerebral haemorrhage: a retrospective population based study. *J Neurol Neurosurg Psychiatry*2005 Nov;76(11):1534-8.
8. Warlow C, Sudlow C, Dennis M, Wardlaw J, Sandercock P. *Stroke*. *Lancet*2003 Oct 11;362(9391):1211-24.



9. Adams HP, Jr., Bendixen BH, Kappelle LJ, Biller J, Love BB, Gordon DL, et al. Classification of subtype of acute ischemic stroke. Definitions for use in a multicenter clinical trial. TOAST. Trial of Org 10172 in Acute Stroke Treatment. *Stroke*1993 Jan;24(1):35-41.
10. Ay H, Benner T, Arsava EM, Furie KL, Singhal AB, Jensen MB, et al. A computerized algorithm for etiologic classification of ischemic stroke: the Causative Classification of Stroke System. *Stroke*2007 Nov;38(11):2979-84.
11. Ay H, Furie KL, Singhal A, Smith WS, Sorensen AG, Koroshetz WJ. An evidence-based causative classification system for acute ischemic stroke. *Ann Neurol*2005 Nov;58(5):688-97.
12. Dirnagl U, Iadecola C, Moskowitz MA. Pathobiology of ischaemic stroke: an integrated view. *Trends Neurosci*1999 Sep;22(9):391-7.
13. Saver JL. Time is brain--quantified. *Stroke*2006 Jan;37(1):263-6.
14. Astrup J, Siesjo BK, Symon L. Thresholds in cerebral ischemia - the ischemic penumbra. *Stroke*1981 Nov-Dec;12(6):723-5.
15. Liebeskind DS. Collateral circulation. *Stroke*2003 Sep;34(9):2279-84.
16. Markus HS. Cerebral perfusion and stroke. *J Neurol Neurosurg Psychiatry*2004 Mar;75(3):353-61.
17. Moustafa RR, Baron JC. Pathophysiology of ischaemic stroke: insights from imaging, and implications for therapy and drug discovery. *Br J Pharmacol*2008 Mar;153 Suppl 1:S44-54.
18. Broughton BR, Reutens DC, Sobey CG. Apoptotic Mechanisms After Cerebral Ischemia. *Stroke*2009 Jan 29.
19. Wu TC, Grotta J. Hypothermia for Acute Ischaemic Stroke. *Lancet Neurol*2013 March;12(3):275-84.
20. Muir KW. Heterogeneity of stroke pathophysiology and neuroprotective clinical trial design. *Stroke*2002 Jun;33(6):1545-50.

21. Hossmann KA. Viability thresholds and the penumbra of focal ischemia. *Ann Neurol*1994 Oct;36(4):557-65.
22. Sundt TM, Jr., Sharbrough FW, Anderson RE, Michenfelder JD. Cerebral blood flow measurements and electroencephalograms during carotid endarterectomy. *J Neurosurg*1974 Sep;41(3):310-20.
23. Branston NM, Symon L, Crockard HA, Pasztor E. Relationship between the cortical evoked potential and local cortical blood flow following acute middle cerebral artery occlusion in the baboon. *Exp Neurol*1974 Nov;45(2):195-208.
24. Astrup J, Symon L, Branston NM, Lassen NA. Cortical evoked potential and extracellular K<sup>+</sup> and H<sup>+</sup> at critical levels of brain ischemia. *Stroke*1977 Jan-Feb;8(1):51-7.
25. Jones TH, Morawetz RB, Crowell RM, Marcoux FW, FitzGibbon SJ, DeGirolami U, et al. Thresholds of focal cerebral ischemia in awake monkeys. *J Neurosurg*1981 Jun;54(6):773-82.
26. Donnan G, Baron JC, Davis S, Sharp FR. *The Ischemic Penumbra*. New York: Informa Healthcare; 2007.
27. Lassen NA. Cerebral Blood Flow and Oxygen Consumption in Man. *Physiological Reviews*1959;39(2):183-238.
28. Baron JC, Bousser MG, Rey A, Guillard A, Comar D, Castaigne P. Reversal of focal "misery-perfusion syndrome" by extra-intracranial arterial bypass in hemodynamic cerebral ischemia. A case study with <sup>15</sup>O positron emission tomography. *Stroke*1981 Jul-Aug;12(4):454-9.
29. Marchal G, Benali K, Iglesias S, Viader F, Derlon JM, Baron JC. Voxel-based mapping of irreversible ischaemic damage with PET in acute stroke. *Brain*1999 Dec;122 ( Pt 12):2387-400.
30. Heiss WD. Ischemic penumbra: evidence from functional imaging in man. *J Cereb Blood Flow Metab*2000 Sep;20(9):1276-93.

31. Lees KR, Bluhmki E, von Kummer R, Brodt TG, Toni D, Grotta JC, et al. Time to treatment with intravenous alteplase and outcome in stroke: an updated pooled analysis of ECASS, ATLANTIS, NINDS, and EPITHET trials. *Lancet* 2010 May 15;375(9727):1695-703.
32. Baird TA, Parsons MW, Phan T, Butcher KS, Desmond PM, Tress BM, et al. Persistent poststroke hyperglycemia is independently associated with infarct expansion and worse clinical outcome. *Stroke* 2003 Sep;34(9):2208-14.
33. Parsons MW, Barber PA, Desmond PM, Baird TA, Darby DG, Byrnes G, et al. Acute hyperglycemia adversely affects stroke outcome: a magnetic resonance imaging and spectroscopy study. *Ann Neurol* 2002 Jul;52(1):20-8.
34. Gray CS, Hildreth AJ, Sandercock PA, O'Connell JE, Johnston DE, Cartlidge NE, et al. Glucose-potassium-insulin infusions in the management of post-stroke hyperglycaemia: the UK Glucose Insulin in Stroke Trial (GIST-UK). *Lancet Neurol* 2007 May;6(5):397-406.
35. McCormick M, Hadley D, McLean JR, Macfarlane JA, Condon B, Muir KW. Randomized, controlled trial of insulin for acute poststroke hyperglycemia. *Ann Neurol* May;67(5):570-8.
36. Rosso C, Corvol JC, Pires C, Crozier S, Attal Y, Jacqueminet S, et al. Intensive Versus Subcutaneous Insulin in Patients With Hyperacute Stroke: Results From the Randomized INSULINFARCT Trial. *Stroke* Sep;43(9):2343-9.
37. Ay H, Koroshetz WJ, Vangel M, Benner T, Melinosky C, Zhu M, et al. Conversion of ischemic brain tissue into infarction increases with age. *Stroke* 2005 Dec;36(12):2632-6.
38. Baltan S, Besancon EF, Mbow B, Ye Z, Hamner MA, Ransom BR. White matter vulnerability to ischemic injury increases with age because of enhanced excitotoxicity. *J Neurosci* 2008 Feb 6;28(6):1479-89.

39. Gokcay F, Arsava EM, Baykaner T, Vangel M, Garg P, Wu O, et al. Age-dependent susceptibility to infarct growth in women. *Stroke* 2011 Apr;42(4):947-51.
40. Bang OY, Saver JL, Alger JR, Starkman S, Ovbiagele B, Liebeskind DS. Determinants of the distribution and severity of hypoperfusion in patients with ischemic stroke. *Neurology* 2008 Nov 25;71(22):1804-11.
41. Allport LE, Parsons MW, Butcher KS, MacGregor L, Desmond PM, Tress BM, et al. Elevated hematocrit is associated with reduced reperfusion and tissue survival in acute stroke. *Neurology* 2005 Nov 8;65(9):1382-7.
42. Tissue plasminogen activator for acute ischemic stroke. The National Institute of Neurological Disorders and Stroke rt-PA Stroke Study Group. *N Engl J Med* 1995 Dec 14;333(24):1581-7.
43. Albers GW, Clark WM, Madden KP, Hamilton SA. ATLANTIS trial: results for patients treated within 3 hours of stroke onset. Alteplase Thrombolysis for Acute Noninterventional Therapy in Ischemic Stroke. *Stroke* 2002 Feb;33(2):493-5.
44. Hacke W, Kaste M, Fieschi C, Toni D, Lesaffre E, von Kummer R, et al. Intravenous thrombolysis with recombinant tissue plasminogen activator for acute hemispheric stroke. The European Cooperative Acute Stroke Study (ECASS). *JAMA* 1995 Oct 4;274(13):1017-25.
45. Hacke W, Kaste M, Fieschi C, von Kummer R, Davalos A, Meier D, et al. Randomised double-blind placebo-controlled trial of thrombolytic therapy with intravenous alteplase in acute ischaemic stroke (ECASS II). Second European-Australasian Acute Stroke Study Investigators. *Lancet* 1998 Oct 17;352(9136):1245-51.
46. Hacke W, Kaste M, Bluhmki E, Brozman M, Davalos A, Guidetti D, et al. Thrombolysis with alteplase 3 to 4.5 hours after acute ischemic stroke. *N Engl J Med* 2008 Sep 25;359(13):1317-29.

47. Hacke W, Furlan AJ, Al-Rawi Y, Davalos A, Fiebach JB, Gruber F, et al. Intravenous desmoteplase in patients with acute ischaemic stroke selected by MRI perfusion-diffusion weighted imaging or perfusion CT (DIAS-2): a prospective, randomised, double-blind, placebo-controlled study. *Lancet Neurol*2009 Feb;8(2):141-50.
48. Hacke W, Albers G, Al-Rawi Y, Bogousslavsky J, Davalos A, Eliasziw M, et al. The Desmoteplase in Acute Ischemic Stroke Trial (DIAS): a phase II MRI-based 9-hour window acute stroke thrombolysis trial with intravenous desmoteplase. *Stroke*2005 Jan;36(1):66-73.
49. Davydov L, Cheng JW. Tenecteplase: a review. *Clin Ther*2001 Jul;23(7):982-97; discussion 1.
50. Haley EC, Jr., Thompson JL, Grotta JC, Lyden PD, Hemmen TG, Brown DL, et al. Phase IIB/III trial of tenecteplase in acute ischemic stroke: results of a prematurely terminated randomized clinical trial. *Stroke* Apr;41(4):707-11.
51. Parsons MW, Miteff F, Bateman GA, Spratt N, Loiselle A, Attia J, et al. Acute ischemic stroke: imaging-guided tenecteplase treatment in an extended time window. *Neurology*2009 Mar 10;72(10):915-21.
52. Parsons M, Spratt N, Bivard A, Campbell B, Chung K, Miteff F, et al. A randomized trial of tenecteplase versus alteplase for acute ischemic stroke. *N Engl J Med*2012 Mar 22;366(12):1099-107.
53. Rha JH, Saver JL. The impact of recanalization on ischemic stroke outcome: a meta-analysis. *Stroke*2007 Mar;38(3):967-73.
54. Bhatia R, Hill MD, Shobha N, Menon B, Bal S, Kochar P, et al. Low rates of acute recanalization with intravenous recombinant tissue plasminogen activator in ischemic stroke: real-world experience and a call for action. *Stroke*2010 Oct;41(10):2254-8.

55. del Zoppo GJ, Poeck K, Pessin MS, Wolpert SM, Furlan AJ, Ferbert A, et al. Recombinant tissue plasminogen activator in acute thrombotic and embolic stroke. *Ann Neurol*1992 Jul;32(1):78-86.
56. Furlan A, Higashida R, Wechsler L, Gent M, Rowley H, Kase C, et al. Intra-arterial prourokinase for acute ischemic stroke. The PROACT II study: a randomized controlled trial. Prolyse in Acute Cerebral Thromboembolism. *JAMA*1999 Dec 1;282(21):2003-11.
57. Ogawa A, Mori E, Minematsu K, Taki W, Takahashi A, Nemoto S, et al. Randomized trial of intraarterial infusion of urokinase within 6 hours of middle cerebral artery stroke: the middle cerebral artery embolism local fibrinolytic intervention trial (MELT) Japan. *Stroke*2007 Oct;38(10):2633-9.
58. Lee M, Hong KS, Saver JL. Efficacy of intra-arterial fibrinolysis for acute ischemic stroke: meta-analysis of randomized controlled trials. *Stroke*2010 May;41(5):932-7.
59. Meyers PM, Schumacher HC, Connolly ES, Jr., Heyer EJ, Gray WA, Higashida RT. Current status of endovascular stroke treatment. *Circulation*2011 Jun 7;123(22):2591-601.
60. Smith WS, Sung G, Saver J, Budzik R, Duckwiler G, Liebeskind DS, et al. Mechanical thrombectomy for acute ischemic stroke: final results of the Multi MERCI trial. *Stroke*2008 Apr;39(4):1205-12.
61. The penumbra pivotal stroke trial: safety and effectiveness of a new generation of mechanical devices for clot removal in intracranial large vessel occlusive disease. *Stroke*2009 Aug;40(8):2761-8.
62. Castano C, Dorado L, Guerrero C, Millan M, Gomis M, Perez de la Ossa N, et al. Mechanical thrombectomy with the Solitaire AB device in large artery occlusions of the anterior circulation: a pilot study. *Stroke*2010 Aug;41(8):1836-40.

63. Davalos A, Pereira VM, Chapot R, Bonafe A, Andersson T, Gralla J. Retrospective Multicenter Study of Solitaire FR for Revascularization in the Treatment of Acute Ischemic Stroke. *Stroke* 2012 Oct;43(10):2699-705.
64. Saver JL, Jahan R, Levy EI, Jovin TG, Baxter B, Nogueira RG, et al. Solitaire flow restoration device versus the Merci Retriever in patients with acute ischaemic stroke (SWIFT): a randomised, parallel-group, non-inferiority trial. *Lancet* 2012 Aug 24.
65. Nogueira RG, Lutsep HL, Gupta R, Jovin TG, Albers GW, Walker GA, et al. Trevo versus Merci retrievers for thrombectomy revascularisation of large vessel occlusions in acute ischaemic stroke (TREVO 2): a randomised trial. *Lancet* 2012 Oct 6;380(9849):1231-40.
66. San Roman L, Obach V, Blasco J, Macho J, Lopez A, Urra X, et al. Single-center experience of cerebral artery thrombectomy using the TREVO device in 60 patients with acute ischemic stroke. *Stroke* 2012 Jun;43(6):1657-9.
67. Broderick JP, Palesch YY, Demchuk AM, Yeatts SD, Khatri P, Hill MD, et al. Endovascular therapy after intravenous t-PA versus t-PA alone for stroke. *N Engl J Med* 2013 Mar 7;368(10):893-903.
68. Ciccone A, Valvassori L, Nichelatti M, Sgoifo A, Ponzio M, Sterzi R, et al. Endovascular treatment for acute ischemic stroke. *N Engl J Med* 2013 Mar 7;368(10):904-13.
69. Powers WJ. Intra-arterial therapies for acute ischemic stroke: unsafe and without proven value. *J Neurointerv Surg* 2012 May;4(3):164-6.
70. Chimowitz MI. Endovascular treatment for acute ischemic stroke--still unproven. *N Engl J Med* 2013 Mar 7;368(10):952-5.
71. Muir KW, Baird-Gunning J, Walker L, Baird T, McCormick M, Coutts SB. Can the ischemic penumbra be identified on noncontrast CT of acute stroke? *Stroke* 2007 Sep;38(9):2485-90.

72. Grond M, von Kummer R, Sobesky J, Schmulling S, Heiss WD. Early computed-tomography abnormalities in acute stroke. *Lancet*1997 Nov 29;350(9091):1595-6.
73. Kucinski T, Majumder A, Knab R, Naumann D, Fiehler J, Vaterlein O, et al. Cerebral perfusion impairment correlates with the decrease of CT density in acute ischaemic stroke. *Neuroradiology*2004 Sep;46(9):716-22.
74. von Kummer R, Bourquain H, Bastianello S, Bozzao L, Manelfe C, Meier D, et al. Early prediction of irreversible brain damage after ischemic stroke at CT. *Radiology*2001 Apr;219(1):95-100.
75. Kucinski T, Vaterlein O, Glauche V, Fiehler J, Klotz E, Eckert B, et al. Correlation of apparent diffusion coefficient and computed tomography density in acute ischemic stroke. *Stroke*2002 Jul;33(7):1786-91.
76. Muir KW, Buchan A, von Kummer R, Rother J, Baron JC. Imaging of acute stroke. *Lancet Neurol*2006 Sep;5(9):755-68.
77. Simard JM, Kent TA, Chen M, Tarasov KV, Gerzanich V. Brain oedema in focal ischaemia: molecular pathophysiology and theoretical implications. *Lancet Neurol*2007 Mar;6(3):258-68.
78. Dzialowski I, Weber J, Doerfler A, Forsting M, von Kummer R. Brain tissue water uptake after middle cerebral artery occlusion assessed with CT. *J Neuroimaging*2004 Jan;14(1):42-8.
79. Barber PA, Demchuk AM, Zhang J, Buchan AM. Validity and reliability of a quantitative computed tomography score in predicting outcome of hyperacute stroke before thrombolytic therapy. ASPECTS Study Group. Alberta Stroke Programme Early CT Score. *Lancet*2000 May 13;355(9216):1670-4.
80. Leys D, Pruvo JP, Godefroy O, Rondepierre P, Leclerc X. Prevalence and significance of hyperdense middle cerebral artery in acute stroke. *Stroke*1992 Mar;23(3):317-24.



81. Koo CK, Teasdale E, Muir KW. What constitutes a true hyperdense middle cerebral artery sign? *Cerebrovasc Dis*2000 Nov-Dec;10(6):419-23.
82. von Kummer R, Meyding-Lamade U, Forsting M, Rosin L, Rieke K, Hacke W, et al. Sensitivity and prognostic value of early CT in occlusion of the middle cerebral artery trunk. *AJNR Am J Neuroradiol*1994 Jan;15(1):9-15; discussion 6-8.
83. Tomsick T, Brott T, Barsan W, Broderick J, Haley EC, Spilker J, et al. Prognostic value of the hyperdense middle cerebral artery sign and stroke scale score before ultraearly thrombolytic therapy. *AJNR Am J Neuroradiol*1996 Jan;17(1):79-85.
84. Kharitonova T, Thoren M, Ahmed N, Wardlaw JM, von Kummer R, Thomassen L, et al. Disappearing hyperdense middle cerebral artery sign in ischaemic stroke patients treated with intravenous thrombolysis: clinical course and prognostic significance. *J Neurol Neurosurg Psychiatry*2009 Mar;80(3):273-8.
85. Leary MC, Kidwell CS, Villablanca JP, Starkman S, Jahan R, Duckwiler GR, et al. Validation of computed tomographic middle cerebral artery "dot"sign: an angiographic correlation study. *Stroke*2003 Nov;34(11):2636-40.
86. Ozdemir O, Leung A, Bussiere M, Hachinski V, Pelz D. Hyperdense internal carotid artery sign: a CT sign of acute ischemia. *Stroke*2008 Jul;39(7):2011-6.
87. Riedel CH, Jensen U, Rohr A, Tietke M, Alfke K, Ulmer S, et al. Assessment of thrombus in acute middle cerebral artery occlusion using thin-slice nonenhanced Computed Tomography reconstructions. *Stroke*2010 Aug;41(8):1659-64.
88. Kim EY, Yoo E, Choi HY, Lee JW, Heo JH. Thrombus volume comparison between patients with and without hyperattenuated artery sign on CT. *AJNR Am J Neuroradiol*2008 Feb;29(2):359-62.
89. Srinivasan A, Goyal M, Al Azri F, Lum C. State-of-the-art imaging of acute stroke. *Radiographics*2006 Oct;26 Suppl 1:S75-95.

90. Ezzeddine MA, Lev MH, McDonald CT, Rordorf G, Oliveira-Filho J, Aksoy FG, et al. CT angiography with whole brain perfused blood volume imaging: added clinical value in the assessment of acute stroke. *Stroke*2002 Apr;33(4):959-66.
91. Wildermuth S, Knauth M, Brandt T, Winter R, Sartor K, Hacke W. Role of CT angiography in patient selection for thrombolytic therapy in acute hemispheric stroke. *Stroke*1998 May;29(5):935-8.
92. Macdougall NJ, McVerry F, Baird S, Baird T, Teasdale E, Muir KW. Iodinated Contrast Media and Cerebral Hemorrhage After Intravenous Thrombolysis. *Stroke*2011 Jul 7.
93. Bartlett ES, Walters TD, Symons SP, Fox AJ. Carotid stenosis index revisited with direct CT angiography measurement of carotid arteries to quantify carotid stenosis. *Stroke*2007 Feb;38(2):286-91.
94. Wardlaw JM, Stevenson MD, Chappell F, Rothwell PM, Gillard J, Young G, et al. Carotid artery imaging for secondary stroke prevention: both imaging modality and rapid access to imaging are important. *Stroke*2009 Nov;40(11):3511-7.
95. Wardlaw JM, Chappell FM, Best JJ, Wartolowska K, Berry E. Non-invasive imaging compared with intra-arterial angiography in the diagnosis of symptomatic carotid stenosis: a meta-analysis. *Lancet*2006 May 6;367(9521):1503-12.
96. Rothwell PM, Eliasziw M, Gutnikov SA, Fox AJ, Taylor DW, Mayberg MR, et al. Analysis of pooled data from the randomised controlled trials of endarterectomy for symptomatic carotid stenosis. *Lancet*2003 Jan 11;361(9352):107-16.
97. Di Tullio MR, Russo C, Jin Z, Sacco RL, Mohr JP, Homma S. Aortic arch plaques and risk of recurrent stroke and death. *Circulation*2009 May 5;119(17):2376-82.

98. Vertinsky AT, Schwartz NE, Fischbein NJ, Rosenberg J, Albers GW, Zaharchuk G. Comparison of multidetector CT angiography and MR imaging of cervical artery dissection. *AJNR Am J Neuroradiol* 2008 Oct;29(9):1753-60.
99. Schramm P, Schellinger PD, Fiebach JB, Heiland S, Jansen O, Knauth M, et al. Comparison of CT and CT angiography source images with diffusion-weighted imaging in patients with acute stroke within 6 hours after onset. *Stroke* 2002 Oct;33(10):2426-32.
100. Schramm P, Schellinger PD, Klotz E, Kallenberg K, Fiebach JB, Kulkens S, et al. Comparison of perfusion computed tomography and computed tomography angiography source images with perfusion-weighted imaging and diffusion-weighted imaging in patients with acute stroke of less than 6 hours' duration. *Stroke* 2004 Jul;35(7):1652-8.
101. Coutts SB, Lev MH, Eliasziw M, Roccatagliata L, Hill MD, Schwamm LH, et al. ASPECTS on CTA source images versus unenhanced CT: added value in predicting final infarct extent and clinical outcome. *Stroke* 2004 Nov;35(11):2472-6.
102. Puetz V, Sylaja PN, Coutts SB, Hill MD, Dzialowski I, Mueller P, et al. Extent of hypoattenuation on CT angiography source images predicts functional outcome in patients with basilar artery occlusion. *Stroke* 2008 Sep;39(9):2485-90.
103. Sharma M, Fox AJ, Symons S, Jairath A, Aviv RI. CT angiographic source images: flow- or volume-weighted? *AJNR Am J Neuroradiol* 2010 Feb;32(2):359-64.
104. Campbell B, Christensen S, Levi C, Desmond P, Donnan G, Davis S, et al. Cerebral Blood Flow Is the Optimal CT Perfusion Parameter for Assessing Infarct Core. *Stroke* 2011;42(12):3435-40.
105. Romero JM. CT angiography source image evaluation for stroke. *Semin Ultrasound CT MR* 2005 Dec;26(6):387-93.

106. Lev MH, Farkas J, Rodriguez VR, Schwamm LH, Hunter GJ, Putman CM, et al. CT angiography in the rapid triage of patients with hyperacute stroke to intraarterial thrombolysis: accuracy in the detection of large vessel thrombus. *J Comput Assist Tomogr* 2001 Jul-Aug;25(4):520-8.
107. Sims JR, Rordorf G, Smith EE, Koroshetz WJ, Lev MH, Buonanno F, et al. Arterial occlusion revealed by CT angiography predicts NIH stroke score and acute outcomes after IV tPA treatment. *AJNR Am J Neuroradiol* 2005 Feb;26(2):246-51.
108. Brandt T, Knauth M, Wildermuth S, Winter R, von Kummer R, Sartor K, et al. CT angiography and Doppler sonography for emergency assessment in acute basilar artery ischemia. *Stroke* 1999 Mar;30(3):606-12.
109. Schonewille WJ, Wijman CA, Michel P, Rueckert CM, Weimar C, Mattle HP, et al. Treatment and outcomes of acute basilar artery occlusion in the Basilar Artery International Cooperation Study (BASICS): a prospective registry study. *Lancet Neurol* 2009 Aug;8(8):724-30.
110. Knauth M, von Kummer R, Jansen O, Hahnel S, Dorfler A, Sartor K. Potential of CT angiography in acute ischemic stroke. *AJNR Am J Neuroradiol* 1997 Jun-Jul;18(6):1001-10.
111. Miteff F, Levi CR, Bateman GA, Spratt N, McElduff P, Parsons MW. The independent predictive utility of computed tomography angiographic collateral status in acute ischaemic stroke. *Brain* 2009 Aug;132(Pt 8):2231-8.
112. Muir KW, Halbert HM, Baird TA, McCormick M, Teasdale E. Visual evaluation of perfusion computed tomography in acute stroke accurately estimates infarct volume and tissue viability. *J Neurol Neurosurg Psychiatry* 2006 Mar;77(3):334-9.
113. Parsons MW. Perfusion CT: is it clinically useful? *Int J Stroke* 2008 Feb;3(1):41-50.

114. Siebert E, Bohner G, Dewey M, Masuhr F, Hoffmann KT, Mews J, et al. 320-slice CT neuroimaging: initial clinical experience and image quality evaluation. *Br J Radiol*2009 Jul;82(979):561-70.
115. Cohnen M, Wittsack HJ, Assadi S, Muskalla K, Ringelstein A, Poll LW, et al. Radiation exposure of patients in comprehensive computed tomography of the head in acute stroke. *AJNR Am J Neuroradiol*2006 Sep;27(8):1741-5.
116. FDA investigates the safety of brain perfusion CT [database on the Internet]2010 [cited Jan]. Available from: [http://www.ncbi.nlm.nih.gov/entrez/query.fcgi?cmd=Retrieve&db=PubMed&dopt=Citation&list\\_uids=19892810](http://www.ncbi.nlm.nih.gov/entrez/query.fcgi?cmd=Retrieve&db=PubMed&dopt=Citation&list_uids=19892810).
117. Kudo K, Sasaki M, Yamada K, Momoshima S, Utsunomiya H, Shirato H, et al. Differences in CT perfusion maps generated by different commercial software: quantitative analysis by using identical source data of acute stroke patients. *Radiology*2009 Jan;254(1):200-9.
118. Axel L. Cerebral blood flow determination by rapid-sequence computed tomography: theoretical analysis. *Radiology*1980 Dec;137(3):679-86.
119. Konstas AA, Goldmakher GV, Lee TY, Lev MH. Theoretic basis and technical implementations of CT perfusion in acute ischemic stroke, part 1: Theoretic basis. *AJNR Am J Neuroradiol*2009 Apr; 30(4):662-8.
120. Mullani NA, Gould KL. First-pass measurements of regional blood flow with external detectors. *J Nucl Med*1983 Jul; 24(7):577-81.
121. Wintermark M, Maeder P, Thiran JP, Schnyder P, Meuli R. Quantitative assessment of regional cerebral blood flows by perfusion CT studies at low injection rates: a critical review of the underlying theoretical models. *Eur Radiol*2001; 11(7):1220-30.

122. Eastwood JD, Lev MH, Azhari T, Lee TY, Barboriak DP, Delong DM, et al. CT perfusion scanning with deconvolution analysis: pilot study in patients with acute middle cerebral artery stroke. *Radiology* 2002 Jan; 222(1):227-36.
123. Meier P, Zierler KL. On the theory of the indicator-dilution method for measurement of blood flow and volume. *J Appl Physiol* 1954 Jun; 6(12):731-44.
124. Calamante F, Gadian DG, Connelly A. Delay and dispersion effects in dynamic susceptibility contrast MRI: simulations using singular value decomposition. *Magn Reson Med* 2000 Sep; 44(3):466-73.
125. Wintermark M. The anterior cerebral artery is an appropriate arterial input function for perfusion-CT processing in patients with acute stroke. *Neuroradiology* 2008; 50:227-36.
126. Wu O, Ostergaard L, Weisskoff RM, Benner T, Rosen BR, Sorensen AG. Tracer arrival timing-insensitive technique for estimating flow in MR perfusion-weighted imaging using singular value decomposition with a block-circulant deconvolution matrix. *Magn Reson Med* 2003 Jul; 50(1):164-74.
127. Schaefer PW, Mui K, Kamalian S, Nogueira RG, Gonzalez RG, Lev MH. Avoiding "pseudo-reversibility" of CT-CBV infarct core lesions in acute stroke patients after thrombolytic therapy: the need for algorithmically "delay-corrected" CT perfusion map postprocessing software. *Stroke* 2009 Aug; 40(8):2875-8.
128. Reichenbach JR, Rother J, Jonetz-Mentzel L, Herzau M, Fiala A, Weiller C, et al. Acute stroke evaluated by time-to-peak mapping during initial and early follow-up perfusion CT studies. *AJNR Am J Neuroradiol* 1999 Nov-Dec; 20(10):1842-50.
129. Wintermark M, Reichhart M, Thiran JP, Maeder P, Chalaron M, Schnyder P, et al. Prognostic accuracy of cerebral blood flow measurement by perfusion computed tomography, at the time of emergency room admission, in acute stroke patients. *Ann Neurol* 2002 Apr; 51(4):417-32.

130. Parsons MW, Pepper EM, Chan V, Siddique S, Rajaratnam S, Bateman GA, et al. Perfusion computed tomography: prediction of final infarct extent and stroke outcome. *Ann Neurol* 2005 Nov;58(5):672-9.
131. Wintermark M, Flanders AE, Velthuis B, Meuli R, van Leeuwen M, Goldsher D, et al. Perfusion-CT assessment of infarct core and penumbra: receiver operating characteristic curve analysis in 130 patients suspected of acute hemispheric stroke. *Stroke* 2006 Apr;37(4):979-85.
132. Wintermark M, Meuli R, Browaeys P, Reichhart M, Bogousslavsky J, Schnyder P, et al. Comparison of CT perfusion and angiography and MRI in selecting stroke patients for acute treatment. *Neurology* 2007 Feb 27;68(9):694-7.
133. Murphy BD, Fox AJ, Lee DH, Sahlas DJ, Black SE, Hogan MJ, et al. White matter thresholds for ischemic penumbra and infarct core in patients with acute stroke: CT perfusion study. *Radiology* 2008 Jun;247(3):818-25.
134. Bivard A, McElduff P, Spratt N, Levi C, Parsons M. Defining the extent of irreversible brain ischemia using perfusion computed tomography. *Cerebrovasc Dis* 2011;31(3):238-45.
135. Dani KA, Thomas RG, Chappell FM, Shuler K, MacLeod MJ, Muir KW, et al. Computed tomography and magnetic resonance perfusion imaging in ischemic stroke: definitions and thresholds. *Ann Neurol* 2011 Sep;70(3):384-401.
136. Christensen S, Mouridsen K, Wu O, Hjort N, Karstoft H, Thomalla G, et al. Comparison of 10 perfusion MRI parameters in 97 sub-6-hour stroke patients using voxel-based receiver operating characteristics analysis. *Stroke* 2009 Jun;40(6):2055-61.
137. Rowley HA. The four Ps of acute stroke imaging: parenchyma, pipes, perfusion, and penumbra. *AJNR Am J Neuroradiol* 2001 Apr;22(4):599-601.

138. Aviv RI, d'Esterre CD, Murphy BD, Hopyan JJ, Buck B, Mallia G, et al. Hemorrhagic transformation of ischemic stroke: prediction with CT perfusion. *Radiology*2009 Mar;250(3):867-77.
139. Dankbaar JW, Hom J, Schneider T, Cheng SC, Lau BC, van der Schaaf I, et al. Dynamic perfusion CT assessment of the blood-brain barrier permeability: first pass versus delayed acquisition. *AJNR Am J Neuroradiol*2008 Oct;29(9):1671-6.
140. Hom J, Dankbaar JW, Schneider T, Cheng SC, Bredno J, Wintermark M. Optimal Duration of Acquisition for Dynamic Perfusion CT Assessment of Blood-Brain Barrier Permeability Using the Patlak Model. *AJNR Am J Neuroradiol*2009 Apr 15.
141. Moseley ME, Kucharczyk J, Mintorovitch J, Cohen Y, Kurhanewicz J, Derugin N, et al. Diffusion-weighted MR imaging of acute stroke: correlation with T2-weighted and magnetic susceptibility-enhanced MR imaging in cats. *AJNR Am J Neuroradiol*1990 May;11(3):423-9.
142. Sevick RJ, Kanda F, Mintorovitch J, Arieff AI, Kucharczyk J, Tsuruda JS, et al. Cytotoxic brain edema: assessment with diffusion-weighted MR imaging. *Radiology*1992 Dec;185(3):687-90.
143. Schlaug G, Benfield A, Baird AE, Siewert B, Lovblad KO, Parker RA, et al. The ischemic penumbra: operationally defined by diffusion and perfusion MRI. *Neurology*1999 Oct 22;53(7):1528-37.
144. Kidwell CS, Saver JL, Mattiello J, Starkman S, Vinuela F, Duckwiler G, et al. Thrombolytic reversal of acute human cerebral ischemic injury shown by diffusion/perfusion magnetic resonance imaging. *Ann Neurol*2000;47(4):462-9.
145. Guadagno JV, Warburton EA, Jones PS, Day DJ, Aigbirhio FI, Fryer TD, et al. How affected is oxygen metabolism in DWI lesions?: A combined acute stroke PET-MR study. *Neurology*2006 Sep 12;67(5):824-9.



146. Kranz PG, Eastwood JD. Does diffusion-weighted imaging represent the ischemic core? An evidence-based systematic review. *AJNR Am J Neuroradiol*2009 Jun;30(6):1206-12.
147. Chemmanam T, Campbell BC, Christensen S, Nagakane Y, Desmond PM, Bladin CF, et al. Ischemic diffusion lesion reversal is uncommon and rarely alters perfusion-diffusion mismatch. *Neurology*2010 Sep 21;75(12):1040-7.
148. Mullins ME, Schaefer PW, Sorensen AG, Halpern EF, Ay H, He J, et al. CT and conventional and diffusion-weighted MR imaging in acute stroke: study in 691 patients at presentation to the emergency department. *Radiology*2002 Aug;224(2):353-60.
149. Lovblad KO, Laubach HJ, Baird AE, Curtin F, Schlaug G, Edelman RR, et al. Clinical experience with diffusion-weighted MR in patients with acute stroke. *AJNR Am J Neuroradiol*1998 Jun-Jul;19(6):1061-6.
150. Gonzalez RG, Schaefer PW, Buonanno FS, Schwamm LH, Budzik RF, Rordorf G, et al. Diffusion-weighted MR imaging: diagnostic accuracy in patients imaged within 6 hours of stroke symptom onset. *Radiology*1999 Jan;210(1):155-62.
151. Chalela JA, Kidwell CS, Nentwich LM, Luby M, Butman JA, Demchuk AM, et al. Magnetic resonance imaging and computed tomography in emergency assessment of patients with suspected acute stroke: a prospective comparison. *Lancet*2007 Jan 27;369(9558):293-8.
152. Parsons MW, Christensen S, McElduff P, Levi CR, Butcher KS, De Silva DA, et al. Pre-treatment diffusion- and perfusion-MR lesion volumes have a crucial influence on clinical response to stroke thrombolysis. *J Cereb Blood Flow Metab*2010 Jun;30(6):1214-25.
153. Albers GW, Thijs VN, Wechsler L, Kemp S, Schlaug G, Skalabrin E, et al. Magnetic resonance imaging profiles predict clinical response to early reperfusion:

the diffusion and perfusion imaging evaluation for understanding stroke evolution (DEFUSE) study. *Ann Neurol* 2006 Nov;60(5):508-17.

154. Davis SM, Donnan GA, Parsons MW, Levi C, Butcher KS, Peeters A, et al. Effects of alteplase beyond 3 h after stroke in the Echoplanar Imaging Thrombolytic Evaluation Trial (EPITHET): a placebo-controlled randomised trial. *Lancet Neurol* 2008 Apr;7(4):299-309.

155. Gaudinski MR, Henning EC, Miracle A, Luby M, Warach S, Latour LL. Establishing final infarct volume: stroke lesion evolution past 30 days is insignificant. *Stroke* 2008 Oct;39(10):2765-8.

156. Tourdias T, Renou P, Sibon I, Asselineau J, Bracoud L, Dumoulin M, et al. Final cerebral infarct volume is predictable by MR imaging at 1 week. *AJNR Am J Neuroradiol* 2011 Feb;32(2):352-8.

157. Ebinger M, Christensen S, De Silva DA, Parsons MW, Levi CR, Butcher KS, et al. Expediting MRI-based proof-of-concept stroke trials using an earlier imaging end point. *Stroke* 2009 Apr;40(4):1353-8.

158. Thomalla G, Cheng B, Ebinger M, Hao Q, Tourdias T, Wu O, et al. DWI-FLAIR mismatch for the identification of patients with acute ischaemic stroke within 4.5 h of symptom onset (PRE-FLAIR): a multicentre observational study. *Lancet Neurol* 2011 Nov;10(11):978-86.

159. Lee KY, Latour LL, Luby M, Hsia AW, Merino JG, Warach S. Distal hyperintense vessels on FLAIR: an MRI marker for collateral circulation in acute stroke? *Neurology* 2009 Mar 31;72(13):1134-9.

160. Kamran S, Bates V, Bakshi R, Wright P, Kinkel W, Miletich R. Significance of hyperintense vessels on FLAIR MRI in acute stroke. *Neurology* 2000 Jul 25;55(2):265-9.

161. Fiebach JB, Schellinger PD, Gass A, Kucinski T, Siebler M, Villringer A, et al. Stroke magnetic resonance imaging is accurate in hyperacute intracerebral

hemorrhage: a multicenter study on the validity of stroke imaging. *Stroke* 2004 Feb;35(2):502-6.

162. Nighoghossian N, Hermier M, Adeleine P, Blanc-Lasserre K, Derex L, Honnorat J, et al. Old microbleeds are a potential risk factor for cerebral bleeding after ischemic stroke: a gradient-echo T2\*-weighted brain MRI study. *Stroke* 2002 Mar;33(3):735-42.

163. Fiehler J, Albers GW, Boulanger JM, Derex L, Gass A, Hjort N, et al. Bleeding risk analysis in stroke imaging before thrombolysis (BRASIL): pooled analysis of T2\*-weighted magnetic resonance imaging data from 570 patients. *Stroke* 2007 Oct;38(10):2738-44.

164. Raghavan P, Mukherjee S, Gaughen J, Phillips CD. Magnetic resonance angiography of the extracranial carotid system. *Top Magn Reson Imaging* 2008 Oct;19(5):241-9.

165. Patel SG, Collie DA, Wardlaw JM, Lewis SC, Wright AR, Gibson RJ, et al. Outcome, observer reliability, and patient preferences if CTA, MRA, or Doppler ultrasound were used, individually or together, instead of digital subtraction angiography before carotid endarterectomy. *J Neurol Neurosurg Psychiatry* 2002 Jul;73(1):21-8.

166. Tomanek AI, Coutts SB, Demchuk AM, Hudon ME, Morrish WE, Sevick RJ, et al. MR angiography compared to conventional selective angiography in acute stroke. *Can J Neurol Sci* 2006 Feb;33(1):58-62.

167. The Thrombolysis in Myocardial Infarction (TIMI) trial. Phase I findings. TIMI Study Group. *N Engl J Med* 1985 Apr 4;312(14):932-6.

168. Dani KA, Thomas RG, Chappell FM, Shuler K, Muir KW, Wardlaw JM. Systematic review of perfusion imaging with computed tomography and magnetic resonance in acute ischemic stroke: heterogeneity of acquisition and

- postprocessing parameters: a translational medicine research collaboration multicentre acute stroke imaging study. *Stroke* 2011 Feb;43(2):563-6.
169. Ebinger M, De Silva DA, Christensen S, Parsons MW, Markus R, Donnan GA, et al. Imaging the penumbra - strategies to detect tissue at risk after ischemic stroke. *J Clin Neurosci* 2009 Feb;16(2):178-87.
170. Parsons MW, Barber PA, Chalk J, Darby DG, Rose S, Desmond PM, et al. Diffusion- and perfusion-weighted MRI response to thrombolysis in stroke. *Ann Neurol* 2002 Jan;51(1):28-37.
171. Calamante F, Christensen S, Desmond PM, Ostergaard L, Davis SM, Connelly A. The physiological significance of the time-to-maximum (Tmax) parameter in perfusion MRI. *Stroke* 2010 Jun;41(6):1169-74.
172. Hand PJ, Wardlaw JM, Rowat AM, Haisma JA, Lindley RI, Dennis MS. Magnetic resonance brain imaging in patients with acute stroke: feasibility and patient related difficulties. *J Neurol Neurosurg Psychiatry* 2005 Nov;76(11):1525-7.
173. Kathuria S, Gregg L, Chen J, Gandhi D. Normal cerebral arterial development and variations. *Semin Ultrasound CT MR* 2011 Jun;32(3):242-51.
174. Lasjaunias P, Santoyo-Vazquez A. Segmental agenesis of the internal carotid artery: angiographic aspects with embryological discussion. *Anat Clin* 1984;6(2):133-41.
175. Quisling RG, Rhoton AL, Jr. Intrapetrous carotid artery branches: radioanatomic analysis. *Radiology* 1979 Apr;131(1):133-6.
176. Gibo H, Lenkey C, Rhoton AL, Jr. Microsurgical anatomy of the supraclinoid portion of the internal carotid artery. *J Neurosurg* 1981 Oct;55(4):560-74.
177. Gibo H, Carver CC, Rhoton AL, Jr., Lenkey C, Mitchell RJ. Microsurgical anatomy of the middle cerebral artery. *J Neurosurg* 1981 Feb;54(2):151-69.
178. Pai SB, Varma RG, Kulkarni RN. Microsurgical anatomy of the middle cerebral artery. *Neurol India* 2005 Jun;53(2):186-90.

179. Buckenham TM, Wright IA. Ultrasound of the extracranial vertebral artery. *Br J Radiol*2004 Jan;77(913):15-20.
180. Pai BS, Varma RG, Kulkarni RN, Nirmala S, Manjunath LC, Rakshith S. Microsurgical anatomy of the posterior circulation. *Neurol India*2007 Jan-Mar;55(1):31-41.
181. Zeal AA, Rhoton AL, Jr. Microsurgical anatomy of the posterior cerebral artery. *J Neurosurg*1978 Apr;48(4):534-59.
182. Molnar Z. Thomas Willis (1621-1675), the founder of clinical neuroscience. *Nat Rev Neurosci*2004 Apr;5(4):329-35.
183. Willis T. Two Discourses Concerning the Soul of Brutes, in his Practice of Physick, Being the Whole Works of That Renowned and Famous Physician Containing These Eleven Several Treatises. London: T. Dring, C. Harper, & J. Leigh; 1684.
184. Mount LA, Taveras JM. Arteriographic demonstration of the collateral circulation of the cerebral hemispheres. *AMA Arch Neurol Psychiatry*1957 Sep;78(3):235-53.
185. Hoksbergen AW, Legemate DA, Ubbink DT, Jacobs MJ. Collateral variations in circle of Willis in atherosclerotic population assessed by means of transcranial color-coded duplex ultrasonography. *Stroke*2000 Jul;31(7):1656-60.
186. Battacharji SK, Hutchinson EC, McCall AJ. The Circle of Willis--the incidence of developmental abnormalities in normal and infarcted brains. *Brain*1967 Dec;90(4):747-58.
187. Lippert H, Pabst R. Arterial Variations in Man. Munich: JF Bergman Verlag; 1985.
188. Hendrikse J, Hartkamp MJ, Hillen B, Mali WP, van der Grond J. Collateral ability of the circle of Willis in patients with unilateral internal carotid artery

- occlusion: border zone infarcts and clinical symptoms. *Stroke* 2001 Dec 1;32(12):2768-73.
189. Hedera P, Bujdakova J, Traubner P. Effect of collateral flow patterns on outcome of carotid occlusion. *Eur Neurol* 1995;35(4):212-6.
190. Pipinos, II, Pisimisis GT, Burjonrappa SC, Johanning JM, Longo GM, Lynch TG. One patent intracranial collateral predicts tolerance of flow reversal during carotid angioplasty and stenting. *Ann Vasc Surg* 2009 Jan-Feb;23(1):32-8.
191. van Laar PJ, Hendrikse J, Klijn CJ, Kappelle LJ, van Osch MJ, van der Grond J. Symptomatic carotid artery occlusion: flow territories of major brain-feeding arteries. *Radiology* 2007 Feb;242(2):526-34.
192. Liebeskind DS, Sansing LH. Willisian collateralization. *Neurology* 2004 Jul 27;63(2):344.
193. Nicholls SC, Kohler TR, Bergelin RO, Primozich JF, Lawrence RL, Strandness DE, Jr. Carotid artery occlusion: natural history. *J Vasc Surg* 1986 Nov;4(5):479-85.
194. Brozici M, van der Zwan A, Hillen B. Anatomy and functionality of leptomeningeal anastomoses: a review. *Stroke* 2003 Nov;34(11):2750-62.
195. Vander Eecken H, Adams R. The Anatomy and Functional Significance of the Meningeal Arterial Anastomoses of the Human Brain *Journal of Neuropathology & Experimental Neurology* 1953;12:132-57.
196. Coyle P, Jokelainen PT. Dorsal cerebral arterial collaterals of the rat. *Anat Rec* 1982 Jul;203(3):397-404.
197. Coyle P. Diameter and length changes in cerebral collaterals after middle cerebral artery occlusion in the young rat. *Anat Rec* 1984 Oct;210(2):357-64.
198. Kidd GA, Dobrucki LW, Brovkovich V, Bohr DF, Malinski T. Nitric oxide deficiency contributes to large cerebral infarct size. *Hypertension* 2000 May;35(5):1111-8.

199. Coyle P, Jokelainen PT. Differential outcome to middle cerebral artery occlusion in spontaneously hypertensive stroke-prone rats (SHRSP) and Wistar Kyoto (WKY) rats. *Stroke*1983 Jul-Aug;14(4):605-11.
200. Coyle P. Middle cerebral artery occlusion in the young rat. *Stroke*1982 Nov-Dec;13(6):855-9.
201. Coyle P. Outcomes to middle cerebral artery occlusion in hypertensive and normotensive rats. *Hypertension*1984 Mar-Apr;6(2 Pt 2):169-74.
202. Coyle P. Dorsal cerebral collaterals of stroke-prone spontaneously hypertensive rats (SHRSP) and Wistar Kyoto rats (WKY). *Anat Rec*1987 May;218(1):40-4.
203. Coyle P. Spatial relations of dorsal anastomoses and lesion border after middle cerebral artery occlusion. *Stroke*1987 Nov-Dec;18(6):1133-40.
204. Coyle P, Heistad DD. Blood flow through cerebral collateral vessels in hypertensive and normotensive rats. *Hypertension*1986 Jun;8(6 Pt 2):1167-71.
205. Gratton JA, Sauter A, Rudin M, Lees KR, McColl J, Reid JL, et al. Susceptibility to cerebral infarction in the stroke-prone spontaneously hypertensive rat is inherited as a dominant trait. *Stroke*1998 Mar;29(3):690-4.
206. Jeffs B, Clark JS, Anderson NH, Gratton J, Brosnan MJ, Gauguier D, et al. Sensitivity to cerebral ischaemic insult in a rat model of stroke is determined by a single genetic locus. *Nat Genet*1997 Aug;16(4):364-7.
207. Zhang H, Prabhakar P, Sealock R, Faber JE. Wide genetic variation in the native pial collateral circulation is a major determinant of variation in severity of stroke. *J Cereb Blood Flow Metab*2010 May;30(5):923-34.
208. Chalothorn D, Faber JE. Formation and maturation of the native cerebral collateral circulation. *J Mol Cell Cardiol*2010 Aug;49(2):251-9.

209. Clayton JA, Chalothorn D, Faber JE. Vascular endothelial growth factor-A specifies formation of native collaterals and regulates collateral growth in ischemia. *Circ Res*2008 Oct 24;103(9):1027-36.
210. Chalothorn D, Zhang H, Smith JE, Edwards JC, Faber JE. Chloride intracellular channel-4 is a determinant of native collateral formation in skeletal muscle and brain. *Circ Res*2009 Jul 2;105(1):89-98.
211. Cabrera CL, Bealer SL, Bohr DF. Central depressor action of nitric oxide is deficient in genetic hypertension. *Am J Hypertens*1996 Mar;9(3):237-41.
212. Huang Z, Huang PL, Ma J, Meng W, Ayata C, Fishman MC, et al. Enlarged infarcts in endothelial nitric oxide synthase knockout mice are attenuated by nitro-L-arginine. *J Cereb Blood Flow Metab*1996 Sep;16(5):981-7.
213. Huang Z, Huang PL, Panahian N, Dalkara T, Fishman MC, Moskowitz MA. Effects of cerebral ischemia in mice deficient in neuronal nitric oxide synthase. *Science*1994 Sep 23;265(5180):1883-5.
214. Dalkara T, Morikawa E, Panahian N, Moskowitz MA. Blood flow-dependent functional recovery in a rat model of focal cerebral ischemia. *Am J Physiol*1994 Aug;267(2 Pt 2):H678-83.
215. Muller M, Schimrigk K. Vasomotor reactivity and pattern of collateral blood flow in severe occlusive carotid artery disease. *Stroke*1996 Feb;27(2):296-9.
216. Todo K, Kitagawa K, Sasaki T, Omura-Matsuoka E, Terasaki Y, Oyama N, et al. Granulocyte-macrophage colony-stimulating factor enhances leptomeningeal collateral growth induced by common carotid artery occlusion. *Stroke*2008 Jun;39(6):1875-82.
217. Zhu M, Bi X, Jia Q, Shangguan S. The possible mechanism for impaired angiogenesis after transient focal ischemia in type 2 diabetic GK rats: different expressions of angiostatin and vascular endothelial growth factor. *Biomed Pharmacother*2009 Mar;64(3):208-13.



218. de Groot D, Pasterkamp G, Hoefer IE. Cardiovascular risk factors and collateral artery formation. *Eur J Clin Invest* 2009 Dec;39(12):1036-47.
219. Weihrauch D, Lohr NL, Mraovic B, Ludwig LM, Chilian WM, Pagel PS, et al. Chronic hyperglycemia attenuates coronary collateral development and impairs proliferative properties of myocardial interstitial fluid by production of angiostatin. *Circulation* 2004 May 18;109(19):2343-8.
220. Anan M, Abe T, Shimotaka K, Kamida T, Kubo T, Fujiki M, et al. Induction of collateral circulation by hypoxia-inducible factor 1alpha decreased cerebral infarction in the rat. *Neurol Res* 2009 Nov;31(9):917-22.
221. Sahinarslan A, Yalcin R, Kocaman SA, Ercin U, Tanalp AC, Topal S, et al. The relationship of serum erythropoietin level with coronary collateral grade. *Can J Cardiol* 2011 Sep-Oct;27(5):589-95.
222. Harder DR, Lange AR, Gebremedhin D, Birks EK, Roman RJ. Cytochrome P450 metabolites of arachidonic acid as intracellular signalling molecules in vascular tissue. *J Vasc Res* 1997 May-Jun;34(3):237-43.
223. Gebremedhin D, Lange AR, Lowry TF, Taheri MR, Birks EK, Hudetz AG, et al. Production of 20-HETE and its role in autoregulation of cerebral blood flow. *Circ Res* 2000 Jul 7;87(1):60-5.
224. Dunn KM, Renic M, Flasch AK, Harder DR, Falck J, Roman RJ. Elevated production of 20-HETE in the cerebral vasculature contributes to severity of ischemic stroke and oxidative stress in spontaneously hypertensive rats. *Am J Physiol Heart Circ Physiol* 2008 Dec;295(6):H2455-65.
225. Omura T, Tanaka Y, Miyata N, Koizumi C, Sakurai T, Fukasawa M, et al. Effect of a new inhibitor of the synthesis of 20-HETE on cerebral ischemia reperfusion injury. *Stroke* 2006 May;37(5):1307-13.
226. Miyata N, Seki T, Tanaka Y, Omura T, Taniguchi K, Doi M, et al. Beneficial effects of a new 20-hydroxyeicosatetraenoic acid synthesis inhibitor, TS-011 [N-(3-

chloro-4-morpholin-4-yl) phenyl-N'-hydroxyimido formamide], on hemorrhagic and ischemic stroke. *J Pharmacol Exp Ther* 2005 Jul;314(1):77-85.

227. Tanaka Y, Omura T, Fukasawa M, Horiuchi N, Miyata N, Minagawa T, et al. Continuous inhibition of 20-HETE synthesis by TS-011 improves neurological and functional outcomes after transient focal cerebral ischemia in rats. *Neurosci Res* 2007 Dec;59(4):475-80.

228. Sieff CA. Hematopoietic growth factors. *J Clin Invest* 1987 Jun;79(6):1549-57.

229. Endres M. Statins and stroke. *J Cereb Blood Flow Metab* 2005 Sep;25(9):1093-110.

230. Amarenco P, Bogousslavsky J, Callahan A, 3rd, Goldstein LB, Hennerici M, Rudolph AE, et al. High-dose atorvastatin after stroke or transient ischemic attack. *N Engl J Med* 2006 Aug 10;355(6):549-59.

231. Atkins D, Psaty BM, Koepsell TD, Longstreth WT, Jr., Larson EB. Cholesterol reduction and the risk for stroke in men. A meta-analysis of randomized, controlled trials. *Ann Intern Med* 1993 Jul 15;119(2):136-45.

232. Hebert PR, Gaziano JM, Chan KS, Hennekens CH. Cholesterol lowering with statin drugs, risk of stroke, and total mortality. An overview of randomized trials. *JAMA* 1997 Jul 23-30;278(4):313-21.

233. Goldstein LB, Amarenco P, Zivin J, Messig M, Altafullah I, Callahan A, et al. Statin treatment and stroke outcome in the Stroke Prevention by Aggressive Reduction in Cholesterol Levels (SPARCL) trial. *Stroke* 2009 Nov;40(11):3526-31.

234. Ovbiagele B, Saver JL, Starkman S, Kim D, Ali LK, Jahan R, et al. Statin enhancement of collateralization in acute stroke. *Neurology* 2007 Jun 12;68(24):2129-31.

235. Willmot M, Ghadami A, Whysall B, Clarke W, Wardlaw J, Bath PM. Transdermal glyceryl trinitrate lowers blood pressure and maintains cerebral blood flow in recent stroke. *Hypertension* 2006 Jun;47(6):1209-15.
236. Glyceryl trinitrate vs. control, and continuing vs. stopping temporarily prior antihypertensive therapy, in acute stroke: rationale and design of the Efficacy of Nitric Oxide in Stroke (ENOS) trial (ISRCTN99414122). *Int J Stroke* 2006 Nov;1(4):245-9.
237. Shuaib A, Butcher K, Mohammad AA, Saqqur M, Liebeskind DS. Collateral blood vessels in acute ischaemic stroke: a potential therapeutic target. *Lancet Neurol* 2011 Oct;10(10):909-21.
238. Suzuki N, Hardebo JE, Kahrstrom J, Owman C. Selective electrical stimulation of postganglionic cerebrovascular parasympathetic nerve fibers originating from the sphenopalatine ganglion enhances cortical blood flow in the rat. *J Cereb Blood Flow Metab* 1990 May;10(3):383-91.
239. Khurana D, Kaul S, Bornstein NM. Implant for augmentation of cerebral blood flow trial 1: a pilot study evaluating the safety and effectiveness of the Ischaemic Stroke System for treatment of acute ischaemic stroke. *Int J Stroke* 2009 Dec;4(6):480-5.
240. Shuaib A, Bornstein NM, Diener HC, Dillon W, Fisher M, Hammer MD, et al. Partial aortic occlusion for cerebral perfusion augmentation: safety and efficacy of NeuroFlo in Acute Ischemic Stroke trial. *Stroke* 2011 Jun;42(6):1680-90.
241. Emery DJ, Schellinger PD, Selchen D, Douen AG, Chan R, Shuaib A, et al. Safety and feasibility of collateral blood flow augmentation after intravenous thrombolysis. *Stroke* 2011 Apr;42(4):1135-7.
242. Berthet K, Lukaszewicz AC, Bousser MG, Payen D. Lower body positive pressure application with an antigravity suit in acute carotid occlusion. *Stroke Res Treat* 2010;2010.

243. Christoforidis GA, Karakasis C, Mohammad Y, Caragine LP, Yang M, Slivka AP. Predictors of hemorrhage following intra-arterial thrombolysis for acute ischemic stroke: the role of pial collateral formation. *AJNR Am J Neuroradiol*2009 Jan;30(1):165-70.
244. Bang OY, Saver JL, Buck BH, Alger JR, Starkman S, Ovbiagele B, et al. Impact of collateral flow on tissue fate in acute ischaemic stroke. *J Neurol Neurosurg Psychiatry*2008 Jun;79(6):625-9.
245. Christoforidis GA, Mohammad Y, Kehagias D, Avutu B, Slivka AP. Angiographic assessment of pial collaterals as a prognostic indicator following intra-arterial thrombolysis for acute ischemic stroke. *AJNR Am J Neuroradiol*2005 Aug;26(7):1789-97.
246. Qureshi AI. New grading system for angiographic evaluation of arterial occlusions and recanalization response to intra-arterial thrombolysis in acute ischemic stroke. *Neurosurgery*2002 Jun;50(6):1405-14; discussion 14-5.
247. Liebeskind D. A Novel CT Angiography scale for Assessment of Collaterals in Acute Stroke. *Stroke*. [Abstract]. 2003;34:265.
248. Tan IY, Demchuk AM, Hopyan J, Zhang L, Gladstone D, Wong K, et al. CT angiography clot burden score and collateral score: correlation with clinical and radiologic outcomes in acute middle cerebral artery infarct. *AJNR Am J Neuroradiol*2009 Mar;30(3):525-31.
249. Tan JC, Dillon WP, Liu S, Adler F, Smith WS, Wintermark M. Systematic comparison of perfusion-CT and CT-angiography in acute stroke patients. *Ann Neurol*2007 Jun;61(6):533-43.
250. Chng SM, Petersen ET, Zimine I, Sitoh YY, Lim CC, Golay X. Territorial arterial spin labeling in the assessment of collateral circulation: comparison with digital subtraction angiography. *Stroke*2008 Dec;39(12):3248-54.

251. Hofmeijer J, Klijn CJ, Kappelle LJ, Van Huffelen AC, Van Gijn J. Collateral circulation via the ophthalmic artery or leptomeningeal vessels is associated with impaired cerebral vasoreactivity in patients with symptomatic carotid artery occlusion. *Cerebrovasc Dis*2002;14(1):22-6.
252. Wu B, Wang X, Guo J, Xie S, Wong EC, Zhang J, et al. Collateral circulation imaging: MR perfusion territory arterial spin-labeling at 3T. *AJNR Am J Neuroradiol*2008 Nov;29(10):1855-60.
253. Powers WJ, Press GA, Grubb RL, Jr., Gado M, Raichle ME. The effect of hemodynamically significant carotid artery disease on the hemodynamic status of the cerebral circulation. *Ann Intern Med*1987 Jan;106(1):27-34.
254. Derdeyn CP, Shaibani A, Moran CJ, Cross DT, 3rd, Grubb RL, Jr., Powers WJ. Lack of correlation between pattern of collateralization and misery perfusion in patients with carotid occlusion. *Stroke*1999 May;30(5):1025-32.
255. Klijn CJ, Kappelle LJ, van Huffelen AC, Visser GH, Algra A, Tulleken CA, et al. Recurrent ischemia in symptomatic carotid occlusion: prognostic value of hemodynamic factors. *Neurology*2000 Dec 26;55(12):1806-12.
256. Essig M, von Kummer R, Egelhof T, Winter R, Sartor K. Vascular MR contrast enhancement in cerebrovascular disease. *AJNR Am J Neuroradiol*1996 May;17(5):887-94.
257. Ozgur HT, Kent Walsh T, Masaryk A, Seeger JF, Williams W, Krupinski E, et al. Correlation of cerebrovascular reserve as measured by acetazolamide-challenged SPECT with angiographic flow patterns and intra- or extracranial arterial stenosis. *AJNR Am J Neuroradiol*2001 May;22(5):928-36.
258. Rutgers DR, Klijn CJ, Kappelle LJ, van der Grond J. Recurrent stroke in patients with symptomatic carotid artery occlusion is associated with high-volume flow to the brain and increased collateral circulation. *Stroke*2004 Jun;35(6):1345-9.

259. Grubb RL, Jr., Derdeyn CP, Fritsch SM, Carpenter DA, Yundt KD, Videen TO, et al. Importance of hemodynamic factors in the prognosis of symptomatic carotid occlusion. *JAMA*1998 Sep 23-30;280(12):1055-60.
260. Fukuyama H, Akiguchi I, Kameyama M, Taki W, Handa H, Higa T, et al. Krypton-81m single photon emission tomography and the collateral circulation in carotid occlusion: the role of the circle of Willis and leptomeningeal anastomosis. *J Neurol*1983;230(1):7-17.
261. Yamauchi H, Kudoh T, Sugimoto K, Takahashi M, Kishibe Y, Okazawa H. Pattern of collaterals, type of infarcts, and haemodynamic impairment in carotid artery occlusion. *J Neurol Neurosurg Psychiatry*2004 Dec;75(12):1697-701.
262. Russell SM, Woo HH, Siller K, Panasci D, Leroux PD. Evaluating middle cerebral artery collateral blood flow reserve using acetazolamide transcranial Doppler ultrasound in patients with carotid occlusive disease. *Surg Neurol*2008 Nov;70(5):466-70; discussion 70.
263. Bisschops RH, Klijn CJ, Kappelle LJ, van Huffelen AC, van der Grond J. Collateral flow and ischemic brain lesions in patients with unilateral carotid artery occlusion. *Neurology*2003 May 13;60(9):1435-41.
264. Bokkers RP, van Laar PJ, van de Ven KC, Kapelle LJ, Klijn CJ, Hendrikse J. Arterial spin-labeling MR imaging measurements of timing parameters in patients with a carotid artery occlusion. *AJNR Am J Neuroradiol*2008 Oct;29(9):1698-703.
265. Derdeyn CP, Powers WJ, Grubb RL, Jr. Hemodynamic effects of middle cerebral artery stenosis and occlusion. *AJNR Am J Neuroradiol*1998 Sep;19(8):1463-9.
266. Smith HA, Thompson-Dobkin J, Yonas H, Flint E. Correlation of xenon-enhanced computed tomography-defined cerebral blood flow reactivity and collateral flow patterns. *Stroke*1994 Sep;25(9):1784-7.

267. Brandt T. Survival with Basilar Artery Occlusion. *Cerebrovasc Dis*1995;5:182-7.
268. Weidner W, Hanafeewmarkham CH. Intracranial Collateral Circulation Via Leptomeningeal and Rete Mirabile Anastomoses. *Neurology*1965 Jan;15:39-48.
269. Kinoshita T, Ogawa T, Kado H, Sasaki N, Okudera T. CT angiography in the evaluation of intracranial occlusive disease with collateral circulation: comparison with MR angiography. *Clin Imaging*2005 Sep-Oct;29(5):303-6.
270. Zappe L, Juhasz J, Vidovszky T. Relationship of collateral circulation and prognosis in cerebral arterial occlusion. *Acta Neurochir (Wien)*1966;14(3):225-37.
271. Uemura A, O'Uchi T, Kikuchi Y, Yashiro N, Ihara N, Shoji K. Prominent laterality of the posterior cerebral artery at three-dimensional time-of-flight MR angiography in M1-segment middle cerebral artery occlusion. *AJNR Am J Neuroradiol*2004 Jan;25(1):88-91.
272. Cross DT, 3rd, Moran CJ, Akins PT, Angtuaco EE, Derdeyn CP, Diringer MN. Collateral circulation and outcome after basilar artery thrombolysis. *AJNR Am J Neuroradiol*1998 Sep;19(8):1557-63.
273. Roberts HC, Dillon WP, Furlan AJ, Wechsler LR, Rowley HA, Fischbein NJ, et al. Computed tomographic findings in patients undergoing intra-arterial thrombolysis for acute ischemic stroke due to middle cerebral artery occlusion: results from the PROACT II trial. *Stroke*2002 Jun;33(6):1557-65.
274. Ringelstein EB, Biniek R, Weiller C, Ammeling B, Nolte PN, Thron A. Type and extent of hemispheric brain infarctions and clinical outcome in early and delayed middle cerebral artery recanalization. *Neurology*1992 Feb;42(2):289-98.
275. Lee KH, Cho SJ, Byun HS, Na DG, Choi NC, Lee SJ, et al. Triphasic perfusion computed tomography in acute middle cerebral artery stroke: a correlation with angiographic findings. *Arch Neurol*2000 Jul;57(7):990-9.

276. von Kummer R, Holle R, Rosin L, Forsting M, Hacke W. Does arterial recanalization improve outcome in carotid territory stroke? *Stroke*1995 Apr;26(4):581-7.
277. Toni D, Fiorelli M, Bastianello S, Falcou A, Sette G, Ceschin V, et al. Acute ischemic strokes improving during the first 48 hours of onset: predictability, outcome, and possible mechanisms. A comparison with early deteriorating strokes. *Stroke*1997 Jan;28(1):10-4.
278. Noguchi K, Ogawa T, Inugami A, Fujita H, Hatazawa J, Shimosegawa E, et al. MRI of acute cerebral infarction: a comparison of FLAIR and T2-weighted fast spin-echo imaging. *Neuroradiology*1997 Jun;39(6):406-10.
279. Kim JJ, Fischbein NJ, Lu Y, Pham D, Dillon WP. Regional angiographic grading system for collateral flow: correlation with cerebral infarction in patients with middle cerebral artery occlusion. *Stroke*2004 Jun;35(6):1340-4.
280. von Kummer R, Hacke W. Safety and efficacy of intravenous tissue plasminogen activator and heparin in acute middle cerebral artery stroke. *Stroke*1992 May;23(5):646-52.
281. von Kummer R. Effects of Recanalization and Collateral Blood Supply on Infarct Extent and Brain Edema after Middle Cerebral Artery Occlusion. *Cerebrovasc Dis*1993;3:252-5.
282. Bozzao L, Bastianello S, Fantozzi LM, Angeloni U, Argentino C, Fieschi C. Correlation of angiographic and sequential CT findings in patients with evolving cerebral infarction. *AJNR Am J Neuroradiol*1989 Nov-Dec;10(6):1215-22.
283. Bozzao L, Fantozzi LM, Bastianello S, Bozzao A, Fieschi C. Early collateral blood supply and late parenchymal brain damage in patients with middle cerebral artery occlusion. *Stroke*1989 Jun;20(6):735-40.
284. Kim Y, Sin DS, Park HY, Park MS, Cho KH. Relationship between flow diversion on transcranial Doppler sonography and leptomeningeal collateral



circulation in patients with middle cerebral artery occlusive disorder. *J*

*Neuroimaging*2009 Jan;19(1):23-6.

285. Mohammad YM, Christoforidis GA, Bourekas EC, Slivka AP. Qureshi grading scheme predicts subsequent volume of brain infarction following intra-arterial thrombolysis in patients with acute anterior circulation ischemic stroke. *J Neuroimaging*2008 Jul;18(3):262-7.

286. Mohammad Y, Xavier AR, Christoforidis G, Bourekas E, Slivka A. Qureshi grading scheme for angiographic occlusions strongly correlates with the initial severity and in-hospital outcome of acute ischemic stroke. *J Neuroimaging*2004 Jul;14(3):235-41.

287. Kucinski T, Koch C, Eckert B, Becker V, Kromer H, Heesen C, et al. Collateral circulation is an independent radiological predictor of outcome after thrombolysis in acute ischaemic stroke. *Neuroradiology*2003 Jan;45(1):11-8.

288. Sanossian N, Saver JL, Alger JR, Kim D, Duckwiler GR, Jahan R, et al. Angiography reveals that fluid-attenuated inversion recovery vascular hyperintensities are due to slow flow, not thrombus. *AJNR Am J Neuroradiol*2009 Mar;30(3):564-8.

289. Higashida RT, Furlan AJ, Roberts H, Tomsick T, Connors B, Barr J, et al. Trial design and reporting standards for intra-arterial cerebral thrombolysis for acute ischemic stroke. *Stroke*2003 Aug;34(8):e109-37.

290. Liebeskind DS. Benign Oligemia Reflects Collateral Perfusion: MRI and Angiography of Low perfusion Hyperemia in Humans. *stroke*. [Abstract]. 2008;39:577.

291. Liebeskind DS. Gradient Echo MRI Phase Mismatching Reveals Angiographic correlated in Acute Ischemic Stroke. *stroke*. [Abstract]. 2006;37:619-46.

292. Liebeskind DS. Clinical Predictors of Angiographic Collaterals in Acute Ischemic Stroke. *Stroke*. [Abstract]. 2005;36:450.
293. Liebeskind DS. Angiographic Collaterals and Outcome in Mechanical Thrombolysis. *Stroke*. [abstract]. 2005;36:449.
294. Arnold M, Nedeltchev K, Schroth G, Baumgartner RW, Remonda L, Loher TJ, et al. Clinical and radiological predictors of recanalisation and outcome of 40 patients with acute basilar artery occlusion treated with intra-arterial thrombolysis. *J Neurol Neurosurg Psychiatry* 2004 Jun;75(6):857-62.
295. Gasparotti R, Grassi M, Mardighian D, Frigerio M, Pavia M, Liserre R, et al. Perfusion CT in patients with acute ischemic stroke treated with intra-arterial thrombolysis: predictive value of infarct core size on clinical outcome. *AJNR Am J Neuroradiol* 2009 Apr;30(4):722-7.
296. Arnold M, Schroth G, Nedeltchev K, Loher T, Remonda L, Stepper F, et al. Intra-arterial thrombolysis in 100 patients with acute stroke due to middle cerebral artery occlusion. *Stroke* 2002 Jul;33(7):1828-33.
297. Meier N, Nedeltchev K, Brekenfeld C, Galimanis A, Fischer U, Findling O, et al. Prior statin use, intracranial hemorrhage, and outcome after intra-arterial thrombolysis for acute ischemic stroke. *Stroke* 2009 May;40(5):1729-37.
298. Gonner F, Remonda L, Mattle H, Sturzenegger M, Ozdoba C, Lovblad KO, et al. Local intra-arterial thrombolysis in acute ischemic stroke. *Stroke* 1998 Sep;29(9):1894-900.
299. Brekenfeld C, Remonda L, Nedeltchev K, Arnold M, Mattle HP, Fischer U, et al. Symptomatic intracranial haemorrhage after intra-arterial thrombolysis in acute ischaemic stroke: assessment of 294 patients treated with urokinase. *J Neurol Neurosurg Psychiatry* 2007 Mar;78(3):280-5.
300. Rosenthal ES, Schwamm LH, Roccatagliata L, Coutts SB, Demchuk AM, Schaefer PW, et al. Role of recanalization in acute stroke outcome: rationale for a

CT angiogram-based "benefit of recanalization" model. *AJNR Am J*

*Neuroradiol*2008 Sep;29(8):1471-5.

301. Maas MB, Lev MH, Ay H, Singhal AB, Greer DM, Smith WS, et al.

Collateral vessels on CT angiography predict outcome in acute ischemic stroke.

*Stroke*2009 Sep;40(9):3001-5.

302. Lima FO, Furie KL, Silva GS, Lev MH, Camargo EC, Singhal AB, et al. The

pattern of leptomeningeal collaterals on CT angiography is a strong predictor of

long-term functional outcome in stroke patients with large vessel intracranial

occlusion. *Stroke*2010 Oct;41(10):2316-22.

303. Soares BP, Tong E, Hom J, Cheng SC, Bredno J, Boussel L, et al.

Reperfusion is a more accurate predictor of follow-up infarct volume than

recanalization: a proof of concept using CT in acute ischemic stroke patients.

*Stroke* Jan;41(1):e34-40.

304. Liebeskind D. Intravascular Deoxygenation of Leptomeningeal Collaterals

Detected with Gradient-Echo MRI. *stroke*. [Abstract]. 2004;35:266.

305. Hermier M, Ibrahim AS, Wiart M, Adeleine P, Cotton F, Dardel P, et al. The

delayed perfusion sign at MRI. *J Neuroradiol*2003 Jun;30(3):172-9.

306. Martel AL, Allder SJ, Delay GS, Morgan PS, Moody AA. Perfusion MRI of

infarcted and noninfarcted brain tissue in stroke: a comparison of conventional

hemodynamic imaging and factor analysis of dynamic studies. *Invest Radiol*2001

Jul;36(7):378-85.

307. Ruland S, Ahmed A, Thomas K, Zhao M, Amin-Hanjani S, Du X, et al.

Leptomeningeal collateral volume flow assessed by quantitative magnetic

resonance angiography in large-vessel cerebrovascular disease. *J*

*Neuroimaging*2009 Jan;19(1):27-30.

308. Schomer DF, Marks MP, Steinberg GK, Johnstone IM, Boothroyd DB, Ross MR, et al. The anatomy of the posterior communicating artery as a risk factor for ischemic cerebral infarction. *N Engl J Med* 1994 Jun 2;330(22):1565-70.
309. Chalela JA, Alsop DC, Gonzalez-Atavales JB, Maldjian JA, Kasner SE, Detre JA. Magnetic resonance perfusion imaging in acute ischemic stroke using continuous arterial spin labeling. *Stroke* 2000 Mar;31(3):680-7.
310. Hermier M, Nighoghossian N, Derex L, Wiart M, Nemoz C, Berthezene Y, et al. Hypointense leptomeningeal vessels at T2\*-weighted MRI in acute ischemic stroke. *Neurology*. [Comparitive study]. 2005 Aug 23;65(4):652-3.
311. Hennerici M, Rautenberg W, Schwartz A. Transcranial Doppler ultrasound for the assessment of intracranial arterial flow velocity--Part 2. Evaluation of intracranial arterial disease. *Surg Neurol* 1987 Jun;27(6):523-32.
312. Zanette EM, Roberti C, Mancini G, Pozzilli C, Bragoni M, Toni D. Spontaneous middle cerebral artery reperfusion in ischemic stroke. A follow-up study with transcranial Doppler. *Stroke* 1995 Mar;26(3):430-3.
313. Reinhard M, Muller T, Guschlbauer B, Timmer J, Hetzel A. Dynamic cerebral autoregulation and collateral flow patterns in patients with severe carotid stenosis or occlusion. *Ultrasound Med Biol* 2003 Aug;29(8):1105-13.
314. Reinhard M, Muller T, Roth M, Guschlbauer B, Timmer J, Hetzel A. Bilateral severe carotid artery stenosis or occlusion - cerebral autoregulation dynamics and collateral flow patterns. *Acta Neurochir (Wien)* 2003 Dec;145(12):1053-9; discussion 9-60.
315. Kaps M, Damian MS, Teschendorf U, Dorndorf W. Transcranial Doppler ultrasound findings in middle cerebral artery occlusion. *Stroke* 1990 Apr;21(4):532-7.
316. Wintermark M, Albers G, Broderick J, Demchuk A, Fiebach J, Fiehler J, et al. Acute Stroke Imaging Research Roadmap II. *Stroke* 2013(44):2628-39.

317. Yoo AJ, Simonsen C, Prabhakaran S, Chaudhry Z, Issa M, Fugate J, et al. Refining angiographic biomarkers of revascularization: improving outcome prediction after intra-arterial therapy. *Stroke* 2013 Sep;44(9):2509-12.
318. Saito I, Segawa H, Shiokawa Y, Taniguchi M, Tsutsumi K. Middle cerebral artery occlusion: correlation of computed tomography and angiography with clinical outcome. *Stroke* 1987 Sep-Oct;18(5):863-8.
319. Marinoni M, Ginanneschi A, Forleo P, Amaducci L. Technical limits in transcranial Doppler recording: inadequate acoustic windows. *Ultrasound Med Biol* 1997;23(8):1275-7.
320. Barber PA, Darby DG, Desmond PM, Gerraty RP, Yang Q, Li T, et al. Identification of major ischemic change. Diffusion-weighted imaging versus computed tomography. *Stroke* 1999 Oct;30(10):2059-65.
321. Furlan AJ, Eyding D, Albers GW, Al-Rawi Y, Lees KR, Rowley HA, et al. Dose Escalation of Desmoteplase for Acute Ischemic Stroke (DEDAS): evidence of safety and efficacy 3 to 9 hours after stroke onset. *Stroke* 2006 May;37(5):1227-31.
322. Whiteley W, Lindley R, Wardlaw J, Sandercock P. Third international stroke trial. *Int J Stroke* 2006 Aug;1(3):172-6.
323. Singer OC, Sitzer M, du Mesnil de Rochemont R, Neumann-Haefelin T. Practical limitations of acute stroke MRI due to patient-related problems. *Neurology* 2004 May 25;62(10):1848-9.
324. Wintermark M, Lev MH. FDA investigates the safety of brain perfusion CT. *AJNR Am J Neuroradiol* 2009 Jan;31(1):2-3.
325. Weisbord SD, Palevsky PM. Radiocontrast-induced acute renal failure. *J Intensive Care Med* 2005 Mar-Apr;20(2):63-75.

326. Lansberg MG, O'Brien MW, Tong DC, Moseley ME, Albers GW. Evolution of cerebral infarct volume assessed by diffusion-weighted magnetic resonance imaging. *Arch Neurol* 2001 Apr;58(4):613-7.
327. van der Worp HB, Claus SP, Bar PR, Ramos LM, Algra A, van Gijn J, et al. Reproducibility of measurements of cerebral infarct volume on CT scans. *Stroke* 2001 Feb;32(2):424-30.
328. Schellinger PD, Thomalla G, Fiehler J, Kohrmann M, Molina CA, Neumann-Haefelin T, et al. MRI-based and CT-based thrombolytic therapy in acute stroke within and beyond established time windows: an analysis of 1210 patients. *Stroke* 2007 Oct;38(10):2640-5.
329. Nagakane Y, Christensen S, Brekenfeld C, Ma H, Churilov L, Parsons MW, et al. EPITHET: Positive Result After Reanalysis Using Baseline Diffusion-Weighted Imaging/Perfusion-Weighted Imaging Co-Registration. *Stroke* 2010 Jan;42(1):59-64.
330. Liebeskind DS. Understanding blood flow: the other side of an acute arterial occlusion. *Int J Stroke* 2007 May;2(2):118-20.
331. Hammer MD, Schwamm L, Starkman S, Schellinger PD, Jovin T, Nogueira R, et al. Safety and feasibility of NeuroFlo use in eight- to 24-hour ischemic stroke patients. *Int J Stroke* 2012 Dec;7(8):655-61.
332. Hsu CY, Norris JW, Hogan EL, Bladin P, Dinsdale HB, Yatsu FM, et al. Pentoxifylline in acute nonhemorrhagic stroke. A randomized, placebo-controlled double-blind trial. *Stroke* 1988 Jun;19(6):716-22.
333. Rordorf G, Cramer SC, Efird JT, Schwamm LH, Buonanno F, Koroshetz WJ. Pharmacological elevation of blood pressure in acute stroke. Clinical effects and safety. *Stroke* 1997 Nov;28(11):2133-8.

334. Lee JH, Han SJ, Kang WY, Lee KH, Yu KH, Song HK, et al. Dominant ipsilateral posterior cerebral artery on magnetic resonance angiography in acute ischemic stroke. *Cerebrovasc Dis*2004;18(2):91-7.
335. Hennerici MG, Kay R, Bogousslavsky J, Lenzi GL, Verstraete M, Orgogozo JM. Intravenous ancrod for acute ischaemic stroke in the European Stroke Treatment with Ancrod Trial: a randomised controlled trial. *Lancet*2006 Nov 25;368(9550):1871-8.
336. Levy DE, del Zoppo GJ, Demaerschalk BM, Demchuk AM, Diener HC, Howard G, et al. Ancrod in acute ischemic stroke: results of 500 subjects beginning treatment within 6 hours of stroke onset in the ancrod stroke program. *Stroke*2009 Dec;40(12):3796-803.
337. Lyden P BT, Tilley B. Improved reliability of the NIH Stroke Scale using video training. *Stroke*1994;25:2220-6.
338. van Swieten JC, Koudstaal PJ, Visser MC, Schouten HJ, van Gijn J. Interobserver agreement for the assessment of handicap in stroke patients. *Stroke*1988 May;19(5):604-7.
339. Bamford J, Sandercock P, Dennis M, Burn J, Warlow C. Classification and natural history of clinically identifiable subtypes of cerebral infarction. *Lancet*1991 Jun 22;337(8756):1521-6.
340. McLeod DD, Parsons MW, Levi CR, Beutement S, Buxton D, Roworth B, et al. Establishing a rodent stroke perfusion computed tomography model. *Int J Stroke* Jan 10.
341. Yang Q. Method and System of Obtaining Improved Data in Perfusion Measurements. PCT International Application PCT/AU2004/000821. WIPO2005.
342. Kidwell CS, Alger JR, Saver JL. Beyond mismatch: evolving paradigms in imaging the ischemic penumbra with multimodal magnetic resonance imaging. *Stroke*2003 Nov;34(11):2729-35.

343. Liebeskind DS. Neuroprotection from the collateral perspective. *IDrugs*2005 Mar;8(3):222-8.
344. Kitagawa K, Matsumoto M, Tagaya M, Hata R, Ueda H, Niinobe M, et al. 'Ischemic tolerance' phenomenon found in the brain. *Brain Res*1990 Sep 24;528(1):21-4.
345. Barone FC, White RF, Spera PA, Ellison J, Currie RW, Wang X, et al. Ischemic preconditioning and brain tolerance: temporal histological and functional outcomes, protein synthesis requirement, and interleukin-1 receptor antagonist and early gene expression. *Stroke*1998 Sep;29(9):1937-50; discussion 50-1.
346. Kitagawa K, Yagita Y, Sasaki T, Sugiura S, Omura-Matsuoka E, Mabuchi T, et al. Chronic mild reduction of cerebral perfusion pressure induces ischemic tolerance in focal cerebral ischemia. *Stroke*2005 Oct;36(10):2270-4.
347. Danesh J, Lewington S, Thompson SG, Lowe GD, Collins R, Kostis JB, et al. Plasma fibrinogen level and the risk of major cardiovascular diseases and nonvascular mortality: an individual participant meta-analysis. *JAMA*2005 Oct 12;294(14):1799-809.
348. Tanne D, Macko RF, Lin Y, Tilley BC, Levine SR. Hemostatic activation and outcome after recombinant tissue plasminogen activator therapy for acute ischemic stroke. *Stroke*2006 Jul;37(7):1798-804.
349. Grotta J, Ostrow P, Fraifeld E, Hartman D, Gary H. Fibrinogen, blood viscosity, and cerebral ischemia. *Stroke*1985 Mar-Apr;16(2):192-8.
350. Reid HA, Chan KE, Thean PC. Prolonged coagulation defect (defibrination syndrome) in Malayan viper bite. *Lancet*1963 Mar 23;1(7282):621-6.
351. Sherman DG, Atkinson RP, Chippendale T, Levin KA, Ng K, Futrell N, et al. Intravenous ancrod for treatment of acute ischemic stroke: the STAT study: a randomized controlled trial. *Stroke Treatment with Ancrod Trial. JAMA*2000 May 10;283(18):2395-403.



352. Hao Z, Liu M, Counsell C, Wardlaw JM, Lin S, Zhao X. Fibrinogen depleting agents for acute ischaemic stroke. *Cochrane Database Syst Rev*2012;3:CD000091.
353. Teasdale EM. Multidetector CT: New Horizons in Neurological Imaging. *Imaging*2007;19:153-72.
354. Dani K, Thomas R, Chappell F, Shuler K, MacLeod M, Muir K, et al. Computed tomography and magnetic resonance perfusion imaging in ischemic stroke: definitions and thresholds. *Annals of Neurology*2011;70(3):384-401.
355. Kamalian S, Maas MB, Goldmacher GV, Payabvash S, Akbar A, Schaefer PW, et al. CT Cerebral Blood Flow Maps Optimally Correlate With Admission Diffusion-Weighted Imaging in Acute Stroke but Thresholds Vary by Postprocessing Platform. *Stroke*2011 Jul;42(7):1923-8.
356. Baron JC. Perfusion thresholds in human cerebral ischemia: historical perspective and therapeutic implications. *Cerebrovasc Dis*2001;11 Suppl 1:2-8.
357. Bivard A, Spratt N, Levi C, Parsons M. Perfusion computer tomography: imaging and clinical validation in acute ischaemic stroke. *Brain*2011;134:3408-16.
358. Youden WJ. Index for rating diagnostic tests. *Cancer*1950 Jan;3(1):32-5.
359. Carrera E, Jones PS, Alawneh JA, Klaerke Mikkelsen I, Cho TH, Siemonsen S, et al. Predicting infarction within the diffusion-weighted imaging lesion: does the mean transit time have added value? *Stroke*2011 Jun;42(6):1602-7.
360. Hill MD, Rowley HA, Adler F, Eliasziw M, Furlan A, Higashida RT, et al. Selection of acute ischemic stroke patients for intra-arterial thrombolysis with pro-urokinase by using ASPECTS. *Stroke*2003 Aug;34(8):1925-31.
361. Dzialowski I, Hill MD, Coutts SB, Demchuk AM, Kent DM, Wunderlich O, et al. Extent of early ischemic changes on computed tomography (CT) before

thrombolysis: prognostic value of the Alberta Stroke Program Early CT Score in ECASS II. *Stroke* 2006 Apr;37(4):973-8.

362. Demchuk AM, Hill MD, Barber PA, Silver B, Patel SC, Levine SR.

Importance of early ischemic computed tomography changes using ASPECTS in NINDS rtPA Stroke Study. *Stroke* 2005 Oct;36(10):2110-5.

363. Parsons MW, Pepper EM, Bateman GA, Wang Y, Levi CR. Identification of the penumbra and infarct core on hyperacute noncontrast and perfusion CT.

*Neurology* 2007 Mar 6;68(10):730-6.

364. Truwit CL, Barkovich AJ, Gean-Marton A, Hibri N, Norman D. Loss of the insular ribbon: another early CT sign of acute middle cerebral artery infarction.

*Radiology* 1990 Sep;176(3):801-6.

365. Patel SC, Levine SR, Tilley BC, Grotta JC, Lu M, Frankel M, et al. Lack of clinical significance of early ischemic changes on computed tomography in acute stroke. *JAMA* 2001 Dec 12;286(22):2830-8.

366. Unger E, Littlefield J, Gado M. Water content and water structure in CT and MR signal changes: possible influence in detection of early stroke. *AJNR Am J Neuroradiol* 1988 Jul-Aug;9(4):687-91.

367. Coutts SB, Demchuk AM, Barber PA, Hu WY, Simon JE, Buchan AM, et al. Interobserver variation of ASPECTS in real time. *Stroke* 2004 May;35(5):e103-5.

368. Brant-Zawadzki M, Enzmann DR. Using computed tomography of the brain to correlate low white-matter attenuation with early gestational age in neonates.

*Radiology* 1981 Apr;139(1):105-8.

369. Hacke W, Donnan G, Fieschi C, Kaste M, von Kummer R, Broderick JP, et al. Association of outcome with early stroke treatment: pooled analysis of

ATLANTIS, ECASS, and NINDS rt-PA stroke trials. *Lancet* 2004 Mar 6;363(9411):768-74.

